Tectonic evolution of the Svecofennian crust in southern Finland –
a basis for characterizing bedrock technical properties
Edited by Matti Pajunen
Geological Survey of Finland, Special Paper 47, 15–160, 2008.

TECTONIC EVOLUTION OF THE SVECOFENNIAN CRUST IN SOUTHERN FINLAND

by

Matti Pajunen, Meri-Liisa Airo, Tuija Elminen, Irmeli Mänttäri, Reijo Niemelä, Markus Vaarma, Pekka Wasenius and Marit Wennerström*

Pajunen, M., Airo, M.-L., Elminen, T., Mänttäri, I., Niemelä, R., Vaarma, M., Wasenius, P. & Wennerström, M. 2008. Tectonic evolution of the Svecofennian crust in southern Finland. *Geological Survey of Finland, Special Paper 47,* 15–160 , 53 figures, 1 table and 9 appendices.

The present-day constitution of the c. 1.9–1.8 Ga old Svecofennian crust in southern Finland shows the result of a complex collision of arc terranes against the Archaean continent. The purpose of this study is to describe structural, metamorphic and magmatic succession in the southernmost part of the Svecofennian domain in Finland, in the Helsinki area. Correlations are also carried out with the Pori reference area in southwestern Finland. A new tectonic model on the evolution of the southern Svecofennian domain is presented. The interpretation is based on field analyses of structural successions and magmatic and metamorphic events, and on interpretation of the kinematics of the structures. The structural successions are linked to new TIMS and SIMS analyses performed on eight samples and to published age data.

The Svecofennian structural succession in the study area is divided into deformation phases D_A-D_I; the post-Svecofennian events are combined as a D_P phase. Kinematics in the progressively-deforming transtensional or transpressional belts complicates analysis of the overprinting relations due to their simultaneous contractional and extensional structures. In this work the Svecofennian structural succession in the study area is related to major geotectonic Events 1–5, E_1-E_5, on the basis of their characteristic kinematics and tectono-metamorphic and magmatic features.

Geotectonic event E_1 includes the D_A deformation (corresponding to the D_1 in the northern Svecofennian units) that deformed the oldest supracrustal sequences, including volcanic Series I. The horizontal D_A structures formed during c. N-S shortening. Event 1 is suggested as an early major thrusting deformation at c. 1.9–1.88 Ga ago. The crust thickened and crustal slices from different depths, and geotectonic and depositional environments, were juxtaposed.

Geotectonic event E_2 includes the D_B deformation (D_2 in the north). It is related to a crustal extension that caused a strong vertical shortening and prograde low-pressure (andalusite-sillimanite type) metamorphism. Extension is related to an island arc collapse; this collapse did not occur in the Archaean domain. The younger volcanic Series II evolved during the collapse and is proposed to represent intra-arc volcanism. Large amounts of syn-/late D_B intermediate igneous rocks were also emplaced. E_2 shows diachronic evolution, getting younger towards south; the age of E_2 in the south is c. 1.88–1.87 Ga.

The E_2 extension was rapidly followed by a N-S shortening event, E_3, that formed the contractional D_C structures (D_3 in the north) in the south at c. 1.87 Ga; E_3 was also a diachronic event. According to the structure and age correlations, the northern Svecofennian units already underwent E_3 contraction during the southern E_2 extensional stage. This supposes that the crust as a whole was under a compressional regime and that E_2 was a southwards-migrating localized event. In the Archaean continent and close to its border zone, the escape of crustal blocks towards the NNW-NNE occurred; movements occurred along the old Archaean or pre-collisional Proterozoic N-S-trending shear zones. After E_3 the Svecofennian and Archaean domains formed a coherent continent and, therefore, the later geotectonic events occurred in this new continental crust.

Geotectonic event E_4 deformed the new continental crust and is in the south predominantly connected to the evolution of the Southern Finland Granitoid Zone (SFGZ). The E_3 N-S stress field rotated into a SW-NE orientation. The pre-SFGZ crust in the south is characterized by the D_{C+D} dome-and-basin interferences formed at c. 1.87 Ga due to the SW-NE transpressional deformation D_D (D_4 in the north). At that time, in the northern units, the wide-scale oblique contractional folding, eastwards transport and clockwise rotation of crustal blocks occurred. The deformation pattern of crustal blocks, like the Pomarkku and Vaasa blocks during D_4 (D_D in the south) and the Central Finland block during D_F at c. 1.86–1.85 Ga, as well as related shear zone patterns, are interpreted as a product of escape tectonics related to the SW-NE transpression. Simultaneously with the termination of the D_4 deformation in the north at 1868 ± 3 Ma, evolution of the Southern Finland Granitoid Zone (SFGZ) was initiated by the early D_E tonalites in the south. The SFGZ shows a very complex pattern of D_E, D_F, D_G and D_H structures that formed in kinematics representing different local stress fields. Intense intermediate to felsic D_E magmatism occurred in the oblique SE-extensional zones between the active N-trending deformation zones, the Baltic Sea-Bothnian Bay Zone (BBZ), Riga Bay Karelia Zone (RKZ) and the Transscandinavian Igneous Belt (TIB). In the erosion level, progressive extensional evolution led to the development of the pull-part basins with supracrustal sequences exemplified by the Jokela supracrustal association. The peak of D_E extensional evolution is represented by gabbro intrusions at c. 1.84 Ga; this mafic and intense intermediate magmatism may be related to the volcanism in the pull-apart basins. The Porkkala-Mäntsälä shear/fault zone and the wide-scale F_G folding are results of a short-lasting N-S shortening D_G at c. 1.85 Ga. In southern Finland the late E_4 evolution, from c. 1.84 to 1.80 Ga, is characterized by SE-NW transpression during D_H. Sinistral movements in the N-trending shear zones, like the Vuosaari-Korso shear/fault zone, oblique dextral movements in the E-W-trending Hyvinkää and Southern Finland shear/fault zones, oblique contractional D_H folds and the oblique extensional or spot-like granites and diabase dykes resulted. The localized D_E SE-NW extension in the SFGZ turned to SE-NW transpression due to rotation of the zone under an overall SW-NE transpression between the major N-trending deformation zones, the Baltic Sea-Bothnian Bay Zone (BBZ), Riga Bay-Karelia Zone (RKZ) and Transscandinavian Igneous Belt (TIB).

The evolution of the major N-trending D_I deformation zones, the BBZ, RKZ and TIB, already started during the D_D deformation, but their latest phase, related here to the E_5, deformed the Southern Finland Granitoid Zone (SFGZ) and the E-W-trending shear zones. The D_{G+H+I} dome-and-basin interferences determining the present exposition of the geotectonic and metamorphic units were formed. The youngest dated Svecofennian rock in the study area is a <1.8 Ga old amphibolite facies diabase dyke, which confines the fade of the Svecofennian orogeny in southernmost Finland.

The post-Svecofennian deformations and magmatic events, included here as a combined D_P, are strongly controlled by the older Svecofennian structures. In the study area the c. 1.65 Ga Bodom and Obbnäs rapakivi granite magmas were channelled by the intersections of the major Svecofennian crustal shear structures, like the southern Finland, Porkkala-Mäntsälä and the D_I shear zones/faults, and the low-angle structures like the $S_{E/H}$ foliation planes controlled their emplacement. On a wider scale, rapakivis are located in close association with the major Svecofennian D_I deformation zones such as the Baltic Sea-Bothnian Bay Zone (BBZ) and Riga Bay-Karelia Zone (RKZ).

Tectonic and kinematic analysis combined with the tectonically-fixed age data on magmatic events establishes that the Svecofennian orogeny was a continuous diachronic event getting younger towards the south/southwest. The Svecofennian island arc system collided obliquely against the Archaean continent simultaneously with the growth of an island arc. The Svecofennian arc components were accreted to the Archaean continent to form a new continental crust. The continent was deformed during the continued transpressional orogen into major crustal blocks that transported and rotated with simultaneously formed extensional zones – e.g. the pull-apart basins and granitoid zones – and strike slip terranes. The tectonic pattern is characteristic for terranes formed by escape tectonics.

In summary, the tectonic evolution of the Svecofennian orogeny is related to one oblique collision of the active, growing Svecofennian island arc system against the Archaean continent, and to subsequent transpressional continental deformation characterized by escape tectonics.

Key words (GeoRef Thesaurus, AGI): crust, tectonics, structural geology, structural analysis, deformation, folds, shear zones, Svecofennian Domain, Proterozoic, Paleoproterozoic, Uusimaa, Southern Finland

* *Geological Survey of Finland, P.O. Box 96, FI-02151 Espoo, Finland*

* *E-mail: matti.pajunen@gtk.fi*

INTRODUCTION

At the very beginning of last century, J. J. Sederholm (1907, 1923, 1926, compiled works in 1967), the architect of modern geological research and mapping in Finland (e.g. Scheinin & Korsman 2007), described with amazing accuracy the 1.9–1.8 Ga Svecofennian supracrustal sequences and migmatites (interpreted as Archaean at his time) in the southernmost part of the country. His main emphasis was on structures and the genesis of migmatites, melting and granitization in the deeper crustal levels. Sederholm (1926) carefully analysed the relationships between different magmatic and migmatization events. For example, mafic dykes intruded into the brittle fractures of Hanko-Inkoo granite, and both the granite and dyke were migmatized by a later granitic event, thus confirming the polyphase tectono-thermal evolution of the crust. The observation definitely evidences that there was a cooling stage between the two granitic events; this discordance was later re-established, for instance, by Pajunen et al. (2008). In the southern Svecofennian domain, Korsman et al. (1984) described a tectono-metamorphic discordance (geosuture in Korsman et al. 1988) between the northern Tonalite Migmatite Belt (TMB) and the southern Granite Migmatite Belt (GMB) (Figure 1). These kinds of discordances, combined with kinematic and thermal data, have a great importance in constructing crustal evolution models. Several models of the history of Svecofennian evolution have been developed since the first plate tectonic model of Hietanen (1975). These accretion and collision-extension models (e.g. Koistinen 1981, Edelman & Jaanus-Järkkälä 1983, Gaál & Gorbatchev 1987, Ekdahl 1993, Korja et al. 1993, Lahtinen 1994, Ruotoistenmäki 1996, Nironen 1997, Kilpeläinen 1998, Korsman et al. 1999, Väisänen 2002, Pajunen et al. 2002, 2004 and Lahtinen et al. 2005), accompanied with considerable age data (e.g. Patchett et al. 1981, Huhma 1986, Vaasjoki & Sakko 1988 and Suominen 1991), are a good basis for further research on Svecofennian evolution. Unfortunately, the interesting results of the Finnish Reflection Experiment FIRE 2001–2005 (Kukkonen & Lahtinen 2006) were published too late to be discussed in details here.

In the northern Tonalite Migmatite Belt (TMB) the crust was largely stabilized at 1.88 Ga ago, whereas in the southern Granite Migmatite Belt (GMB) the thermal peak was achieved c. 50 Ma later (Korsman et al. 1984 and 1999). The differences in timing of thermal and deformation events, and the depth of concurrent deformations between the units (e.g. Kilpeläinen 1998), have a crucial bearing on characters of concomitant tectonic structures in these regions. While ductile deformation occurred in the south, the northern units behaved in a more rigid and brittle way (Pajunen et al. 2001b). Recently, more reasonable information on the semi-brittle to brittle structures has been needed, because society has increased the requirements for geological information. Especially the analysis of semi-ductile to brittle structural data has prime importance for several applications. The late Svecofennian ductile to semi-ductile tectonic events are important for the present-day arrangement of tectonic units and distribution of lithologies, but are only seldom described (Ehlers et al. 1993, Pietikäinen 1994 and Pajunen et al. 2001a). How the Svecofennian structures influenced the post-Svecofennian geotectonic structures, like the extension-related rapakivi magmatism at c. 1.65–1.57 Ga ago (Vaasjoki 1977a, Rämö 1991, Korja & Heikkinen 1995, Kosunen 2004 and Haapala et al. 2005), the subsequent formation of the sandstone basin (Kohonen et al. 1993) and related mafic magmatism at 1.25 Ga in the Pori area, or the Caledonian or even post-glacial events, is still an open question.

The aim of this paper is to explain how tectonic, magmatic and thermal evolution yielded the present configuration of rock types and structures in the study area in the surroundings of Helsinki (Figure 1). The results presented in a preceding unpublished report by Pajunen et al. (2002) showed that tectono-metamorphic and magmatic evolution in southernmost Finland is more complicated than can be summarized from the earlier studies. There are several reasons for this complexity, for example: 1) the tectono-thermal events and their products cover the whole time-scale of Svecofennian history, from 1.9 to 1.8 Ga; the crust was strongly modified during the anorogenic rapakivi-stage c. 1.65–1.54 Ga ago (Vaasjoki 1977a, Korsman et al. 1997 and Haapala et al. 2005) and later Mesoproterozoic extension and magmatism 1.25 Ga ago (Kohonen et al. 1993); some reactivation occurred during the Caledonian orogeny c. 450 Ma ago (Vaasjoki 1977b and Mertanen et al. 2008) and even the post-glacial time (Kuivamäki et al. 1998), 2) the bedrock is characterized by a complex polyphase tectonic history (e.g. Laitala 1973a, Hopgood 1984 and Pajunen et al. 2008) that caused strong fragmentation and reorganization of the various tectonic units, 3) the thermal state and rigidity of different units varied during the concomitant deformation, causing differing kinematic behaviour and deformation patterns that are difficult to correlate between the separate units, 4) several metamorphic mineral growth stages (e.g. Korsman et al. 1984, 1999 and Kilpeläinen 1998),

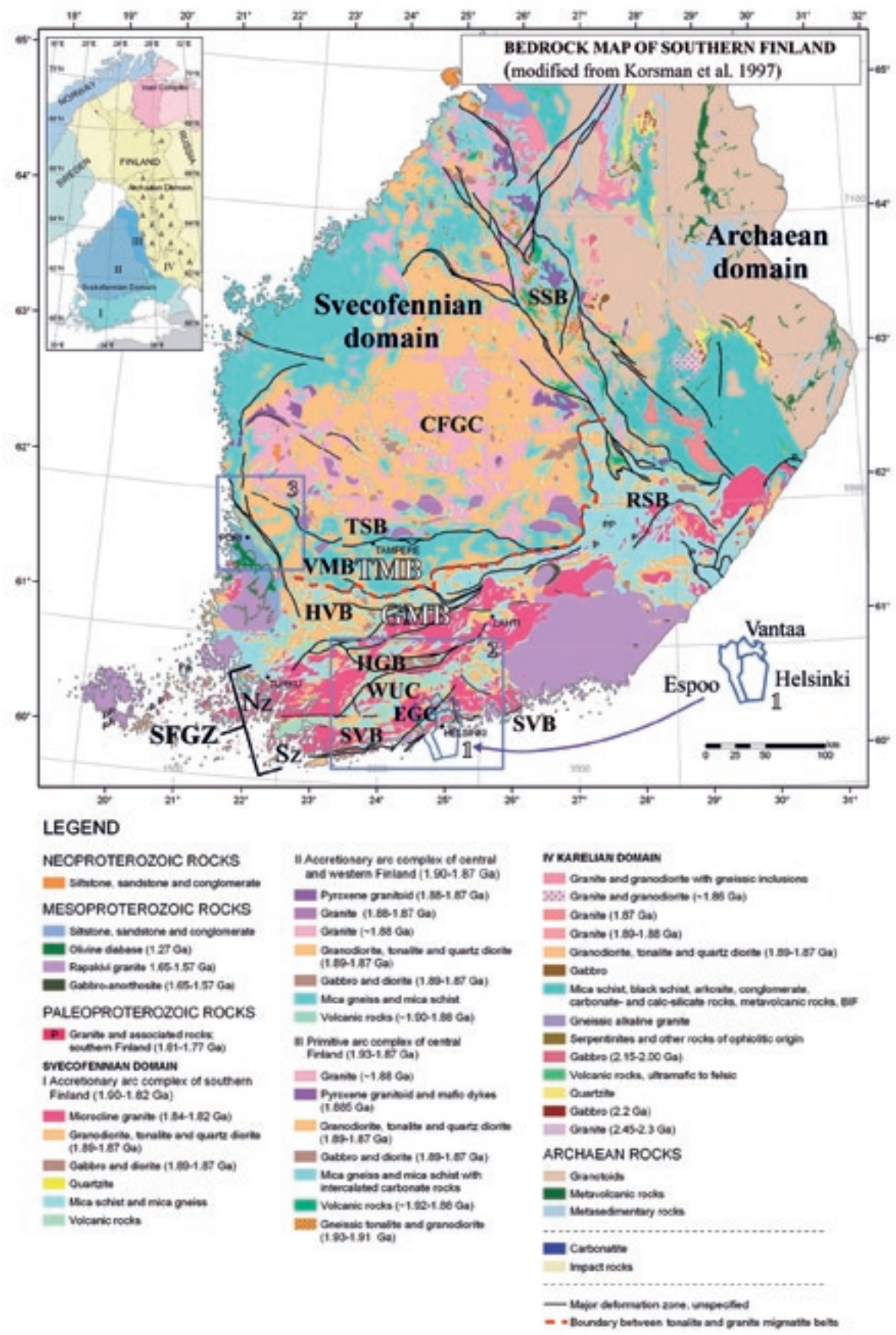

Figure 1. The study areas on the geological map of Finland (Korsman et al. 1997): 1. Detailed study area in Espoo, Helsinki and Vantaa; 2. Study area for the observations on key outcrops and interpretation of the pre-existing data; and 3. Pori reference area (Pajunen et al. 2001a). Abbreviations: GMB = Granite Migmatite Belt (I in inset), TMB = Tonalite Migmatite belt (II in inset), SSB = Savo Schist Belt (III in inset), Karelian unit (IV in inset), RSB = Rantasalmi-Sulkava area, VMB = Vammala Migmatite Belt, TSB = Tampere Schist Belt, HVB = Häme Volcanic Belt, HGB = Hyvinkää Gabbroic-volcanic Belt, WUC = West Uusimaa Complex, SVB = Southern Volcanic-sedimentary Belt, CFGC = Central Finland Granitoid Complex, SFGZ = Southern Finland Granitoid Zone, northern zone of the SFGZ = Nz, southern zone of the SFGZ = Sz and EGC = Espoo Granitoid Complex. Base map © National Land Survey of Finland, permit No. 13/MML/08.

strong melting and granitization (e.g. Härme 1965), have often destroyed the earlier structures and effectively obscure the preceding metamorphic signatures, 5) primary supracrustal features are largely destroyed and the stratigraphic interpretations generally justify only tectonic strathigraphy of variable crustal slices, and 6) isotopic information on early events is sometimes difficult to obtain due to later higher-grade overprint, inheritance or rejuvenation.

Analysis of tectonic evolution of the southern Svecofennian domain is based on detailed field observations on structures in the study area; much weight will be put on descriptions of structures in the field. The descriptions and interpretations focus predominantly on the Granite Migmatite Belt (GMB) in Espoo, Helsinki and Vantaa (Figure 1, area 1). In understanding regional Svecofennian evolution in the southernmost part of Finland, it was also necessary to carry out some studies and correlations outside the detailed area (Figure 1, area 2). Some revision of the early observations of Pajunen et al. (2001a) was also made in the Tonalite Migmatite Belt (TMB) in the Pori area (Figure 1, area 3). Some characteristic structures in the study area are impossible to analyze without considering a wider, Fennoscandian context. Supporting interpretations outside the detailed study area are separately described in Appendices 1–7. The structural model is fixed with some new TIMS and SIMS age data on the key rocks (Appendix 8). Figures in the Appendices are referred to in the main text in the form Appendix-Fig. 1-1a (Figure 1a in Appendix 1); the main text Figures are referred to in the Appendices correspondingly to the main text. Tables in appendices are named as App-Table 1–4. Postulations on how the southern Svecofennian structures controlled post-Svecofennian deformation, especially during the Palaeoproterozoic-Mesoproterozoic rapakivi event, are briefly discussed.

The results represented here are based on projects organized by the Geological Survey of Finland (GTK): 1) "Construction potential modelling of bedrock in urban areas" during 1999–2002 near Helsinki in southernmost Finland (Pajunen et al. 2001b and preliminary report, Pajunen et al. 2002), with field revision during the field seasons 2003 and 2004; 2) "Shear/fault zone research and rock engineering", which was carried out in 1998–1999 in the Pori area in western Finland (Pajunen et al. 2001a), where some revision was made in 2006–2007 by the "Bedrock stress field in Satakunta/GeoSatakunta" project.

M. Pajunen takes the full responsibility for the geological interpretations presented in this paper. M.-L. Airo modified and interpreted the geophysical data and constructed the cross-sections (cf. Airo et al. 2008). T. Elminen and M. Wennerström interpreted the semi-brittle to brittle structures that are discussed in more detail in Elminen et al. (2008) and Wennerström et al. (2008). M. Pajunen, T. Elminen, M. Wennerström, Vaarma, R. Niemelä and P. Wasenius took part in the regional and thematic mapping necessary for this analysis. I. Mänttäri performed the U-Pb age determinations.

GEOLOGICAL OUTLINE

Svecofennian evolution

The Palaeoproterozoic 1.9–1.8 Ga Svecofennian domain is situated in the central part of the Fennoscandian Shield area (Koistinen et al. 2001). According to refraction seismic studies (e.g. Luosto et al. 1990, Grad & Luosto 1992 and Korsman et al. 1999), the crust in southernmost Finland is c. 48–50 km thick. In the central and eastern parts of the Svecofennian domain, in the Proterozoic-Archaean border zone, it is considerably thicker, up to 65 km. The reflection seismic data of FIRE (Kukkonen & Lahtinen 2006) and BABEL (Korja & Heikkinen 1995 and 2005) indicate a layered crust with wide-scale, low-angle tectonic structures characterizing large areas in central and southern Finland.

The complex collision of the Svecofennian units against the Archaean domain occurred along a suture zone at 1.90–1.88 Ga (e.g. Wegmann 1928, Koistinen 1981, Lahtinen 1994 and Korsman et al. 1999). The suture is verified by remnants of a c. 1.95 Ga oceanic crust (Kontinen 1987) and turbiditic sediments (area IV in inset in Figure 1) that was overthrusted towards the NNE over the Archaean continent (Koistinen 1981). The effects of Svecofennian tectonic activity extended far northeast of the suture zone (e.g. Kontinen et al. 1992 and Pajunen & Poutiainen 1999). Pajunen and Poutiainen (1999) identified two Svecofennian tectono-thermal overprinting events in the Archaean domain. The first event was related to barrowian-type (kyanite-staurolite) heating after collision at c. 1.90 Ga and the later one to c. 1.85 Ga dilatational fluid activity (Mg-metasomatism in sillimanite stability field) and magmatism. The later event was caused by magmatic underplating, resulting in the thick crust of the area (cf. Luosto et al. 1990, Korja et al. 1993 and Korsman et al. 1999). The U-Pb zircon ages in mafic

granulite xenoliths from the lower crust in kimberlites in eastern Finland evidence high temperatures in the lower crust still occurring c. 1.80–1.73 Ga ago (Hölttä et al. 2000 and Peltonen et al. 2006).

The Svecofennian domain consists of juvenile (Huhma 1986) crust showing increasing maturity of island arcs towards south and west. The NW-SE trending Savo Schist Belt (SSB, the Pyhäsalmi primitive island arc, c. 1.93–1.91 Ga) borders the Archaean unit. In the southern and western part of the Svecofennian domain, more mature island arc belts, like the Tampere Schist Belt (TSB, c. 1.9–1.89 Ga) and the Häme Volcanic Belt (HVB) (Kähkönen 1989, Lahtinen 1994 and Hakkarainen 1994), are located. The volcanic sequences (c. 1.90–1.87 Ga) in the Orijärvi area of the Southern Volcanic-sedimentary Belt (SVB) show back-arc basin geochemical characteristics (Väisänen & Mänttäri 2002). Laitala (1973a) described the structures in the volcanic series (c. 1.89 Ga) in the eastern part of the belt in Pellinki. The Hyvinkää Gabbroic-volcanic Belt (HGB) shows several large, c. 1.88 Ga gabbro intrusions (Patchett et al. 1981) in a volcanic environment (Härme 1978). Wide areas between the volcanic units are characterized by predominantly migmatized pelitic to psammitic rocks. In the southernmost Svecofennian domain, near the coast and in the archipelago, the volcanic rocks are felsic to mafic, sometimes with well-preserved pillow lava structures. Layers of carbonate rocks and silicate-facies iron formations indicate a shallow-marine depositional environment of the sediments (e.g. Ehlers & Lindroos 1990). Carbonate rocks and pillow lavas diminish northwards and volcanism changes to intermediate, pyroclastic and epiclastic (Kähkönen 1987). Sedimentary rocks deposited in deep water with intermediate to mafic volcanic rocks dominate further north in the Tonalite Migmatite Belt (TMB) (Korsman et al. 1984 and Kähkönen 1987). The majority of these supracrustal rocks were deposited at c. 1.9 Ga during the earliest stage of Svecofennian evolution (Huhma et al. 1991), but some, like the Tiirismaa quartzite near Lahti (Lehijärvi 1964), have younger zircons indicating deposition after 1.87–1.86 Ga (Lahtinen et al. 2002).

Several pulses of magmatic rocks representing different tectono-magmatic settings intrude the supracrustal sequences. Sederholm (1932a) divided the intrusive rocks in Finland into four groups that essentially still represent a helpful basis for classification: I – synorogenic mafic to felsic intrusive rocks (c. 1.89–1.87 Ga); II – late-orogenic felsic intrusive rocks (c. 1.84–1.81 Ga); III – post-orogenic granites and mafic dykes (c. 1.80–1.77 Ga); IV – anorogenic rapakivi granites and related intrusive rocks (c. 1.65–1.57 Ga) (cf. Vaasjoki 1977a, Nurmi & Haapala 1986 and Suominen 1991). The Central Finland Granitoid Complex (CFGC) is a coherent area of predominantly felsic granitoids with narrow zones of supracrustal rocks (Korsman et al. 1997). The CFGC shows a two-stage magmatic history: the older syntectonic plutonic pulse is c. 1.89–1.88 Ga in age and the later late/post-orogenic granitoids are c. 1.88–1.87 Ga old (Nironen 2003). A crustal component older than 1.92 Ga in the CFGC (e.g. Lahtinen & Huhma 1997) is postulated by Lahtinen et al. (2005) as the signature of an unexposed early microcontinent. A large amount of late-orogenic granites are exposed in a c. 100 km wide ENE-WSW-trending zone along the coast of the Gulf of Finland, in the southernmost Svecofennian area (Sederholm 1932a and Korsman et al. 1997), which is named Southern Finland Granitoid Zone (SFGZ). Related granitic rocks also cut the Archaean crust in eastern Finland; Sm-Nd data demonstrate Archaean contamination in these granitoids (Huhma 1986). Corresponding granitic units also exist in Sweden and northern Estonia (Koistinen et al. 1996 and 2001). Rämö et al. (2004) found variations in the Sm-Nd isotopic compositions in the late-orogenic granites between the northern (Nz in Figure 1) and southern zones (Sz in Figure 1) of the SFGZ. The c. 1.80–1.79 Ga old (Suominen 1991 and Vaasjoki 1995) post-tectonic granite intrusions locally caused metamorphic contact aureoles into the Granite Migmatite Zone (GMB) country rocks (Rastas 1990).

The tectono-metamorphic discordance between the Tonalite Migmatite Belt (TMB) and the Granite Migmatite Belt (GMB) (Korsman et al. 1984) forms a rather sharp boundary zone (Koistinen et al. 1996 and Korsman et al. 1999); Korsman et al. (1988) proposed that it represents a geosuture between the belts. The Rantasalmi-Sulkava area (RSB) was overthrusted towards north upon the Savo Schist Belt (SSB). In spite of the differences in crustal structure, the pressure estimates representing the Svecofennian peak metamorphic conditions are consistently around 5 kbar in the whole Svecofennian area (Korsman et al. 1999), and even in the Archaean domain (Tuisku & Laajoki 1990 and Pajunen & Poutiainen 1999).

The high-T/low-p (andalusite-sillimanite-type) metamorphism in the Savo Schist Belt (SSB) was connected to the c. 1.89–1.88 Ga magmatic activity. The crust stabilized soon after emplacement of 1884 ± 5 Ma pyroxene-bearing granitoids. The contact metamorphism generated by these rocks overprints the regional metamorphism (e.g. Korsman et al. 1984, Hölttä 1988, Hölttä et al. 1988 and Hölttä & Pajunen 1988). In western Finland, corresponding post-tectonic pyroxene-bearing granitoids are younger, c. 1.87 Ga (Mäkitie & Lahti 2001). In the tectono-metamorphic model of Korsman et al. (1999), based on the

refraction seismic structure of the crust (Luosto et al. 1984), magmatic underplating was proposed as the main source of crustal heat flow and the reason for the invariable pressure estimates. Pajunen and Poutiainen (1999) also supported the idea of lower-crustal disturbance as a heat source for the 1.85 Ga tectono-thermal process in the Archaean domain.

In the Rantasalmi-Sulkava area (RSB) of the Granite Migmatite Belt (GMB), penetrative tectonic, metamorphic and magmatic processes peaked c. 1.82–1.81 Ga ago (Korsman et al. 1984, 1988 and 1999). However, in the southern Savo Schist Belt (SSB) c. 1.84 Ga lamprophyre dykes intruded into an already cooled crust (Neuvonen et al. 1981). In the RSB the high-T/low-p metamorphism shows prograde zoning from andalusite stability in the north to granulite facies migmatitic garnet-cordierite gneisses in the south (Korsman 1977 and Korsman et al. 1984). However, the intrusion age of a pyroxene-bearing granitoid in the Granite Migmatite Belt (GMB) in the Turku area is 1878 ± 19 Ma (Väisänen et al. 2002), and the results of Hopgood et al. (1983) indicate that there was an earlier, c. 1.88–1.87 Ga, tectono-metamorphic event in the GMB.

Several models for the metamorphic evolution in the GMB have been proposed. An early interpretation of Korsman (1977) explained the progressive metamorphic zoning in the Rantasalmi-Sulkava area (RSB) as due to crustal thickening. Schreurs and Westra (1986) connected the granulite facies metamorphism in the West Uusimaa granulite Complex (WUC, cf. Parras 1958) to CO_2 influx. Väisänen (2002), on the other hand, proposed that the high heat flow in the granulite area in Turku (Väisänen & Hölttä 1999) was caused by crustal collapse (cf. model of Platt & England 1993). Ehlers et al. (1993) interpreted the late-orogenic granite magmatism in the Southern Finland Granitoid Zone (SFGZ) as syntectonic with SE-NW transpression at c. 1.84–1.81 Ga. According to Puura et al. (2004), further south in Estonia the ages of 1778 ± 2 Ma for monazite and 1728 ± 24 Ma for garnet in high-grade gneisses refer to still later events or cooling than in southern Finland.

Post-Svecofennian events

The late Palaeo- to Mesoproterozoic rapakivi stage (group IV of Sederholm 1932a) is the latest major tectono-magmatic event producing great amounts of mafic and granitic rocks (e.g. Sederholm 1932a, Rämö 1991, Heeremans 1997, Kosunen 2004 and Haapala et al. 2005). The rocks of the rapakivi suite are younger in western Finland (1.59–1.54 Ga) and in Russian Karelia (1.5–1.3 Ga) than in the detailed study area near Helsinki (1.67–1.62 Ga) (Vaasjoki 1977a and Haapala et al. 2005). The formation of the rapakivi suite, including related anorthosites and diabase dyke swarms, represented an extensional event that affected the whole crust, as suggested by listric faults identified below the Åland rapakivi batholith (Korja & Heikkinen 1995). In the Pori area, Mesoproterozoic c. 1.25 Ga mafic sills and laccoliths occur within the sandstone basin (Korsman et al. 1997 and Kohonen et al. 1993). These events reactivated older faults (Mertanen 2001, Mertanen et al. 2001, 2004, 2008 and Elminen et al. 2008), and later during the Caledonian orogeny some heating and reactivation (Vaasjoki 1977b and Mertanen et al. 2008) of the predominantly brittle faults occurred. The more systematic joint patterns were also formed during these latest stages of crustal evolution (Pajunen et al. 2001a and Wennerström et al. 2008). The present-day seismic activity and several post-glacial faults demonstrate that the recent c. WNW-ESE-oriented stress field (Stephansson et al. 1986), and even the local stress variations due to present gravity contrasts caused by differences in densities of rock types (Elo et al. 2007), still causes reactivation in the old fracture zones (e.g. Kuivamäki et al. 1998).

METHODS AND DATA

Field data

Tectonic interpretation is based on the field analyses of rock types and structures. The majority of observations are from the detailed study area (Figure 1, area 1). Approximately 1550 outcrops (Figures 2a, Pajunen et al. 2002) were studied; c. 200 exposures were investigated more carefully for their structural, metamorphic and magmatic characteristics, but detailed metamorphic analysis was beyond the scope of this study. Nearly 400 thin sections, including those collected during the regional mapping (see below), were investigated for structural and metamorphic characterization. Some correlations and sampling outside the detailed area (Figure 1, area 2) was concentrated on key outcrops hosting important geological information. The tectonic interpretation made in the Pori area (Figure 1, area 3) by Pajunen et al. (2001a) was based on c. 650 outcrops (Figure 2b), some of which are revisited during this study.

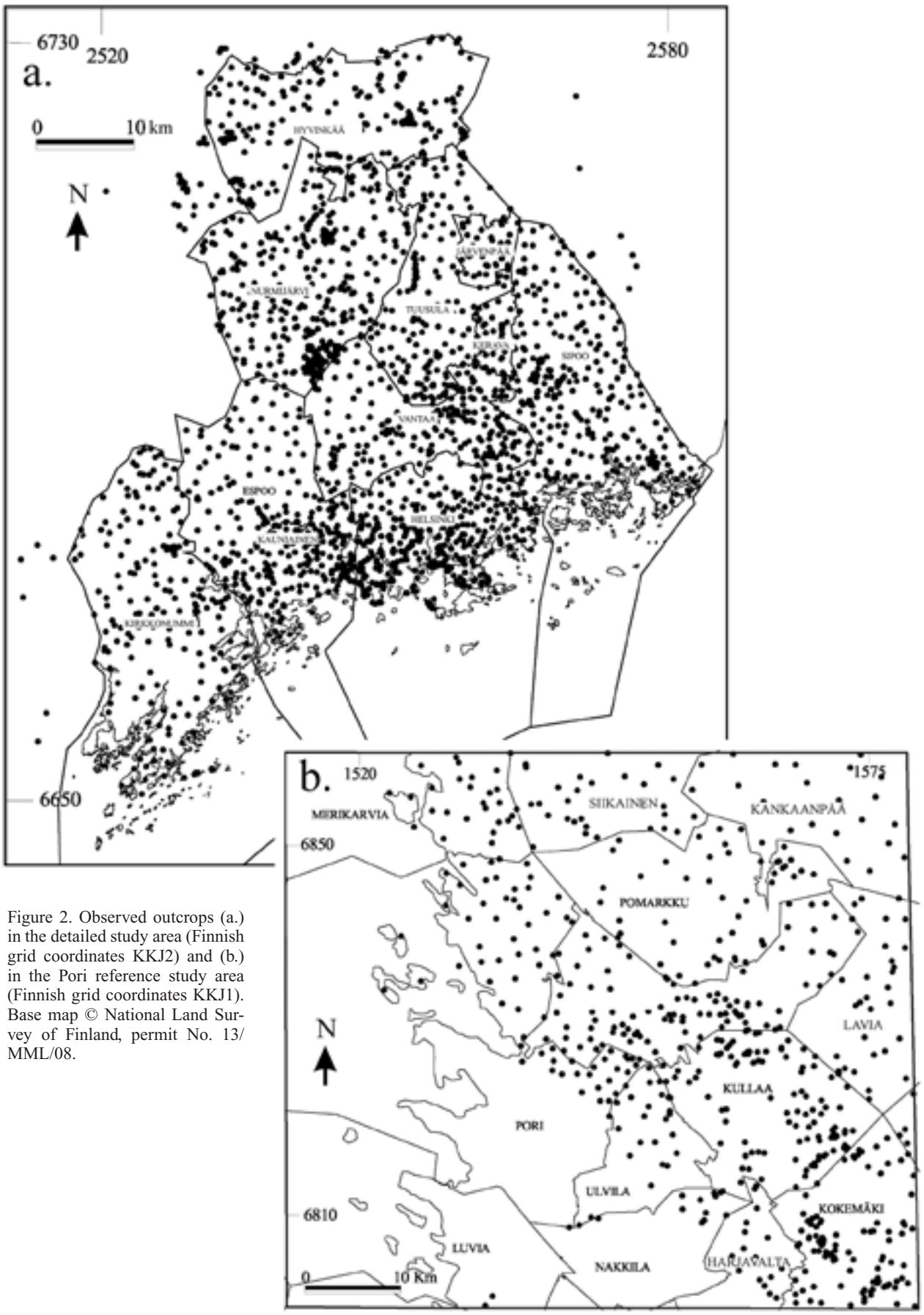

Figure 2. Observed outcrops (a.) in the detailed study area (Finnish grid coordinates KKJ2) and (b.) in the Pori reference study area (Finnish grid coordinates KKJ1). Base map © National Land Survey of Finland, permit No. 13/MML/08.

Structural analysis

Analysis of structural sequences is based on overprinting relationships of tectonic, magmatic and metamorphic events. The sequences of different structural features were established by analyzing the relationships of the structures and interference patterns on outcrops using the method described by Hopgood (1980, 1984 and 1999). To be able to make a regional correlation of structural sequences in and between the polydeformed and metamorphosed areas, the thermal history, mineral growth and magmatic events have to be considerated, as well as the relative ages of events. Regional variation in strain during deformation has an important effect on the resulting tectonic configuration (e.g. Ramsay & Huber 1983); strain and stress terminology follows Marrett and Peacock (1999). In this work, the kinematic reconstructions are based on the analysis of tectonic transport directions in the high strain shear zones, folding, foliation, boudinage structures, stretching/intersection lineations and shear band structures in the field. Rough estimations of strain are based on folding patterns, foliation intensities and the behaviour of competent objects in ductile groundmass.

When dealing with the Svecofennian history (e.g. Korsman et al. 1999, Pajunen et al. 2004 and Lahtinen et al. 2005) of the study area, it is not easy to correlate structures of one area to another. Where did the earliest events occur with respect to their present-day neighbouring units or tectonic slices? When were different crustal units/slices accreted to each other? Even though the crustal units share their primary lithology, earliest deformation events and even ages with each other whether it is not always self-evident, if they were together during the tectonic process. This problem is represented schematically in Figure 3. Especially in the strongly metamorphosed and tectonically segmented areas, like in southern Finland, correlation of the earliest tectonic structures from one area to another is difficult. Missing structures, not developed in sheltered blocks, may also confuse the structural succession.

In polydeformed and metamorphosed areas the analysis of structural succession is not straightforward; the metamorphic mineral growth history and age dating of processes are needed. The deformation products differ in the deeper parts of the crust from those simultaneously forming shallower crustal levels. Some rocks may have been affected by deformation under low-grade brittle conditions, or were even still depositing, whereas the lower crust already suffered a high-grade metamorphism and ductile metamorphism. Infra-supracrustal structures of this kind were exemplified by Kilpeläinen (1998),

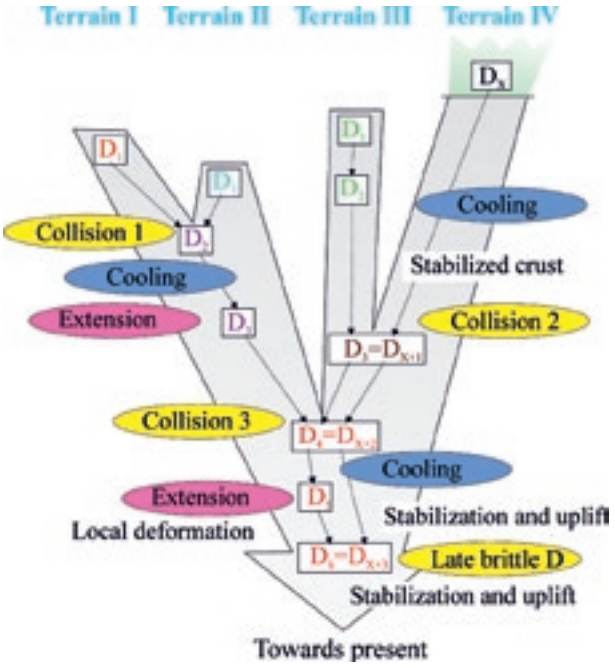

Figure 3. Schematic model describing the successive series of deformation events in different units; the oldest D_1 deformation event is overprinted by the subsequent deformations $D_{1, 2, 3...}$. Depending on the timing of the collisional, extensional and stabilization stages of the crust, the deformation history is the same or different in different units. Generally, the latest deformation events show a coherent history over wide areas, such as in the Fennoscandian Shield.

who noted that the well-preserved lower-grade rocks in the Tampere Schist Belt (TSB) were not affected by the earliest deformation seen in the corresponding high-grade gneisses south of it in the Vammala Migmatite Belt (VMB) (Figure 1). On the other hand, Rutland et al. (2004) proposed an age difference and discordance between them. As discussed above, Sederholm already presented similar ideas of the "tectono-thermal discordances" from southern Finland in 1926.

Heterogeneous strain partitioning during deformation complicates the correlation of tectonic structures. Strain localization into narrow shear zones may show some bending or folding restricted to these zones, whereas wide areas may be left unaffected. Thus, an important structure for reconstructing the regional tectonic history may be absent or very weak. This kind of partitioning is common under low-grade upper crustal conditions during the earliest and latest episodes of crustal history. Under higher-grade conditions, deformation is more penetrative and partitioning affects the rock on a smaller scale, e.g. along the fold limbs. When dealing with multistage tectono-magmatic history, deformation partitioning due to temperature and ductility contrasts is a phenomenon that strongly controls the tectonic construction. Local irregularities in the distribution of heat input or syntectonic magmatism may disturb the otherwise regular fold interference

patterns. These kinds of regional variations in strain and heat flow characterize, for example, the regions deformed in transpressional/-tensional belts (Holdsworth et al. 1998), or orogen-parallel extension zones in compressional orogens, like in the Himalayas (Zhang et al. 2000 and Murphy 2002). Tectonic structures indicating simultaneous shortening and dilatation in different parts of the region were developed.

The small-scale structures identified on outcrops do not necessarily reflect the major structures of the crust, like those seen in the reflection seismic data. For example, steeply- and tightly-folded units often represent on a wider scale a quite horizontal, only internally steep and tightly-folded slice. Internal structures are often unaffected by horizontal deformations such as overthrusting or extensional shearing/flattening (Figure 4). Such situations are typical in the southern Svecofennian domain. On a wider scale, thermal-driven differences in the competences of rocks or units may cause drastic modifications, even to the major crustal structure; Koistinen (1981) and Koistinen et al. (1996) described such effects in the boundary zone of the Archaean domain.

A range of magmatic intrusions and dykes are useful for structural correlation (cf. Sederholm 1926). They are often widespread and intruded into different tectonic domains, thus fixing the structural history of the domains. Intrusive rocks show tectonic structures such as foliation, shear bands or metamorphic mineral assemblages that are often easier to interpreted than those distinguished, for instance, in the complexly deformed pelitic rocks. However, magmatic rocks representing the same event may have different styles of intrusion depending on the local tectonic-metamorphic conditions or emplacement depth.

On the other hand, intrusive rocks and alteration caused by magmatic fluids may obscure and destroy pre-existing structures. Fortunately, early structures may sometimes still be identifiable, although their manifestation has changed. Figures 5a and b show an example of remnant foliation after granitization (cf. Härme 1965) on an outcrop scale. Sometimes only small remnants of original gneisses are preserved in schlieren migmatites (Figure 5c). On a regional scale, the remnants of gneiss belts may remain as narrow remnant chains between or within the intrusive or strongly migmatitic areas. Belts of this kind are often still interpretable from the geophysical data.

Crustal-scale long-wavelength folds, bends and warps (cf. Pajunen et al. 2008) are mostly difficult to observe on an outcrop scale, especially on the flat ice-polished outcrops. Nevertheless, they are significant in analyzing the major characteristics of tectonic units, e.g. the distribution of litho-stratigraphic units, exposures from various crustal depths evident from variations in the metamorphic grade and characters in magmatism, variation of crustal

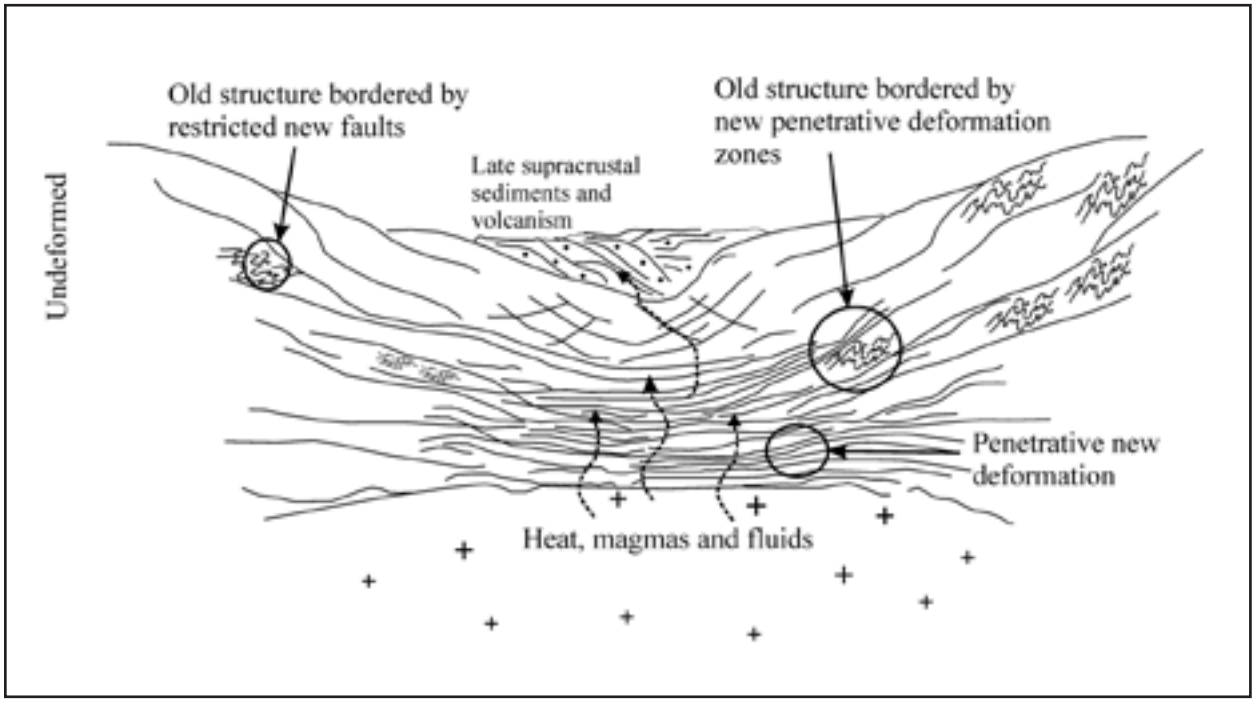

Figure 4. The type of deformation, penetrative or zoned, varies with crustal depth and thermal conditions. For example, the deformation pattern in the extensional event may produce penetratively deformed parts in the crust, where the pre-existing structures are totally destroyed. The less deformed parts of the crust locally show the older deformation structures preserved; depending on the strength of deformation, the directions of the old structures may also be preserved. Near the surface the deformation may, however, show only weak and narrow deformation zones and fault structures that are often overlain by soft sediments.

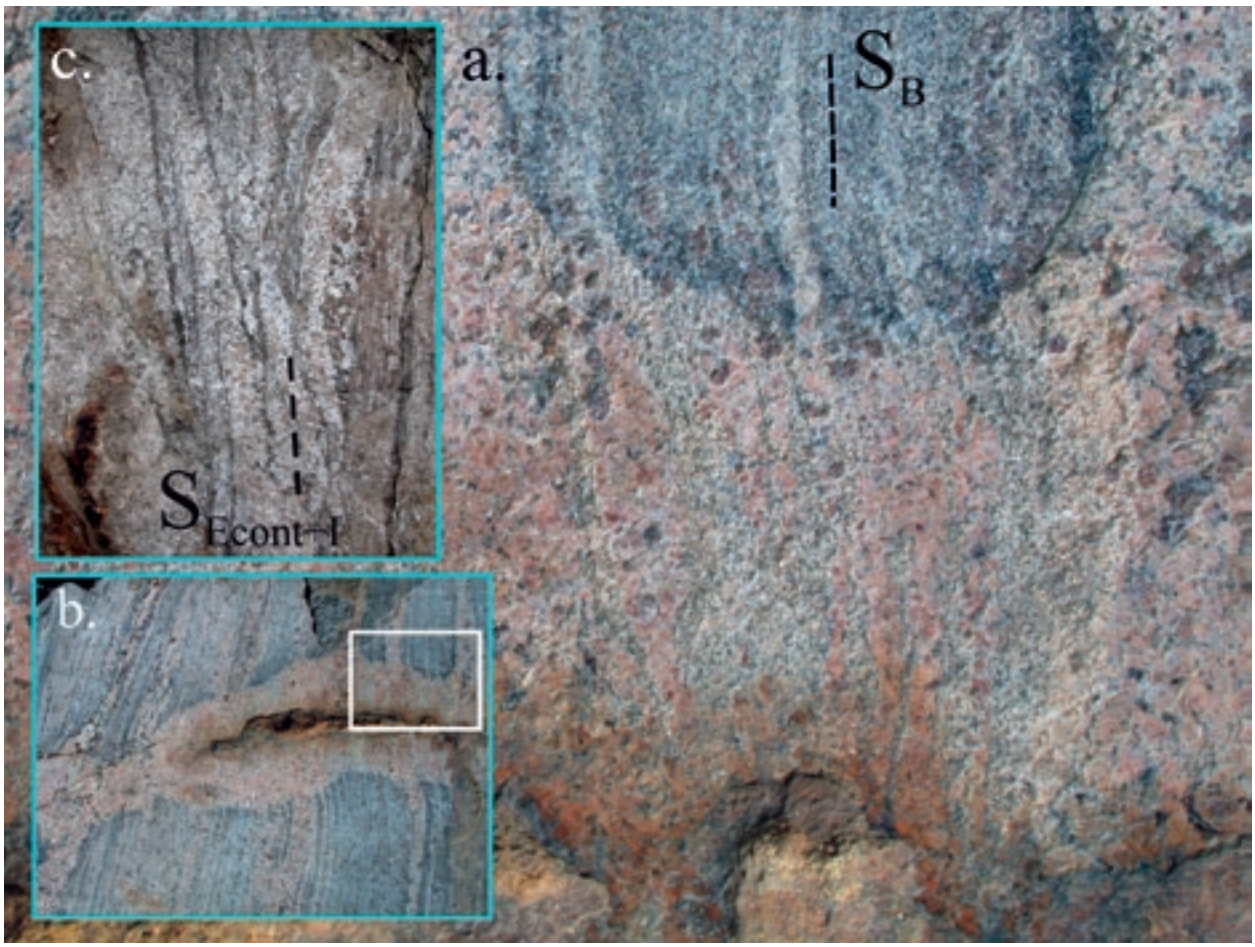

Figure 5. Granitized garnet-bearing mica gneiss in Sipoo (Finnish grid coordinates KKJ2 2568.78E 6695.45N). Figure (a.) shows a detail of the granitization surroundings of the fracture in figure (b.). The pre-existing structure is still visible in the altered gneiss. Width of the area of the figure is c. 1.5 m. (c.) Granitization and melting is almost penetrative in schlieren mica gneiss in Nurmijärvi, Klaukkala (Finnish grid coordinates KKJ2 2542.76E 6696.12N). The pre-existing structure is hardly visible, but the major trends of the gneisses are often preserved and identifiable on geophysical maps. Width of the area of the figure is c. 1 m. Photos by M. Pajunen.

deformation style, and so on. According to several metamorphic studies (e.g. Korsman et al. 1984 and 1999), strong magmatic activity under a high thermal gradient caused a rapid temperature increase downwards during the peak metamorphism in the southern Svecofennian domain. Therefore, the late/post-metamorphic open fold structures and faults have an important effect on the metamorphic configuration on the present-day erosion level, e.g. in antiformal or synformal tectonic settings. The results of these open fold deformations vary depending on the pre-existing structural setting; areas with steep and horizontal structures produce very different patterns, as schematized in Figure 6.

The open structures form a framework into which the earlier structures should be fixed. The small-scale structures are the results of major tectonic processes, but they are often affected by local heterogeneities. Our approach is first to deal with the structures from a regional point of view to reconstruct the tectonic framework in which the detailed study area is located. Our purpose is not to try to explain all the structures caused by local heterogeneities, but to provide a generalized structural framework by describing several examples for further, more detailed analyses (e.g. Hopgood et al. 1983, Hopgood 1984 and Pajunen et al. 2008) that are helpful in resolving local structural problems.

The general structural framework of the Fennoscandian Shield was compiled by using the published geological (e.g. Korsman et al. 1997 and Koistinen et al. 2001), magnetic (Korhonen et al. 2002a), gravity (Korhonen et al. 2002b) and Moho depth (Korsman et al. 1999) maps, and the low- and high-altitude aeromagnetic magnetic data of the Geological Survey of Finland (GTK). By correlating structural information on lithological and magnetic or gravity maps, it is evident that the "post- and late orogenic" magmatic and migmatization events locally effectively reduced or destroyed the early structures of supracrustal belts. Remnants of supracrustal belts are commonly more poorly exposed than granitoids characterizing the geological maps. Even though the pre-migmatization rock was supracrustal in origin, the large granitic component (>50%) determines the rock as granitoid on

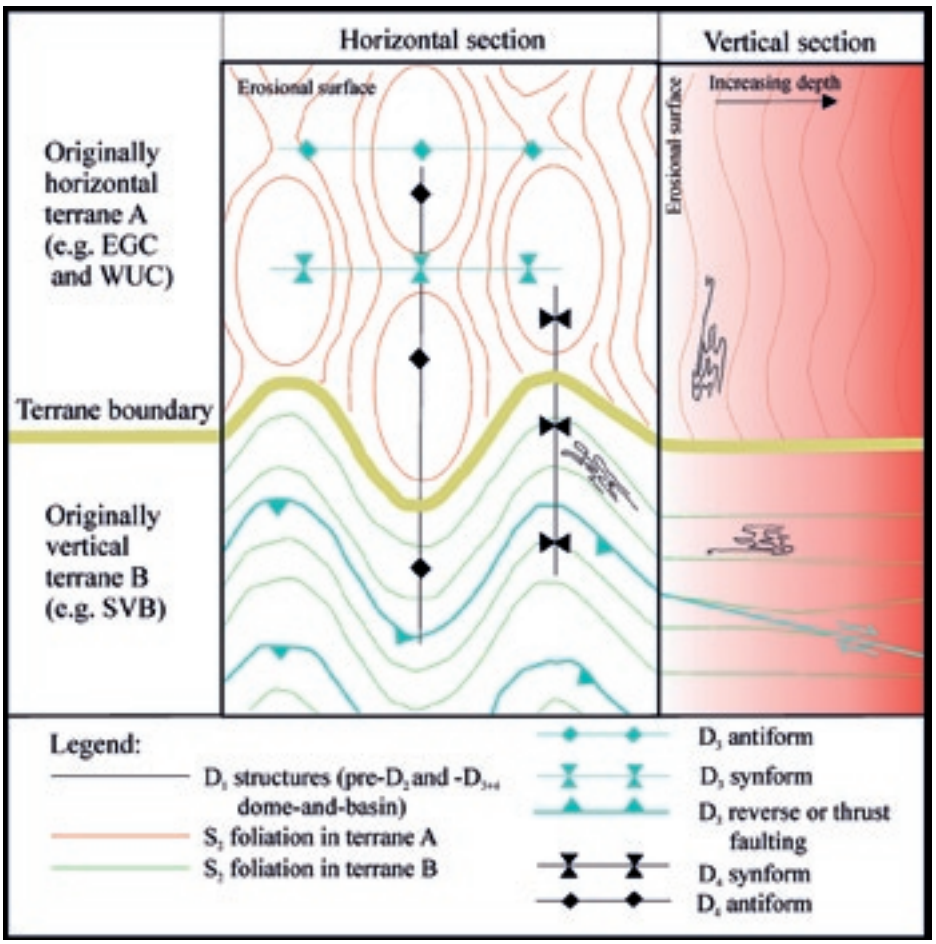

Figure 6. Two generations of open folding in originally steeply and horizontally deformed areas in horizontal and vertical sections. The characters of the deformation structures and the regional pattern vary between tectonic units. The structural analysis thus demands careful correlation of structures with metamorphic and magmatic events. $D_{1, 2, 3...}$ refer to successive deformation events and the abbreviations (EGC = Espoo Granitoid Complex, WUC = West Uusimaa granulite Complex and SVB = Southern Finland Volcanic-sedimentary Belt) exemplify the units in the study area (see Figure 1).

the lithological maps of GTK. Thus, we suggest that the relic geophysical signatures, indicating the pre-magmatic/migmatization structural trends of the belts, are often still identifiable. The structural interpretations represented here are based on these assumptions.

As discussed previously, the problems in analysing the succession of tectonic structures are multiple. The structural events of this study are not directly consistent with the previously published descriptions, because some structures identified in the study area are missing as such in the other domains, or the way structures are interpreted differs. To avoid confusion while keeping doors open for later modification, we label the structures as follows. The structures formed by the first identified regional deformation phase D_A are F_A = folding, S_A = foliation or axial plane, L_A = lineation and M_A = metamorphism; the second, respectively, D_B, F_B, S_B, L_B, M_A; the third D_C, F_C, S_C, L_C, M_A… The bedding is termed S_0. When discussing or referring to the earlier published results, we follow the labels applied by the previous authors. The naming of structures follows a regional scheme: the earliest structure in a late rock series is named according to the regional structural succession. For example, the foliation S_E in older sequences may represent the first foliation in a sequence formed later; we also label it as S_E. We prefer this solution because the structures in both the old and the young series are related to the same tectonic event. Such naming requires the identification of key features such as regional folding, characteristic foliation or dated magmatic rocks (volcanic/intrusive) that enable correlation. Difficulties arise in naming structures formed during continued transcurrent events comprising simultaneous shortening/contraction (labelled e.g. $D_E$cont), dilatation/extension (labelled e.g. $D_E$ext), which overprint during progressive deformation. In the descriptions we primarily follow the overprinting relations on outcrops.

The field structures are then assigned to regional major geotectonic events labelled Event 1 – E_1, Event 2 – E_2, Event 3 – E_3…

Pre-existing geological data

Structural domains and tectonic formlines were constructed using structural field data, tectonic elements from geological maps and the digitalized geological data sets of the Geological Survey of Finland (GTK). The following geological bedrock maps of scale 1:100 000 were used: 2013 (Jussarö, Laitala 1973b), 2014 (Tammisaari, Koistinen 1992), 2023 (Suomusjärvi, Salli 1955), 2024 (Somero, Simonen 1955 and 1956), 2032 (Siuntio, Laitala 1960), 2034 (Helsinki, Laitala 1967 and 1991), 2041 (Lohja, Laitala 1994), 2042 (Karkkila, Härme 1953), 2043 (Kerava, Härme 1969), 2044 (Riihimäki, Kaitaro 1956), 2113 (Forssa, Neuvonen 1954), 2131 (Hämeenlinna, Simonen 1949), 2133 (Kärkölä, Lehijärvi 1961), 3012 (Pellinki, Laitala 1965), 3021 (Porvoo, Laitala 1964), 3022 (Lapinjärvi, Laitakari & Simonen 1962 and 1963), 3023+3014 (Kotka, Simonen & Laitala 1970), 3024 (Karhula, Simonen 1965), 3111 (Lahti, Lehijärvi 1964), and 3113 (Kouvola, Simonen & Lehijärvi 1963).

The majority of the maps are old; at the time of their production, modern tectonic study methods were just being developed. Generally, the main foliations on outcrops are shown on the maps. The foliation trends in Figure 7 were constructed by combining several foliation measurements with average dip values. Each trend line represents the foliation trend inside a certain lithological unit. Without familiarity with the tectonic and magmatic history of the rock it is not possible in most cases to identify the deformation event that produced the depicted foliation. According to our observations, especially the horizontal structures, which seem to characterize wide areas of southern Finland, are underestimated on the maps. For example, the dome-and-basin structures that characterize the magnetic maps are difficult to construct from these tectonic elements. Similar problems arose when dealing with fold axes (which fold phase?) and lineations (stretching or intersection lineation, or slicken line striation?). According to our experience, most granitic areas show measurable foliations on outcrops, but these are not shown on the maps.

Magmatic processes are important when interpreting the tectonic evolution of the crust. In southern Finland, different types of granitoids are not sufficiently classified and outlined on the maps. Their composition and amount of strain vary from foliated tonalites to weakly-deformed granites and, finally, to non-deformed pegmatitic granites and even migmatitic mica gneisses. Therefore, the regional distribution of various granitoids can only be discussed in a very general sense.

Aerogeophysical data

The field observations on outcrops mostly show the structures on a “miniature” scale. The magnetic data were useful for the regional tectonic analyses. Wide areas only show small variations in the intensity of the magnetic field. In such areas, different methods of processing the aeromagnetic data were used for detailed analyses; the methods are described in detail in Airo (1999) and Airo et al. (2008). Topographic maps were often useful in constructing the regional structures. They were informative in granitoid dominant areas, which were homogeneous in the geophysical data, but clearly show structural trends in the topographic patterns. Geophysical interpretations were confirmed by detailed field observations on the key outcrops.

Aeroradiometric data were used in estimating the distribution of some late magmatic events (Th/U ratio). The use of radiation data is limited, because it often reflects the soil properties or radiation may be buffered in lakes and swamps. The non-geological noise diminishes the usefulness of aeroelectromagnetic data. Regional gravity data with a 5 km and a denser grid of 250 m collected by the Geodetic institute and by the Geological Survey of Finland (GTK) were of benefit in analyzing wide-scale structures, unit boundaries and crustal fracture zones.

Geochronology

The major tectonic events are dated using the U-Pb TIMS and SIMS methods. Samples were fixed to the successive structural and magmatic events observed in the field. The dating methods and results are provided in Appendix 8. The ages for the rocks that are structurally fixed into tectonic evolution are presented in App-Table 3.

Figure 7. Lithology and foliation trends in the study area. Foliation trends are compiled using the bedrock maps on the scale 1 : 100 000 of GTK. Ev = Evitskog, Ka = Kauklahti, Ko = Kopparnäs and Sf = Sarfvik. Base map © National Land Survey of Finland, permit No. 13/MML/08.

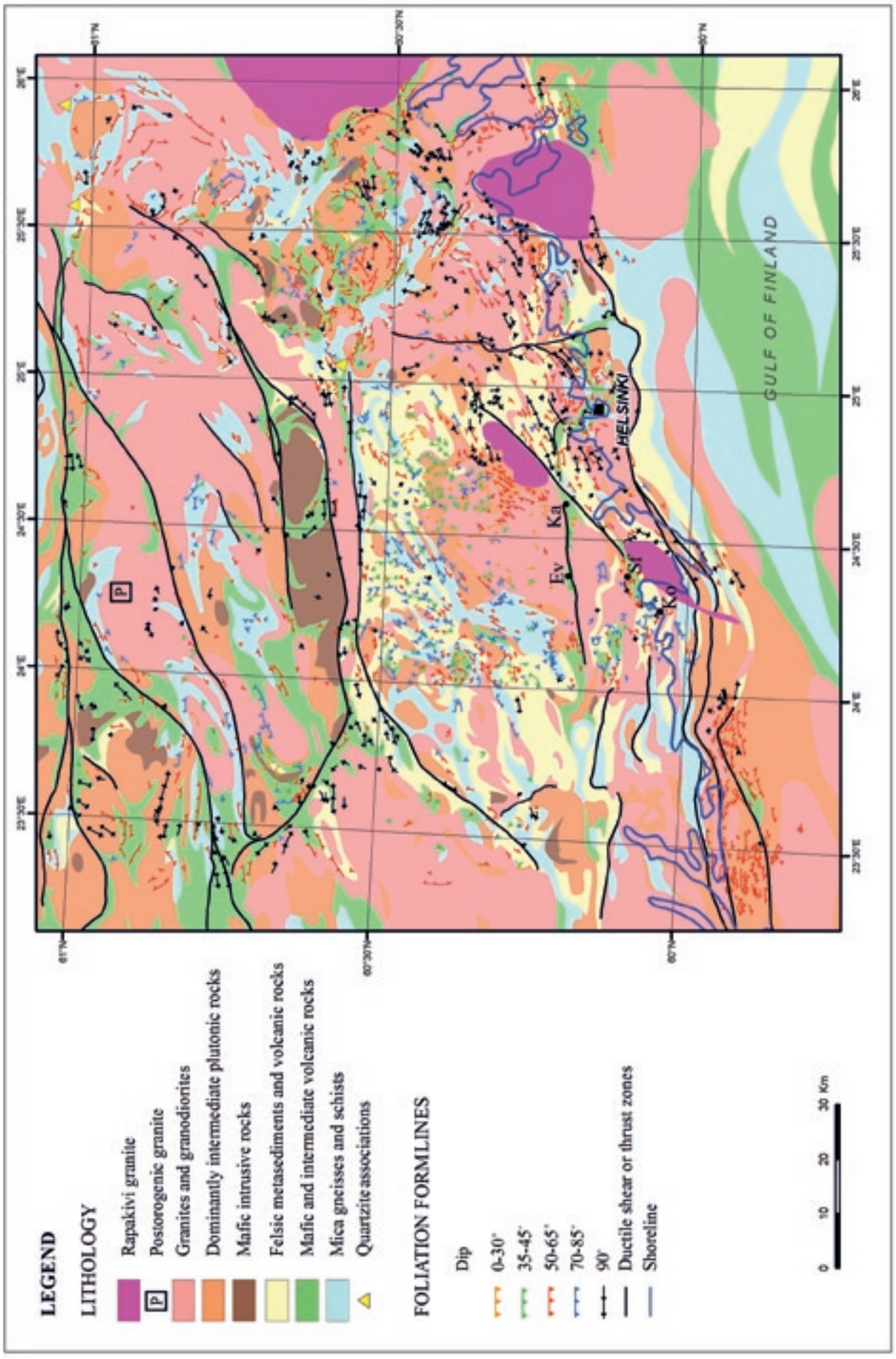
LEGEND
LITHOLOGY
Rapakivi granite
Postorogenic granite
Granites and granodiorites
Dominantly intermediate plutonic rocks
Mafic intrusive rocks
Felsic metasediments and volcanic rocks
Mafic and intermediate volcanic rocks
Mica gneisses and schists
Quartzite associations
FOLIATION FORMLINES
Dip
0-30°
35-45°
50-65°
70-85°
90°
Ductile shear or thrust zones
Shoreline
0 10 20 30 Km
GULF OF FINLAND
HELSINKI
Ka
Ev
Sf
Ko
P
61°N
60°30'N
60°N
23°30'E
24°E
24°30'E
25°E
25°30'E
26°E

TECTONIC FRAMEWORK OF THE STUDY AREAS IN THE SOUTHERN FENNOSCANDIAN SHIELD IN FINLAND

The lithology and timing of major tectonic events of the Fennoscandian Shield are represented on the geological map of Koistinen et al. (2001). Recently, Lahtinen et al. (2005) compiled a tectonic model for the shield. Relating the local structures in the study areas to structural evolution on the crustal scale first requires the determination of their setting in the structural framework of the southern Fennoscandian Shield in Finland.

The Archaean and Svecofennian domains can be divided into different tectonic units using major tectonic boundaries, shear/fault zones of varying origin. The southern Svecofennian domain of the Fennoscandian Shield is divided into c. N-trending tectonic units along the eastern margin of the Transscandinavian Igneous Belt (TIB, see Högdahl et al. 2004) in Sweden, the deformation zones from the southern Baltic Sea to the eastern coast of the Bothnian Bay (Baltic Sea-Bothnian Bay Zone, BBZ) and from Riga Bay, Lithuania, to the Vyborg rapakivi and to Karelia in southeastern Finland (Riga Bay-Karelia Zone, RKZ). These deformation zones are shown on the magnetic map of Korhonen et al. (2002a) (Figure 8).

The Transscandinavian Igneous Belt (TIB) is dominated by magmatism that overprints the earlier

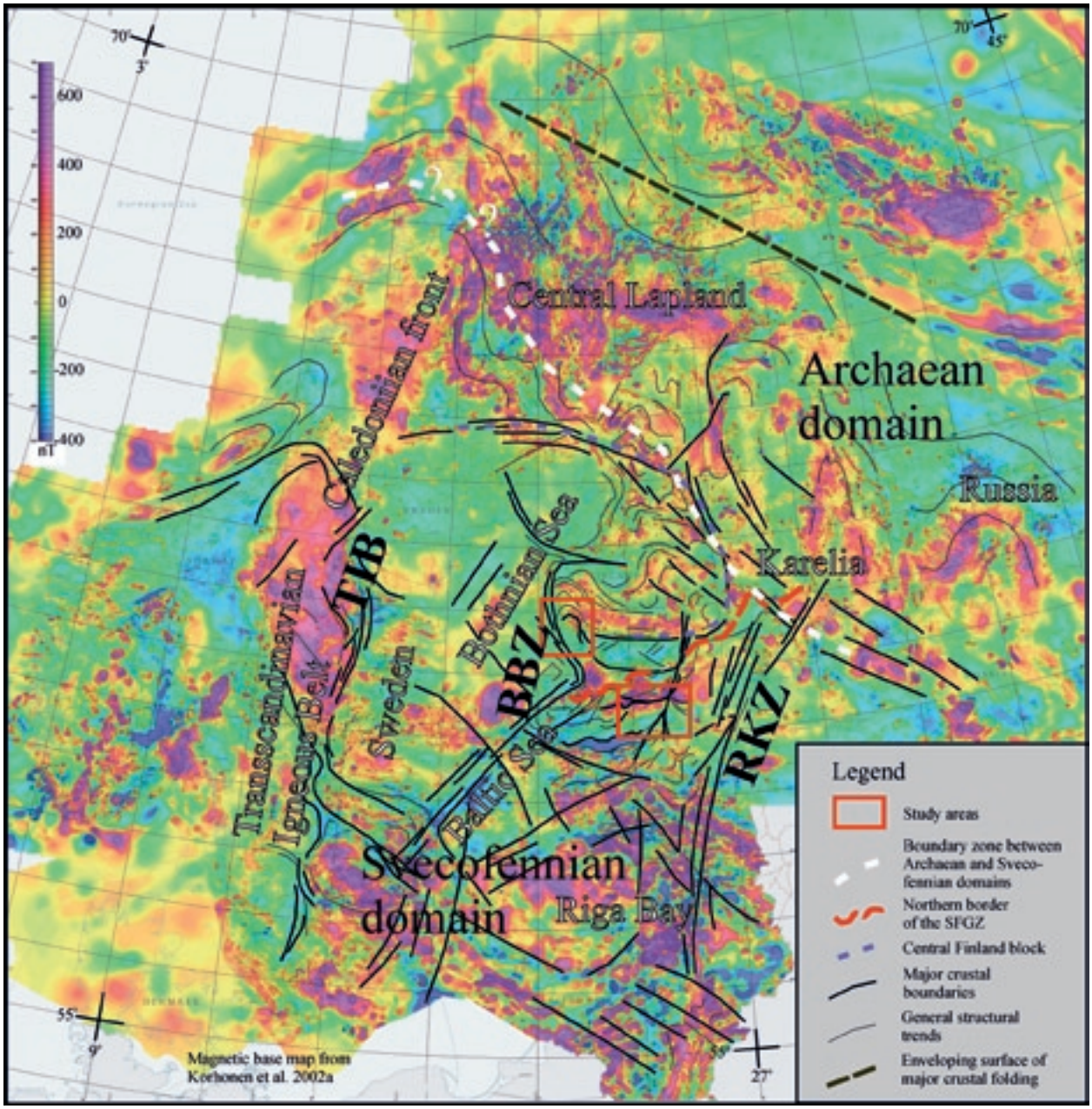

Figure 8. The major crustal structures and domains of the southern Fennoscandian Shield on the magnetic map of Korhonen et al. (2002a). BBZ = Baltic Sea-Bothnian Bay Zone, RKZ = Riga Bay-Karelia Zone and TIB = Transscandinavian Igneous Belt.

Svecofennian structural trends. The age of the TIB magmatism ranges from 1.85 to 1.65 Ga (Högdahl et al. 2004). The oldest granitoids are situated in the eastern margin of the belt (Koistinen et al. 2001). A c. N-trending deformation zone characterizes the TIB. To the east of the zone the structural trend is bent from c. WNW to NW due to a crustal-scale dextral drag of the earlier structures. The magnetic anomalies are weaker below the Caledonian front to the west of the TIB, where the large-scale crustal bend shows a NNE-trending axial trace (Figure 8). According to Bergman et al. (2006), the so-called Storsjön-Edsby Deformation Zone is a dextral transpressional zone that was active in the time interval of c. 1.7–1.3 Ga.

The Baltic Sea-Bothnian Zone (BBZ) is exposed in its northernmost part in the Pori area. The structural characteristics established from the magnetic pattern supports the more ductile deformation in the northern part (ductile bended shear zones) of the BBZ than in its southern parts (more sharply cutting faults). The Pori area is characterized by NNW-trending crustal blocks, e.g. the Pomarkku block (Po in Figure 9) (Pietikäinen 1994 and Pajunen et al. 2001a), that are bordered by the major sinistral NNW-SSE-/N-S-trending Kynsikangas shear/fault zone in the west and the dextral shear zones like the Kankaanpää shear zone in the east (Figure 10). A similar block structure is exposed towards the north up to the Vittinki zone, and is also characteristic in the east, in the Central Finland Granitoid Complex (CFGC) (Figures 9 and 10). The northern end of the BBZ is located in the Vaasa area (Va in Figure 9) along the Vittinki shear/fault zone (Figure 10). According to Rutland et al. (2004), the Vaasa area was pushed into its present setting from the WNW.

In its southern parts, in the Paleozoic area of the Baltic countries, the Riga Bay-Karelia Zone (RKZ) appears as sharp faults. It disappears in the Vyborg rapakivi massive area and forms a complex, ductile structural pattern to the north and northeast of the rapakivi intrusion. The crustal segment between the BBZ and RKZ in southern Finland is characterized by large-scale warping with a c. N-trending axial plane. Closer to the BBZ and RKZ zones the folds become tighter and the major shear and fault zones parallel to the axial planes of the folds (see also Lindroos et al. 1996). The detail study area is situated in the western branch of the RKZ. The area is characterized by wide-scale open to tight folding with a c. N-trending axial plane paralleling the Vuosaari-Korso shear/fault zone (Figure 10).

An ENE-trending belt of late Svecofennian granitoids, the Southern Finland Granitoid Zone (SFGZ), characterizes the southern study area. The major crustal N-trending deformation zones, the Riga Bay-Karelia Zone (RKZ) and Baltic Sea-Bothnian Zone (BBZ), deform the SFGZ.

STRUCTURAL UNITS IN THE SOUTHERN SVECOFENNIAN DOMAIN

The southern Svecofennian domain is composed of several tectonic units showing varying depositional, tectono-metamorphic and magmatic characteristics (Figure 9). The shapes of the units are determined by wide-scale folding and faulting patterns, and by the competences of rock and tectonic units during deformation. The major crustal high-strain and fault/shear zones and stacked zones/units are indicated in Figure 10. Naturally, this kind of division is somewhat artificial; the units often show features in common or they may simply represent corresponding rocks from different crustal depths. In fact, the division should be carried out in three dimensions constrained in time; an ambitious challenge only shortly assessed here.

The study areas are situated in the major tectonic units of the Granite Migmatite Belt (GMB) and Tonalite Migmatite Belt (TMB). Our observations are from key outcrops in the Southern Volcanic-sedimentary Belt (SVB), West Uusimaa granulite Complex (WUC), Hyvinkää Gabbroic-volcanic Belt (HGB), Jokela supracrustal association (Jo in Figure 9) and the Espoo Granitoid Complex (EGC). We place the main emphasis on the EGC, because it excellently shows the wide variation in magma phases, and on the SVB, which was preserved from the intense magmatism of the EGC. Supracrustal rocks within the EGC show characteristics similar to those in the SVB and WUC. The HGB represents a tectonic slice lying upon the EGC and WUC. The Jokela supracrustal association is a late sedimentary-volcanic sequence. These units include the majority of the lithological and structural characteristics important in constructing the tectono-metamorphic and magmatic scheme for the southernmost Svecofennian domain.

The Hämeenlinna shear/fault and the stacked zone north of it border the Granite Migmatite Belt (GMB) against the Tonalite Migmatite Belt (TMB). The stacked slices of the GMB are NW-trending in the west and N- and NE-trending in the east (Figure 10). The western end of the TMB-GMB discordance was mapped later by Korsman et al. (1997). The general structural trend of the TMB is E-W, but it is

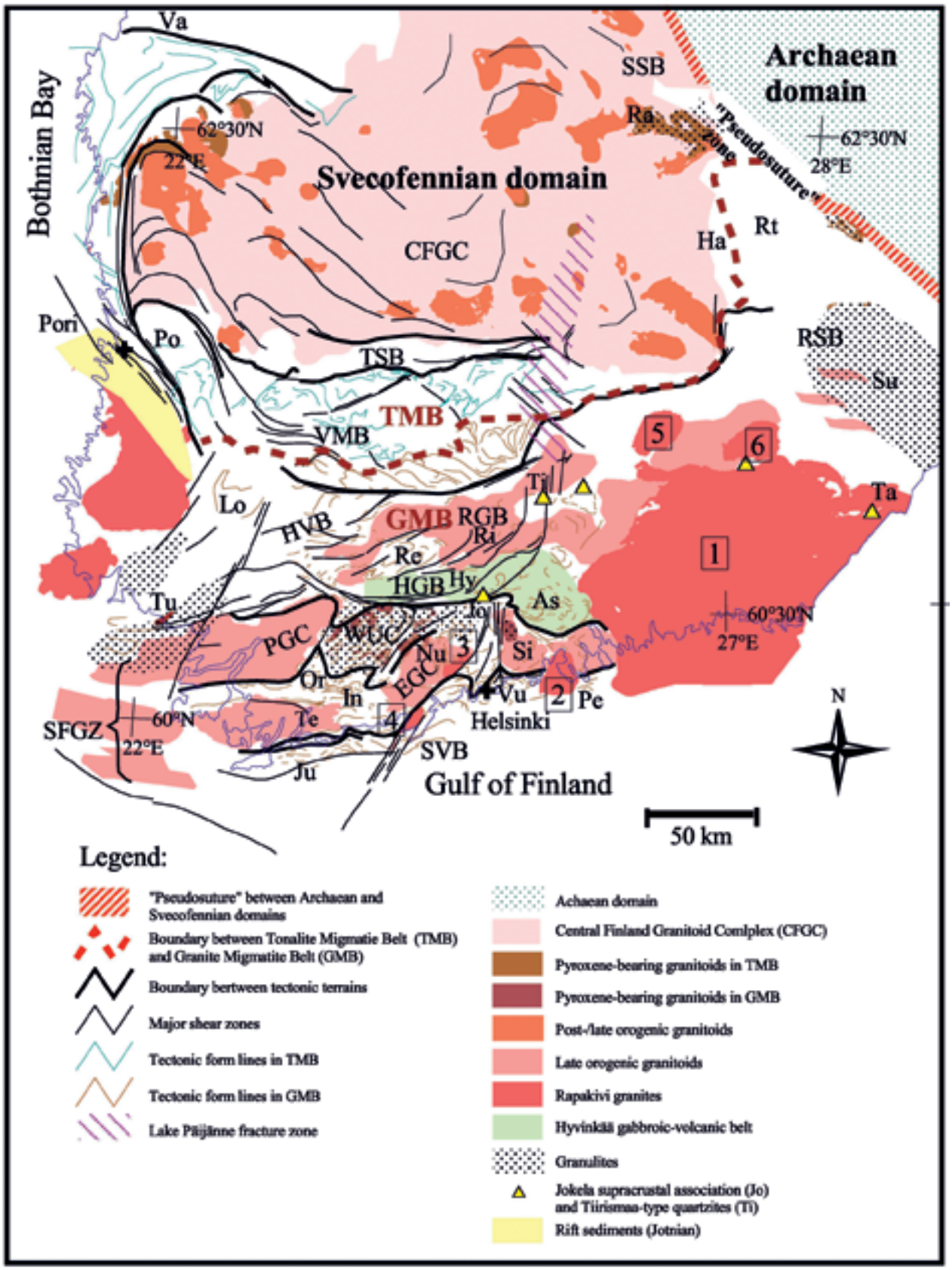

Figure 9. Geotectonic units in southern Finland. Abbreviations: SFGZ = Southern Finland Granitoid Zone, CFGC = Central Finland Granitoid Complex, TMB = Tonalite Migmatite Belt, GMB = Granite Migmatite Belt, SSB = Savo Schist Belt, RSB = Rantasalmi-Sulkava area/Belt, TSB = Tampere Schist Belt, VMB = Vammala Migmatite Belt, HVB = Häme Volcanic Belt, HGB = Hyvinkää Gabbroic-volcanic Belt, WUC = West Uusimaa granulite Complex, SVB = Southern Volcanic-sedimentary Belt, EGC = Espoo Granitoid Complex, RGC = Riihimäki Granitoid Complex, PGC = Perniö Granitoid Complex; Po = Pomarkku block, Nu = Nuuksio area, Va = Vaasa area, Lo = Loimaa area, Tu = Turku area, Re = Renko area, Pe = Pellinki area, In = Inkoo area Or = Orijärvi area, Ju = Jussarö area, Vu = Vuosaari area, Hy = Hyvinkää area, As = Askola area; Jo = Jokela supracrustal association, Ti = Tiirismaa quartzite, Rt = Rantasalmi area, Su = Sulkava area, Ra = Rautalampi area, Ha = Haukivuori area, Ta = Taalikkala "roof pendant"; rapakivi granites: 1 = Vyborg, 2 = Onäs, 3 = Bodom, 4 = Obbnäs, 5 = Ahvenisto and 6 = Suomenniemi. Base map © National Land Survey of Finland, permit No. 13/MML/08.

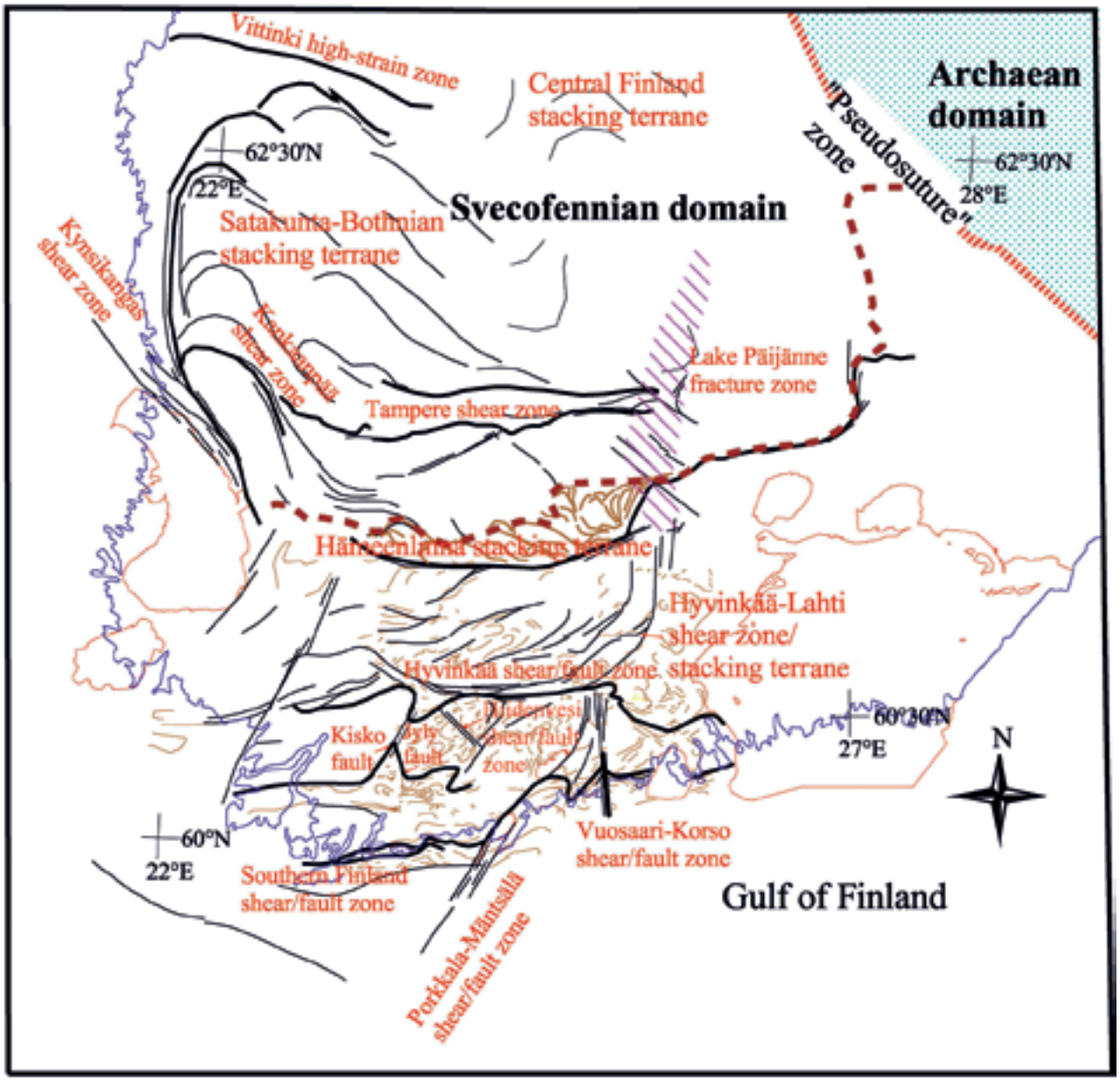

Figure 10. Major unit boundaries, shear and fault zones, in Southern Finland. Base map © National Land Survey of Finland, permit No. 13/MML/08.

bent towards the NW in the Pori area (e.g. Pomarkku block, Po in Figure 9) and reoriented into the N-NW trend near the Archaean-Proterozoic border zone in the east (e.g. Koistinen et al. 1996 and Korsman et al. 1997). The lower-grade Tampere Schist Belt (TSB) is bordered by the TMB in the south and by the Central Finland Granitoid Complex (CFGC) in the north. The CFGC is characterized by crustal-scale NW-stacked structures (Figures 8 and 10). The structural characteristics of the northern units, the Central Finland Granitoid Complex (CFGC), Vammala Migmatite Belt (VMB), Hämeenlinna Volcanic Belt (HVB), Tampere Schist Belt (TSB), Rantasalmi-Sulkava area (RSB) and Savo Schist Belt (SSB) are briefly discussed.

The volcanic and sedimentary sequences of the Southern Volcanic-sedimentary Belt (SVB) in southernmost Finland form continuous E-trending belts ranging from the southwestern archipelago (e.g. Ehlers & Lindroos 1990) to the Inkoo (e.g. Eskola 1914, Sederholm 1926, Hopgood 1984, Bleeker & Westra 1987 and Kilpeläinen & Rastas 1990) and Pellinki areas (e.g. Sederholm 1923 and Laitala 1973a and 1984) (Figure 9). The SVB is cut and bent by the Porkkala-Mäntsälä and Vuosaari-Korso shear/fault structures (Figure 10) (Elminen et al. 2008). Psammitic-pelitic metasediments with carbonaceous interlayers, various felsic gneisses and mafic to intermediate volcanic rocks characterize the SVB supracrustal lithology. Generally, the rocks are migmatitic and intruded by the later granitoids. The pelitic layers are intensely affected by melting. Felsic gneisses are felsic volcanic rocks, psammitic metasediments or, locally, even deformed granitoids; mostly the related rock associations give reference to their origin. Non-migmatitic, amphibolite

facies areas such as in the Pellinki (Pe in Figure 9) (Laitala 1973a and 1984), Orijärvi (Or in Figure 9) (e.g. Eskola 1914, 1915 and Tuominen 1957) and Vuosaari areas (Vu in Figure 9) clearly show the primary features like bedding, pillow lava, amygdale and porphyric structures. The Orijärvi area is characterized by Zn-Cu-Pb ores, associated with altered rocks such as coarse-grained cordierite-anthophyllite rocks (Eskola 1914 and 1915), and skarn-iron ores, iron formations (e.g. Eskola 1914, Latvalahti 1979 and Saltikoff et al. 2002) and carbonate rock horizons (Bleeker & Westra 1987 and Reinikainen 2001), indicating a shallow-water depositional environment. Väisänen and Mänttäri (2002) proposed a back-arc basin origin for the volcanogenic rocks and divided them into two sequences at c. 1.90–1.89 Ga and c. 1.88–1.87 Ga; in the following they are referred to as volcanic Series I and II, respectively. The Orijärvi granodiorite was interpret as syngenetic with the earlier volcanic sequences (Väisänen & Mänttäri 2002). Hopgood et al. (1976 and 1983) and Hopgood (1984) described gabbroic-tonalitic associations from the Jussarö-Skåldö area (Ju in Figure 9): mafic magmatic series have the same age as the early volcanism (Hopgood et al. 1983).

The granulite-facies West Uusimaa granulite Complex (WUC) (Eskola 1914, 1915 and Parras 1958) is exposed between amphibolite-facies gneisses and granitoid complexes. It is sharply bordered by the Hyvinkää high strain zone in the north (Figures 9 and 10) against the Hyvinkää Gabbroic-volcanic Belt (HGB). Lithologically, the WUC represents the granulite-facies counterpart of the Southern Volcanic-sedimentary Belt (SVB) and the Espoo Granitoid Complex (EGC) rocks (e.g. Eskola 1914, 1915, Parras 1958, Schreurs & Westra 1986 and Kilpeläinen & Rastas 1990); the occurrence of orthopyroxene- and two-pyroxene-bearing assemblages is characteristic. Small granulite remnants overprinted by retrograde parageneses occur in the central Sipoo area (Si in Figure 9).

The Hyvinkää Gabbroic-volcanic Belt (HGB) has a complex internal structure and is squeezed between the Hyvinkää shear/fault zone and the sheared structures bordering the Renko area (Re in Figure 9). The Hyvinkää-Lahti shear zone, in the continuation of the combined Porkkala-Mäntsälä and Vuosaari-Korso shear/fault zones, continues further north to the Päijänne fracture pattern, already described by Sederholm (1932b) (Figures 9 and 10). The Hyvinkää-Lahti shear/fault zone separates the Hyvinkää unit of the HGB (Hy in Figure 9) from the eastern Askola unit (As in Figure 9). Large layered gabbro massifs and supracrustal sequences characterize the western part. Volcanic rocks and mica gneisses locally show primary features such as bedding, agglomerate and pillow lava structures. Roundish dome-and-basin structures with gabbroic-volcanic rock associations squeezed between the domes typify the eastern part. The dome interiors are composed of granodioritic-tonalitic intrusive rocks and migmatitic mica gneisses.

The supracrustal Jokela association (Jo in Figure 9), including quartzites similar to those in Tiirismaa (Ti in Figure 9) (Lehijärvi 1964), is exposed near Hyvinkää. The association shows a depositional succession composed of sedimentary and volcanic sequences. It is important in establishing the regional structures and metamorphism because of its young depositional age dated by Lahtinen et al. (2002) using detrital zircons.

The ENE-trending Southern Finland Granitoid Zone (SFGZ) cuts the structural trend of the Granite Migmatite Belt (GMB) and is thus tectonically differentiated from the GMB. It also penetrates the Archaean domain. The southern belt, from Tenhola (Te in Figure 9) to Nuuksio (Nu) and Sipoo (Si), is here referred to as the Espoo Granite Complex (EGC) (Figure 9). It is cut by the Vyborg rapakivi (1 in Figure 9) massive in the east. The northern zone, the Riihimäki Granite Complex (RGC), extends ENE to the Rantasalmi-Sulkava area (RSB) and the Archaean domain, up to the Riga Bay-Karelia Zone (RKZ). In the west, the Perniö Granite Complex (PGC) continues from the Kisko fault (Figure 10) to Turku. According to our limited observations, the lithology and structural settings of the Perniö (PGC) and Riihimäki Granite Complexes (RGC) are quite similar to that of the Espoo Granitoid Complex (EGC) (cf. Ehlers et al. 1993 and Lindroos et al. 1996). Rämö et al. (2004) described some geochemical differences between the northern (Nz in Figure 1) and southern granitic units (Sz in Figure 1).

The Espoo Granitoid Complex (EGC) covers a significant part of the detailed study area. Its contacts with the supracrustal associations of the Southern Volcanic-sedimentary Belt (SVB) are generally tectonic, e.g. along the Southern Finland shear/fault zone (cf. Koistinen et al. 1996). The EGC is bordered in the north along low-angle shear zones with the granulitic West Uusimaa granulite Complex (WUC), which, according to tectonic observations, underlies the EGC. The observation is supported by the continuation and weakening of the magnetic anomalies of the WUC below the EGC. Felsic and intermediate intrusive rocks characterize the EGC. Gneissic tonalites were intruded and migmatized by later granites; thus, many rocks shown as granitic-granodioritic on the geological maps were originally more tonalitic in composition. Gabbroic rocks occur as restricted intrusions or fragments within granitoids. Intermediate and to a lesser extent mafic

dykes form important reference features in analyzing the deformation scheme. We have not studied the lamprophyre dykes described by Eskola (1954) and Suominen (1997); the first one is situated in the courtyard of a prison and the other in a wastewater tunnel in Helsinki.

The Palaeo- to Mesoproterozoic rapakivi granites and related diabase dykes cut the rocks of the Espoo Granitoid Complex (EGC) and the Southern Volcanic-sedimentary Belt (SVB) in a semi-ductile to brittle manner. The names of the rapakivis in the study are given in Figure 9. Diabase dykes form at least two sets of dykes that are c. WNW- and NW-trending; some dykes showing a W trend may be related to a younger dyke group (Mertanen et al. 2008). Near the Vuosaari-Korso shear/fault zone occur penetratively-altered diabase dykes showing ghost-like blasto-ophitic structure. Some diabase dykes intruded close to the erosion level and rapidly cooled, as evidenced by their shock-like and chilled microstructures.

The over 600 m thickness of the Mesoproterozoic sandstone and related mafic laccoliths (Kohonen et al. 1993) in the fault-bounded basin in the Pori area (Figure 11) also indicates that late brittle movements distinctly modified the crustal structure (Pajunen et al. 2001a). The movements must have been even larger than is estimated from the thickness of the very low-grade sandstone sequence, because the recent cross-section represents a locally ductiley drag-folded section. Late NW-trending normal fault structures exist in the study area (Elminen et al. 2008); their effect on the metamorphic pattern is still an open question.

OVERVIEW OF STRUCTURES IN THE STUDY AREA

A two-stage thermal evolution of the southern Svecofennian domain has been established in several studies since the interpretations of Sederholm (1926) and Korsman et al. (1984). However, the data of Pajunen et al. (2002) demonstrated that the tectonic evolution is more complex. In order to follow the structural succession, we provide a short overview prior to the descriptions. The early structures, D_A-D_D, deformed the early supracrustal sequences and magmatic rocks. The high- to medium-grade horizontal structure, predominantly D_B, was folded into tight, ellipsoidal dome-and-basin patterns, D_{C+D} (Figure 11) with an originally c. E-trending longitudinal axis. A complex series of dilatational to contractional structures followed the D_A-D_D. We label the earliest dilatational and flat-lying structures as D_E, and related intrusive rocks are divided into early, mid- and late D_E phases according to their relationships to the successive magmatic sequence. The D_E structures were followed by structures formed by N-S-shortening D_G and later NW-SE shortening D_H, which was accompanied by strong granitic magmatism. D_F deformation appears as E-W-contractional structures that caused major block movements in the northern Svecofennian domain in eastern Finland; it was simultaneous with the D_E in the south, where only local shear zones are related to this deformation. The large-scale warping with N- to NNE-trending steep axial planes has deformed all the earlier structures and is labelled as D_I. The post-Svecofennian structures, e.g. those related to the rapakivi event, are generalized as D_P structures.

WIDE-SCALE FOLD STRUCTURES – FRAMEWORK FOR DETAILED STRUCTURAL ANALYSIS

The thermal gradient was high during Svecofennian evolution (Korsman 1977 and Korsman et al. 1984 and 1999). It caused rapid changes in metamorphic conditions with depth. This had an important effect on regional variation in metamorphic grade, magma production and the characters of tectonic structures. In the southern Svecofennian domain the late, wide-scale folding and warping structures (D_G, D_H and D_I) substantially modified the tectonic geometry. These structures also deformed the magmatic rocks of the Southern Finland Granitoid Zone (SFGZ), although to varying extents. The regional-scale open fold or warp structures with unpretentious axial plane properties are generally difficult to identify on outcrops. However, the interference structures formed a wide synform-antiform pattern that is clearly visible on lithological, tectonic (Figures 7 and 11) and magnetic maps. This interference pattern is accompanied by major shear and fault zones (Figure 10) and determines the recent regional distribution of lithological, structural and metamorphic units in the southern Svecofennian domain (Figure 11). The folds are therefore described prior to the older structures.

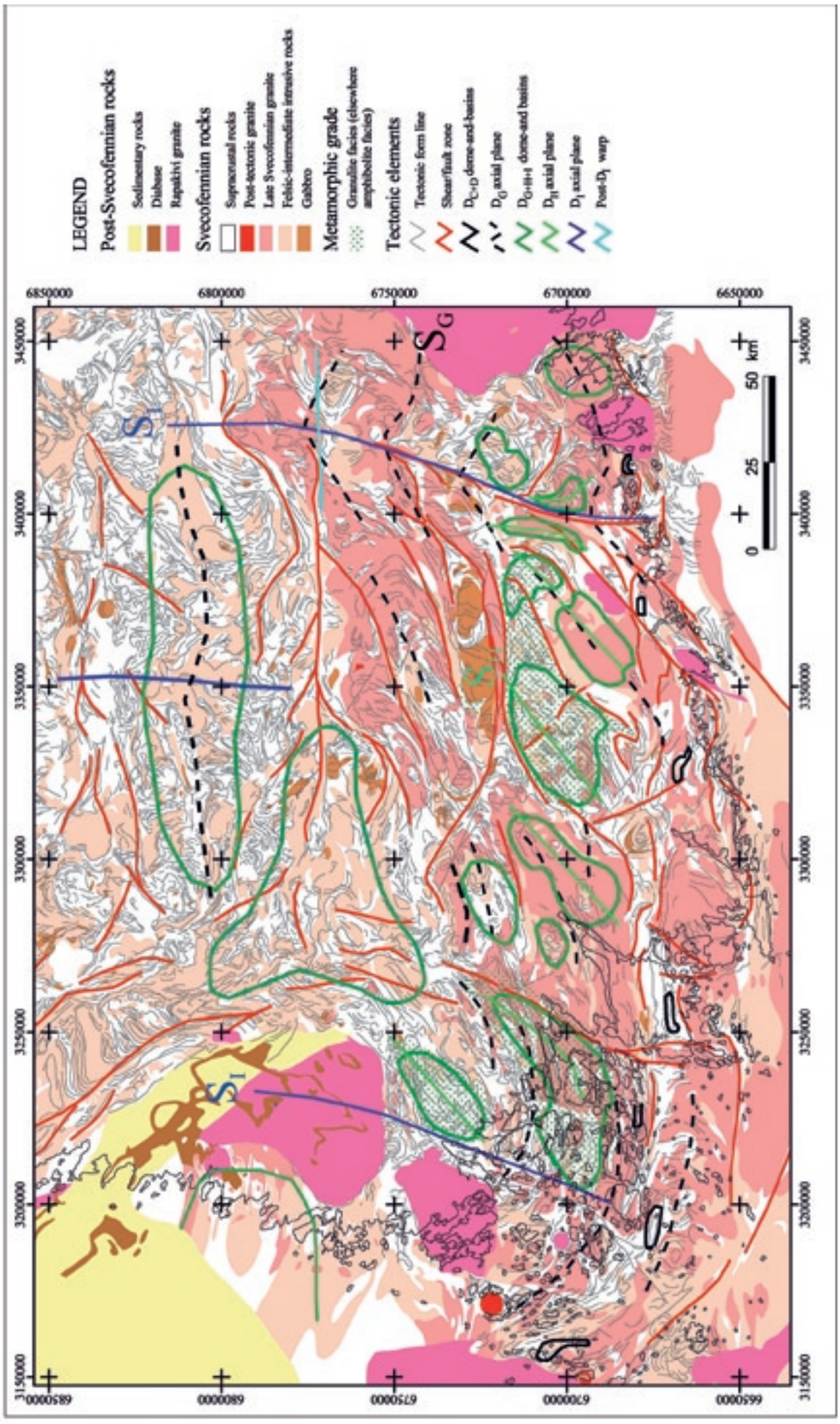

Figure 11. Large-scale fold structures and tectonic formlines in southern Finland. The formlines are constructed predominantly by using magnetic and structural element data of the Geological Survey of Finland (Finnish grid coordinates KKJ3). Base map © National Land Survey of Finland, permit No. 13/MML/08.

Open folds with E-trending axial planes (F_G)

Originally open folds and warps (F_G), with an approximately vertical E-trending axial planes, indicate N-S shortening of the crust. On the present-day erosion level these folds determine the distribution of the E-W-trending granitoid-dominant complex, such as the Espoo Granitoid Complex (EGC) and Riihimäki Granitoid Complex (RGC), and the earlier supracrustal-magmatic units (Figure 11). This fold structure, together with the regional folds with NE-trending axial planes (F_H), determines the large-scale NE-trending dome-and-basin pattern characterizing the study area; the exposure of the West Uusimaa granulite Complex (WUC) and granitoid areas southeast of it, provides a good example. These folds are seldom identified on an outcrop scale.

Open folds with NE-trending axial planes (F_H)

Large-scale folds with NE-trending axial planes (F_H) (Figure 11) are constructed in Figures 12a and b from magnetic and gravity data. Up to 3 km for the amplitude and c. 8 km for the wavelength of the folding can be estimated. The axial plane estimated from field observations and the magnetic anomaly pattern is NE-trending, indicating NW-SE shortening. The folds are open and overturned northwestwards on the western limb of the major fold with a N-trending axial plane (F_I) (Figure12c). The structure on the upwards-continued aeromagnetic map in Figure 12a indicates that shortening (D_{H+I}) extended into deeper levels of the crust. This ductile folding is identifiable in the southern part of the Svecofennian domain, especially in the Southern Finland Granitoid Zone (SFGZ). In the north, e.g. in the Tonalite Migmatite Belt (TMB), the crust deformed in a more localized manner, e.g. along the ENE-NE- and WNW-NW-trending crustal shear/fault zones that deform the major folds with E-trending axial planes (Figure 11). This indicates that the folding (F_H) represents a high-T event in the south, whereas stabilization/cooling at that time occurred far in the north. The foliation trends in the border zones of the tectonic units often reveal south-eastwards dipping high-strain zones (Figure 12b), e.g. the West Uusimaa granulite Complex-Espoo Granitoid Complex (WUC-EGC) boundary zone (Figure 9).

Open warps with N-trending axial planes (F_I)

In southern Finland the early tight (D_{C+D}) and also the less strained dome-and-basins (D_{G+H}) trend approximately E-ENE (Figure 11). These structures are openly warped/folded (D_I) with wavelength up to 300 km and a steep axial plane trending c. N (010º).

The most intense bends exist in the detailed study area and in western Finland, from the SW archipelago to the Pori area. These coincide with the Baltic Sea-Bothnian Bay Zone (BBZ) and Riga Bay-Karelia Zone (RKZ), exemplified by the Vuosaari-Korso shear/fault zone in the detailed study area (Figures 8 and 10). In the northern parts of the detailed study area, ductile folding with a N-NNE-directional axial plane developed, indicating E-W shortening. The early dome-and-basin structures (D_{G+H}) tightened and were refolded/drag-folded into a N direction, especially near the Vuosaari-Korso zone. The open folds with a NW-trending axial plane to the west of Obbnäs rapakivi granite (4 in Figure 9) are related to this deformation (D_I) (Figure 11); its axial plane (S_I) is bent into a N-NNE-trend further north. The axial structure shows varying ductility characters; it is more ductile in the granite-dominant areas and deforms the NE-trending axial plane (S_H). Corresponding folds also exists in the southern Sipoo area, where they form complex dome-and-basin interferences (D_{G+H+I}).

The shapes and setting of the granulite-facies areas, the West Uusimaa granulite Complex (WUC) and central Sipoo area (Si in Figure 9), are a consequence of the large-scale dome-and-basin geometry ($D_{G+H\pm I}$) (Figure 11). The high-grade rocks are exposed in the antiformal settings of the structures. The corresponding interference pattern (predominantly D_{G+H}) also defines the large, open tectonic dome-and-basins such as the Nuuksio synform (Nu in Figure 9), which was reoriented in the N-trending Vuosaari-Korso axial zone (S_I). The supracrustal Southern Volcanic-sedimentary Belt (SVB) is predominantly characterized by the earlier isoclinal dome-and-basin geometry (D_{C+D}), which in the study area is complexly deformed by the crustal-scale the Vuosaari-Korso (D_I) and Porkkala-Mäntsälä shear/fault zones (D_G) (Figures 10 and 11).

Small amounts of granite veins locally intruded into the N-trending axial planes (S_I), indicating high temperatures during deformation, but the latest semi-brittle axial plane structures provide evidence of decreasing temperatures during its later stages. Semi-brittle to sharp brittle faults with a N-NNE orientation, and dense jointing cutting the open fold pattern described from the Vuosaari-Korso shear/fault zone, indicate late reactivation of the zone (Elminen et al. 2008 and Wennerström et al. 2008). The character of the structure (D_I) changes from ductile in the area of the Southern Finland Granitoid Zone (SFGZ) to brittle in the Lake Päijänne fracture

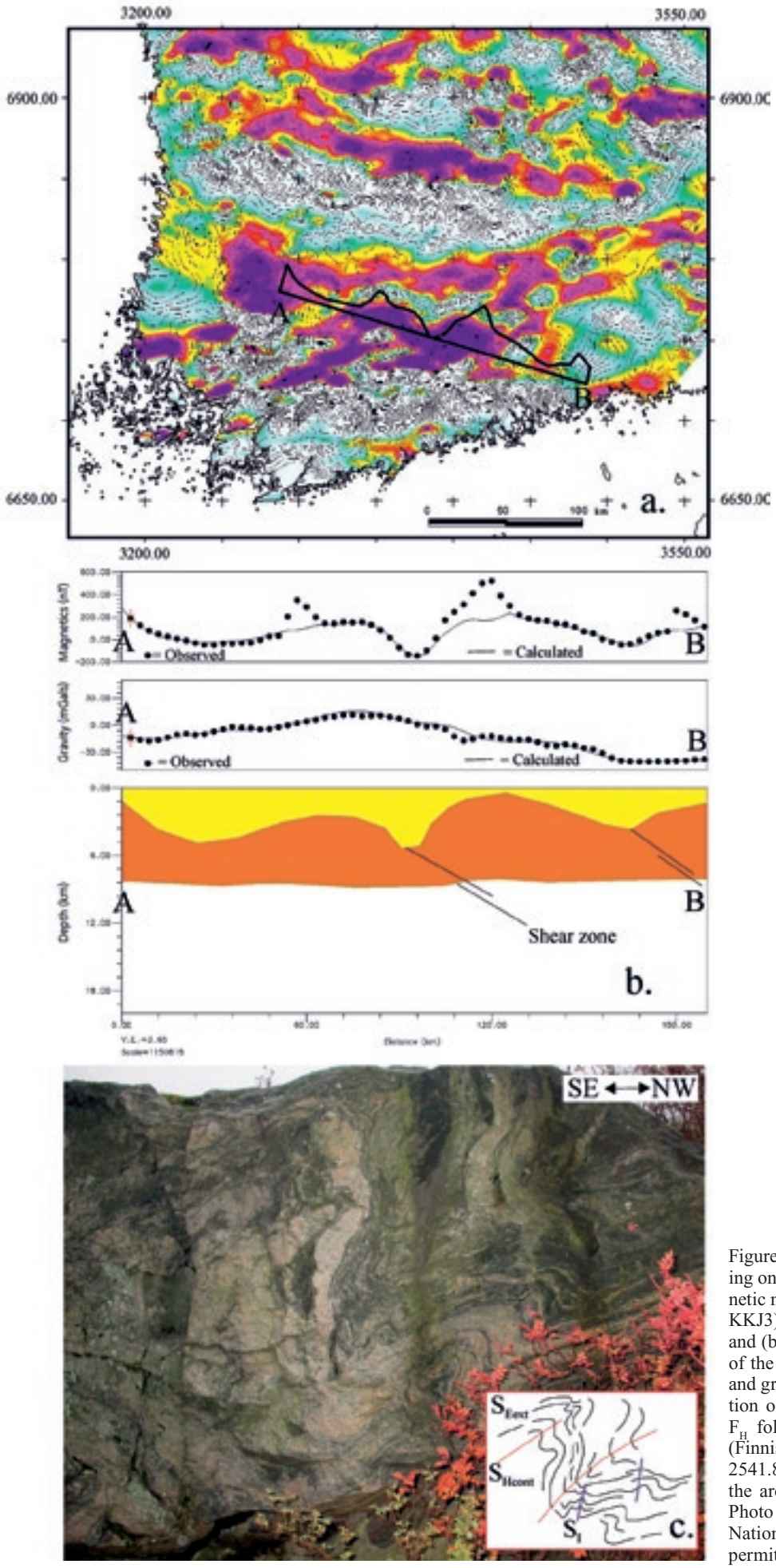

Figure 12. (a.) Large-scale D_H folding on the upwards-continued magnetic map (Finnish grid coordinates KKJ3) with the interpreted profile and (b.) geophysical interpretations of the structure from aeromagnetic and gravity data. (c.) A vertical section of northwestwards overturned F_H fold in Nurmijärvi, Klaukkala (Finnish grid coordinates KKJ2 2541.83E 6696.47N); width of the area of the figure is c. 1.5 m. Photo by M. Pajunen. Base map © National Land Survey of Finland, permit No. 13/MML/08.

zone (Figure 10 and Sederholm 1932b), in the Tonalite Migmatite Belt (TMB) and the Central Finland Granitoid Complex (CFGC). This suggests different thermal evolutions in the areas; the northern units were cooled at the time of ductile deformation and magmatism in the south.

Open warps with E-trending axial planes (post-D_I)

The ductile N-S axial plane (S_I) is openly warped in c. N-NNE-shortening: the post-D_I warp in Figure 11. The semi-brittle structures in the Vuosaari-Korso shear/fault zone also show such open bending and the early tight domes-and-basins (D_{C+D}) are deformed in a complex manner south of the Vuosaari area (Vu in Figure 9). We have not established whether these late structures are related to the latest Svecofennian events that occurred essentially later in Estonia (Puura et al. 2004) than observed so far in Finland. The latest movements in the N-trending axial zones (D_I) are related to post-Svecofennian events (D_P) prior to or during the rapakivi stage, and even to later stages of crustal evolution (cf. Mertanen et al. 2001, 2008 and Bergman et al. 2006).

DETAILED DESCRIPTION OF STRUCTURAL SUCCESSION

Structural evolution preceding the Southern Finland Granitoid Zone

Primary associations and D_A deformation

The earliest identified tectonic structures in the study area are the intrafolial isoclinal F_A folds preserved in the compositionally-layered volcanic or metasedimentary rocks. A migmatitic mica gneiss outcrop in the Espoo Granitoid Complex (EGC) at the Hakkila site, Vantaa, excellently shows the relations between the early structural events and the primary sedimentary-volcanic structure (Figure 13a). In a schollen fragment of the mica gneiss, a layered felsic rock, a psammitic portion of the mica gneiss, is cut by a zoned mafic dyke (Figure 13b). The felsic rock has a weak, nearly bedding/S_0-parallel S_A foliation (Figure 13c). It was lithified and D_A-deformed before the intrusion of the mafic dyke into a brittle fracture at a high angle to S_0 and S_A. The dyke has narrow, altered, chilled margins, seen as a grain-size decrease towards the contact, indicating intrusion into a cool environment. On the same outcrop the primary bedding, S_0, of psammitic metasediment shows remnant isoclinal F_A folds (Figure 13d) with weak penetrative S_A foliation, which was later strengthened and migmatized by D_B. The S_A foliation and a weak F_A folding remnant beside the mafic dyke (Figure 13c; white arrow) constrains the structure in the schollen fragment to those (Figure 13d) in the gneiss nearby. The mafic dyke was M_B-metamorphosed and D_B-deformed. The D_B structures in the surrounding mica gneiss are strongly overprinted by later deformations. The mafic fragmentary (possible agglomerate, Figure 13e) and layered volcanic rocks (Figure 13f) show M_B metamorphic parageneses, but their relations to D_A are not known.

Garnet-bearing migmatitic felsic gneiss (Figures 14a-d) from the Southern Sedimentary-volcanic Belt (SVB) at the Kalkkiranta site, on the Sipoo coast, includes intra-folial F_A folds (Figure 14c) in a D_B-foliated rock. It also has D_B-boudinaged and rotated amphibolite fragments (Figure 14d). F_A folds also occur in the associated, shallow-water, impure limestones/marbles in the Kalkkiranta mine. Due to later higher-grade processes, carbonates were often remobilized into dilatational fractures, like in the West Uusimaa granulite Complex (WUC, Appendix 2). A garnet-bearing, intermediate dyke with chilled margins cut the F_A-folded gneiss (Figures 14a and b) and was deformed and metamorphosed in D_B. This post-D_A to pre-/early D_B dyke shows a corresponding setting to the volcanic dykes in Hakkila. Boudinaged mafic fragments have a strong lineation (Figure 14e) similar to the F_A-folded felsic host gneiss; it is an intersection lineation, $L_{A+B/C}$ (structural relations summarized in the inset in Figure 14).

Thus, two tectonically-differentiated volcanic sequences occur: the earlier volcanic Series I (pre-D_A) including the F_A folds, and the later volcanic Series II (post-D_A to pre-/early D_B) cutting the D_A structures. Both are deformed and metamorphosed during the D_B. The described tectonic relationships also support the view that at least part of the psammitic to pelitic sediments were lithified and deformed, before the mafic dykes and the closely-associated volcanic rocks were formed.

The F_A folds are flame- or sharp-hinged with thickened hinges and thinned limbs (Figure 15a). The flame-shaped F_A hinges are interpreted as being a result of low-temperature deformation, which caused a brittle to semi-brittle, spaced, fracture foliation in the S_A axial plane. The spaced segments were transposed along the foliation planes under continuous D_A flattening. Later higher-grade ductile

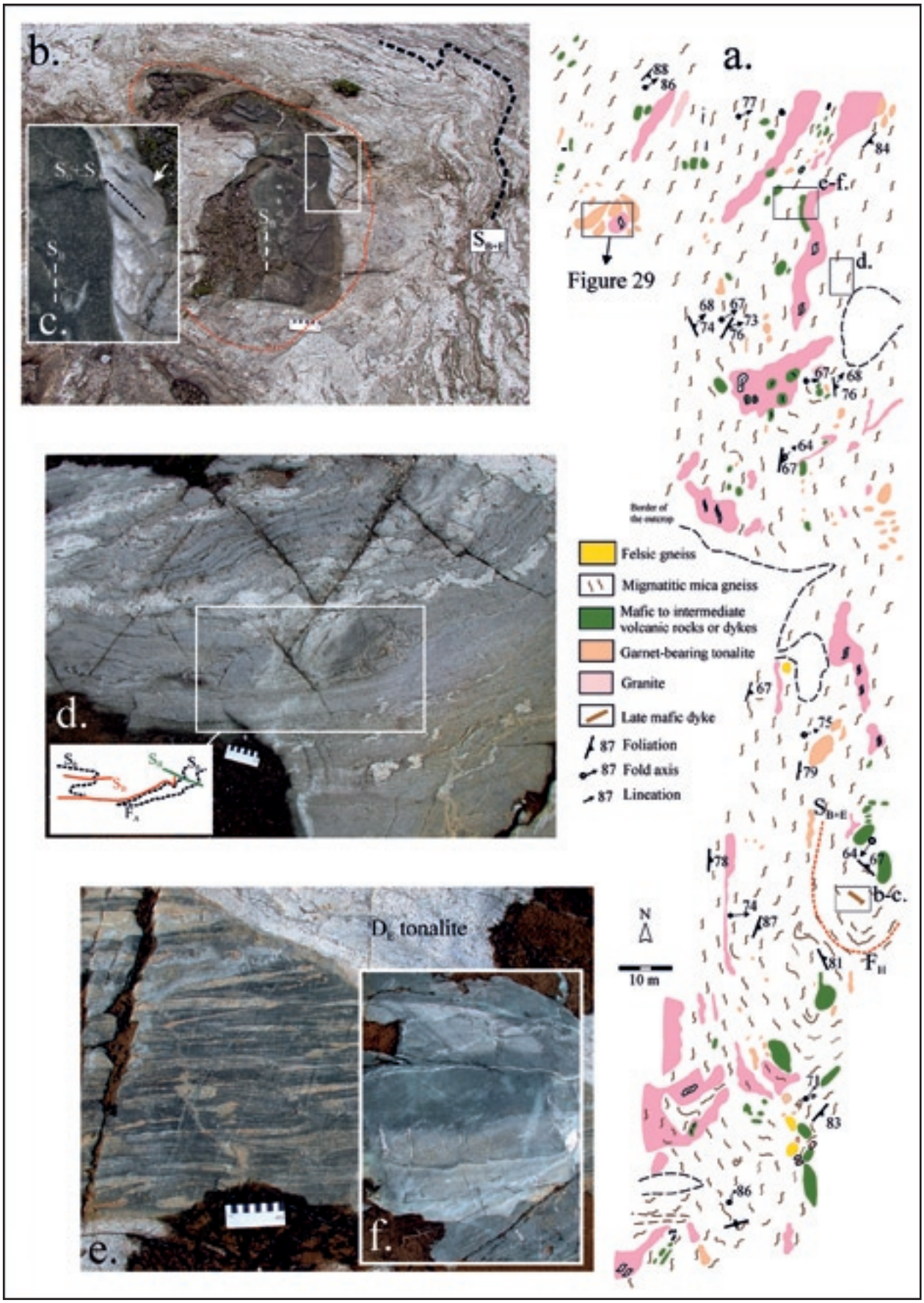

Figure 13. (a.) Detailed map of a migmatitic mica gneiss outcrop in Hakkila, Vantaa (Finnish grid coordinates KKJ2 2560.64E 6687.59N). The locations of Figures 29 and 13b-f are shown with boxes. (b.) Fragment of an amphibolitic dyke (red dot line) in migmatitic mica gneiss. Scale bar is 10 cm in length. (c.) A detail in (b.) (white box) showing the dyke edge against the psammitic portion of the mica gneiss; the dyke was intruded into D_A-deformed rock; (d.) F_A and F_B folding in psammitic layers of migmatitic mica gneiss. Scale bar is 10 cm in length. (e.) Fragment of fragmentary mafic volcanic rock cut by D_E tonalite. Scale bar is 10 cm in length. (f.) Layered volcanic rock in migmatitic mica gneiss. Width of the area of the figure is c. 2 m Photos by M. Pajunen.

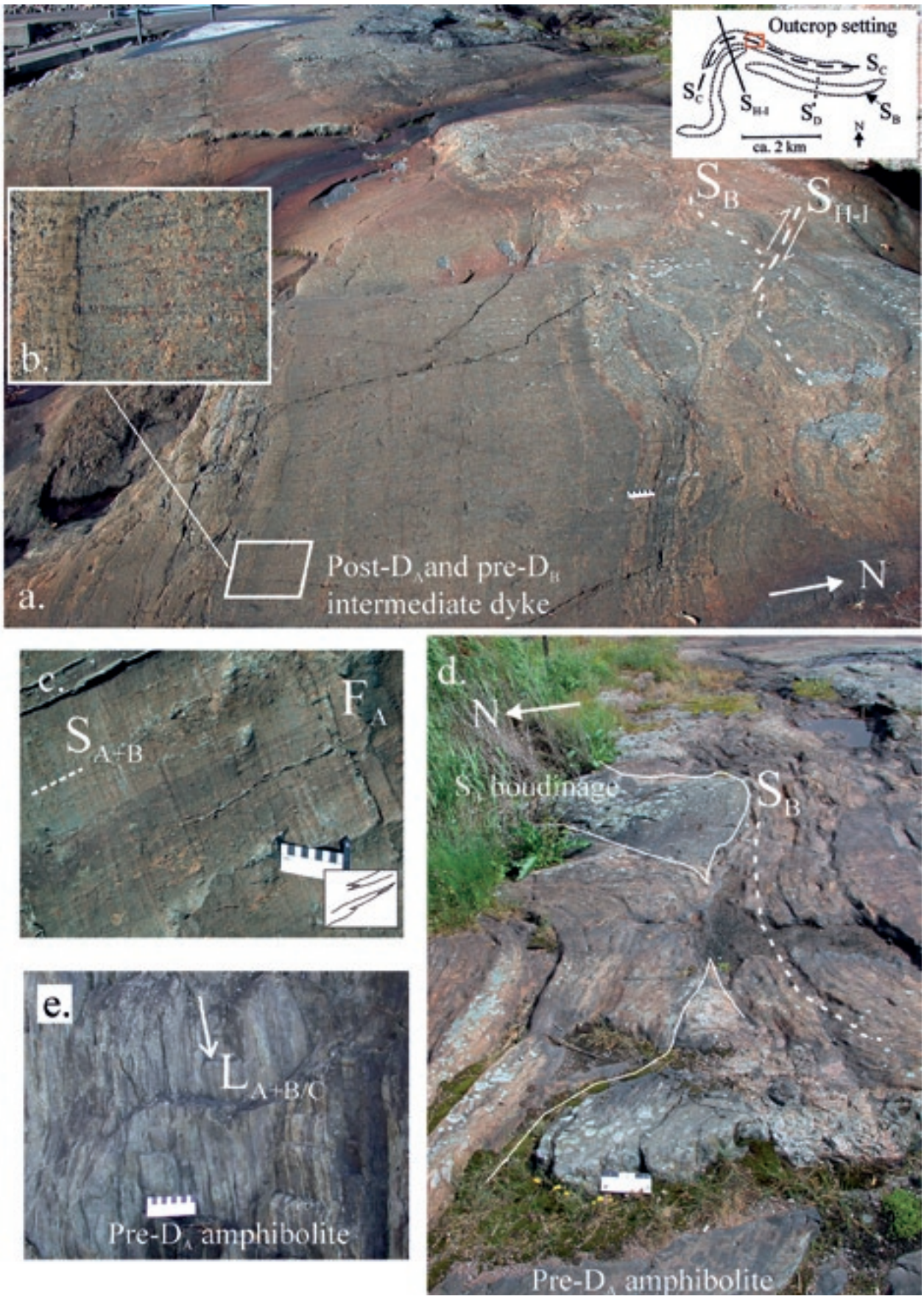

Figure 14. (a.) A metamorphosed intermediate dyke cutting migmatitic garnet-bearing felsic gneiss with a chilled margin in an intermediate dyke shown in Figure (b.). Scale bar is 10 cm in length. (c.) F_A folds in felsic gneiss. Scale bar is 10 cm in length. (d.) D_B boudinage structure of amphibolitic layers in migmatitic felsic gneiss. Scale bar is 15 cm in length. (e.) $L_{A+B/C}$ lineation in a D_B-boudinaged amphibolite. Scale bar is 10 cm in length. Kalkkiranta, Sipoo (Finnish grid coordinates KKJ2 2577.26E 6683.23N). Photos by M. Pajunen.

deformation and metamorphism transformed the folds into a flame shape. These types of "low-temperature" fold hinges also characterize the earliest fold phases elsewhere (cf. Koistinen 1981, Hopgood 1984 and Pajunen et al. 2008). However, the later more ductile folds, refolding the earlier schistosity or foliation, show more or less rounded and unbroken hinges. S_A is weak foliation. At present it is composed of biotite and is sometimes crenulated by S_B. It parallels the F_A limbs and bedding S_0. Generally, D_A phases were consumed by the later mineral growth, particularly D_B; pelitic layers were effectively melted during the later high-grade events. No mineral, veining or melting phase can be connected to D_A. Hitherto, there are no direct indications of metamorphic conditions during D_A. The brittle character of the contact relations between the felsic gneiss and the post-D_A volcanic dyke, and the "low-temperature" flame-hinged F_A folds, indicate low-grade conditions during D_A. Kilpeläinen and Rastas (1990) described early, low-T quartz segregations from the andalusite schists of the Orijärvi area; we relate the quartz veins in the Vetio andalusite-cordierite schist to a later prograde metamorphism following the cooling stage after the early tectonothermal events D_{A-D}; the veins are related to D_H (Appendix-Fig. 4-1).

The isoclinal F_A folds are identified from the steep supracrustal units, in sections perpendicular to S_0; in horizontal sections, F_A folds are seldom recognisable (cf. Figure 6). Indications on depositional top directions are rare and not helpful for lithostratigraphic analysis. The primary associations show strong shortening, but the original D_A strain cannot be estimated, because the following D_B shows the main compressional axis roughly paralleling that of D_A. In the E-W-trending, upright parts of the Southern Volcanic-sedimentary Belt (SVB), not strongly affected by the later high-grade crustal bends, the sub-horizontal F_A axes trend c. E-W (cf. Pajunen et al. 2008), roughly referring to N-S-directional tectonic transport. However, the axes can be followed only a few meters on the outcrops and, when taking into account the effects of the later deformations, like rotation due to D_B shearing (Figures 14d and 15b), this estimation should be regarded as suggestive. The rarity of the F_A folds may indicate that they were originally very large.

Age of D_A deformation and correlations

According to recent observations the age of D_A deformation in the Espoo Granitoid Complex (EGC) and Southern Sedimentary-volcanic Belt (SVB) is between the ages of the early volcanic rocks (Series I) and later volcanic rocks (Series II), i.e. 1.90–1.88 Ga and 1.88–1.87 Ga, respectively (Väisänen & Mänttäri 2002). The age of Series II is approximately the same as that of intrusive D_B magmatism: these relations are discussed in more detail later. The 1.90–1.89 Ga age of volcanism in the Tampere Schist Belt (TSB) (Kähkönen 1989), corresponds to that of the early volcanic Series I.

The oldest dated granitoid in the study area is the 1898 ± 2 Ma Orijärvi granodiorite, which is interpreted as co-magmatic with the bimodal volcanism in the Orijärvi area (Väisänen & Mänttäri 2002). According to Suominen (1991), the syntectonic Algersö granodiorite in Föglö, in the southwestern archipelago SW of Turku, is 1899 ± 8 Ma in age (Southern Volcanic-sedimentary Belt, SVB). There have so far been no descriptions of the relations between D_A structures and these oldest granitoids.

The earliest structurally-fixed magmatic rocks in the study area are mafic rocks dated by Hopgood et al. (1983) in the Jussarö-Skåldö area (Ju in Figure 9) (ages are discussed under D_B). Hopgood et al. (1983) proposed a primary volcanic-volcanogenic origin for the rock assemblage. Hopgood (1984) described two intrafolial fold sets from the Skåldö-Jussarö area, F_{aa} and F_{ab}; S_{aa} is folded around F_{ab} fold hinges. The tightly refolded, round-hinged folds (Figure 13d) are rare in our data and we relate them to the D_B flattening. This does not contradict the possibility of local isoclinal folds (F_{ab}) between F_A and F_B of this study – we have limited data from the well-exposed, clean coastal outcrops studied by Hopgood (1984). Hopgood et al. (1983) and Hopgood (1984) did not describe F_A folds from the mafic agmatitic rocks, but they related the gabbro foliation to the earliest deformation phase in the area. Nevertheless, the foliation-forming mineral assemblage of the rocks indicates metamorphism under amphibolite facies conditions, which according to our observations points to conditions not achieved until D_B. We relate the post-D_A/pre-D_B mafic and intermediate dykes (Figures 13b and 14a and b) of the study area to the later volcanic rocks, Series II.

Summarizing, we have not identified D_A structures from the later volcanic Series II (post-D_A to pre/early-D_B) or from the gabbroic-tonalitic association (pre-/early D_B) in the Southern Sedimentary-volcanic Belt (SVB, see D_B description). The Hyvinkää Gabbroic-volcanic Belt (HGB, Appendix 3) and the high-grade gneisses of an upper tectonic unit of the southern Svecofennian domain, referred to here as the Upper Tectonic Unit (UTU) (Appendix 6), do not show F_A folds either. The evolution of the Jokela sedimentary-volcanic association is dated to considerably later, post-dating D_C (Appendix 5). No F_A folds are defined from the Vetio andalusite-cordierite schist in the Orijärvi area (Appendix 4), either.

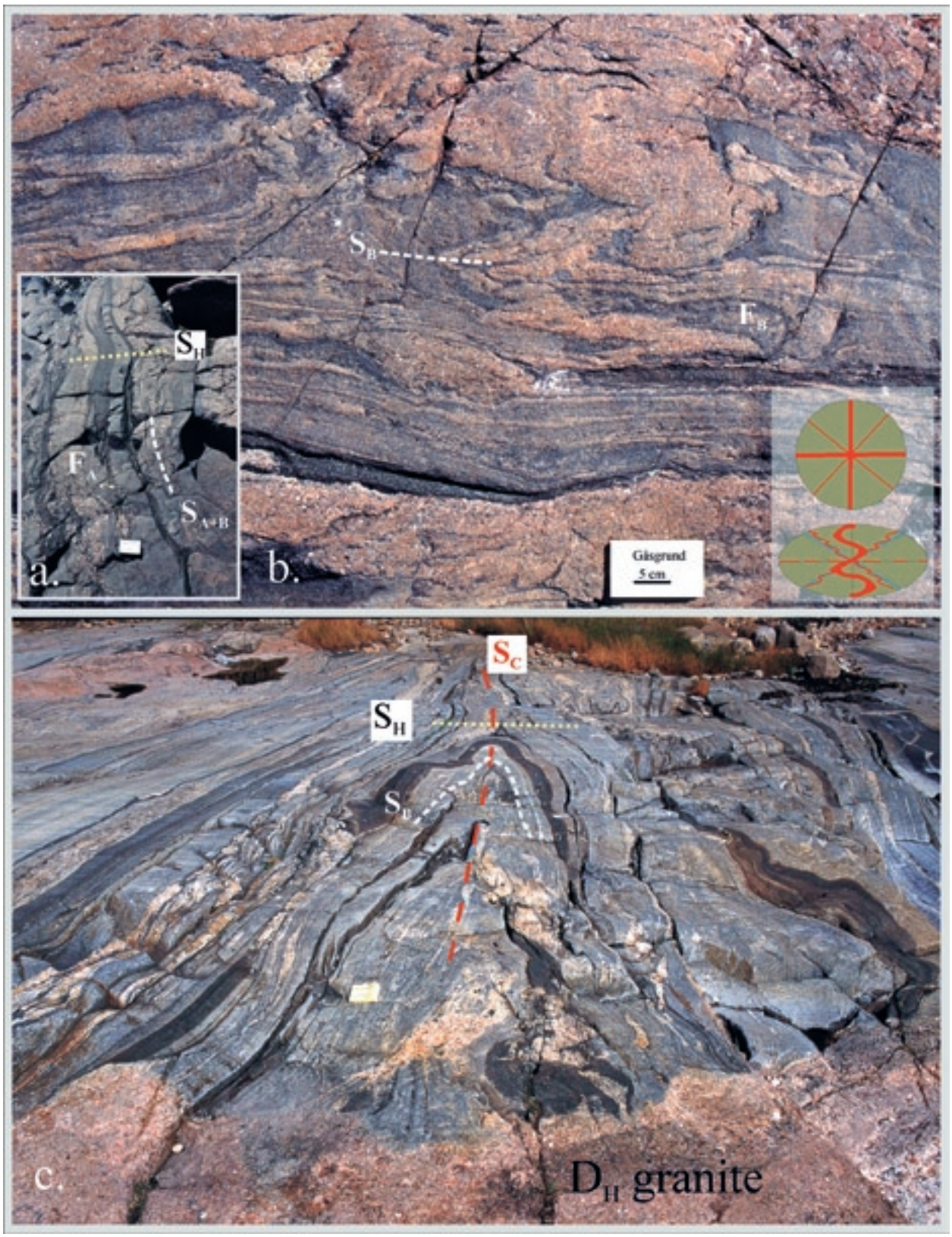

Figure 15. (a.) Flame-hinged F_A folding in felsic gneiss with mafic layers. The F_A axis is close to horizontal. S_{A+B} is c. ENE-WSW-trending; scale bar is 7 cm in length. (b.) D_B folding and migmatization in mica gneiss. Anti-clockwise D_B rotation of competent fragments and shearing parallel to S_B foliation planes indicate that the D_B strain was not pure shear strain in the study area (the pure shear strain flow model with related folding and boudinage patterns is shown in the inset). S_B is c. ENE-WSW-trending. (c.) An F_C fold in layered felsic gneiss cut by a D_H granite dyke. S_C is c. ENE-WSW-trending; scale bar is 7 cm in length. Gåsgrundet, Espoo (Finnish grid coordinates KKJ2 2541.86E 6664.80N). Photos by M. Pajunen.

D_B deformation – extensional event with intense crustal flattening

The D_A structures and the early supracrustal sequences, including both the volcanogenic Series I and II, were deformed in a strong, penetrative D_B deformation that occurred under progressive metamorphic conditions. D_B structures also characterize the gabbroic associations described by Hopgood (1984). Intense vertical shortening deformation, melting and intense intrusive magmatism typify the D_B.

F_B folds are isoclinal to tight with thickened, roundish hinges and thinned or boudinaged limbs (Figures 13d and 15b). Penetrative, or locally zoned, S_B mineral foliation developed sub-parallel/parallel to S_0 and S_A. The F_B folds are only occasionally observed to refold the primary bedding S_0 or S_A (Figure 13d), because the early structures were originally close to horizontal position. Generally, D_B only strengthened the F_A folds. However, isoclinal to tight F_B folds in the syn-D_B migmatizing neosome veins are typical (Figures 15b). Deformation was often localized in D_B shear zones along the F_B fold limbs and, in places, competent boudinage fragments were rotated due to D_B shearing (Figure 14d). A melt fraction developed into the pressure minimums of the boudinaged necks. L_B lineation is weak, but an intersection lineation is evident, for example, in amphibolites; $L_{A+B/C}$ in the early volcanic amphibolites (Series I, Figure 14e) and $L_{B/C}$ in the later ones (Series II, Appendix-Fig. 3-2c).

The D_B neosome veins are quartzo-feldspathic or trondhjemitic in composition during the early stages; later more granitic melts were formed (Figure 13b and 15b). According to Mouri et al. (1999), the composition of neosomes depends on the activity (aH_2O) of participating fluid components and the primary rock composition. D_B migmatization was polyphase due to successive melting and intrusive magma events under continuous flattening and heating. In the Southern Finland Granitoid Zone (SFGZ) it is sometimes impossible to fix the neosome phase to just the D_B because of strong later melting events. On an outcrop scale, the D_B structures often are quite similar to $D_{E\pm H}$ structures, especially where a weak D_B is overprinted by a strong $D_{E\pm H}$. The S_B represents the main foliation in the supracrustal areas of weak $D_{E\pm H}$. The similarity of the D_B and $D_{E\pm H}$ structures has been one of the major "stumbling blocks" in analyzing the structural successions in the southern Svecofennian domain: they may both represent the second deformation event in a particular area, but there is an important time gap between them. The problem becomes particularly evident in areas where only a few structurally-fixed date determinations are in use. The identification is straightforward if a cooling stage can be established between the events (e.g. Sederholm 1926 and Pajunen et al. 2008).

Koistinen et al. (1996, Figures 26 and 27, page 50) provide an example of weakly lineated, chocolate tablet D_2 boudinage from Uusikaupunki, c. 80 km SSW of Pori, indicating weakly ellipsoidal flattening strain. We have not found good three-dimensional sections to analyze the kinematics of D_B boudinage structures. The subhorizontal to horizontal position of the S_B can be constructed by analyzing the position of the enveloping surface of F_{C+D} domes, but only on an outcrop-scale. On a map-scale, the ductile D_B shearing and later structures between the domes complicate such analysis. The observations suggest that the main strain was sub-/horizontal flattening; the strain was not just pure shear, as modelled in the inset Figure 15b, but the rotated D_B boudinages (Figure 14d) and shearing along the F_B limbs (Figure 15b) refer to some shear component during the deformation.

Structures in magmatic rocks related to D_B deformation

The early Svecofennian magmatic rocks are foliated, complexly deformed and intruded by several later magma and migmatization events. They have amphibolite to granulite facies mineral parageneses. Analysis of the tectonic setting of these intrusive rocks necessitates the description of their field relations with respect to the early structures in their hosts as well as to the later structures existing in them. Hence, the following examples also describe the post-D_B structures that will be discussed in more detail later.

Structures in pre-/early D_B gabbroic associations

The earliest magmatic rocks related to deformation are banded or layered mafic rocks showing variation in composition from assimilated ultramafic remnants to gabbros and diorites in the Jussarö-Skåldö area (Ju in Figure 9). Hopgood et al. (1983) and Hopgood (1984) proposed a primary volcanic-volcanogenic origin for the rock assemblage. The gabbros were intruded and injected by tonalitic magmas and by amphibolitic dykes. In Simijärvi (Si in Figure 16), to the south and east of the Orijärvi area (Or in Figure 9), occur corresponding, locally sheared, gabbroic rocks (Figures 17a and b). The Salittu ultramafic rock (Sa in Figure 16) is situated to the N of Simijärvi. The association is exposed along a rather coherent zone in the southern coast and archipelago in the Southern Volcanic-sedimentary Belt

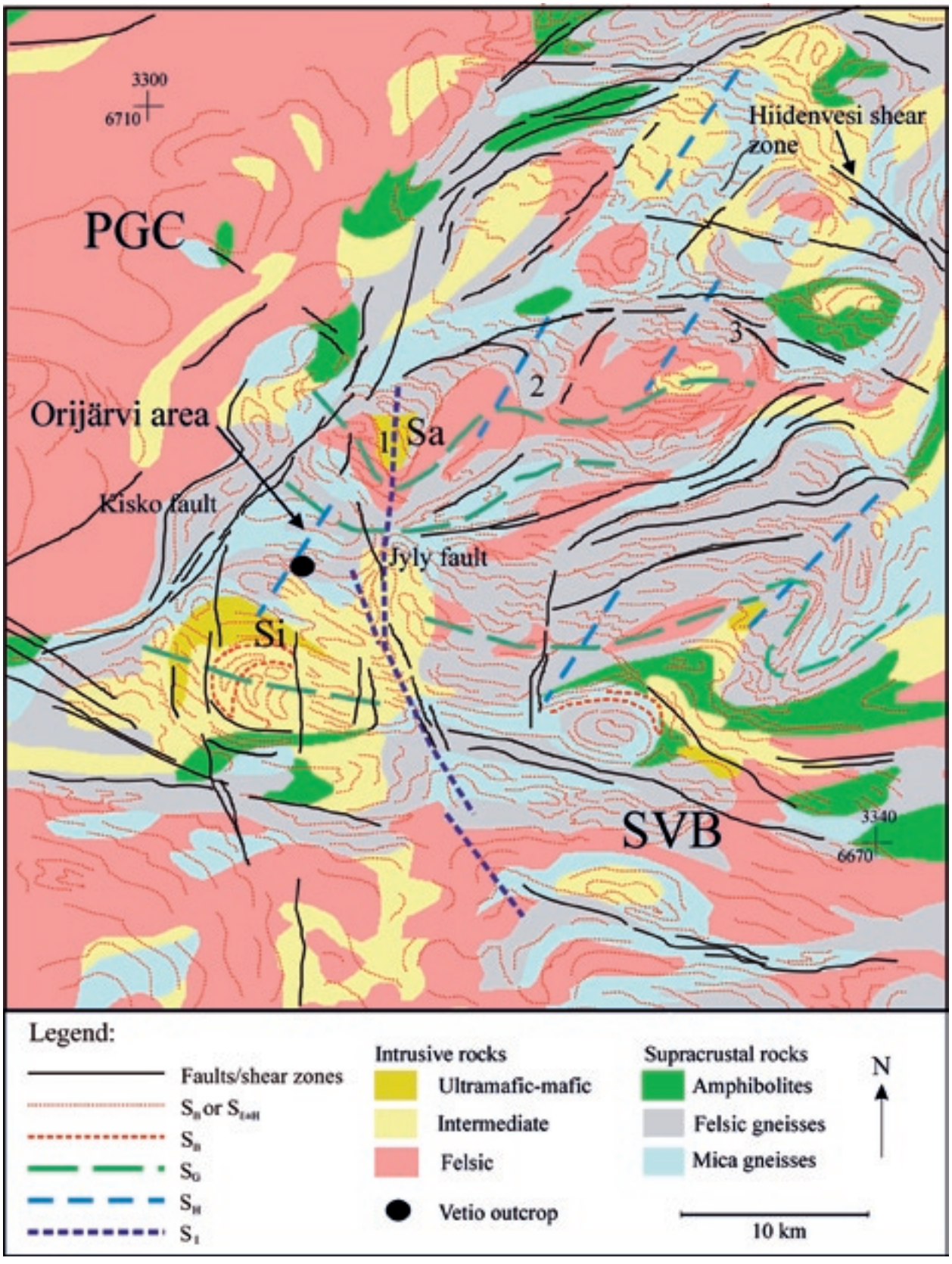

Figure 16. Tectonic structure of the Orijärvi area. Si = Simijärvi, Sa = Salittu, 1–3 mafic to ultramafic rock in tectonically similar settings (see text) (Finnish grid coordinates KKJ3).

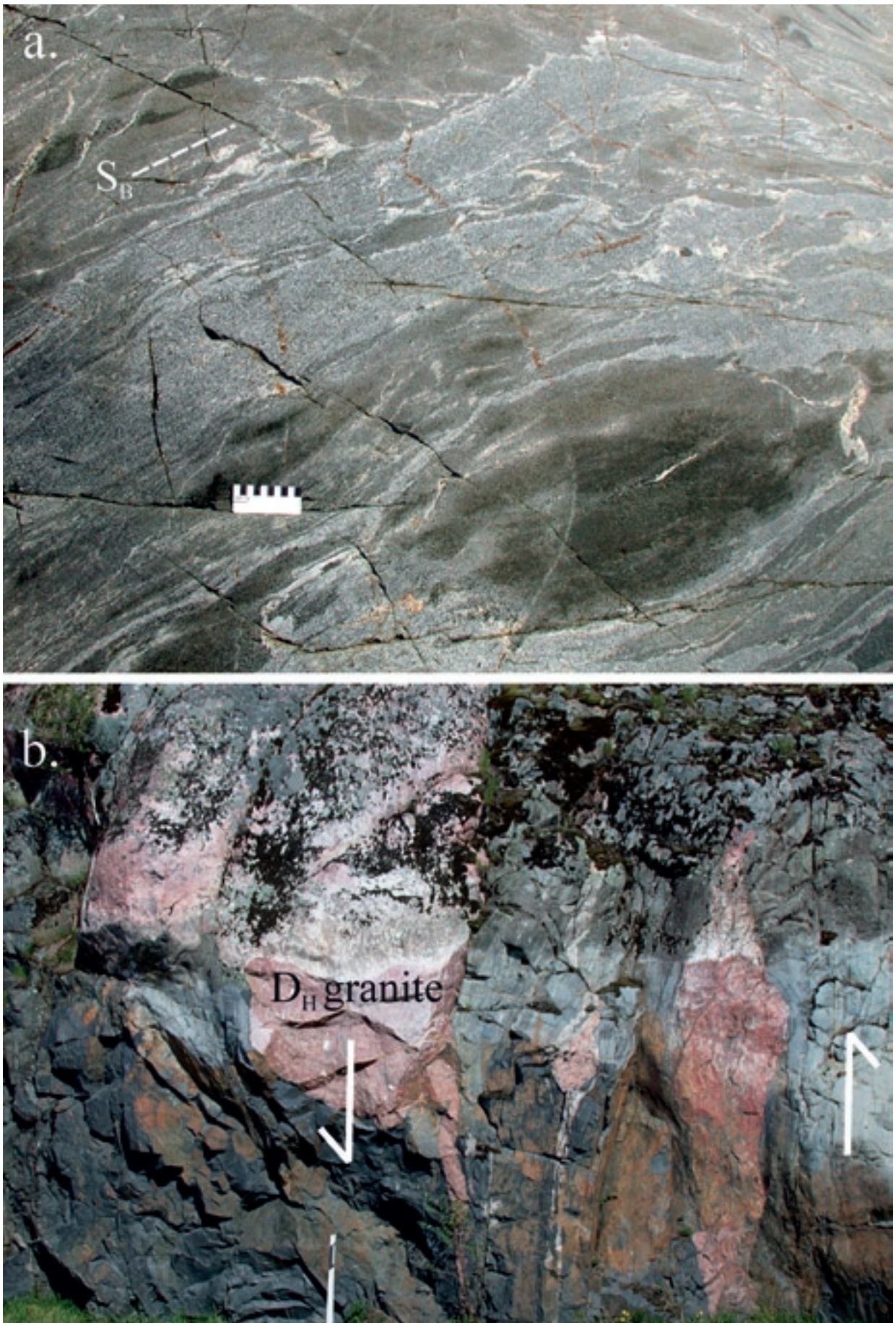

Figure 17. (a.) A pre-/early D_B gabbroic-tonalitic association with tonalitic magma cutting and assimilating the gabbro and ultramafic fragments. Scale bar is 10 cm in length. (b.) Strongly-sheared gabbroic rock on the same outcrop representing deformation in the Southern Finland shear zone. Width of the area of the figure is c. 3 m. Bollstad N, Inkoo (Finnish grid coordinates KKJ2 2494.50E 6661.50N). Photos by M. Pajunen.

(SVB), e.g. Kopparnäs in Siuntio, Sarfvik and Evitskog in Kirkkonummi, and Kauklahti in Espoo (locations are shown in Figure 7). The sinistral Porkkala-Mäntsälä shear zone in the east cuts the zone.

The Sarfvik site is an example of the structural relationships of the gabbroic association and the Porkkala-Mäntsälä crustal bend. The medium-grained gabbro (Figure 18a) was intruded by a gneissic tonalite (Figure 18b). The gabbro has an amphibolite-facies, penetrative mineral foliation, S_B, which locally appears as shear foliation. The gabbro shows weakly rotated D_B boudinage structures (Figure 18c). We have not identified D_A structures in the rocks. Hopgood et al. (1983) also did not describe folds that can be correlated to F_A of this study from the Jussarö-Skåldö area. They related the foliation to the first deformational phase. We suggest that it corresponds to S_B: the metamorphic assemblages related to the penetrative foliation and weakly rotated boudinages are characteristic for D_B. Thus, we link the rocks to a pre-/early D_B gabbroic association. The D_B structures were later cut by granitoids (Figures 18a and b) showing a retrograde reaction rim against the gabbro (Figure 18d) and overprinted by later metamorphic events, such as high-grade melt patches related to the late stage of D_B or $D_{E/H}$ (Figure 18e). The D_E granitoid in Sarfvik does not show such high-grade mineral assembages.

The post-D_B deformations in the gabbroic rocks have been studied at the Kauklahti site (Figure 21a), in the amphibolitic wedge shown on the geological map (Laitala 1960 and 1961, Ka in Figure 7) to the

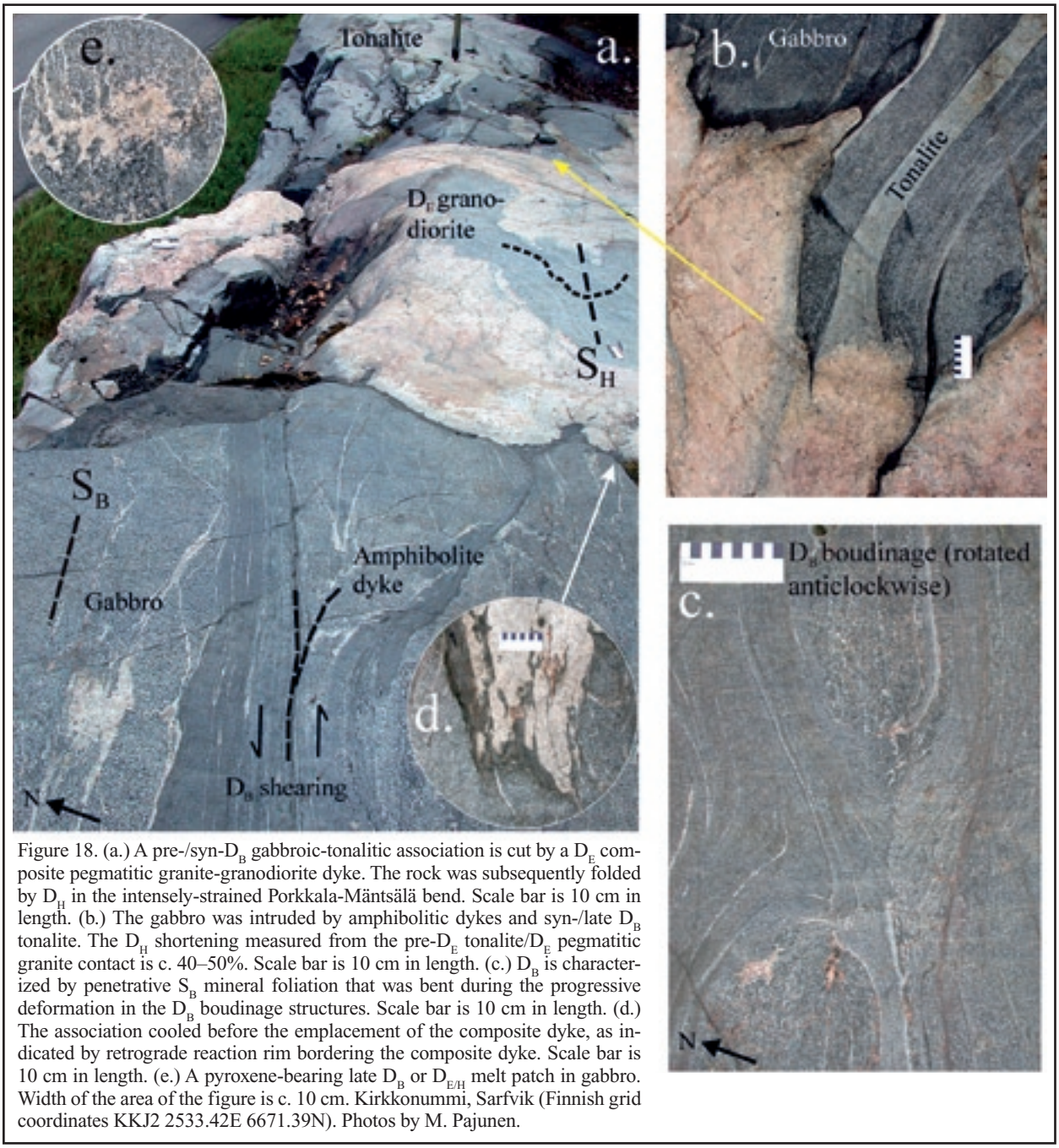

Figure 18. (a.) A pre-/syn-D_B gabbroic-tonalitic association is cut by a D_E composite pegmatitic granite-granodiorite dyke. The rock was subsequently folded by D_H in the intensely-strained Porkkala-Mäntsälä bend. Scale bar is 10 cm in length. (b.) The gabbro was intruded by amphibolitic dykes and syn-/late D_B tonalite. The D_H shortening measured from the pre-D_E tonalite/D_E pegmatitic granite contact is c. 40–50%. Scale bar is 10 cm in length. (c.) D_B is characterized by penetrative S_B mineral foliation that was bent during the progressive deformation in the D_B boudinage structures. Scale bar is 10 cm in length. (d.) The association cooled before the emplacement of the composite dyke, as indicated by retrograde reaction rim bordering the composite dyke. Scale bar is 10 cm in length. (e.) A pyroxene-bearing late D_B or $D_{E/H}$ melt patch in gabbro. Width of the area of the figure is c. 10 cm. Kirkkonummi, Sarfvik (Finnish grid coordinates KKJ2 2533.42E 6671.39N). Photos by M. Pajunen.

southwest of the Bodom rapakivi intrusion (3 in Figure 9) and to the west of the Porkkala-Mäntsälä shear/fault zone (Figure 10). A low-angle, E-W-trending gabbroic wedge dips gently towards the north, below the granitoids of Nuuksio (Nu in Figure 9). The gabbro was foliated, boudinaged and sheared and resembles a layered volcanic rock (Figure 19b); we interpret the layered structure as tectonic caused by the shearing of an originally heterogeneous ultramafic-mafic to tonalitic rock. The structures indicate intense flattening with contemporaneous shearing in amphibolite facies conditions. The S-C intersection and slicken line lineations in the shear planes indicate reverse top-to-SE faulting with a dilatation zone in the NW, i.e., in the direction of the West Uusimaa granulite Complex (WUC). We relate the shear planes to the $D_E$ext dilatation; further NW from the Porkkala-Mäntsälä shear/fault zone the $S_E$ext foliation is only gently to openly folded by later deformations, which is typical for the D_E, but not the case with the tightly D_{C+D}-folded D_B structures. Instead, the S_B, corresponding to that in Sarfvik, is preserved as penetrative mineral foliation in the gabbroic boudinage fragments. Recumbent F_E folds are very small and deform the felsic veins or, due to progressive deformation, more seldomly the sheared layering S_E itself. The kinematic setting (D_E) is exactly the same as at the Klaukkala site, described later. The described $D_E$ext structures are re-boudinaged during $D_H$ext with pegmatitic granitic melt emplaced in the boudinage neck (Figure 19c). The S_E-layered structure was overturned towards the south, supposedly as F_G folds, and refolded by the $F_H$cont folds overturned northwestwards (Figure 19d). The latest granites of the Espoo Granitoid Complex (EGC) cut the gabbroic association and the shear foliation (S_E). In the western extension of the Kauklahti gabbroic association, in Evitskog, Kirkkonummi (Ev in Figure 7), the strongly deformed and assimilated remnants of mafic rock, corresponding to that in Kauklahti, are preserved as inclusions in a D_H granite. This supports the view that the main deformation in the Kauklahti site occurred before the D_H deformation.

According to the structural interpretation, based on field observations, regional geophysical data and

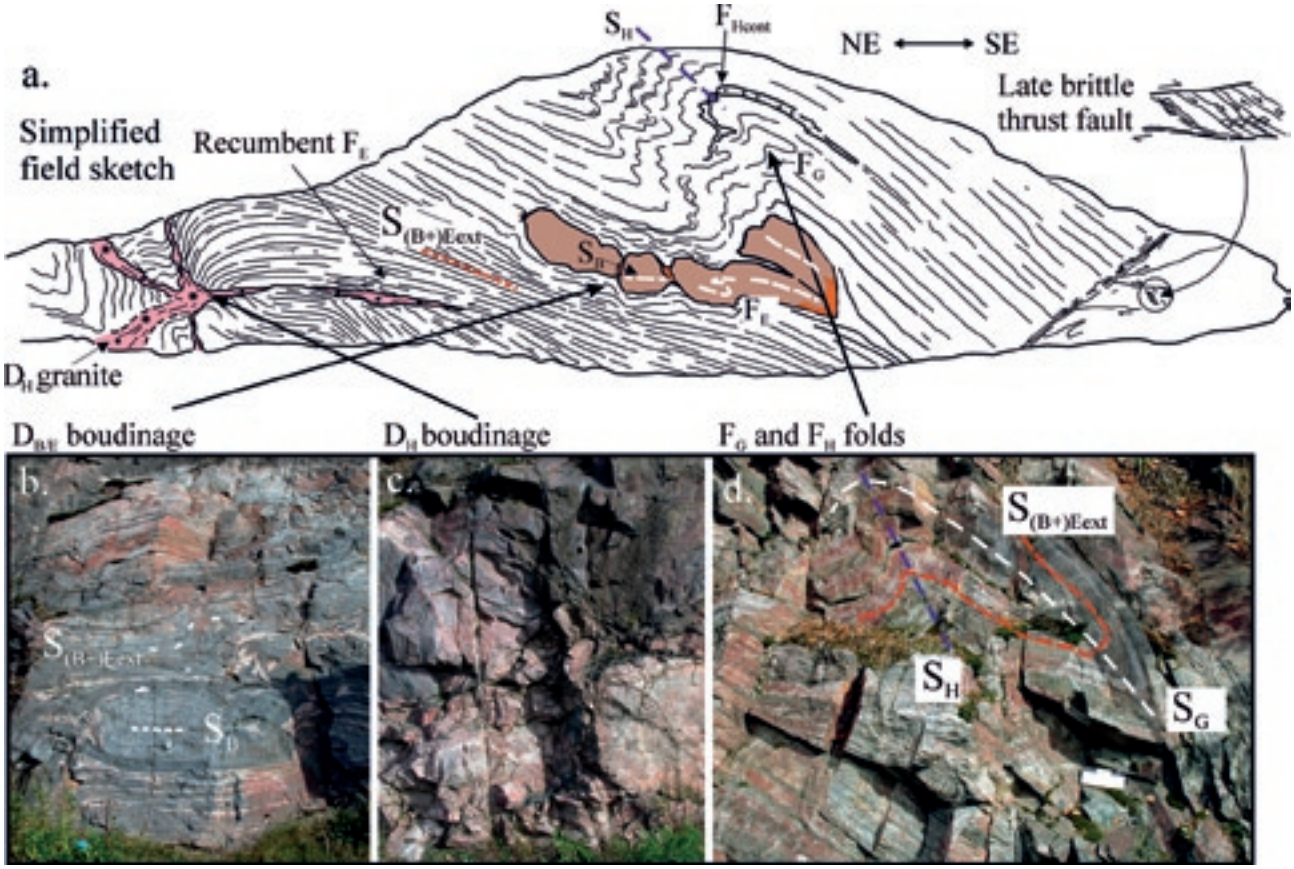

Figure 19. (a.) A simplified field sketch of a road cut showing layered amphibolitic gneiss interpreted as strongly D_E-deformed pre-/early D_B gabbroic rock. (b.) S_B is preserved in the gabbroic boudinage fragments; the main foliation is linked to $S_E$ext, indicating top-to-SE movement. The initiation of D_E boudinaged gabbroic fragments possibly has its roots in D_B (cf. Figure 18c). Width of the area of the figure is c. 2 m. (c.) The D_E structures are re-boudinaged by the D_H with pegmatitic granite intruded into the boudinage neck. Width of the area of the figure is c. 1.5 m. (d.) The D_E structures are refolded by the c. south-eastwards overturned F_G and c. north-westwards overturned $F_H$cont folds. The post-Svecofennian brittle thrust fault deforms all the structures. Scale bar is 15 cm in length. Kauklahti, Espoo (Finnish grid coordinates KKJ2 2532.08E 6675.58N). Photos by M. Pajunen.

the geological map of Koistinen (1992), the locally-sheared gabbroic association (Figures 17a and b) at Simijärvi (Si in Figure 16) forms a refolded synformal structure that can be correlated to the D_{C+D} domes-and-basins in the surrounding Southern Volcanic-sedimentary Belt (SVB). This D_{C+D} structure was refolded by F_G folding with an E-trending axial plane and by F_I folding with a NNW-trending axial plane. The S_I axial plane bends to a north trend further north and refolds the E-W-trending S_G at Salittu (Sa in Figure 16). The Salittu ultramafic rock (cf. Mikkola 1955) is situated in a northwards-opening fold structure (F_{G+I}), near the northern border of the granitic zone. The tectonic setting of the granitic zone is controlled by the F_G folding. Mafic rocks (amphibolites) in corresponding settings exist to the ENE of Salittu (2 and 3 in Figure 16). On a structural basis the Salittu (1) and mafic rocks ENE of it (2 and 3) are related to the mafic association in Simijärvi due to the large-scale, open F_G folding. Thus, the tectonic setting of the Simijärvi and Salittu ultramafic-mafic associations suggests their close relations (Figure 16). Their genetic relation to the lower-grade rocks in Orijärvi has not yet been based on structure.

Due to their high competence the ultramafic-gabbroic rocks were resistant to small-scale folding, but a regional folding pattern (Figure 16) can be constructed from the mapping and geophysical data. These medium-grained rocks are S_B-foliated with amphibolite facies assemblages, but locally strong later events overprint the D_B structures, like D_{E-H} in Kauklahti. The magmatic structures in the medium-grained rocks, such as assimilation and mobile magma contacts without chilled effects (Figure 17a), point to processes that occurred quite deep in the crust. The compositional variation from ultramafic and gabbroic to dioritic and tonalitic may represent a differentiated magma evolution. For these reasons, we suppose that these rocks are not tightly associated with the lower-grade, volcanic rocks in Orijärvi nearby, but the contacts are tectonic as often suggested by the discordant geophysical features and by the sheared structures (Figure 17b and 18a). This does not preclude a genetic connection to the volcanic associations as postulated by Hopgood et al. (1983) and Väisänen and Mänttäri (2002). We have not identified D_A structures from these rocks to support the possibility that D_A transported these rocks close to the lower-grade gneisses. It is also possible that these kinds of rocks evolved at different times with respect to D_A, just as is the case with the volcanic sequences, Series I and II. Our observations so far fix these S_B-foliated rocks, without identified D_A structures, to formation during the early stage of D_B.

Structures in syn-/late D_B tonalitic rocks

In the southern Svecofennian units, gneissic intrusive rocks are widespread. They cut the supracrustal associations, except for the Jokela supracrustal association (Appendix 5). These intrusive rocks are homogeneous and vary in composition from tonalites to granodiorites. Tonalites locally have pyroxene (cf. the West Uusimaa granulite Complex, WUC), which generally retrogressed to pale clino-amphibole, like in Sipoo (Si in Figure 9). Several pulses of later magmatic rocks cut these granitoids (e.g. Figure 18a and b). The following key examples from Pornainen and Sipoo summarize the characteristics of these gneissic tonalites.

The contact relationships between the gneissic tonalite and migmatitic mica gneiss are exposed at the Hirvensuo site, Pornainen, within a wide, open synform with a N-trending axial plane. On the outcrop, migmatitic mica gneiss forms a tight synform few meters wide in tonalite (Figure 20a). A strong S_B foliation and isoclinally F_B folded neosome veins of the gneiss indicate intense D_B deformation. The D_B structures were deformed by the synform F_C, with a moderately plunging F_C axis. The D_C structures are refolded by F_I folding; the synform thus represents a D_{C+I} structure. The tonalite intruded along the S_B plane and was folded by F_C. S_C is the first dominant mineral foliation identified in the tonalite. Close to the contacts, tonalite is only weakly S_B-oriented (Figure 20a), but farther from the contact, in the homogeneous parts, a steep S_C dominates; thus, it is syn-/late tectonic to D_B. A narrow, folded intermediate dyke cuts the mica gneiss, tonalite and the D_C synform (Figure 20b). Dykes cut S_C foliation in tonalite with bulging contacts (Figure 20c). We relate these post-D_C dykes to the D_E event; the syn-/late D_B tonalite and the dykes underwent a new prograde metamorphism during the proceeding D_E. In the following we refer to the intermediate D_E dykes in the corresponding tectonic setting as microtonalites, even though they show small variations in their composition and in their relations to D_E structures. Weak spaced foliation $S_E$cont formed in tonalites; it is penetrative in microtonalites. New granitic melt and segregation patches locally destroyed the S_C and $S_E$cont foliations. The prograde metamorphism also produced garnet-bearing granitic dykes and granite dykes (D_E or D_H) with a pegmatitic margin and medium-grained centre (Figure 20d) showing a pinch-and-swell-structure. The continuing magmatism (D_E-D_H) indicates that rather high temperatures prevailed during late deformation events.

Often the contacts between tonalite and supracrustal rocks are strongly deformed, or gradational due to later migmatization or magma pulses. Figure

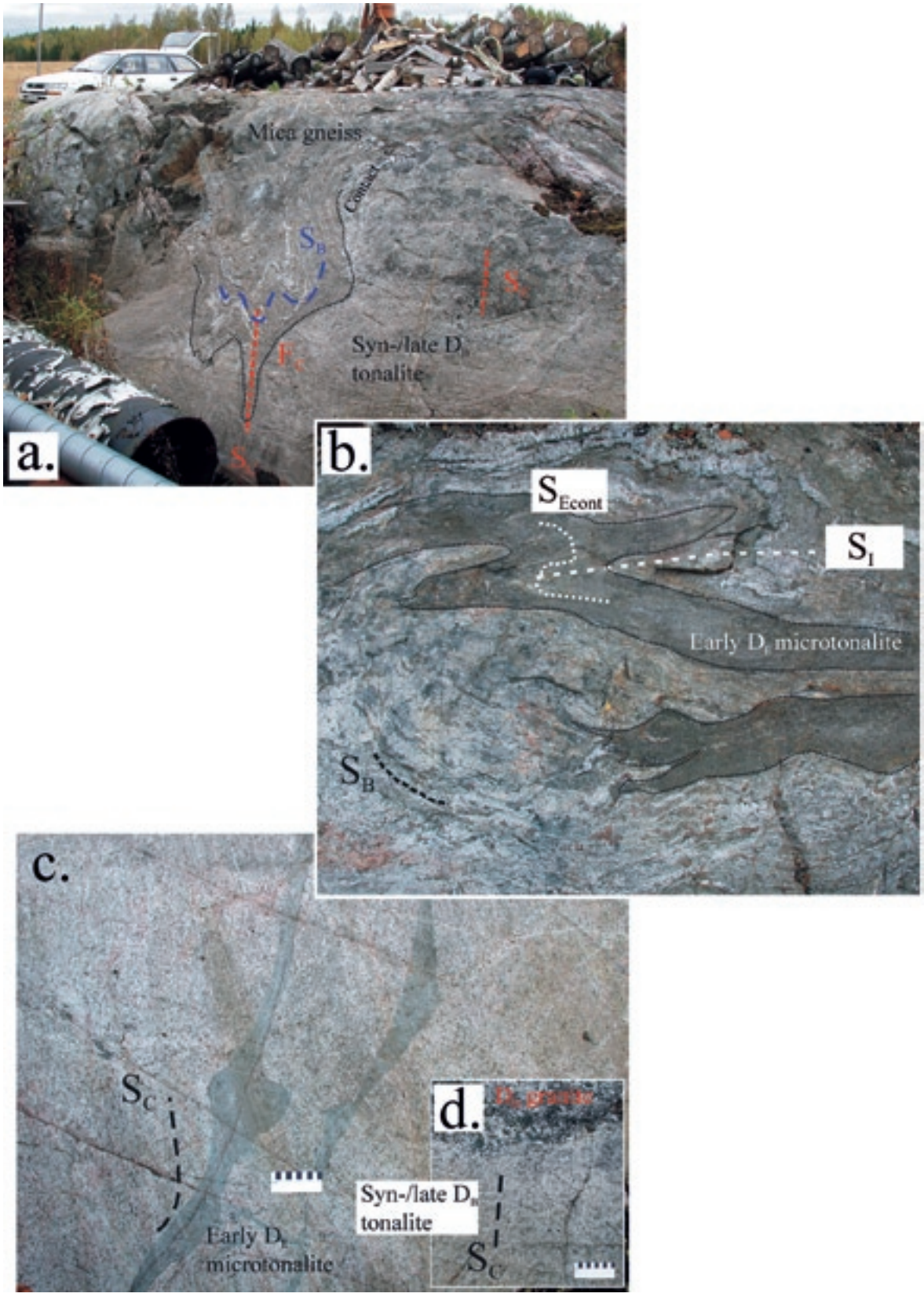

Figure 20. (a.) D_B deformed and migmatized mica gneiss forming a synformal structure in syn-/late D_B tonalite. Tonalite was intruded into the S_B plane, but its first penetrative foliation is S_C; S_B formed only close to contact. N is to the right; width of the area of the figure is c. 5 m. (b.) The gneiss and synformal structure are cut by intermediate early D_E microtonalite dyke. Folding with a c. N-trending axial plane is interpreted as F_I; the synform is thus a $D_{C\text{-}I}$ structure. The dyke aquired foliation $S_E$cont before the folded structure, indicating an increase in temperature following the dyke intrusion. (Note: the earliest stages of D_E and the latest D_D were produced by the same regional stress field close to each other during progressive deformation – The F_D folding can not be exluded in this case). N is to the right; width of the area of the figure is c. 1 m. (c.) The microtonalite dykes in the tonalite are bulbous and cut the S_C, indicating emplacement into a ductile environment under elevated temperatures; the M_E temperature increase is also indicated by the melt segregation patches in tonalite. Scale bar is 10 cm in length. (d.) A D_H pegmatitic granite dyke cuts the tonalite and S_C. Scale bar is 10 cm in length. Hirvensuo, Pornainen (Finnish grid coordinates KKJ2 2572.79E 6704.48N). Photo by M. Pajunen.

21a illustrates a sheared and folded contact against the migmatitic mica gneiss, locally including amphibolitic remnants, at the Vilonoja site, Pornainen. It is a primary magmatic contact, which was extensively deformed to an isoclinally-folded structure (sketch in Figure 21b). The D_B neosome veins of mica gneiss in the isoclinal folds, squeezed into tonalite, are strongly deformed; a less deformed mica gneiss structure is shown in Figures 22a and b. The tonalite is S_C-foliated and cut by later magmatic and migmatitic pulses. It is interpreted as syn-/late tectonic to D_B. It was intruded by felsic granitoid with a dark retrograde alteration zone along the contact (Figure 21c); the rock was deformed and migmatized by later granite melt that often concentrated into shear bands. We relate the felsic granitoid dyke to the early/mid-D_E tonalites and the granite to the later D_E or D_H phase. Correspondingly, the mica gneiss was also intruded by D_E melts (see Figure 22a) and in places shows a strong, steep, spaced $S_{E\text{-}cont}$ foliation that developed during proceeding deformation to form extensional shear bands (Figure 22c, the pre-$S_E$cont structure is shown in Figure 22a and b). The horizontal S_E foliation is interpreted as extensional $S_E$ext and the steep S_E as contractional $S_E$cont occurring rather simultaneously. The later D_H, characterized by intense granite production cannot be ruled out, because c. E-W-trending shearing also occurred during it. However, the axial planes of contradictional $F_H$cont folds are NE-trending (see later). In places, penetrative D_E structures completely destroy the early $D_{A\text{-}D}$ structures.

The Hindsby tonalite is c. 5*3 km wide, homogeneous, medium-grained and intrusive, and is exposed in a c. SSE-plunging open antiformal setting at the Staffas site in Sipoo (Hindsby tonalite location in Appendix-Fig. 6-2d). It clearly shows the internal structural evolution of this intrusive phase. Its contacts are mostly covered; the observed ones are against the later pegmatitic granite displacing the foliated tonalite (Figure 23a), or tectonic along the Vuosaari-Korso structure (Figure 23b). The

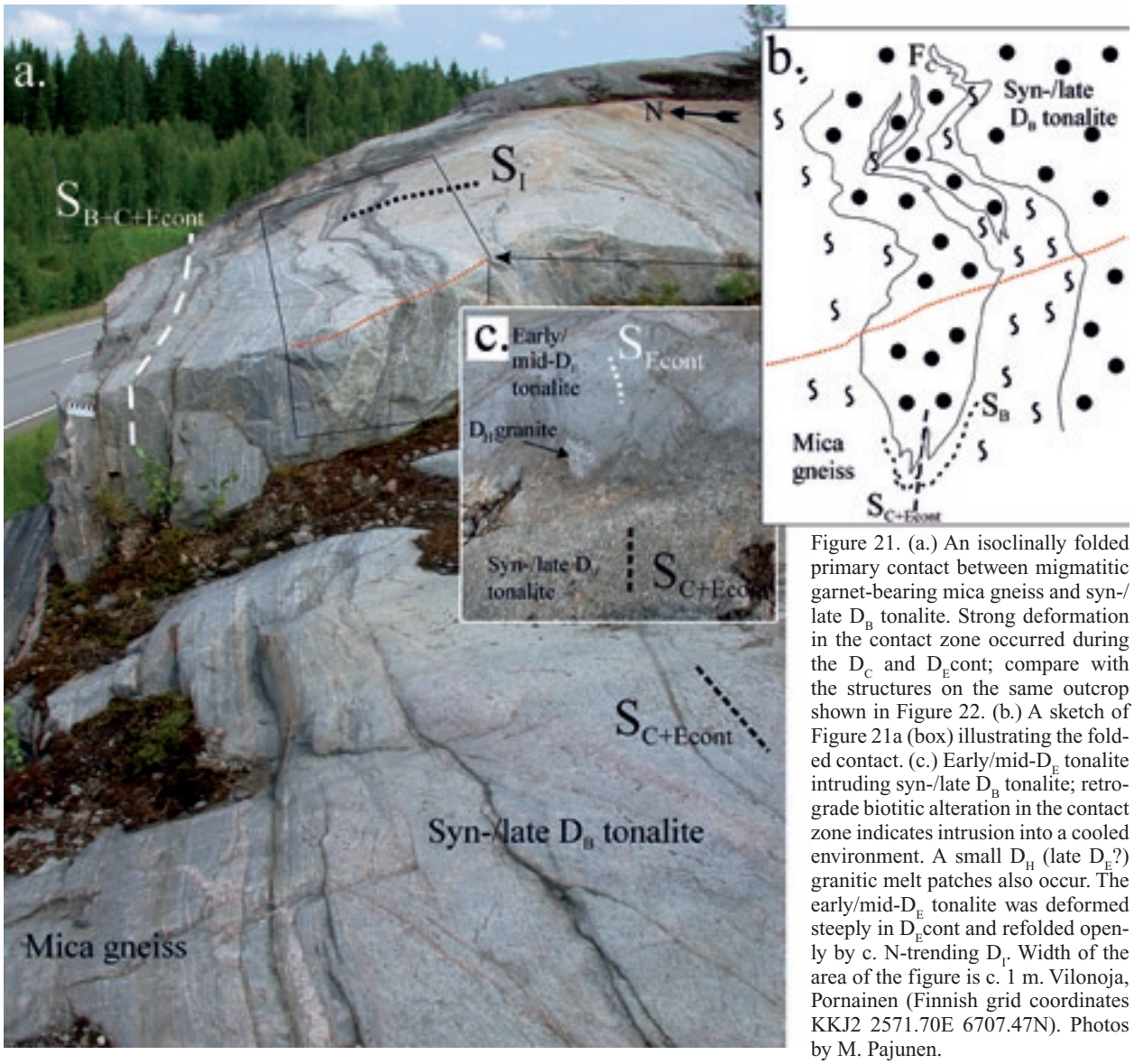

Figure 21. (a.) An isoclinally folded primary contact between migmatitic garnet-bearing mica gneiss and syn-/late D_B tonalite. Strong deformation in the contact zone occurred during the D_C and $D_E$cont; compare with the structures on the same outcrop shown in Figure 22. (b.) A sketch of Figure 21a (box) illustrating the folded contact. (c.) Early/mid-D_E tonalite intruding syn-/late D_B tonalite; retrograde biotitic alteration in the contact zone indicates intrusion into a cooled environment. A small D_H (late D_E?) granitic melt patches also occur. The early/mid-D_E tonalite was deformed steeply in $D_E$cont and refolded openly by c. N-trending D_I. Width of the area of the figure is c. 1 m. Vilonoja, Pornainen (Finnish grid coordinates KKJ2 2571.70E 6707.47N). Photos by M. Pajunen.

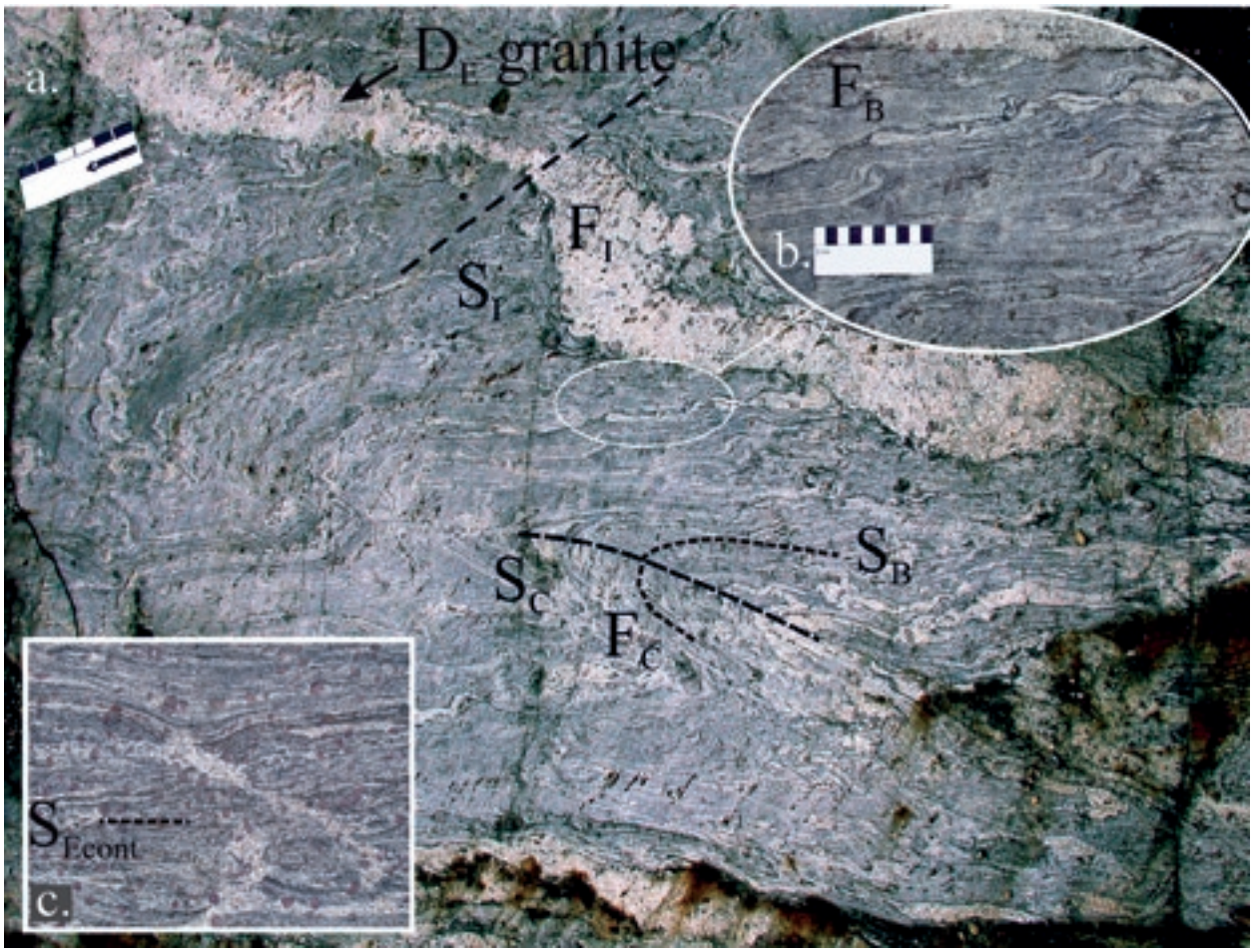

Figure 22. (a.) Migmatitic garnet-bearing mica gneiss showing the relationships between the D_B, D_C, D_E and D_I structures and related migmatization events. Scale bar is 15 cm in length. (b.) F_B folds in trondhjemitic neosome in mica gneiss. Scale bar is 10 cm in length. (c.) Extensional granitic D_E melt fraction in mica gneiss. Width of the area of the figure is c. 1 m. Vilonoja, Pornainen (Finnish grid coordinates KKJ2 2571.70E 6707.47N). Photos by M. Pajunen.

deformation succession of the tonalite (Figure 24a) is determined by the following structures: 1) intrusion (likely as described above); 2) the formation of early foliation S_C – preserved in a dextrally-rotated fragment in the microtonalite dyke, elsewhere strengthened by later events (see point 4); 3) the generation of early quartz veins indicating low-grade fracturing deformation; 4) the intrusion of an intermediate microtonalite dyke with chilled margins (Figure 24b), which along with the fragments in the dyke (Figure 24c) demonstrates intrusion into cool tonalite; 5) the formation of new steep spaced foliation, $S_E$cont (Figures 24a, b and c), which also developed as penetrative in the dyke; 6) an increase in temperature causing partial decomposition of biotite to form garnet and granitic melt, and forming an amphibolite-facies assemblage in the dyke; patchy destruction of the previous structures (Figure 25a); 7) the formation of D_E shear bands with medium-grained coarsening or granitic melt/segregation in the highest-strained zones (Figure 25b); 8) foliated, slightly pinching-and-swelling D_H pegmatitic granite dykes (Figure 24a, upper left corner); 9) the formation of shear bands with granite or quartz in the highest-strained zones – they are less common and locally lower-grade shearing is related to them (Figure 25c), and we interpret that they represent D_I (correlate to point 10); 10) semi-ductile shearing (Figure 23b) along the border zone – the eastern contact is bordered by the steep Vuosaari-Korso shearing structures showing east-side-up movement of $D_{I+(P?)}$ (cf. Elminen et al. 2008).

The structures in the syn-/late D_B tonalites give evidence for a cooling stage before the intrusion of the intermediate microtonalite dykes (e.g. early quartz veins, straight contacts of dykes with chilled margins). The evolution was followed by an increase in temperature that caused the continuing processes, the generation of a foliation, the formation of extensional shear bands and the decomposition of biotite forming garnet and granitic melt patches; these are related to the complex extensional D_E-D_H events. We relate the retrogression of pyroxene in the D_B tonalites to this new D_E melting and fluidization, and prograde metamorphism. Open warping of the main foliation and later lower-grade shear bands, representing the later shortening events, also give evidence for cooling towards the end of the succession.

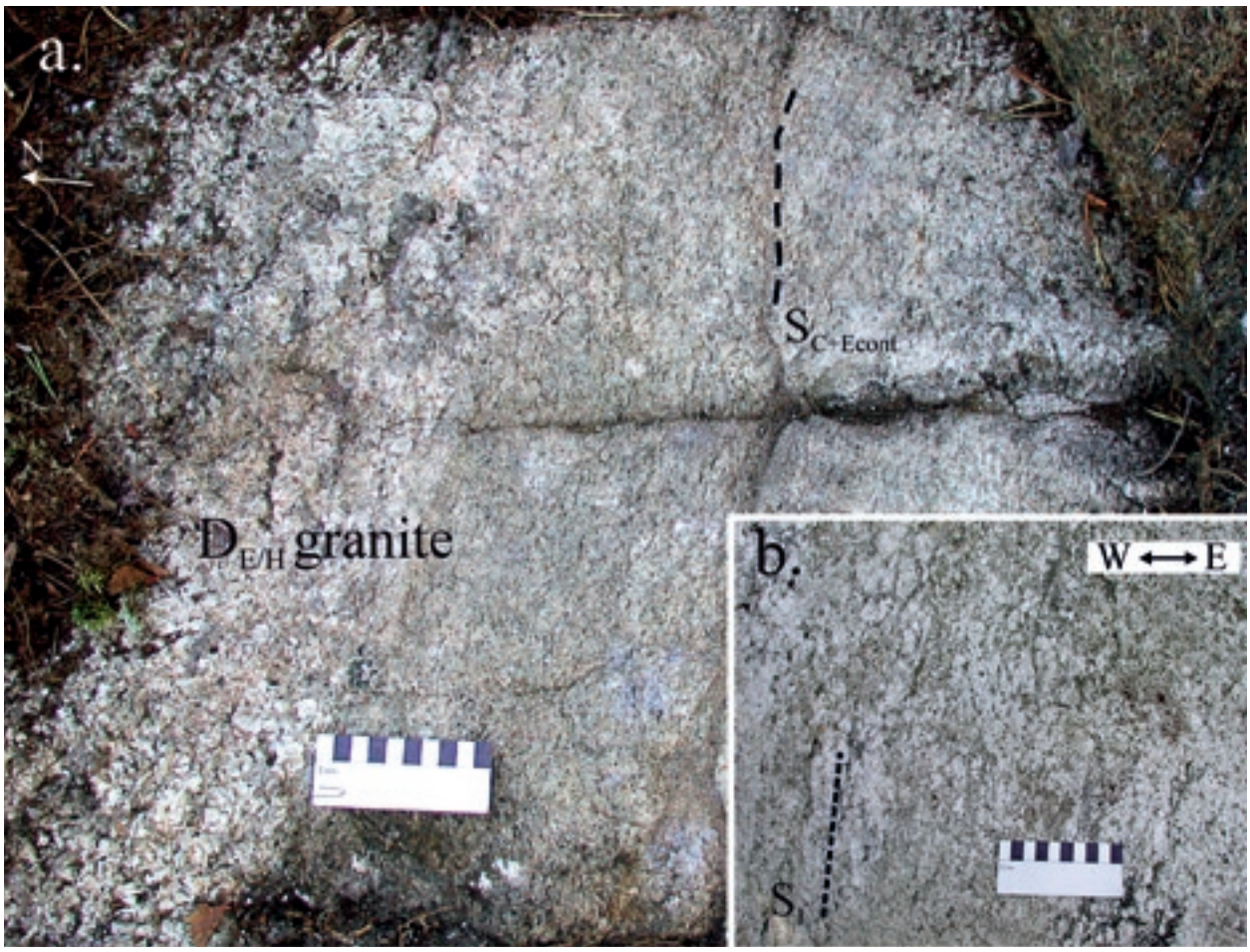

Figure 23. (a.) The E-trending northern contact between the Hindsby syn-/late D_B tonalite and D_E pegmatitic granite. Scale bar is 10 cm in length. Högbacka, Sipoo (Finnish grid coordinates KKJ2 2565.71E 6694.91N). (b.) Vertical section of sheared contact of the Hindsby tonalite against the Vuosaari-Korso shear/fault zone. Scale bar is 10 cm in length. Stormossen, Sipoo (Finnish grid coordinates KKJ2 2565.36E 6691.71N). Photos by M. Pajunen.

Age of D_B deformation and correlations

The earliest structurally-fixed magmatic rocks in the Southern Volcanic-sedimentary Belt (SVB) are the rocks of the gabbroic association showing a penetrative S_B. Hopgood et al. (1983) dated magmatic gabbros at 1885 ± 7 Ma, and banded dioritic gneiss, a neosome for agmatite, at 1895 ± 13 Ma from the Jussarö-Skåldö area. Structurally comparable mafic rocks in the Hyvinkää Gabbroic-volcanic Belt (HGB) show similar D_B evolution of the gabbros and the closely-related supracrustal associations without D_A structures (Appendix 3). The published age of the Hyvinkää gabbro (Patchett & Kouvo 1986 and Patchett et al. 1981) is 1880 ± 5 Ma, which is same as the age of 1880 ± 3 Ma for the plagioclase porphyrite in Hyvinkää (Suominen 1988). Within the error limits, this is the same age as for the younger, post-D_A to early-D_B volcanic Series II, dated from Orijärvi (Väisänen & Mänttäri 2002). The post-D_A/pre-D_B mafic and intermediate dykes (Figures 13b and 14a and b) of the study area belong to the younger volcanic Series II. The ages from Jussarö-Skåldö (Hopgood et al. 1983) have such a large error that both alternatives, the pre-D_A volcanic Series I and early D_B Series II, hold true. Thus, further work is needed to establish the setting of these mafic associations and to test whether the gabbroic associations represent two different sequences. The ages from the Hyvinkää gabbros prove their intrusion close to the regional D_B, because the age is close to that obtained from the syn-/late D_B tonalites. The structures formed in D_A were weak and could have been destroyed by the stronger D_B. This leaves the possibility that the southern gabbroic association belongs to the older, pre-D_A phase.

The maximum age of D_B in the Southern Volcanic-sedimentary Belt (SVB) and in the Espoo Granitoid Complex (EGC) can be established by the age of the post-D_A and pre-D_B volcanic sequence at c. 1.88–1.87 Ga. The syn-/late D_B tonalites intruded into the S_B plane of coexisting supracrustal rocks with strong D_B flattening and migmatization. The first penetrative foliation in these tonalite is S_C. These observations bind D_B deformation and migmatization between the ages of the later volcanic sequence and the tonalite intrusion. A magmatic age of 1873 ± 7 Ma (SIMS U/Pb zircons) was obtained

Figure 24. (a.) A metamorphosed early D_E intermediate microtonalite dyke cutting the syn-/late D_B tonalite (Hindsby intrusion) and pegmatitic D_H granite dykes (black arrow, upper-left corner). Hammer is 47 cm in length; N is to the left. (b.) The dyke shows a chilled margin that indicates intrusion into cooled rock. Width of the area of the figure is c. 0.4 m. (c.) The tonalite is S_C foliated and overprinted by the steep spaced $S_E$cont, which also deforms the dyke as penetrative foliation. The $S_E$cont shows a small shear component deforming the dyke margins. In the central part of the dyke $S_E$cont foliation is c. dyke-parallel. The fragment of tonalite in the dyke (c.) is S_C foliated, slightly rotated, and $S_E$cont is bent to surround it; the observation provides evidence of emplacement of the dyke post-D_C and prior to the strongest $D_E$cont deformation. The medium-grade metamorphic parageneses in the dyke indicates the new metamorphic event after intrusion into cooled rock. Width of the area of the figure is c. 0.7 m. Staffas, Sipoo (Finnish grid coordinates KKJ2 2568.93E 6694.67N). Photos by M. Pajunen.

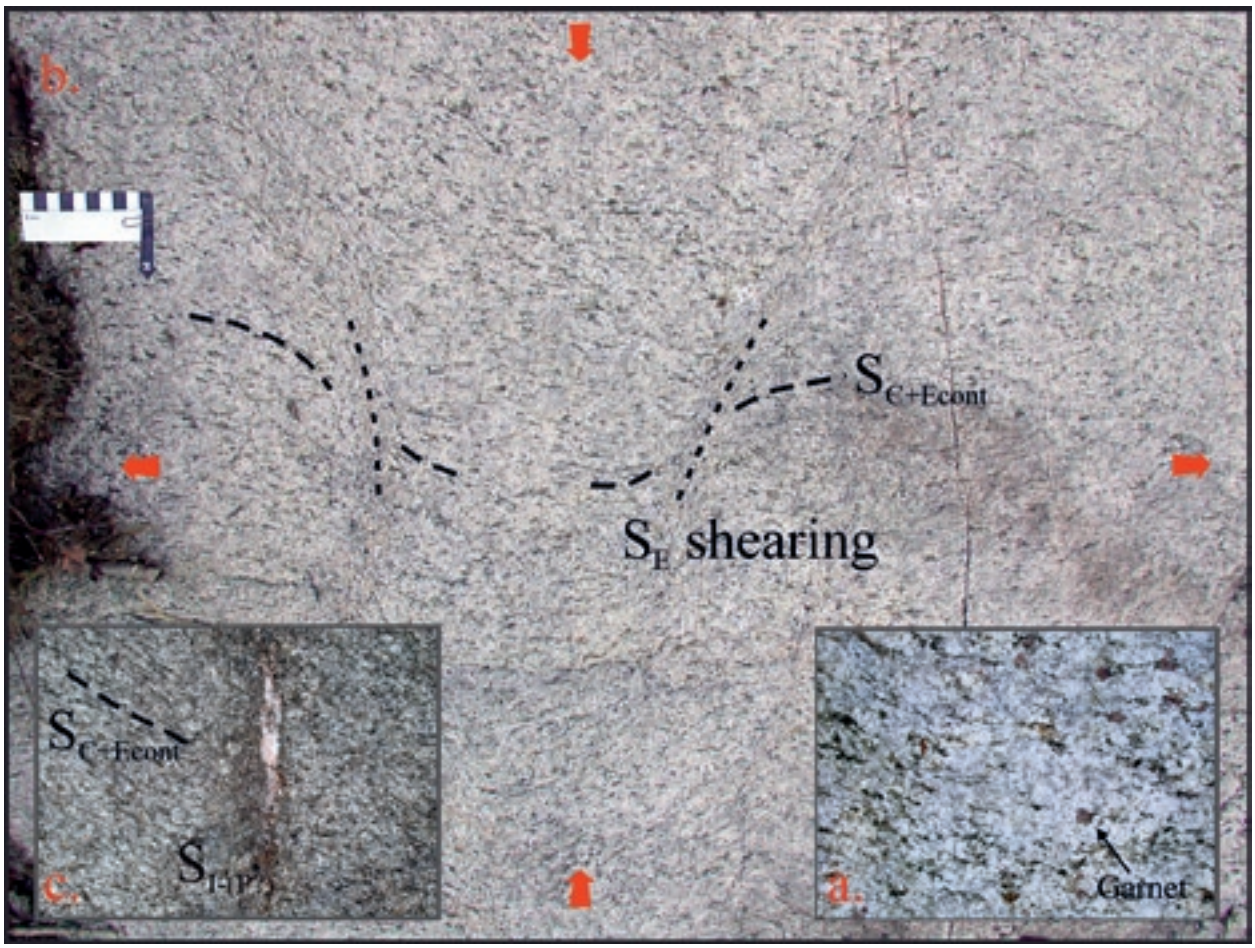

Figure 25. (a.) D_E granitic remelting patches in the syn-/late D_B tonalite. Biotite has decomposed to garnet and granitic melt. Width of the area of the figure is c. 20 cm. (b.) D_E shear band structures in syn-/late D_B tonalite; shear bands are characteristic for this magma phase. The shear bands are formed in N-S contraction. Scale bar is 10 cm in length. (c.) Later lower-grade shear bands in syn-/late D_B tonalite include quartz veining, instead of granite, in the shear plane. Drag folds related to shearing indicate c. E-W contraction that is characterizing the D_I. Width of the area of the figure is c. 30 cm. Stormossen, Sipoo (Finnish grid coordinates KKJ2 2565.36E 6692.07N). Photos by M. Pajunen.

from the Bollstad syn-/late D_B tonalite in Inkoo (mixed age of 1855 ± 6 Ma for zircons was obtained by TIMS method) (Appendix 8). A concordant age of 1829 ± 3 Ma (TIMS U/Pb monazite) for metamorphic monazite in this tonalite was obtained (Appendix 8). The Hindsby syn-/late D_B tonalite (sample A1738 Staffas), Sipoo, gives ages of 1876 ± 8 Ma (SIMS U/Pb zircons, Appendix 8) for the older zircon population, and of 1841 ± 4 Ma and 1801 ± 7 Ma for younger zircons. On the structural basis the age group of 1876 ± 8 Ma could represents the age of the intrusion, whereas the age of 1841 ± 4 Ma could be related to later metamorphism and lead loss; the tonalite shows typically small melt patches related to D_E (Figure 25a). The youngest ages are related to M_H metamorphism and older zircons are inherited.

The ages of 1.88–1.87 Ga are typical for the "syntectonic granitoids" and neosomes in southern Finland (Hopgood et al. 1983, Huhma 1986, Vaasjoki & Sakko 1988, Nironen 1999, Mouri et al. 1999, Väisänen et al. 2002 and Skyttä et al. 2006). The ages are on average 10 Ma younger than corresponding rocks in the northern units in the Tonalite Migmatite Belt (TMB) (e.g. Huhma 1986, Vaasjoki & Sakko 1988 and Nironen 1989). The tectono-metamorphic characteristics of the northern units (Pietikäinen 1994, Koistinen et al. 1996, Kilpeläinen 1998, Korsman et al. 1999, Nironen 1999, Pajunen et al. 2001a and Rutland et al. 2004), like the strong nearly-horizontal S_2 and flat-lying recumbent F_2 folds, prove strong vertical shortening deformation D_2 at c. 1.89–1.88 Ga; "syntectonic" intrusive rocks of this age also characterize the major parts of the Central Finland Granitoid Complex (CFGC) (Nironen 2003). The intense magmatism and migmatization, oblate horizontal flattening strain (cf. Koistinen et al. 1996) and widespread high-T/low-p metamorphism support an extensional D_2 event. D_2 is very similar to the c. 10 Ga younger D_B in the southern Granite Migmatite Belt (GMB). This suggests a different evolution of northern D_2 from the southern D_B, or that evolution was diachronic, becoming younger towards the south. In such a model

the Tonalite Migmatite Belt (TMB) was situated in the border zone of the intense D_B extensional belt. During the stage of local D_B extension in the south the TMB was already under contraction (D_3, see later). To the north of the GMB-TMB border, in the TMB, there are also granitoids of 1.88–1.87 Ga in age (cf. Kilpeläinen 1998), like the syn-/late D_B tonalite ages in the south. This suggests that the TMB and GMB were close to each other during their intrusion. Thus, the original accretion of the GMB and TMB already occurred during the southern D_A.

In the low-grade gneisses in Orijärvi area (Vetio outcrop, Appendix 4), the first foliation and the early andalusite-cordierite growth are related to the D_B, corresponding the higher-grade extensional D_B deformation in the lower crustal sections. Heating occurred under subsidence of the upper crustal sections. The metamorphic evolution is very similar in the andalusite schists in the Tampere schist belt (TSB, Kilpeläinen 1998) and in the Rantasalmi area (Ra in Figure 9, Korsman 1977 and Korsman & Kilpeläinen 1986). Large andalusite porphyroblasts are c. S_0-parallel and are overprinted by prograde metamorphism. Correspondingly, the TSB began to subside during the northern D_2 extension. The TSB is situated upon an E-W-trending electric conductive zone dipping north (Korja 1990) between the Vammala Migmatite Belt (VMB) and the Central Finland Granitoid Complex (CFGC). The zone has been regarded as a suture zone along which the conductive schists of an accretionary prism of the VMB were pushed below the CFGC (e.g. Lahtinen 1994, Kilpeläinen 1998 and Korsman et al. 1999).

Deformation D_C – N-S shortening

The predominantly horizontal D_B flattening was followed by a high-T, ductile shortening event, D_C, which deformed the early supracrustal and magmatic series to isoclinal or tight, originally E-W-trending folds with steep axial planes. In the study area, the D_C structures are best preserved in the Southern Volcanic-sedimentary Belt (SVB) in areas that were not effectively overprinted by the later D_E-D_H events. Examples of D_C structures are given in Figures 11, 15c, 20 a, 22a, 26b, 27a and b and 28 a and c. Figures 27a and b give an example of a garnet-amphibole rock, a silicate-facies iron formation of the

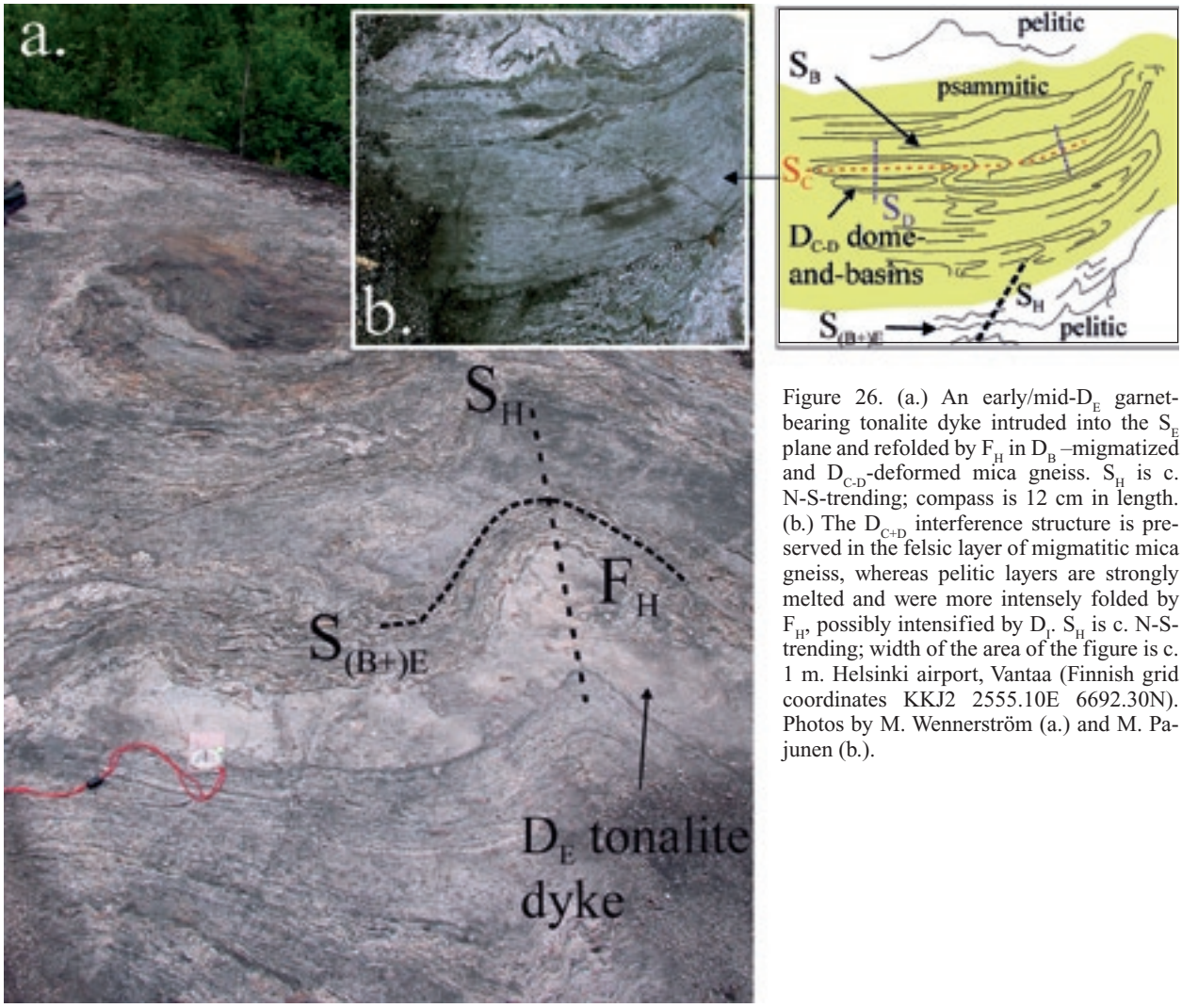

Figure 26. (a.) An early/mid-D_E garnet-bearing tonalite dyke intruded into the S_E plane and refolded by F_H in D_B –migmatized and D_{C-D}-deformed mica gneiss. S_H is c. N-S-trending; compass is 12 cm in length. (b.) The D_{C+D} interference structure is preserved in the felsic layer of migmatitic mica gneiss, whereas pelitic layers are strongly melted and were more intensely folded by F_H, possibly intensified by D_I. S_H is c. N-S-trending; width of the area of the figure is c. 1 m. Helsinki airport, Vantaa (Finnish grid coordinates KKJ2 2555.10E 6692.30N). Photos by M. Wennerström (a.) and M. Pajunen (b.).

Southern Volcanic-sedimentary Belt (SVB), from Nöykkiö, Espoo. The outcrop is situated close to the Porkkala-Mäntsälä high-strain zone. The competent garnet-amphibole rock, however, shows only moderately strained D_{C+D} structures refolding S_B. The D_{C+D} structures are overprinted by steep shear zones (Figure 27c) and weak folding that are related to the Porkkala-Mäntsälä shear/fault zone. The rock also shows patchy melting structures due to D_E.

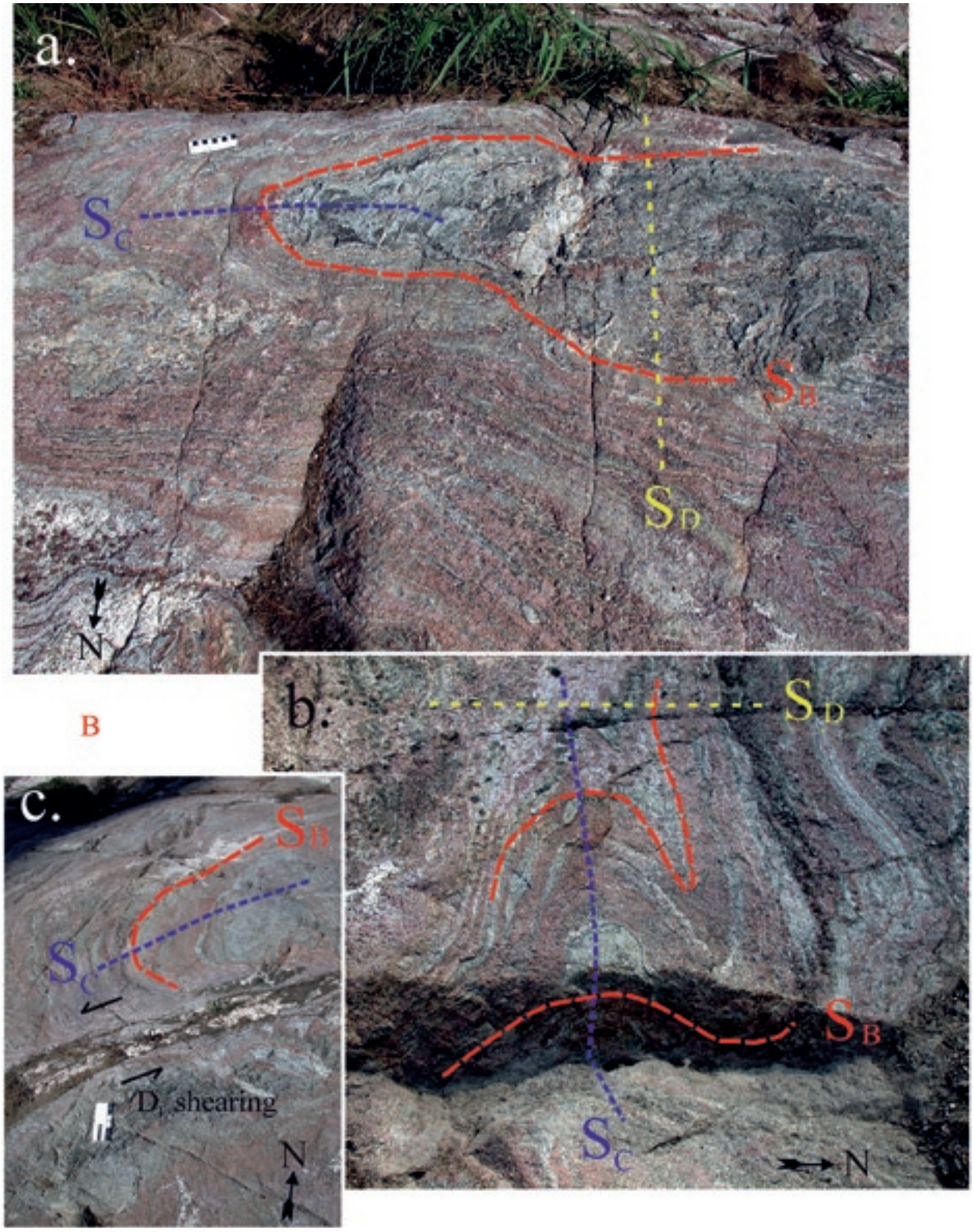

Figure 27. (a.) D_{C+D} interference pattern in a competent garnet-amphibole rock (silicate facies iron formation); the F_C axis is dipping towards W. Scale bar is 10 cm in length. (b.) Vertical section of the same interference structure; the F_C axis is dipping towards W. Width of the area of the figure is c. 1 m. (c.) A D_F shear zone, related to deformation in the Porkkala-Mäntsälä zone under N-S contraction, cuts the D_{C-D} dome-and-basin structure; the F_C axis is dipping towards E. Scale bar is 15 cm in length. Nöykkiö, Espoo (Finnish grid coordinates KKJ2 2536.88E 6672.79N). Photos by M. Pajunen.

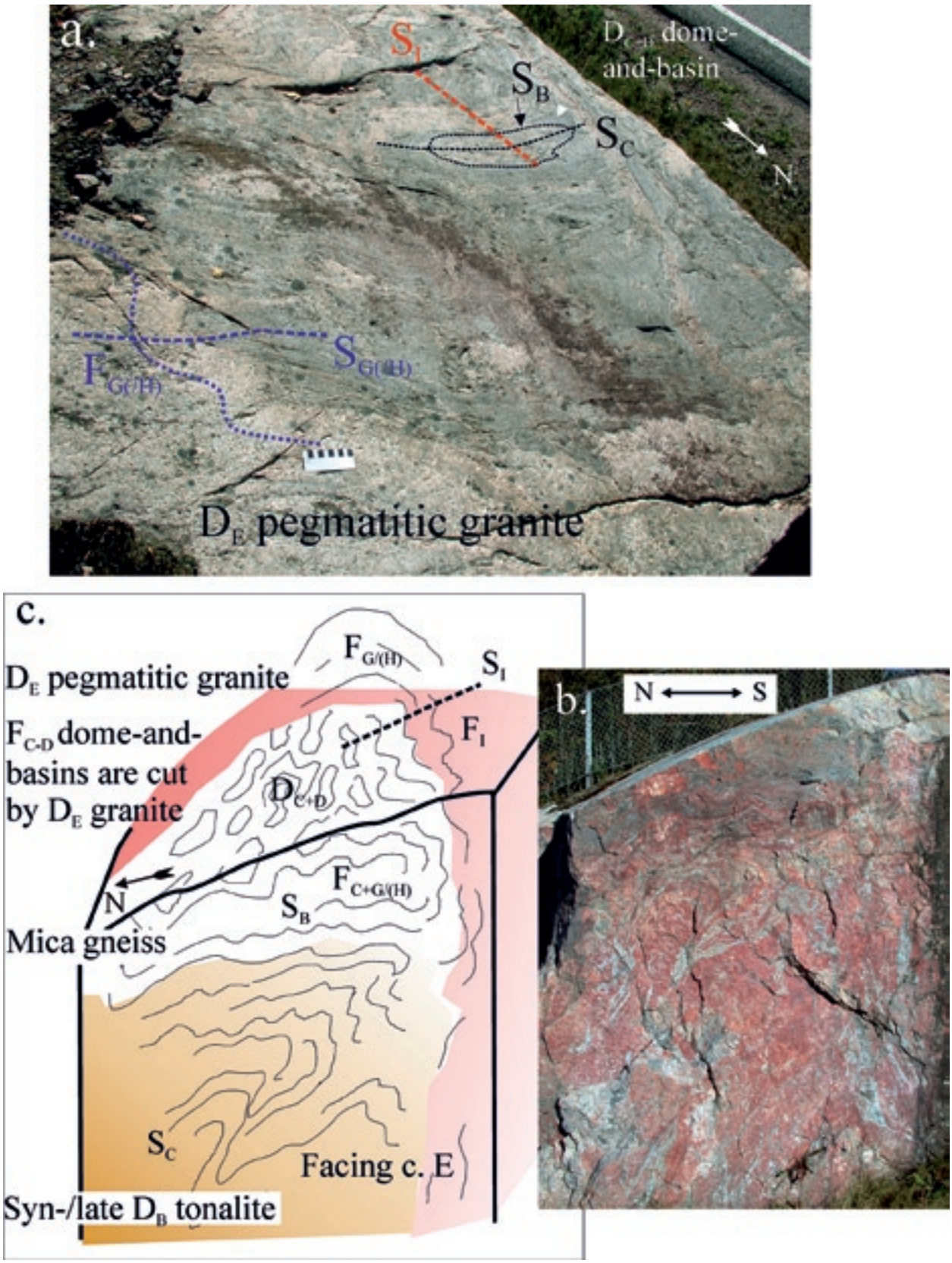

Figure 28. Migmatitic felsic gneiss with a deformed S_{C+D} dome-and-basin interference structure on the horizontal surface (a.); scale bar is 10 cm in length. Vertical surface is shown in (b.); width of the area of the figure is c.2 m. Indistinct relations between the gneiss and tonalitic rock are due to strong granitic melting and intruded dykes. (c.) Interpretation of structure: The S_B foliation plane in felsic gneiss is folded to form D_{C+D} dome-and-basin structures. The D_{C+D} dome-and-basin interference structure is cut by $F_{G/(H)}$-folded D_E pegmatitic granite. $F_{G/(H)}$ intensified the F_C folds, because the axial planes S_C and $S_{G/(H)}$ are approximately parallel. The first foliation in the strongly granitized syn-/late D_B tonalite including remnants of the mica gneiss is S_C (cf. the mica gneiss-tonalite contact in Figure 21). Thus, in the mica gneiss $F_{G/(H)}$ refolds the foliation $S_{B+later}$, whereas in the tonalite it refolds $S_{C+later}$. The vertical section shows a southwards-overturned structure, interpreted as $F_{G/(H)}$, which was refolded by F_I with a c. NW-trending axial plane. This complicated structure is preserved in between the strongly migmatitic rocks characterizing the southern Sipoo area. Söderkulla, Sipoo (Finnish grid coordinates KKJ2 2571.49E 6689.11N). Photos by M. Pajunen.

In the Espoo Granitoid Complex (EGC) the D_C structures have been hidden or destroyed by later deformations, metamorphism and magmatism. The vast majority of the felsic magmatism in the EGC post-dates D_C. For example, in the southern Sipoo area, to the east of the Vuosaari-Korso shear/fault zone, granitic rocks are often nebulitic or schlieren migmatitic. The complexity of structures is exemplified by migmatitic granite at the Söderkulla site, Sipoo (Figures 28a-c). A mica gneiss-tonalite remnant within the granitic unit shows D_{C+D} dome-and-basins deforming the early D_B migmatization and S_B foliation of the mica gneiss, and the S_C foliation of tonalite. No D_A features were preserved/identified. These structures were cut by D_E pegmatitic granite, which, along with the early structures, was overturned southwards by $F_{G/(H)}$ folds with c. E-trending axial planes. There are some kinematic observations indicating to D_G tectonic transport southwards (Figure 19). However, the F_H folds are mostly overturned towards NW, such as to the west of the Vuosaari-Korso zone (Figure 12c). The latest ductile deformation identified at e Söderkulla site is open D_I folding with c. NW-trending axial planes. The deformations $D_{G/(H)+I}$ form an open dome-and-basin structure upon the D_{C+D} ones.

The tight to isoclinal F_C folds are round-hinged, without significant thickening of hinges or thinning on limbs. In the pre-D_C rocks, with strong S_B foliation and migmatization, no significant mineral growth occurred in the S_C axial plane. S_C is indistinct, or weak crenulation and only locally some melt remobilization sometimes occurred in the axial planes. S_C is the first penetrative foliation in the syn-/late D_B tonalites. Minor new D_C mineral growth suggests a decrease in temperature after the peak metamorphic conditions during the D_B. However, close timing of D_B and D_C is suggested by the large amounts of syn-/late D_B tonalites showing S_C as their first foliation. The biotitic-hornblendic tonalite foliation indicates amphibolite facies conditions.

D_D deformation – E-W shortening and D_{C+D} dome-and-basin structures

Refolding of F_C folds by the ductile F_D folds with c. N-trending, steep axial planes formed the dome-and-basin interferences, D_{C+D}, seen on both the map scale (Figure 11) and outcrop scale (Figures 26b, 27a and b, 28a and c). The F_D folds are open to tight, more open than the F_C folds. No significant mineral growth in the S_D axial plane has been identified. The D_{C+D} dome-and-basin structures are deformed by the later tectonic events, e.g. by the less-strained, map-scale D_{G+H+I} interference structures (Figure 11). On outcrops they only openly to weakly refold the D_{C+D} structures (Figures 22, 26a and b).

Regional analysis of the F_G and F_D folding patterns requires investigation of their foliation-fold axis-lineation relationships, which is not possible by using our limited-area field observations alone. On the outcrop scale the structures are mostly small, only partly exposed or reoriented by the later deformations, so that the analysis does not give regionally correlative results. A generalized idea of D_{C+D} dome-and-basin forms and related kinematics can be obtained by studying the D_{C+D} structures using the geological maps of the GTK on the scale 1 : 100 000. The following preliminary analysis is carried out using tectonic measurements on the maps, in the areas not intensely intruded by magmas of the Southern Finland Granitoid Zone (SFGZ) or not located in zones of intense D_{H-I} deformation.

The Pellinki area (Pe in Figure 9) shows a D_{C+D} structural pattern with S_C dipping steeply south (the main foliation S_B is mostly dipping 90–70° towards south). The orientations of F_C fold axes and $L_{A+B/C}$ lineations (generations established by correlation to the study area) give steeply a northwards overturned, isoclinal-tight fold pattern for the F_C, and a westwards overturned moderate pattern for the F_D (the interpreted F_C fold axes are generally steeper on the western end of the D_{C+D} domes than on the eastern end, and opposite for the synformal structures). This indicates N-S shortening during D_C and E-W shortening during D_D. Analysis from the southwestern archipelago to the SW of Turku gives similar kinematics for the D_C, but F_D folds show an eastwards overturned pattern. Analysis of the borders of the major N-trending tectonic block, between the Baltic Sea-Bothnian Bay Zone (BBZ) and the Riga Bay –Karelia Zone (RKZ), suggests opposite overthrusting patterns in the western and eastern parts of the block during the D_D (Figure 8). This may indicate that the bordering structure of the block dips towards the west in the BBZ and towards east in the RKZ. A rough estimate of D_C shortening based on the forms of the F_C folds in the Southern Volcanic-sedimentary Belt (SVB) gives a value of about 40–50%; that of D_D is somewhat less, with shortening of c. 20–30%. These analyses are preliminary and further research is needed to specify the regional variations in D_C and D_D kinematics more comprehensively.

Ages of D_C and D_D deformations and correlations to the northern tectonic units

Structural and mineral growth relations indicate that the compressional D_C evolution rapidly followed the formation of the later volcanic Series II and the

syn-/late D_B tonalites at c. 1.88–1.87 Ga. The D_3 deformation in the Tonalite Migmatite Belt (TMB) can be dated at c. 1.89–1.88 Ga by following the deformation succession of Kilpeläinen (1998), and the ages of syntectonic Hämeenkyrö and Värmälä intrusions (Nironen 1989) (Appendix 1). The E-W-trending D_3 in the northern units is slightly older than D_C in the south; it is about the age range of the southern D_B. Compression in the north was, accordingly, simultaneous with D_B in the south. Because of the rapid evolution from D_B to D_C in the study area, and the contemporaneous extensional D_B in the south and contractional D_3 in the north, we suggest that the crust was in its entity under a compressional stress field, i.e., under continuous collision towards the north. The northern D_2 and southern D_B are similar strong deformations, accompanied by prograde, high-T/low-p metamorphism (e.g. Korsman et al. 1999). We suggest they represent an extensional crustal evolution between the compressional D_A (or D_1 in the north) and D_C (or D_3 in the north). The evolution from the northern D_2 at c. 1.88–1.89 Ga to the southern D_B at 1.88–1.87 Ga was a diachronic process that progressed southwards. Similarly, the D_3 (north) and D_C (south) represent evolution that was diachronic, getting younger southwards. The end of D_C is determined by the rotation of the N-S stress field to SW-NE during D_D. In the study area the setting of the oldest dated early D_E Hakkila tonalite cutting the D_D structures is 1868 ± 3 Ma old (see later discussion and Appendix 8).

The $D_{C\text{-}D}$ folding pattern in the Southern Finland Volcanic-sedimentary Belt (SVB) is systematic, but is more complex further north. In the Pori area Pajunen et al. (2001a) described F_4 folding with a N-trending axial plane deforming the $D_{2–3}$ structures, and Nironen (1999) described a D_4 structure refolding earlier structures into the Pomarkku block structure in the Loimaa area (see Figures 9 and 11). The tectonic formline pattern shown in Figure 11 suggests that corresponding dome-and-basin deformation ($D_{3–4}$) also occurred in the Vammala migmatite belt (VMB), but it was deformed by a complex sliced structural pattern with c. NW- and NE-trending deformation zones. These zones characterize the Hämeenlinna stacked terrane (Figure 10) in the border zone between the Granite Migmatite Belt (GMB) and the Vammala Migmatite Belt (VMB) in the Tonalite Migmatite Belt (TMB). The Pomarkku block structure represents the western end of this structure; we relate the block formation to c. SW-NE transpression D_4/D_D (Appendix 7 and Appendix-Fig. 7-1c).

In the Central Finland Granitoid Complex (CFGC), D_3 produced the northwestwards stacked structure (Figures 8, 9 and 10) that was later sliced by NW-trending D_4 (D_b shear zones of Pajunen 1986) and later N-trending (D_d shear zones of Pajunen 1986) shear zones. The 1.89–1.88 Ga (Vaasjoki & Sakko 1988) granitoids in the CFGC are generally deformed and locally show low-angle foliation dipping SE (S_3). Kilpeläinen (2007) also described a low-angle shear zone from the Savo Schist Belt (SSB) and CFGC border. Primarily, we suggest this to correspond to the D_3 stacking shear structures. The generation of this magmatic complex followed the accretion of the CFGC against the 1.93–1.91 Ga old primitive island arc of the Savo Schist Belt (SSB) and the Archaean continent. The CFGC was fixed to the SSB along a complex structure; originally it was deformed by the D_3 stacking northwestwards and slicing, which during later evolution was folded and fragmented by the zonal D_4 NW-trending shearing. The shear zones are characterized by a strong granite magmatism and granitization (Pajunen 1986 and Pääjärvi 1991) and by a linear gravity low (Korhonen et al. 2002b). Thus, D_3 resulted in a continued northwards collision, forming stacked units that became folded and fragmented during D_4.

No age determination has been carried out to date for the D_D folding structures in the Granite Migmatite Belt (GMB), but correlation with the northern units is supportive. The D_4 block deformation can be dated with post-/late tectonic granitoids emplaced into the arched structures characterizing the block structure of the areas of Pomarkku block (Appendix 7 and Appendix-Fig. 7-1c) and Central Finland Granitoid Complex (CFGC) (Figure 9). The transpressional N-NW slicing, D_4, together with the earlier NW-stacked D_3 structure, formed the arched structures into which these late/post-tectonic granitoids were intruded. According to our interpretation, these granitoids are syn-D_4 intrusions emplaced in oblique dilatational settings during the NE-SW transpression. These granitoids effectively destroyed the older collisional D_3 thrust structures in the CFGC. In the west, to the north of the Pomarkku block, a weakly deformed quartz monzonite, dated at 1872 ± 2 Ma (Mäkitie & Lahti 2001), is a typical syn-D_4 intrusion. In the CFGC corresponding intrusions vary in age, being younger towards the west: 1886 ± 6 to 1885 ± 5 Ma (E part), 1882 ± 2 to 1880 ± 3 Ma (central part), 1880 ± 5 to 1874 ± 4 Ma (SE part), 1875 ± 2 Ma (S part) and 1872 ± 2 to 1870 ± 4 (W part) (ages from Mäkitie & Lahti 2001 and Nironen 2003; dating with large errors is excluded). The age of the ductile D_D folding in the south can be bracketed between the syn-/late D_B tonalite ages (1.88–1.87 Ga) and the early D_E tonalite dykes (the oldest dated Hakkila dyke is 1868 ± 3 Ma). Because the stress field remained in a NE-SW direction

during the early D_E deformation, a transitional transformation from D_D to D_E is suggested.

In eastern Finland, in the Proterozoic allochthonous sequences lying upon the Archaean basement, the earliest deformations, D_{1-2}, are related to thrusting and crustal thickening at c. 1.9 Ga ago (Koistinen 1981). This collision juxtaposed a 1.93–1.91 Ga old primitive island arc (Lahtinen 1994, Kousa et al. 1994 and Korsman et al. 1999) – the Savo Schist Belt (SSB) – and the Archaean domain, causing the obduction of 1.95 Ga ophiolites, described by Kontinen (1987), together with the early rift and passive margin sediments (Koistinen 1981). Prior to the 1.95 Ga rifting the Archaean continent was covered by platform sediments that are now preserved near the craton border zone and between the wide tectonic slices of the Archaean unit. These tectonic slices of the Archaean domain have a surprisingly similar geometry to the D_4 slices in the northern Svecofennian unit, e.g. the Pomarkku block. These structures formed earlier in the east than in the west. The Proterozoic-Archaean boundary zone was already strongly deformed before the intrusion of the 1884 ± 5 Ma orthopyroxene-bearing monzonites (Hölttä 1988). Their contact aureoles cut the regional fold structures in the Savo Schist Belt (SSB), but some ductile shearing in the contact aureole (Hölttä et al. 1988) proves that deformation was already localized at the time of monzonite intrusion. These intrusions terminate the main stage of deformation and metamorphism near the craton boundary. We propose a corresponding generation for the major geometry in the Archaean domain and in its boundary zone to that further west: D_3 N-S compression and $D_{4/D}$ SW-NE transpression. The craton boundary area did not undergo an extensional event characterizing its evolution, such as $D_{2/B}$ in the southern Svecofennian domain. The thick crust is preserved in the craton boundary area, and it thins towards the southwest (Luosto et al. 1990). The continued $D_{3/C}$ north-south compression followed by $D_{4/D}$ SW-NE transpression prevented the major extensional thinning of the crust. Korsman et al. (1999) already suggested this kind of continuous compression model to explain the preservation of the thick crust.

We suggest that the syn-D_4 granitoids determine the age of the D_4 arching and fragmentation in the north. The younger Härkmeri quartz monzonite, dated at 1868 ± 3 Ma (Lehtonen et al. 2005), caused a metamorphic contact aureole on regional metamorphic assemblages and cut the D_4 block structure in the north (Appendix 7). The age of the intrusion establishes the end of D_4 in the western Tonalite Migmatite Belt (TMB) and the Central Finland Granitoid Complex (CFGC). To the north of the Vittinki zone the strongly migmatitic Vaasa area (Va in Figure 9), which continues to the Swedish coast, has, according to Rutland et al. (2004), been pushed from the west to its present setting. We agree with the eastward movement of the unit and suppose the deformation to be related to syn-D_4. Movements have occurred still later during the D_F deformation (see later). Thus, the termination of the D_4 in Central Finland occurred primarily between 1884 ± 5 Ma in the east and 1868 ± 3 Ma in the west. D_4 development thus shows a similar diachronic evolution, becoming younger towards southwest that became evident from the earlier tectonic events $D_{2/B}$ and $D_{3/C}$. In the south the ductile F_D folding occurred simultaneously with the northern D_4 fragmentation, but it continued longer due to the continuing NE-SW stress field under increasing high heat flow.

Structures related to the evolution of the Southern Finland Granitoid Zone

In the Southern Finland Granitoid Zone (SFGZ), structures in intrusive rocks play a key role in analyzing the geotectonic evolution of the zone; therefore, the structural relationships of intrusive rocks on representative outcrops will be discussed in detail.

From D_D to D_E deformation – begin of the Southern Finland Granitoid Zone evolution

In the study area the Hakkila early D_E garnet-bearing tonalite dyke (Figure 29) has an age of 1868 ± 3 Ma (SIMS U/Pb zircons, Appendix 8). This granitoid phase intruded into dilatational structures in a hot and ductile environment, into migmatitic mica gneiss, that was already deformed into D_{C-D} dome-and-basin structures. Thus, D_D is at least partly older than these tonalitic intrusives. These early D_E tonalitic intrusions determine the beginning of D_E deformation in the study area; they also establish the beginning of evolution of the Southern Finland Granitoid Zone (SFGZ). The tonalite age is exactly the same as that of the Härkmeri quartz monzonite (Lehtonen et al. 2005) cutting the D_4 structure to the north of the Pomarkku block (Appendix 7). The monzonite determines the termination of the major deformations in the north.

The age data demonstrate that tectonic evolution changed rapidly from the extensional D_B to the contractional D_C and transpressional D_D, and finally to the dilatational events labelled here as D_E. These changes occurred in the study area between the intrusion of the syn-/late D_B tonalites at c. 1876 ± 8 Ma and the garnet-bearing early D_E tonalites at c. 1868 ± 3 Ma. This also means that the discordances

described as characterizing the southern Svecofennian domain are transitional and the evolution was more continuous. Deformation did not affect the whole crust, accreted during its early tectonic evolution, to the same extent, but began to deform it in more zoned and patchy pattern.

The SFGZ, formed predominantly during the D_E and D_H, shows large variations in magmatic, metamorphic and structural characteristics in different parts of the zone and during different stages of the evolution of the zone. The composition of magmatism changed with time; it was tonalite-dominant in the early stages (D_E) and changed to granitic during its late evolution (D_H); small amounts of mafic intrusive rocks also evolved. The major N-trending Baltic Sea-Bothnian Bay Zone (BBZ) and Riga Bay Karelia Zone (RKZ) are related to the D_I deformation; the evolution of these structures was partly concurrent with the SFGZ evolution, but the late stages of the D_I structures deformed the SFGZ (Figure 11).

D_E deformation – oblique extension under NE-SW transpression

D_E structures and syn-tectonic intrusions overprint the D_{C+D} dome-and-basin structures. On outcrops, D_E structures are sometimes very similar to those of the D_B and need identification based on their relationships to the D_{C+D} or D_G and D_H structures. The depositional evolution of the Jokela supracrustal association is predominantly related to the D_E and is described in detail in Appendix 5.

Structures in early to mid-D_E tonalite-granodiorite dykes and intrusions

Metamorphosed, folded and fragmented garnet-bearing tonalitic dykes and larger intrusive bodies cut migmatitic gneisses in the Espoo Granitoid Complex (EGC), like at the Hakkila site in Vantaa (Figure 29, sketch of outcrop in Figure 13a) and the Hyrylä site in Tuusula (Figure 30a). The Hakkila rock cuts typical veined garnet-mica gneiss with preserved volcanic remnants, intense D_B migmatization and D_C deformation described above. Closeby, to the north of Helsinki-Vantaa airport, a corresponding garnet-bearing tonalite-granodiorite dyke intruded into the S_E plane (Figure 26a) and cuts the D_{C+D} (Figure 26b). The Hyrylä tonalite (Figure 30a) cuts a strongly foliated and migmatitic garnet-cordierite gneiss. The primary features of the gneiss almost disappeared and the dyke is less fragmented than that in Hakkila; this indicates more proceeded deformation in Hyrylä than in Hakkila. The contact zone of these dykes is granitic-pegmatitic, suggesting that the early magma/migmatite phase intruded in slightly cooler conditions than the later medium-grained central tonalite pulse. The dykes have an early $S_E$cont mineral foliation parallel to the dykes. The folds have granitic neosome in axial planes and show mobile fragmentation. The folds are related to $F_{H\pm I}$ and the composite pegmatitic granite-tonalite dykes are related to early D_E. These garnet-bearing tonalitic rocks represent the earliest D_E magma phases generated during the evolution of the Southern Finland Granitoid Zone (SFGZ) and cutting the D_{C+D} structures.

In Hyrylä, a larger garnet-bearing tonalite body, closely associated with and tectonically corresponding to the tonalite dyke, shows a nice layered pattern (Figure 30b). The steeply NW-dipping layers are systematic in showing narrow biotite-rich planes bordered against a coarser-grained granitic portion that in part grades into finer-grained tonalite. These layers are repeated and in places the new set cuts the earlier one with a low angle. We interpret the layers as magmatic; they formed during repeated magma injections and continuous dilatation. Some crystallization occurred between pulses, but the ductile character of the layer relations and garnet microstructure suggest crystallization from magma and indicate a high-temperature environment during the layer generation. The pegmatite-granite contacts locally show in-situ melting characteristics with the country rock migmatites. However, the central dykes sometimes sharply cut the pegmatite, indicating their longer transport distance. Dilatation occurred perpendicular to the NW-directional magmatic layering (Figure 30b) and is consistent with the SE extension; the dextral shear zone in Hyrylä (Figure 30c) was generated concurrently with the SE extension.

A similar pegmatitic granite-granodiorite dyke cuts the pre-D_B gabbro-tonalite association in Kirkkonummi, at the Sarfvik site. Discordance between the gabbro and the D_E dyke is shown in Figure 18a. The gabbro was cooled before the intrusion of the dyke, as shown by the retrograde alteration zone surrounding the dyke (Figure 18d). Medium-grained granodiorite in the dyke centre represents hotter magma with a longer transport distance – the same granodiorite cuts close by the country rock with intrusive contacts. The dyke intruded into a dilatational fracture, but the contact character indicates intrusion into a cooler environment than in Hakkila and Hyrylä, which are closer to the granulitic unit of the West Uusimaa granulite Complex (WUC). It also differs from the previous dykes by its more granitic composition and absent garnet. The intrusion into a cooler environment indicates either a later intrusion event or intrusion in the margin area of the major D_E

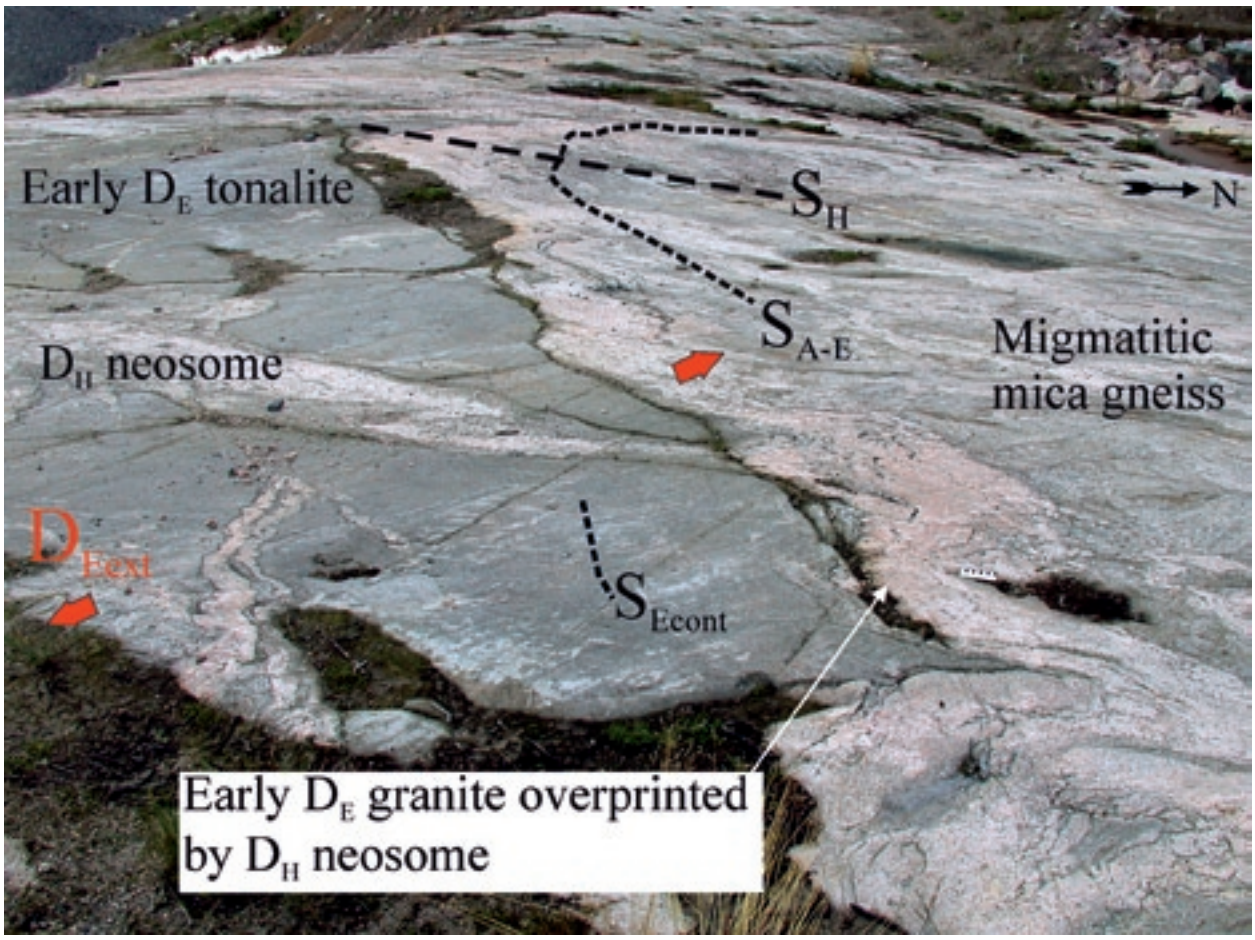

Figure 29. Garnet-bearing early D_E tonalite cutting migmatitic mica gneiss (see location in Figure 13). The dyke cuts the D_{A-D} structures (cf. Figure 26). The early intrusive phase of the dyke is represented by pegmatitic granite in the dyke margins. Tonalite intruded during progressive dilatation into the pegmatitic dyke phase. The composite dyke was deformed by progressive D_E ($S_E$cont) and fragmented by later by $D_{H(-I)}$. A new granitic melt was also generated and it intruded into the $S_{H(-I)}$ axial planes. Scale bar is 10 cm in length. Hakkila, Vantaa (Finnish grid coordinates KKJ2 2560.64E 6687.59N). Photo by M. Pajunen.

event; there is no age data, but a situation close to the margin of the D_E granitoid area holds true. In Sarfvik, the later granite plays a minor role; only narrow pegmatitic veins cut the dyke there, but they blend into a pegmatitic border zone. This is why we suppose this granodiorite-pegmatitic granite phase to also be younger than the tonalitic phases and relate it to late D_E. The Sarfvik composite dyke was folded by c. ENE-trending D_H (Figure 18a) that caused shortening of c. 40–50% (Figure 18b).

Structural relationships of the widespread tonalitic intrusive rocks are often difficult to establish accurately. At the Jamppa site, Järvenpää, a garnet-bearing tonalite-granodiorite intruded into nearly horizontal and strongly sheared $S_E$ext foliation planes of a mica gneiss (Figure 31 a and b). Its intrusion occurred during the main phase of the D_E extensional shearing phase. Similar homogeneous, penetratively foliated tonalitic intrusions are common in the Southern Finland Granitoid Zone (SFGZ).

In all studied cases the early to mid-D_E garnet-bearing tonalitic-granodioritic compositions are intruded, migmatized or cut by later granitic pulses. The tonalites were dated using zircon U-Pb SIMS. The age of 1868 ± 3 Ma was interpreted to represent the magmatic age of the Hakkila dyke. An exceptionally old age of 3.30 Ga for one inherited zircon grain was observed in Hakkila (Appendix 8). The Hyrylä dyke was dated at 1860 ± 3 Ma; inherited zircon gave an age of c. 1.95 Ga (Appendix 8). The Maikkala pyroxene tonalite from Vihti (charnockite) represents a granulitic magmatic rock from the West Uusimaa granulite Complex (WUC); it gives TIMS ages of 1860 ± 5 Ma on zircon and of 1837 ± 3 Ma on monazite (Appendix 8); the U-Pb SIMS analysis of zircons give an age of 1862 ± 4 Ma for the rock and c. 1.83 Ga was obtained for a metamorphic zircon phase (Appendix 8). The ages of c. 1.86 Ga are regarded as magmatic ages of the early D_E tonalitic rocks, and the monazite and younger zircon ages of c. 1.84–1.83 Ga reflect metamorphism related to late D_E or D_H.

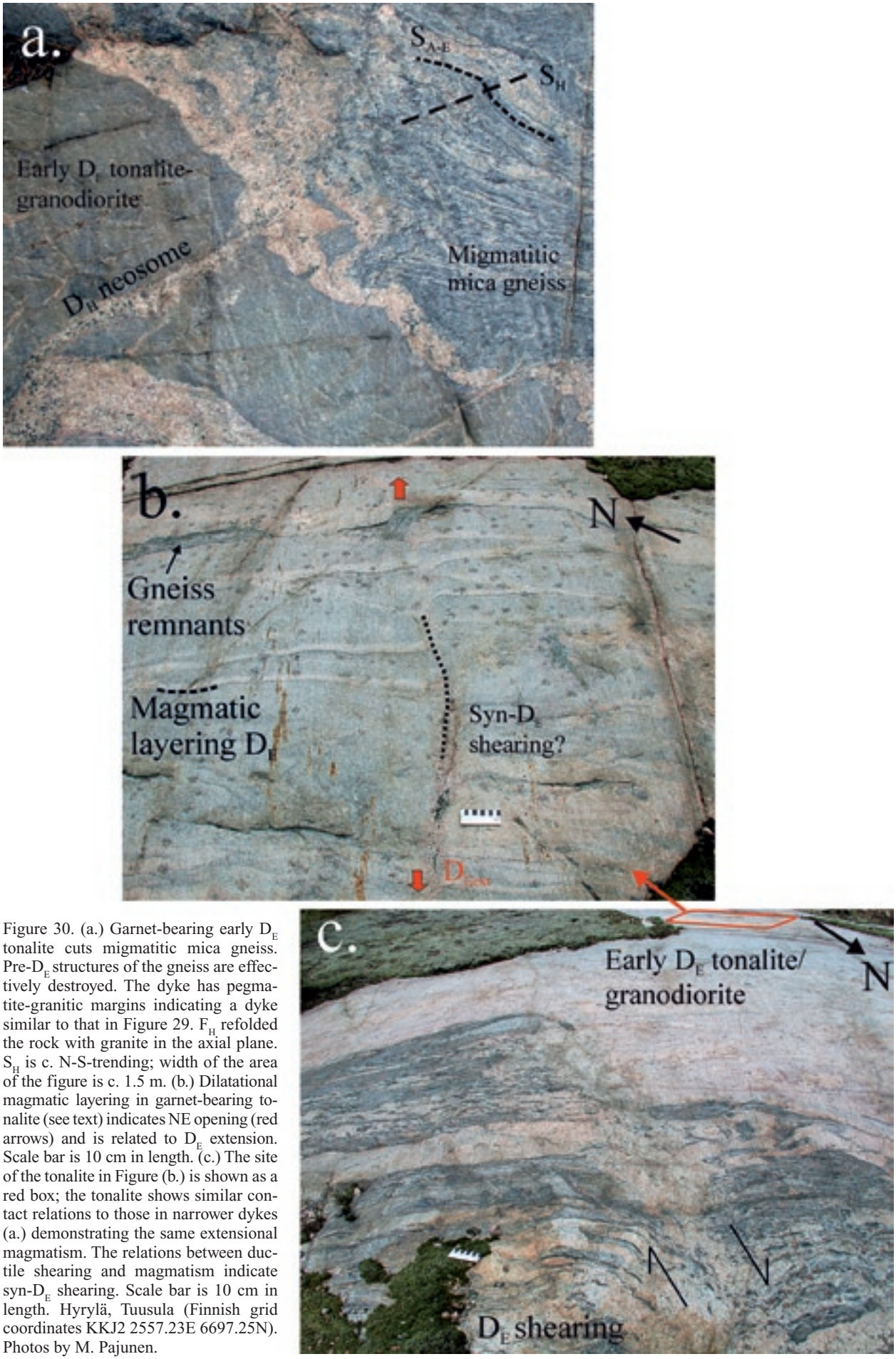

Figure 30. (a.) Garnet-bearing early D_E tonalite cuts migmatitic mica gneiss. Pre-D_E structures of the gneiss are effectively destroyed. The dyke has pegmatite-granitic margins indicating a dyke similar to that in Figure 29. F_H refolded the rock with granite in the axial plane. S_H is c. N-S-trending; width of the area of the figure is c. 1.5 m. (b.) Dilatational magmatic layering in garnet-bearing tonalite (see text) indicates NE opening (red arrows) and is related to D_E extension. Scale bar is 10 cm in length. (c.) The site of the tonalite in Figure (b.) is shown as a red box; the tonalite shows similar contact relations to those in narrower dykes (a.) demonstrating the same extensional magmatism. The relations between ductile shearing and magmatism indicate syn-D_E shearing. Scale bar is 10 cm in length. Hyrylä, Tuusula (Finnish grid coordinates KKJ2 2557.23E 6697.25N). Photos by M. Pajunen.

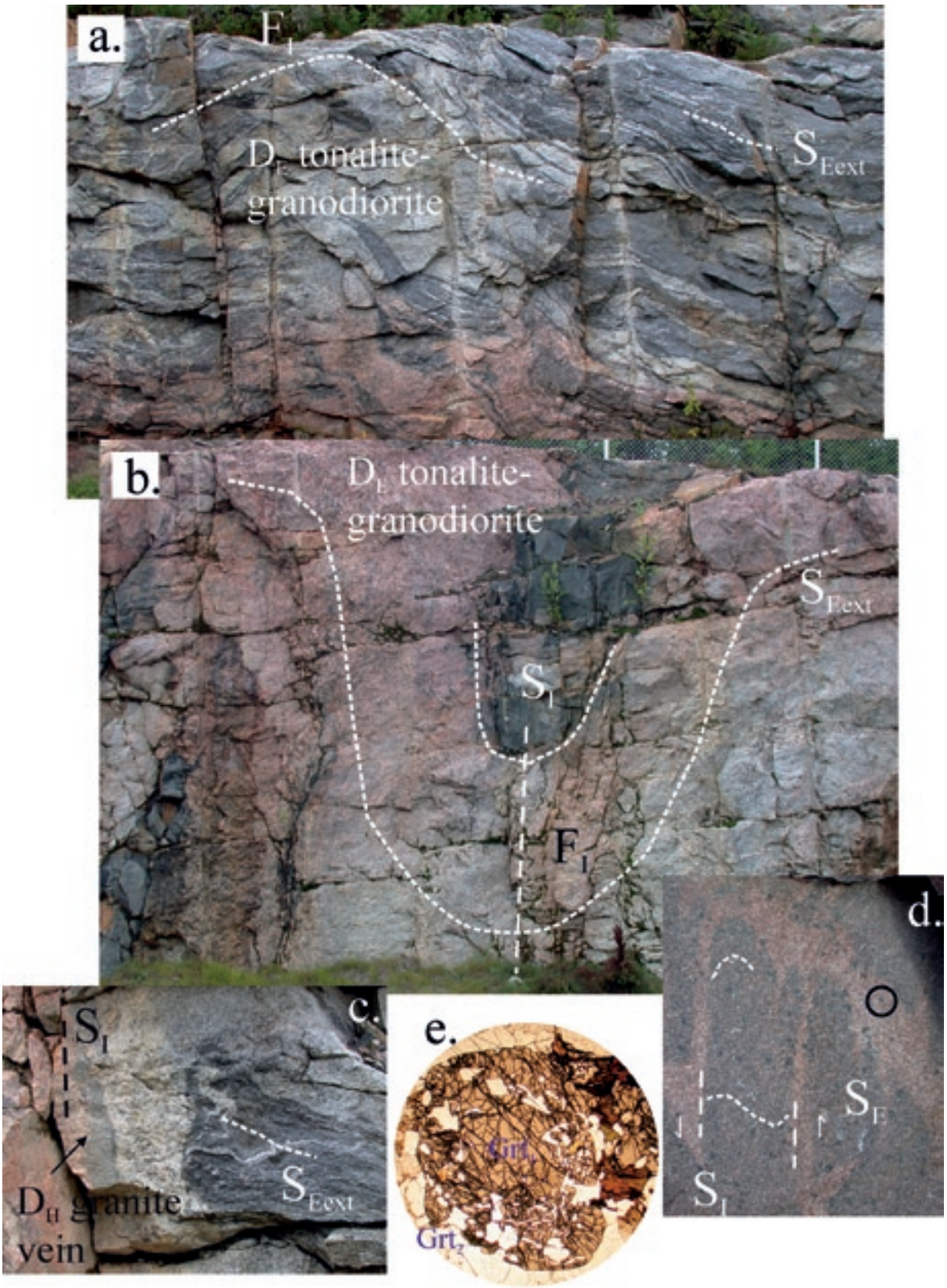

Figure 31. Nearly horizontal $S_E$ext foliation intensely destroyed the pre-existing D_{A-D} structures and the early migmatization events in garnet-bearing mica gneiss. Garnet-bearing tonalite was intruded into the $S_E$ext plane and refolded by open N-trending F_I. Width of the area of the figure is c. 5 m; E is to the right. (b.) Large, tight to isoclinal F_I folds (or F_H folds re-oriented by D_I) with steep axial planes S_I; the F_I folds in this figure are exceptionally tight. The site is located close the major D_I axial zone near the Vuosaari-Korso shear zone in the northern Espoo Granitoid Complex (EGC). Width of the area of the figure is c. 5 m; E is to the right. (c.) Medium-grained D_I granite intruded into the F_I axial plane. Width of the area of the figure is c. 1 m; E is to the right. (d.) D_I structure with granite in the ductile D_I shear planes. Width of the area of the figure is c. 0.5 m; E is to the right. (e.) The high temperature during D_I in the northern EGC is indicated by the new garnet$_2$ generation surrounding the earlier garnet$_1$ core; the microstructure in both garnet generations indicates crystallization from melt. Diameter of the figure c. 1 cm. Jamppa, Järvenpää (Finnish grid coordinates KKJ2 2558.23E 6710.45N). Photo by M. Pajunen.

Structures in early to mid-D_E intermediate dykes – microtonalites

Intermediate intrusive dykes, microtonalites in the following, vary slightly in their composition. Such dykes are found in the southern archipelago (Sederholm 1926), in the western study area (Pajunen et al. 2008), widely in the Espoo Granitoid Complex (EGC) and in the Askola area of the Hyvinkää Gabbroic-volcanic Belt (HGB) (As in Figure 9 and Appendix 3). Generally, they are found/preserved in those areas where the latest granitic pulses of the Southern Finland Granitoid Zone (SFGZ) were not extensive or penetrative. These dykes exhibit quite well their relationships to their country rocks and are good reference rocks for structural analysis.

The contact structures of the dyke at the Staffas site, Sipoo (Figure 24), demonstrate microtonalite emplacement into the cooled syn-/late D_B tonalite. The microtonalite (Figures 20b and 24c) cuts the S_C foliation and was metamorphosed and partially melted by the later D_E events. In the granite-dominant areas the later D_H granites normally assimilate the dykes. Nevertheless, they still often show their sharp cutting relationships against their syn-/late D_B tonalitic and locally against the D_{A-D}-deformed migmatitic mica gneiss hosts. An example from the Hirvensuo site in Sipoo, in the eastern Espoo Granitoid Complex (EGC), describes the relationships of a microtonalite dyke to the migmatitic mica gneiss of a so-called Upper Tectonic Unit (UTU, Appendix 6) and to the syn-/late D_B tonalite (Appendix-Figs. 6-2a–d). The mica schist – dyke relations indicate that the mica gneiss was situated in the upper crust under low-grade conditions at the time of dyke emplacement, and the dyke contacts suggest already-cooled syn-/late D_B tonalite.

The studied microtonalite dykes have metamorphic mineral parageneses and predate the major granite events of D_H. At the Palojoki site, in Nurmijärvi, a weakly S_H-foliated microtonalite dyke cuts a high-grade migmatitic garnet-cordierite gneiss and pegmatitic granite (Figure 32a). The contacts to the granite are ductile and refer to intrusion into a hot rock shortly after the pegmatitic granite dykes related to D_E (Figure 32b). There is weak later shearing along the contacts of the dyke and assimilated granitic fragments in the dyke, but in general the effects of later alteration in the dyke are minor. The host rock shows ESE-WNW-trending, dextral $D_E$cont shear bands (Figure 32c) predating the D_E pegmatitic dykes. The structural setting of the dyke differs from those emplaced in tonalites (e.g. Figure 24a). The outcrop is located in the transitional area between the Espoo Granitoid Complex (EGC) and the West Uusimaa granulite Complex (WUC). The dyke intruded into a deeper depth, which is supported by the tectonic D_{G+H} antiformal setting of the outcrop. In these deeper levels temperature also began to increase earlier and remained high for longer (the thermal gradient was high) than in the upper crustal levels. Our interpretation is that the dyke represents the corresponding intermediate magma to those microtonalites intruded in brittle conditions, but was intruded into an environment that had already achieved a higher temperature before dyke emplacement. The weak S_H as a only foliation in the rock also establishes it younger than the D_E tonalites and microtonalites described above.

The dykes are often steeply cutting their hosts, like the dyke in Nuuksio (Figure 33) that indicates dilatation in a c. SE-direction, but nearly horizontal dykes also occur, e.g. in the Sipoo area. The field observations provide evidence on the one hand of intrusion into a cool, brittle crust (Figure 24) that later underwent higher-grade metamorphism and, on the other hand, emplacement in a more ductile and heated environment (Figure 32b). Structurally, these dykes are in corresponding setting to the D_E tonalites described above. Thus, the microtonalites also show some variation in time of their emplacement.

No age has been determined from these sharply-cutting dykes from the study area. Microtonalites are widely distributed in eastern Finland, where they intrude the Proterozoic cover overthrusted on the Archaean continent, in a N-trending zone of Svecofennian reactivation, close the craton boundary zone. Koistinen (1981) described fold structures in eastern Finland with N-trending axial planes, belonging to his structure D_4 (cf. Koistinen et al. 1996). It comprises zoned ductile folding that left large areas untouched. The deformation has been dated with the help of the syntectonic Maarianvaara granite to c. 1.86–1.85 Ga (Huhma 1981).

Structures in late D_E gabbros

Post-D_D mafic intrusive rocks are not common. We have found only few gabbros from in the northern Espoo Granitoid Complex (EGC). Often it is difficult to distinguish between these and the early/syn-D_B gabbros of the Hyvinkää Gabbroic-volcanic Belt (HGB) (Appendix 3) or the gabbroic-tonalite association in the south without linking them to the structural succession. An example from the Jyskelä site in Mäntsälä (Figure 34a) shows a medium-grained, foliated gabbro with local coarser-grained later ophitic portions – gabbro pegmatite (Figure 34b). In places the gabbro is homogeneous, medium-grained and only weakly deformed. The gabbro with a mingling-like structure with tonalite shows

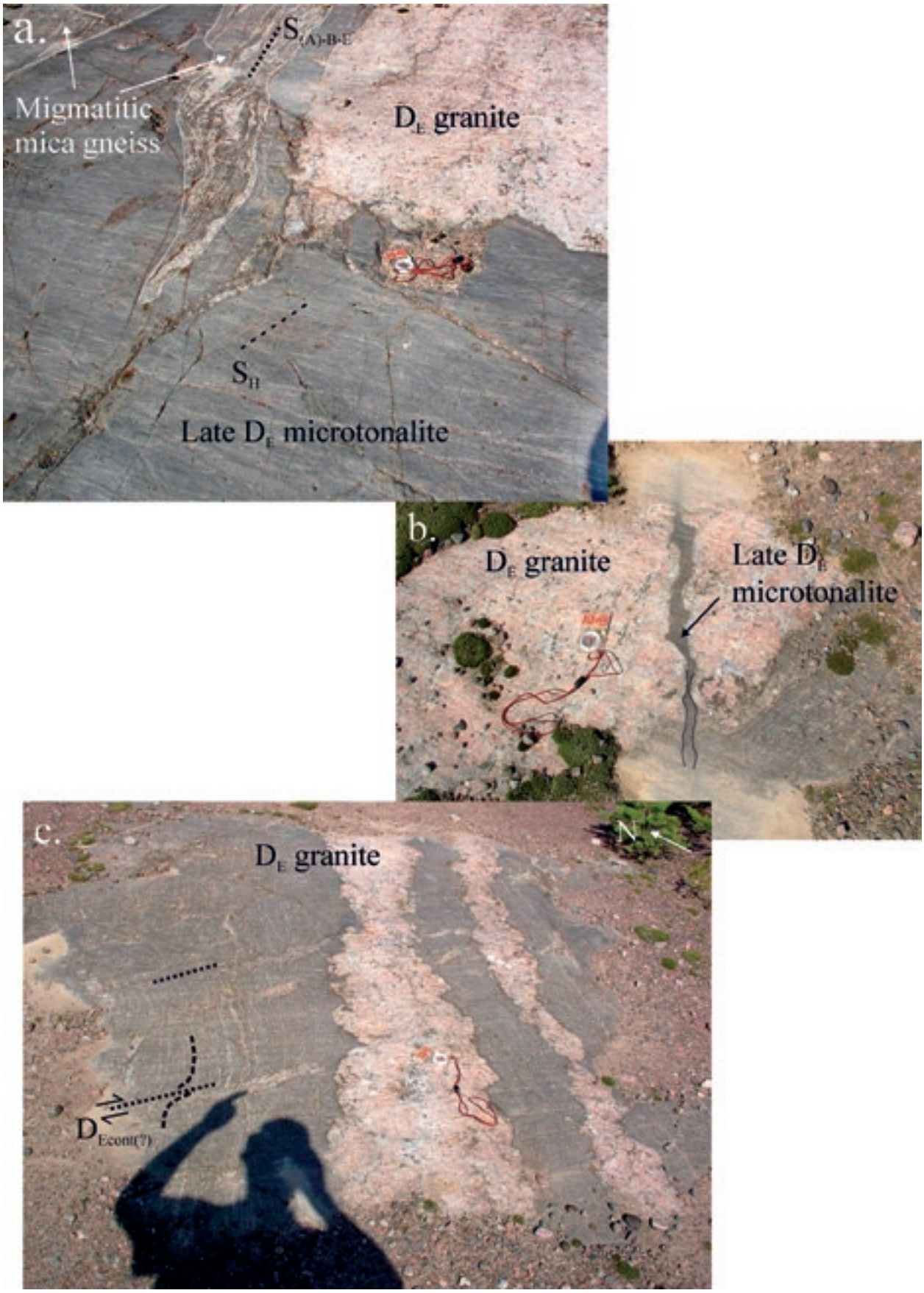

Figure 32. (a.) An intermediate weakly S_H-foliated microtonalite dyke cuts the high-grade, $D_{(A)-B-E}$-deformed migmatitic mica gneiss represented by narrow zones in the upper-left part of the figure. Contacts against the D_E pegmatitic granite are sharp, but in figure (b.) the microtonalite is cutting the pegmatitic granite with bulbous margins suggesting ductile high-grade conditions during the microtonalite emplacement. (c.) The host migmatitic mica gneiss shows c. ESE-WNW-trending dextral $D_E$cont(?) shear bands that predate the pegmatitic D_E granite dykes. Compass is 12 cm in length. Palojoki, Nurmijävi (Finnish grid coordinates KKJ2 2548.41E 6703.32N). Photos by M. Vaarma.

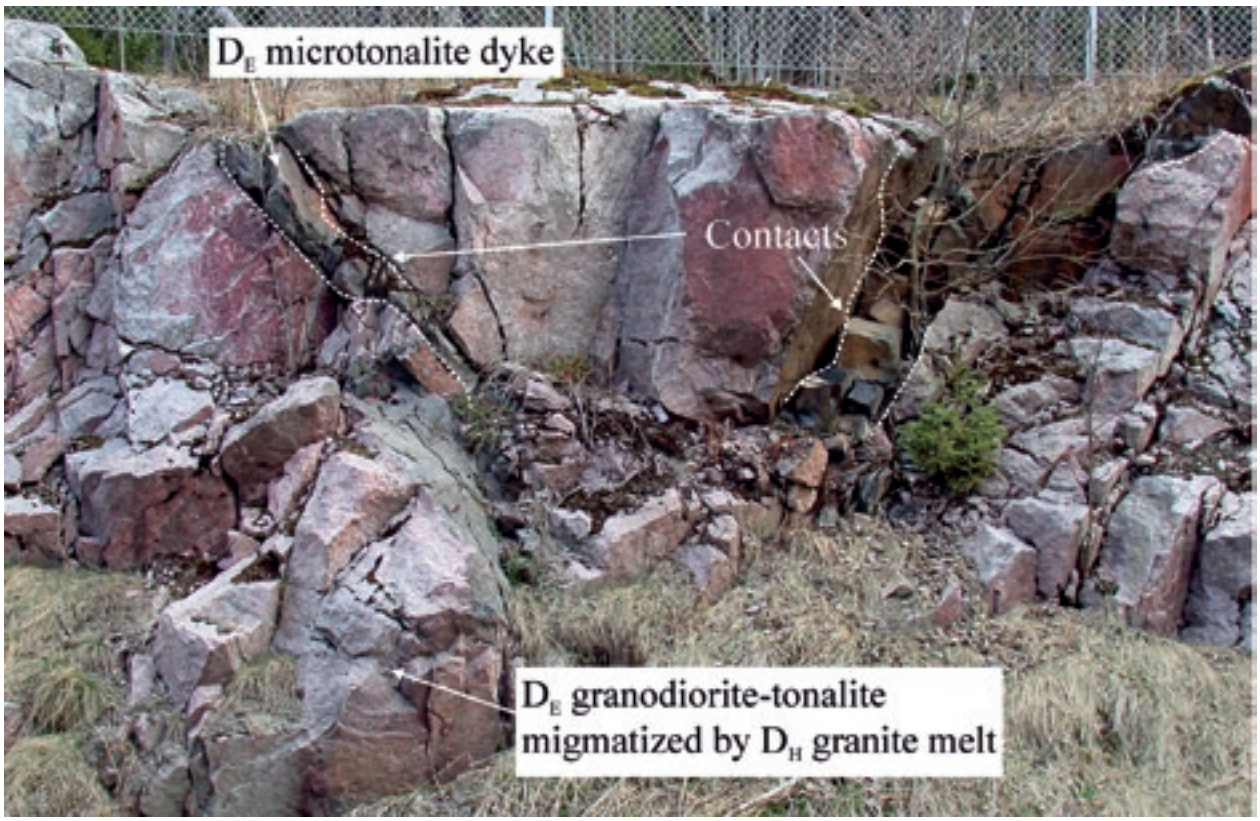

Figure 33. An intermediate dyke cutting the mid-D_E granodiorite/tonalite. The dyke and tonalite are both strongly altered by D_H granite-migmatization. Mustakallio, Nuuksio, Espoo (Finnish grid coordinates KKJ2 2533.28E 6684.02N). Width of the area of the figure is c. 5 m; S is to the right. Photo by M. Pajunen.

weak foliation that formed in ductile and high-temperature conditions rapidly after the gabbro emplacement. We relate it the extensional low-angle $S_E$ext foliation (Figures 34b and c). Granitic dykes intruding the gabbro show recumbent folding, and a retrograde alteration zone in the gabbro (Figure 34d); the reaction rim indicates a cooling period between the gabbro and granite intrusion. We relate the granite to the D_H that is associated with the recumbent folding to $F_H$ext with low-angle $S_H$ext foliation. The low-angle $S_H$ext overprints the earlier $S_E$ext and both are openly $F_{G\text{-}H\text{-}I}$-folded (Figure 34a and b). N-trending shear zones cutting the gabbro can be related to the late phase of the regional D_I or even to D_P. Thus, according to the structural observations, this gabbro is syn-D_E and nearly contemporaneous with tonalitic magmatism, as supported by the mingling-like structure. In the northern EGC in Karhunkorpi, Nurmijärvi, a gabbro has a similar tectonic setting. It is openly folded and it intruded into a horizontal S_E plane. The kinematic observations made from the horizontal $S_E$ext structures indicate extensional top-to-SE movement, so the extension is directed outwards from the granulite facies WUC area (see later).

The gabbro magmatism indicates a deep-seated heat source and the generation of magmas at this stage. The increase in temperature also caused the high-grade metamorphism that characterizes the northern parts of the Espoo Granitoid Complex (EGC) and the West Uusimaa granulite Complex (WUC). The homogeneous portion of the gabbro contains some zircon that was dated by the TIMS method to 1841 ± 7 Ma; the U-Pb SIMS analyses on zircons give, within error limits, the same age of 1838 ± 4 Ma (Appendix 8 and App-Table 3). The structural setting of intruding granite corresponds to the D_H pegmatitic granite in Bollstad (described later and Appendix 8), but the temperature has increased higher in Jyskelä, as indicated by more ductile deformation and the mingling-like structures. The gabbro is slightly older than the pegmatitic dykes in Bollstad (cf. Appendix 8); we relate it to late D_E, because it precedes the major D_H granite pulses. This also indicates that the horizontal $S_E$ext foliation was generated at 1.84 Ga; the observation made in the West Uusimaa Complex (WUC) established its generation after the intrusion of the Maikkala pyroxene-bearing tonalite (charnockite) (Appendix 8).

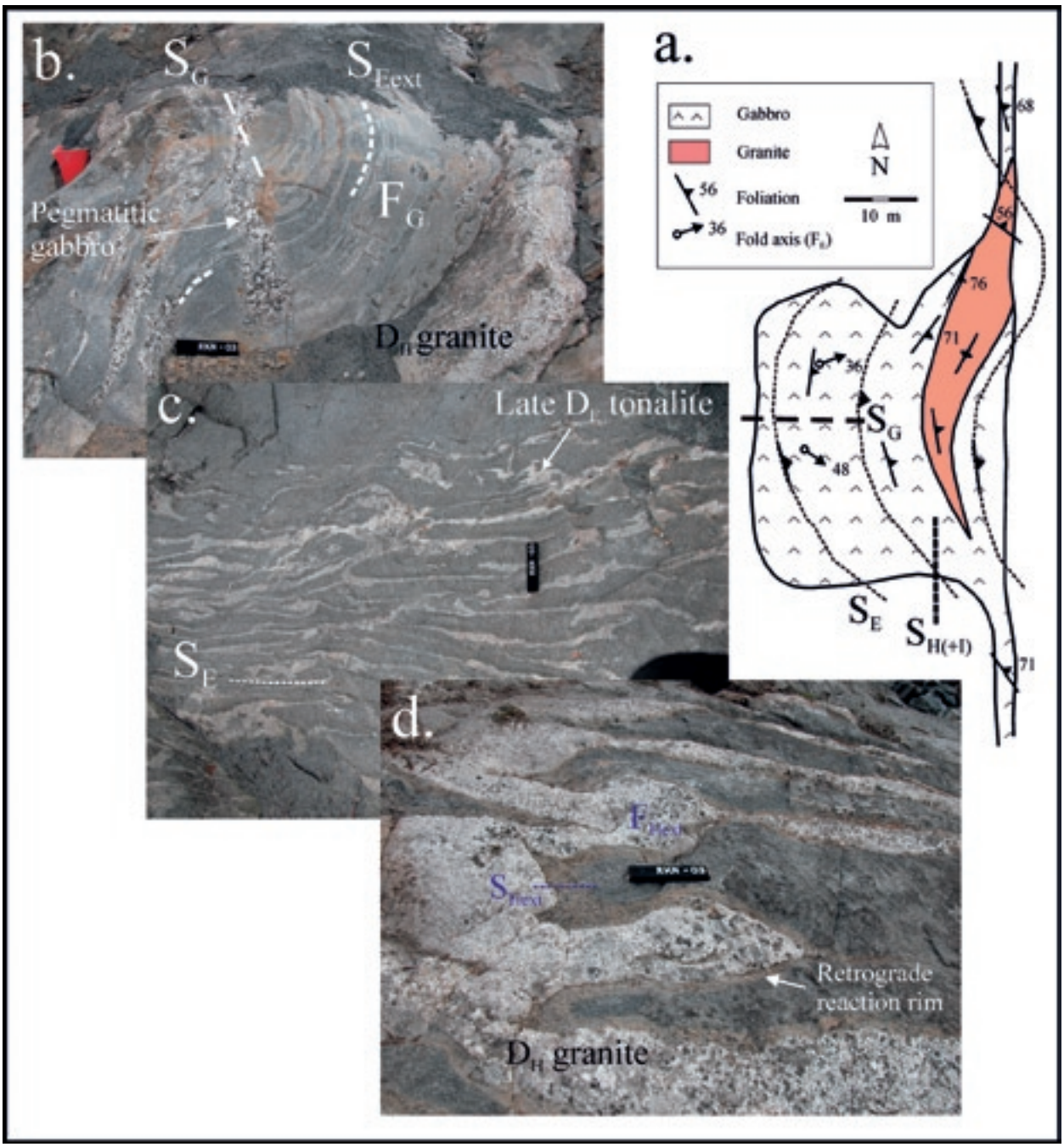

Figure 34. (a.) A sketch of the structural setting of the late D_E gabbro outcrop in Jyskelä, Mäntsälä (Finnish grid coordinates KKJ2 2562.56E 6711.55N). (b.) Late D_E gabbro is cut by a late D_H granite dyke and coarse-grained gabbro-pegmatite veins cutting the $S_E$ext foliation refolded by F_G. Scale bar is 10 cm in length. (c.) A mingling structure between the gabbro and contemporaneous tonalite. $S_E$ext foliation was rapidly generated after intrusion in high temperature conditions. The structure was later deformed by D_H (see d.). Scale bar is 10 cm in length. (d.) Intense D_H vertical shortening of gabbro is indicated by the isoclinal recumbent F_H folding of D_H granite dykes; a new foliation $S_H$ext formed. Scale bar is 10 cm in length. Photos by R. Niemelä.

D_E structures and kinematics

The intensity and character of the D_E structures vary regionally due to deformational depth (schematized in Figure 4) and the time of their formation. The oldest dated D_E intrusion, the garnet-bearing early D_E tonalite in Hakkila, intruded into an approximately E-trending dilatational zone (Figure 29). Dilatation during the emplacement of the slightly younger garnet-bearing Hyrylä tonalite was c. SE-directional (Figure 30a); a similar direction of dilatation is also interpreted from the layered Hyrylä tonalite (Figure 30b) and from the shear zones related to its contacts (Figure 30c). However, the homogeneous Jamppa tonalite was emplaced into horizontal S_E shear planes (Figures 31a and b) in the migmatitic mica gneiss.

The most intense D_E structure in the D_A-D_D deformed rocks is S_E foliation that developed as a

spaced crenulation cleavage. A map from the Klaukkala site in Nurmijärvi (Figure 35) shows the characteristic D_E-D_H relationships (Figure 12c). S_E is a regional, nearly horizontal shear foliation in the migmatitic gneiss. The horizontal S_E foliation plane intersects the pre-existing foliation (S_B of the mica gneiss), forming a SW-trending intersection lineation L_E (Figure 35d). Drag bends of the previous foliation by the S_E shearing indicate extensional top-to-SE movement – the dilatation zone is towards the NW, towards the high-grade West Uusimaa granulite Complex (WUC). Similar kinematic patterns of S_E were identified further south, e.g. at the Kauklahti site, Espoo (Figure 19). In the WUC and the northern Espoo Granitoid Complex (EGC), S_E is often developed as a spaced foliation that transposed and intensely fragmented the early D_B migmatite structures (Figures 12c and 36). Sometimes, the earlier D_A-D_D structures are completely destroyed, as in the felsic pyroxene gneiss in the WUC (Appendix-Fig. 2-1). The age of S_E in the WUC is younger than 1.86 Ga (Appendix 2). Contractional $S_E$cont is a spaced foliation in the syn-/late D_B tonalites (Figure 24). Shear bands with granitic melt are characteristic (Figures 22c and 25b). In the early D_E intrusive rocks, oblique contractional $S_E$cont is penetrative mineral foliation paralleling the dykes.

The age of Hakkila tonalite is precisely the same as the age of the granitoid that blocked the SW-transpressional $D_{4/D}$ evolution in the northern units (Appendix 7). Kinematically, the early D_E dilatational structures in the Espoo Granitoid Complex (EGC) fit well with this NE-SW transpressional stress field that acted during the $D_{4/D}$ between the major N-trending Baltic Sea-Bothnian Bay (BBZ) and the Riga Bay-Karelia Zones (RKZ) (Figure 8). D_E extension occurred in the oblique NE-E-trending dilatation zones in between the active dextral N-trending shear zones, the BBZ and RKZ. The continued NE-SW transpression caused local rotations of the dykes to produce closely related metamorphic steep penetrative $S_E$cont foliation paralleling the dykes. In addition to the early D_E tonalite dykes, these structures are also typical in the microtonalitic dykes. Under continuing extension and increasing temperature, oblique dilatation developed to horizontal extensional shearing with top-to-SE movement. Increased tonalitic to granodioritic magma emplaced into these $S_E$ext shear foliation planes. Thermal gradient was high during the late D_E and gabbroic intrusions emplaced into corresponding $S_E$ext shear planes. The increasing temperature produced polymetamorphic characters in the older syn-/late D_B tonalites that are intensely shear-banded and re-melted, which is not the case with the intermediate D_E granitoids.

The evolution of the Jokela supracrustal association (Jo on Figure 9) began during the early D_E deformation. In the upper crustal levels the oblique extension between the major N-trending BBZ and RKZ opened dilatational regions into a c. NE-E trend, into which the supracrustal sedimentary association began to accumulate. The continuing extension and clockwise rotation caused rapid deformation of the sequences, and increased heat flow due to the thinning crust caused volcanic activity in the subsiding sedimentary basin. We interpret the Jokela supracrustal association as a pull-apart basin formed in between the major N-trending deformation zones – the evolution of the association is discussed in detail in Appendix 5.

In summary, the D_E evolution in the Southern Finland Granitoid Zone (SFGZ) was a result of SW-NE transpression causing oblique SE-dilatation, extensional top-to-SE shearing and clockwise rotation between the active dextral N-trending transcurrent shear zones – the Baltic Sea-Bothnian Bay Zone (BBZ) and Riga Bay Karelia Zone (RKZ).

D_F deformation – E-W movement of the Central Finland block

The sinistral NW-trending Hiidenvesi shear zone (Figures 10 and 16) in the West Uusimaa granulite Complex (WUC) predates the major D_H granitic events; the NE-trending border zone of the Nuuksio granite area, characterized by a strong D_H granite magmatism, cuts it at the southeastern end. According to interpretation made from magnetic maps the shear zone continues below the Espoo Granitoid Complex (EGC), where it still acted as a zone of weakness during the rapakivi-related diabase magmatism. The generation of the shear zone indicates E-W contraction. However, in the study area the fold structures with c. N-trending axial planes are related to D_D deformation or, in the vicinity of the major N-trending, like the Vuosaari-Korso shear/fault zone, to D_I deformation. Folds related to this E-W contraction have not so far been found in the study area.

The observations of Koistinen (1981) in eastern Finland indicate contractional folding with N-trending axial planes at c. 1.86–1.85 Ga ago (see also Huhma 1981). The major sinistral ENE-E-trending deformation zone at the northern end of the Bothnian Bay (cf. Korja & Heikkinen 2005) and dextral movements in the Hyvinkää and southern Finland shear zones indicate the push of a large-scale crustal Central Finland block towards the east (Figure 8). This kind of deformation would explain the zones of folds with N-trending axial planes, the 1.85 Ga fluid activity in NW-trending shear zones and the

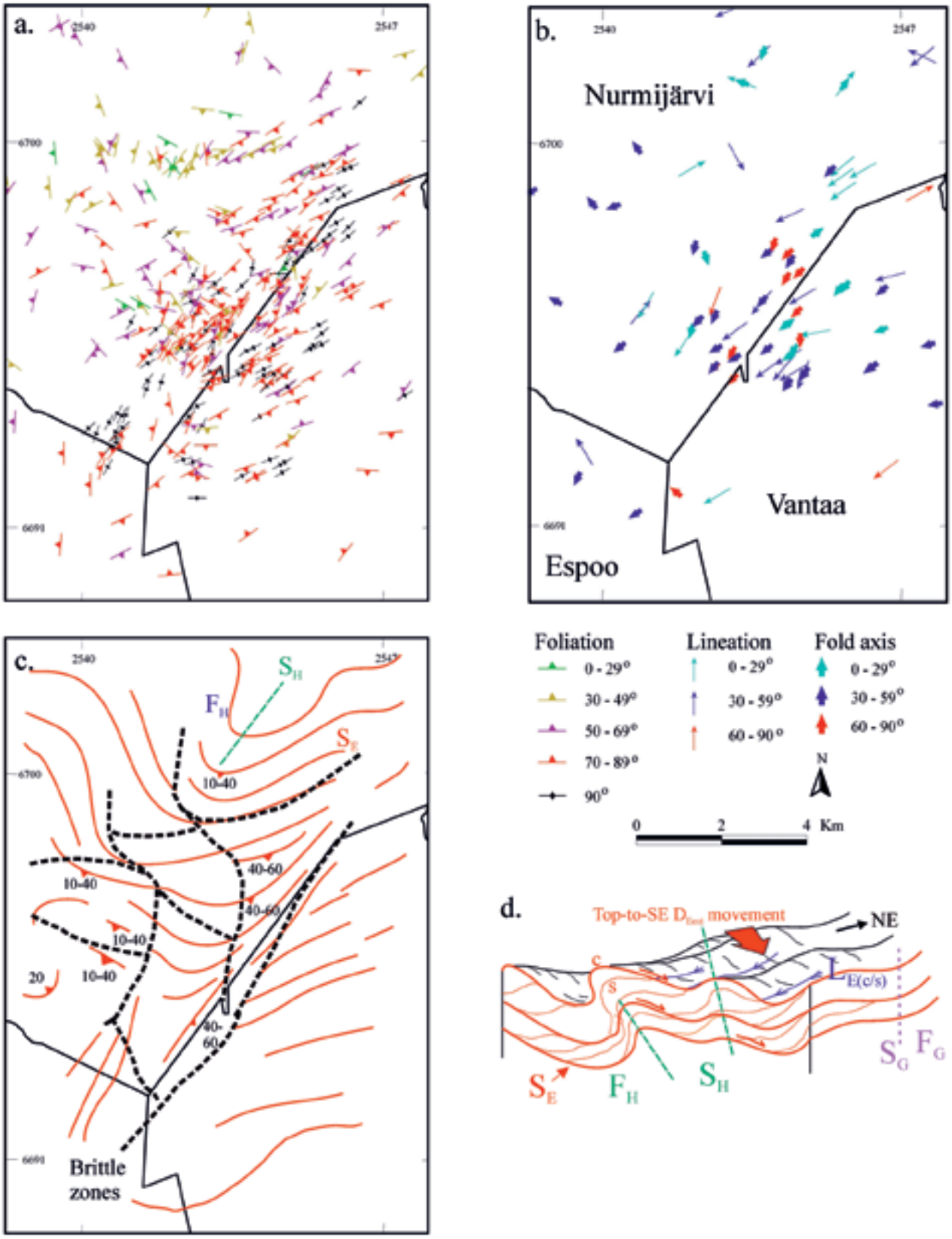

Figure 35. Tectonic element maps, Klaukkala, Nurmijärvi area (Finnish grid coordinates KKJ2): (a.) foliations, (b.) lineations and (c.) S_E foliation plane formlines deformed by D_H, and major ductile to brittle shear/fault zones. (d.) A schematic tectonic model showing the relationships between structures and tectonic transport: lineation dipping towards the SW is predominantly an intersection lineation on the $S_E$ext shear planes (intersection between the S-C planes) that point to low-angle top-to-SE movement during D_E extension. The S_E planes are moderately to openly refolded by the D_H with a NE-trending axial plane (see Figure 12c.). Base map © National Land Survey of Finland, permit No. 13/MML/08.

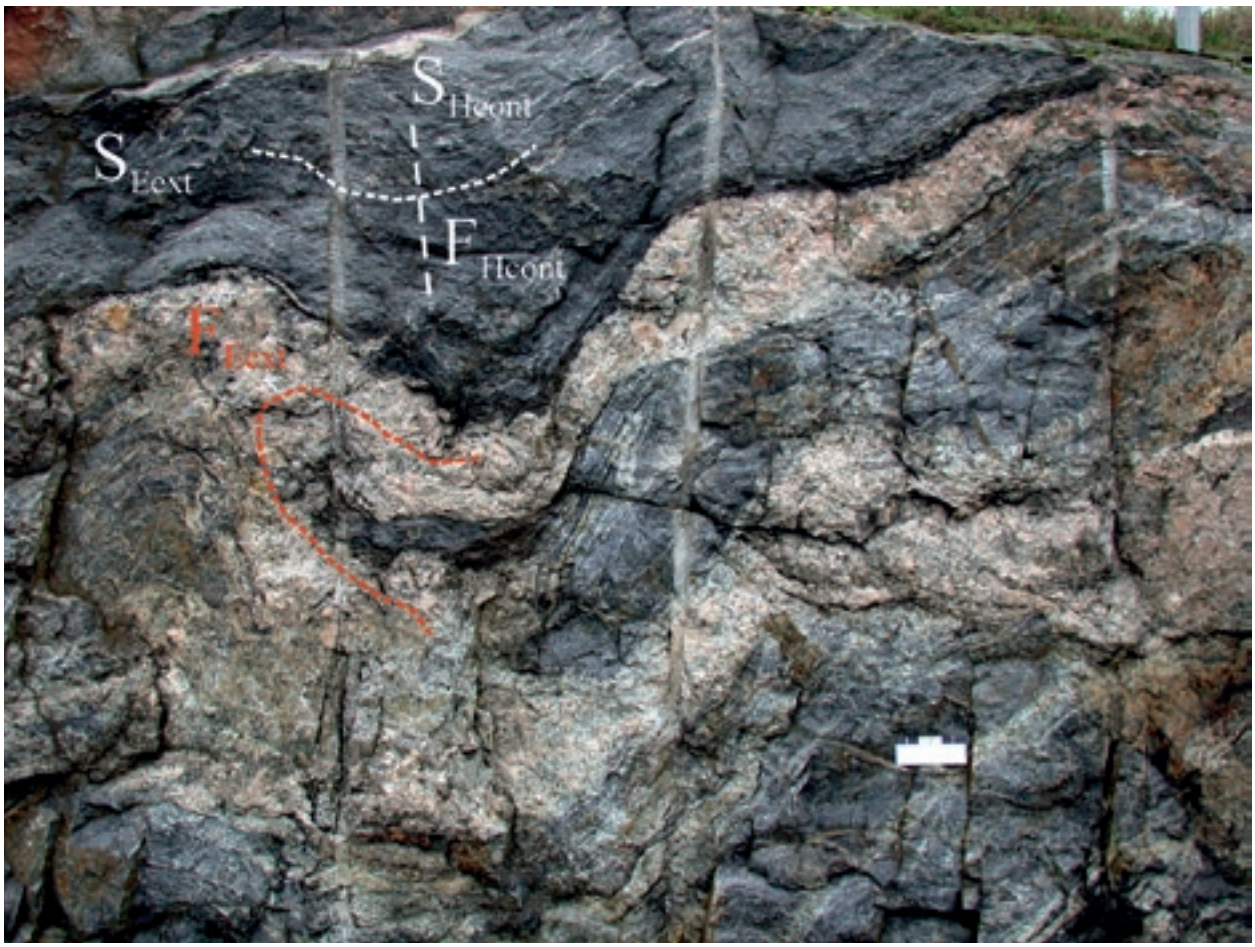

Figure 36. A migmatitic garnet-bearing mica gneiss, cut by D_{E-H} pegmatitic granite, shows strong extensional $S_E$ext foliation, presumably overprinted by the later $S_H$ext, and is refolded by $F_H$cont. The D_{A-D} structures are completely destroyed; relics of the early D_B neosome appear as remnants elongated in the direction of the S_E foliation planes. Scale bar is 15 cm in length; E is to the right. Bockbärget NE, Vantaa (Finnish grid coordinates KKJ2 2550.98E 6687.43N). Photo by M. Pajunen.

emplacement of felsic granitoids of that age in eastern Finland (Pajunen & Poutiainen 1999). Near the craton boundary, there are several NW-trending faults, sometimes showing sinistral movement (e.g. D_c in Pajunen 1986), and NE-trending dextral faults, such as the Auho fault (e.g. Kärki 1995) cutting the Kainuu schist belt. The fold structures and the shear zones were formed during E-W contraction labelled here as D_F deformation.

The SW-NE transpression during the D_E turned into E-W-directional contraction during the D_F at c. 1.86–1.85 Ga. The E-W-push of the Central Finland block did not have major effects on the structures in the southernmost part of Finland, because stress predominantly released along the major E-W-trending shear zones. The main reason for the D_F block movements is considered to exist further west; a large-scale ductile folding with N-NNE-trending axial planes in the western Fennoscandian Shield (Figure 8) may be causing pushing of the coherent Central Finland block towards the east. The E-W contraction may also represent a local rotation of the NE-SW transpressional stress, especially because in the south the SW-NE transpression D_E occurred at the same time.

D_G deformation – N-S shortening

D_G deformation comprises N-S-oriented shortening that produced large-scale open folding with c. E-W-trending axial planes (Figure 11). The F_G folds developed in the intensely D_E-migmatized zones to gentle and sometimes even tight folds. S_G foliation is weak or missing. The D_G effects are difficult to distinguish in the areas where the earlier D_{C-D} dome-and-basins are in the same direction – only tightening or shearing of these early structures occurred. On outcrops the characters of D_G structures can be identified in those areas where the horizontal S_E and D_E granitoids predominate; they were not affected by the D_A-D_D events. The scarce observations on tectonic transport during the D_G indicate overturning towards south in Kauklahti (Figure 19d) and in southern Sipoo (Figure 28c). Although poorly detectable on the outcrop scale, the D_G has an important effect on the regional tectonic $D_{G+H\pm I}$ dome-and-

basin pattern, which strongly determined the present exposing of different tectonic units, such as the West Uusimaa granulite Complex (WUC) and Espoo Granitoid Complex (EGC) (Figure 11). Wide-scale folding with E-W-trending axial planes can be identified in the area of the whole Granite Migmatite Belt (GMB) (Figure 11). It could also partly explain the metamorphic pattern in the Tonalite Migmatite Belt (TMB), where the granitoid-dominant E-trending central zone is surrounded by lower-grade bordering areas (Figure 11).

Sinistral shearing of the Porkkala-Mäntsälä shear zone, bending the pre-D_G structures to sinistral drag folds, can be explained by the N-S shortening related to D_G deformation. Torvela et al. (2008) describe the dextral NW-trending South Finland shear zone from SW Finland in the southwestern archipelago. They dated its beginning at 1.85 Ga and related it to the Southern Finland shear zone of this study. However, according to our interpretation from aeromagnetic maps, the shear zone continues more or less straight towards the ESE**.** We relate it contemporaneously to the Porkkala-Mäntsälä shear zone produced due to c. N-S compression during the D_G. We suggest the age of c. 1.85 Ga for the D_G deformation.

D_H deformation – a major granitic event in the Southern Finland Granitoid Zone

In the Southern Finland Granitoid Zone (SFGZ), weakly oriented, medium to coarse-grained, reddish or greyish, often K-feldspar-porphyric or "layered" granitic rocks (Figure 37a) are widely distributed. They are accompanied by several rather contemporaneous and heterogeneous magmatic, often pegmatite granitic, and migmatitic events. They intrude or migmatize the described D_E granitoids, including the pegmatite granitic border zones of the early/mid-D_E dykes (Figures 29 and 30a). In the Espoo Granitoid Complex (EGC), the Nuuksio area (Nu in Figure 9) forms a large open synformal D_{G+H} structure (Figure 11). It is one of the key areas illustrating how the late granitic intrusive and melting events "eat and hide" the structures formed during the earlier D_{A-E} evolution, and how the D_H magmatism and migmatization are related to the D_H structures. The Riihimäki Granitoid Complex (RGC), the Perniö Granitoid Complex (PGC) and the southern Sipoo area of the Espoo Granitoid Complex (EGC) are corresponding granitic units. However, early D_H evolution can be best examined outside the major D_H granite units; there, the relationships to the early structural evolution are better preserved. Some mafic dykes, cutting the Southern Volcanic-sedimentary Belt (SVB), are closely related to the D_H granite magmatism and represent the latest magmatic events identified in the study area.

Description of D_H granites

The D_H granites cut the older structures in different ways; the melting structures and intrusives change from place to place due to characteristics of the syntectonic D_H deformation processes. Heterogeneous patchy melting of the older granitoids is a general phenomenon (Figure 37b); biotite decomposes to garnet and/or cordierite and granitic melt. Melt formed non-oriented in-situ patches sometimes accompanied by intruded granite dykes. In places, D_H granite occurs in shear bands (Figure 32c) that cut the foliated granitoids or gneisses. In the areas of horizontal deformation and strong granitic melting, the D_H granite was emplaced into the foliation or shear planes (Figure 37c) forming heterogeneously "layered" granites; they are characteristic, for example, in the Nuuksio synform. Non-foliated coarse-grained, garnet-bearing granite and older, foliated granitoid alternate within them (Figure 37a). When the amount of granite increases the older granitoids or gneisses are decomposed to biotite-rich schlierens in the younger granite (Figure 5c). If the contacts with pre-existing rocks are not visible on the outcrops, it is seldom possible to determine whether the pre-existing host rock was a metapelitic-psammitic metasedimentary rock, which is typical in the northern part of the Nuuksio and southern Sipoo areas, or a granitoid. In the Nuuksio area the weakly-oriented porphyritic granites show open folds with steep axial planes trending NE (S_H) or N ($S_{H\pm I}$).

The areas dominated by the widespread D_H granites show a low U/Th radiation ratio, differing from the surrounding granitoid areas (Figure 38). The disturbing effects of water cover and overburden by glacial sediments place restrictions on analysis of the ratio (see Airo et al. 2008). When taking these restrictions and the featureless magnetic anomalies characterizing these areas into account, some estimation of the distribution of corresponding magmatic rocks can be carried out. Our conclusion is that the D_H granitic pulse does not appear as penetrative feature in the Southern Finland Granitoid Zone (SFGZ), but is concentrated in areas determined by local late heat flow and dilatation. The decreased U/Th ratios in granitic rocks indicate that repeated melting processes produced them. Some of these granites have very small amounts of zircon (M. Vaasjoki, pers. comm. 2004). We suppose that the low U/Th ratio was predominantly a result of remelting of earlier syn-/late D_B and early/mid-D_E intermediate granitoids. The early U-bearing phases were decomposed and soluted under increasing

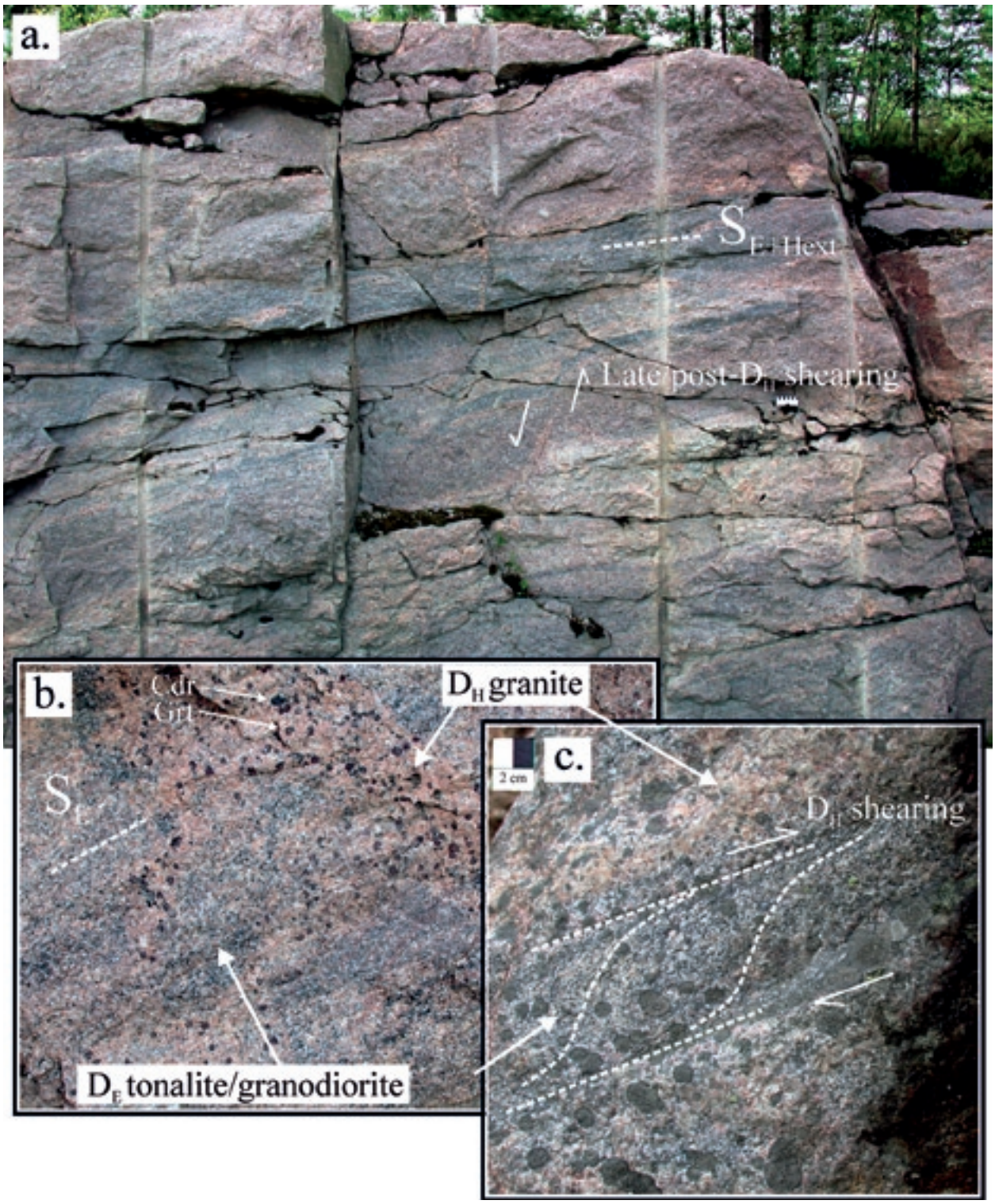

Figure 37. (a.) D_H remelting of early/mid-D_E tonalite/granodiorite producing a layered appearance characterizing the granitoids in the Nuuksio synform area. Scale bar is 10 cm in length; N is to the right. Ämmänsuo, Espoo (Finnish grid coordinates KKJ2 2531.22E 6681.43N). (b.) Patchy D_H remelting of early/mid-D_E granodiorite/tonalite in the Nuuksio synform. Biotite has decomposed to garnet, cordierite and granitic melt. Width of the area of the figure is c. 1 m. Solvalla, Espoo (Finnish grid coordinates KKJ2 2531.02E 6687.27N). (c.) Extensional D_H shearing deforming the pre-/syn-D_E tonalite. The shear plane was deformed by progressive $F_H$cont folding into a secondary thrust zone position. The D_H granite intruded into the extensional $S_H$ext shear plane. NE is to the right. Haramossen, Nuuksio, Espoo (Finnish grid coordinates KKJ2 2534.15E 6685.25N). Photos by M. Pajunen.

temperature and magmatic fluid production. Uranium was fixed into the increased metamorphic melt/fluids and escaped to the upper horizons in the crust. Indeed, this is supported by the uranium showings (Saltikoff et al. 2002) that are concentrated in semi-ductile/-brittle structures of the overlying tectonic sequences.

To the west of the Espoo Granitoid Complex (EGC), in the Bollstad site at Inkoo, the syn-/late D_B tonalite (cf. E_b tonalite of Pajunen et al. 2008) is cut by D_H pegmatitic dykes and granitic veins that show isoclinal recumbent folding with horizontal axial planes (Figures 39a and c) indicating vertical shortening. The pegmatitic dyke was originally intruded into an upright position into a brittle crust that is suggested by the semi-ductile shearing structures related to the early development of the horizontal S_H foliation in the tonalite (Figure 39b). No retrograde mineral phases were formed during shearing, but a continuing vertical shortening under increased

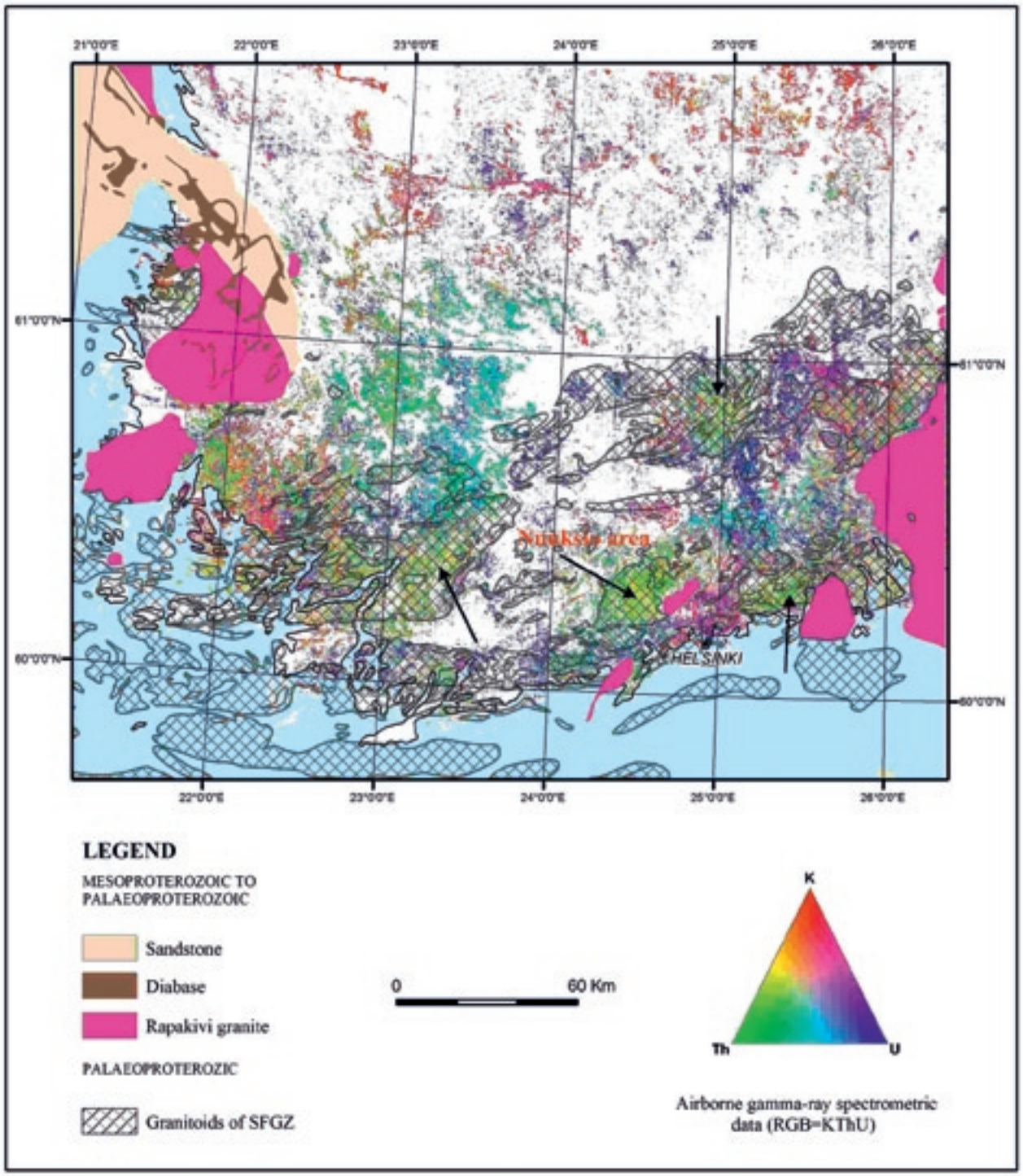

Figure 38. An aeroradiometric map showing the belt characterized by the D_E and D_H granitoids (Southern Finland Granitoid Zone, SFGZ – hatched). The area of intense D_H remelting of the early tonalitic/granodioritic rocks (Figure 37) in the Nuuksio area shows a lower U/Th ratio than in its surroundings. A similar ratio in the radiometric data is also found in the other granitoid complexes, as indicated by the arrows. Base map © National Land Survey of Finland, permit No. 13/MML/08.

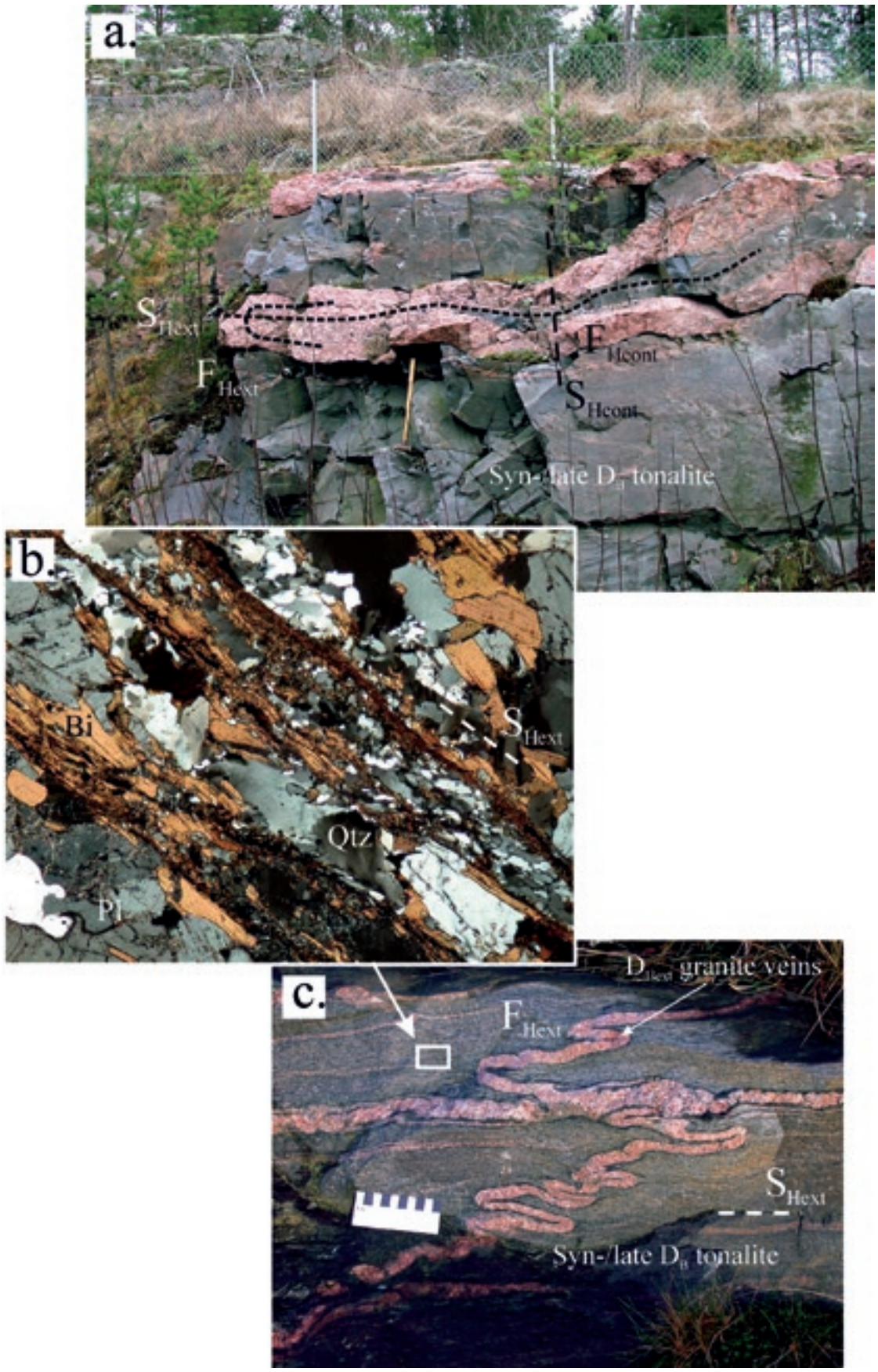

Figure 39. (a.) Isoclinal recumbent $F_H$ext folding in a D_H pegmatitic granite dyke strongly cutting deformed gneissic syn-/late D_B tonalite. The intrusion of the dyke indicates emplacement into steep position in the beginning of the D_H granite phase in the area; the outcrop is located in the marginal area of the most intense D_H granitic area of Nuuksio (cf. Figure 38). Hammer is c. 65 cm in length; SE is to the right. (b.) Photo of microstructures in the tonalite. The development of S_H began as semi-ductile shearing, and under the increasing temperature spaced biotite foliation was produced; Bi = biotite, Pl = plagioclase and Qtz = quartz. Width of the figure area is c. 6 mm. (c.) Vertical D_H shortening in narrow granite veins in the gneissic tonalite that shows a strong $S_H$ext foliation. Scale bar is 10 cm in length. Bollstad, Inkoo (Finnish grid coordinates KKJ2 2497.78E 6662.16N). Photos by M. Pajunen.

temperature caused a horizontal penetrative S_H biotite foliation that characterizes wide areas in the environments. The pegmatitic dyke folded isoclinally and new syn-D_H granite veining developed (Figure 39c). Similar structures elsewhere deform the D_{C+D} dome-and-basins and also the earlier D_E structures and intrusions, like the late D_E gabbros (Figure 34d). The emplacement of the pegmatitic dyke represents the beginning of the D_H granitic event in Bollstad, outside the major D_H granite unit EGC. Open folds with c. NE-trending steep axial planes refold the recumbent F_H folds and form interference dome-and-basins with the F_G and F_I. The open large-scale folds were developed during the progressive D_H deformation into oblique contractional settings; the tectonic relationships of the recumbent fold interpreted as extensional $F_H$ext and the steep $F_H$cont folds are discussed below.

Description of D_H diabase dykes

In the southernmost Southern Finland Volcanic-sedimentary Belt (SVB), near the coast and on the islands of the Gulf of Finland, fine-grained diabase dykes occur showing fresh amphibolite facies hornblende-plagioclase paragenesis. They are found in places that were not intensely intruded by the D_H granites. The dykes cut the gneisses in a c. N-NNE or E-W direction and were, in all the studied cases, emplaced into central parts of the pegmatitic granite dykes.

Figure 40a shows an example in Espoo, the Rövaren site. The E-W-trending dyke cuts felsic gneiss that was intruded by pre-/early D_B amphibolite dyke boudinaged by D_B and folded by F_C. There are magmatic hybrid-/mingling-like structures between the diabase and granite margin (Figure 40b). At the Kopparnäs site, Inkoo, structurally and compositionally corresponding diabase dyke (Figure 40d) cuts the old structure of the gabbro-tonalite association in a N-S direction. The Rövaren dyke was weakly F_H folded with ENE-trending axial planes (Figure 40c) and the diabase dyke in Kopparnäs shows ductile, sinistral N-S-trending $D_{H\text{-}I}$ shearing (Figure 40d) close to the contacts. The metamorphic paragenesis in the dykes and contact structures between the dykes and the pegmatitic granite supposes intrusion into a high temperature environment.

Age of D_H magmatism and metamorphism

The U-Pb TIMS age for the monazite of the Bollstad pegmatitic granite is 1828 ± 3 Ma (Appendix 8). This age provides a reference for the beginning of the D_H deformation in the area and suggests a discordance of c. 40 Ma after the intrusion of the syn-/late D_B tonalite at 1873 ± 7 Ma in Bollstad (Appendix 8). Several studies since Sederholm (1927) have provided evidence that the crust of the Granite Migmatite Belt (GMB) stabilized and cooled between tectono-thermal events (e.g. Korsman et al. 1984, 1999 and Pajunen et al. 2008). Such cooling stages are described between the syn-/late D_B tonalites and the early/mid-D_E microtonalite dykes (Figures 24a and b), and retrograde reaction rims surrounding the mid-D_E granodiorites (Figures 18a and d) also indicate the preceding cooling stage of the country rock.

However, continuous thermal and magmatic evolution is supported by structural relationships between magma phases and by the ages of structurally-fixed magmatic rocks. For example, in the northern Espoo Granitoid Complex (EGC) compositionally varying magmatic and metamorphic activity continued in a ductile state practically without a break throughout the described 40 Ma period. High-T metamorphic conditions during this cap are supported by several observations of metamorphic zircons and monazites (Appendix 8). The Bollstad granite dykes indicate the beginning of the D_H pulse outside the major D_H granite units, but in the granitoid-dominant areas like the EGC (Figures 9 and 38) huge amounts of granodioritic to granitic magmas were produced. Kurhila et al. (2005) dated the granitic magmatism from the detailed study area in Nuuksio at c. 1.85–1.82 Ga. On the basis of structures and remelting characteristics in the area (Figures 37a-c), we suppose that the youngest ages represent the D_H magmatism and remelting event of the earlier intrusive or supracrustal rocks. This is supported by the ages of the D_H leucosomes of granulitic metapelites ranging between 1.82–1.81 Ga (Korsman et al. 1984, 1988, 1999 and Väisänen et al. 2004). Intense crustal melting also produced wide, locally porphyritic granite intrusions. The cooled parts of the crust, beside the areas of intense D_H granitic magmatism, medium-grained to pegmatitic granite dykes with sharp contact were intruded, as exemplified in Figure 15c from the Southern Volcanic-sedimentary Belt (SVB).

The D_H diabase dyke from Kopparnäs yielded a small amount of zircon. For the most part, it has a SIMS U-Pb age of c. 1.83 Ga and only a few zircon grains with deviating appearance poorly determined an age of c. 1.78 Ga. It is considered, that the 1.83 Ga zircon undoubtedly is inherited and the 1.78 Ga is a maximum age for the diabase as mafic fine-grained rocks very seldom contain co-magmatic zircon. Three discordant U-Pb data points analyzed using TIMS reflect an average of c. 1.84 Ga for the very tiny inherited zircon in Kopparnäs diabase. The dyke shows an amphibolite facies mineral

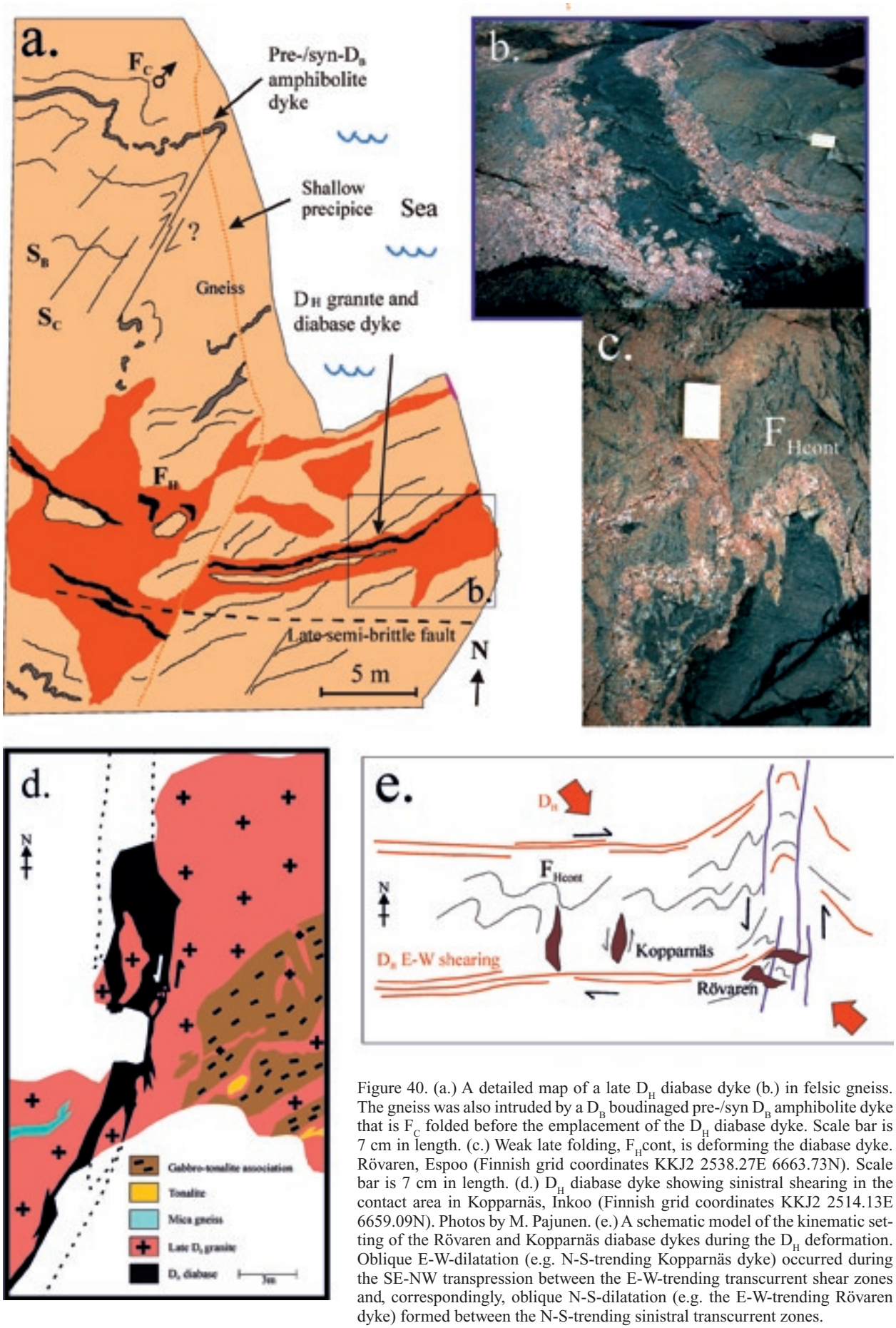

Figure 40. (a.) A detailed map of a late D_H diabase dyke (b.) in felsic gneiss. The gneiss was also intruded by a D_B boudinaged pre-/syn D_B amphibolite dyke that is F_C folded before the emplacement of the D_H diabase dyke. Scale bar is 7 cm in length. (c.) Weak late folding, $F_H$cont, is deforming the diabase dyke. Rövaren, Espoo (Finnish grid coordinates KKJ2 2538.27E 6663.73N). Scale bar is 7 cm in length. (d.) D_H diabase dyke showing sinistral shearing in the contact area in Kopparnäs, Inkoo (Finnish grid coordinates KKJ2 2514.13E 6659.09N). Photos by M. Pajunen. (e.) A schematic model of the kinematic setting of the Rövaren and Kopparnäs diabase dykes during the D_H deformation. Oblique E-W-dilatation (e.g. N-S-trending Kopparnäs dyke) occurred during the SE-NW transpression between the E-W-trending transcurrent shear zones and, correspondingly, oblique N-S-dilatation (e.g. the E-W-trending Rövaren dyke) formed between the N-S-trending sinistral transcurrent zones.

assemblage; therefore the younger zircon age may represent a late metamorphism. However, no metamorphic rims on the young zircon grains have so far been detected. This age is within the error limits approximately the same as that of the post-F_I pegmatitic granite (cf. Pajunen et al. 2008). In Estonia, even later ages for metamorphic minerals (1778 ± 2 Ma for monazite and 1728 ± 24 Ma for garnet) have been published (Puura et al. 2004).

D_H structures and kinematics

The most pronounced D_H structures are the recumbent F_H folds with horizontal S_H axial planes exemplified by the folded Bollstad (Figures 39a and c) or Jyskelä (Figure 34d) granite dykes. Vertical shortening estimated from the folded pegmatitic granite dykes is c. 70–75%. Some shearing along the S_H planes and a weak c. E-tending L_H lineation, indicating with weak E-W dilatation in Bollstad and Västerviken (Pajunen et al. 2008), suggest somewhat smaller vertical shortening. The N-S or E-W trend of the D_H diabase dykes in the Southern Volcanic-sedimentary Belt (SVB) supposes E-W or N-S dilatation during their emplacement. In the NE margin of the Nuuksio granite area (Nu in Figure 9), spaced shear structures indicate c. horizontal top-to-NW movement along the S_H planes (Figure 37c; note that later $F_H$cont folding, discussed later, turned the shear foliation S_H to a thrust fault position). Extensive magmatism and migmatization, vertical shortening and a contemporaneous increase in heat flow resulting in high-T/low-p metamorphism indicate that D_H deformation was related to crustal extension. Although on an outcrop scale the extensional D_H touched the rock often quite homogeneously, regionally there is much variation in its extent. In general, extensional D_H structures and related magmatism were more penetrative in the central parts of the granitoid areas (e.g. EGC), whereas in the bordering areas shearing or faulting left wide areas untouched (schematized in Figure 4). Our limited observations (extensional D_E and D_H structures are very similar on outcrops) on the directions of the extensional movements during the D_H refer to extension outwards from the granitic centres, for example from the Nuuksio area (Nu in Figure 9). This is supported by the patchy distribution of the D_H granites interpreted from the radiometric map (Figure 38).

Folds with NE-trending steep axial planes deform granitoids of different ages to different extents: they deform openly to tightly the earlier S_E foliated rocks (Figure 12c and 36), form gentle folds in the D_H granites (Figure 39a) and refold only weakly and zoned the D_H diabases (Figure 40c). The decreasing contractional strain during this steep F_H folding, from the earlier structures and magmas to the later ones, suggests this folding was concurrent with the evolution of the extensional deformation D_H. Thus, there are two types of F_H folding related to the late Southern Finland Granitoid Zone evolution: the extensional recumbent $F_H$ext folds and the contractional $F_H$cont folds with steep NE-trending axial planes. Due to progressive deformation the contractional and extensional F_H folds may occur on the same outcrops overprinting each other – slightly later contractional F_H folds overprint the extensional F_H folds (Figures 36 and 39a) – or they may form simultaneously in different areas**.**

The $F_H$cont refolded the earlier large-scale F_G folds with E-W-trending axial planes to D_{G+H} dome-and-basins (Figure 11). Locally, the steep $F_H$cont folds are overturned towards the NW (Figure 12c and 19a and d). It is possible that overthrusting along the pre-existing extensional SE-dipping S_E planes also occurred, but we have not observed this so far. The $F_H$cont folds only seldom have distinct axial plane foliation. In the tightly deformed high-T D_H zones, as in Klaukkala, Nurmijärvi (Figure 35), a weak gneissic $S_H$cont foliation exists in the D_H granites. The NE trend of the S_H planes is bent E-W in the northern border zone of the West Uusimaa Complex (WUC). This bending can be explained by the stopping effect during the collision of the hot WUC against the cooled Hyvinkää Gabbroic-volcanic Belt (HGB) along the dextral Hyvinkää shear zone.

The close relations of SE contractional $F_H$cont folds and the E-W dilatational structures is explained by D_H SE-NW transpression between the active E-W-trending transcurrent faults such as the southern Finland shear/fault zone and the Hyvinkää shear/fault zone. The evolution of these shear/fault zones shows a polyphase history that began during the D_E. Hitherto, we have had no observations of high-T, sinistral steep shearing that could be related to $D_E$cont in these zones; thus, rotation of the $D_E$ext into a steep position is suggested. Dextral shearing in these steep zones may have already started during the Central Finland block movements during the D_F, and continued dextral during the D_H transpression. The Hyvinkää gabbros were rotated clockwise during the dextral shear deformations (Appendix 3). The oblique overthrusting of the Hyvinkää Gabbroic-volcanic Belt (HGB) on the West Uusimaa granulite Complex (WUC) occurred due to the D_H SE-NW transpression. The transpression caused oblique E-W dilatation and simultaneous the patchy melting and intrusion of D_H granites that, in the lower-T areas, intruded into N-S-directional oblique dilatation fractures sharply cutting the earlier structures (Figure 15c).

The D_H SE-NW transpression also caused sinistral shearing in the N-S-trending shear zones. The N-S- and E-W-trending D_H diabase dykes indicate dilatation c. perpendicular to each other. The oblique E-W dilatation, the N-S-directed dykes, can be related to SE-NW transpression in between the active E-W-trending shear/fault zones (e.g. Hyvinkää and Southern Finland shear/fault zones). Similarly, the E-W-directed dykes were formed as oblique extension zones in between the N-S-directed shear/fault zones (e.g. in the Vuosaari-Korso shear/fault zone). Indeed, there are several minor shear/fault zones paralleling these major structures in the study area (cf. Elminen et al. 2008), suggesting several possibilities for such oblique dilatational settings. The kinematic setting of the D_H diabase dykes under SE-NW transpression is schematized in Figure 40e. As indicated by the diabase age, the D_H transpression still acted at c. 1.8 Ga ago, suggesting that the transformation to the D_I deformation is more or less transitional.

D_I deformation

The evolution of major N-trending crustal-scale high-strain D_I zones, the Baltic Sea-Bothnian Bay Zone (BBZ), the Riga Bay-Karelia Zone (RKZ) and the Transscandinavian Igneous Belt (TIB) (Figure 8), began at least during D_D (Appendix 7). The Southern Finland Granitoid Zone (SFGZ) predominantly formed during the $D_{E\text{-}H}$. The late phase of the major N-trending high-strain zones, such as the Vuosaari-Korso shear/fault zone, deforms all the structures from the D_A to D_H and hence we prefer to differentiate the deformation event as a new phase D_I. D_I bent the SFGZ, and also the southern Finland and Hyvinkää shear/fault zones (Figure 11) sinistrally into a N-NNE direction.

The Vuosaari-Korso Shear/fault zone (Figure 10) represents a western branch of the Riga Bay-Karelia Zone (RKZ). In the strongest part of the Vuosaari-Korso D_I zone the F_G and F_H folds were refolded or bent to a N-S direction in a ductile manner; the structural relationships are represented by the structures at the Jamppa site, in Järvenpää, in the northern Espoo Granitoid Complex (EGC). The area is intensely D_E deformed with a strong nearly horizontal $S_E$ext that destroyed almost completely the earlier $D_{(A\text{-})B\text{-}D}$ migmatite structures (Figure 31a). The $S_E$ext is a spaced or penetrative mineral foliation; D_E biotite is coarser-grained than D_B biotite. Garnet-bearing tonalite-granodiorite intruded into the S_E planes and was refolded by F_I folding with N-trending axial planes (Figure 31b), which may represent a rotated F_H intensified by D_I. The F_{H+I} folds developed to nearly isoclinal indicating c. E-W shortening. New generation of pegmatitic to medium-grained granite intruded into the N-trending S_I axial plane, which shows shearing with east-side-up movement (Figure 31c). This late granite also cuts or replaces the tonalitic-granodioritic D_E rock. Two garnet generations have been detected in the granite; a new garnet rim overgrows the earlier core. Both generations have a microstructure indicating crystallization from melt (Figure 31d and e). This leads to the conclusion that the thermal conditions were still high during this late phase of structural evolution, especially close to the D_I axial zone in the Espoo Granitoid Complex (EGC) and West Uusimaa Complex (WUC).

The drag folds bending the earlier major structures in the D_I zones indicate sinistral movement on the horizontal surface; the observations of vertical sections (Figure 31d) prove east-side-up movement. These structures and contractional F_I folding showing varying intensity can be explained by c. ESE-WNW transpression during the D_I deformation. In the southern part of the Vuosaari-Korso D_I axial zone, in the Vuosaari triangle (Vu in Figure 9) and to the south of it in the Gulf of Finland, a complex pattern of magnetic anomalies was generated; the D_I deforms the early D_{C+D} dome-and-basin structures. Sederholm (1932b) described brittle structures seen in bathymetric configuration in lake Päijänne, Central Finland: the Lake Päijänne fracture zone in Figure 10. Structurally, Päijänne is on the continuation of the axial trace D_I. As described above, the bedrock to the north of Southern Finland Granitoid Zone (SFGZ) was already stabilized after D_D at c. 1.87–1.86 Ga ago. Thus, the D_I was brittle in the Päijänne area at the time of ductile deformation in the southern part of the zone. The fracture pattern described by Sederholm (1932b) is consistent with c. E shortening characterizing the D_I.

The tight-isoclinal ductile F_{H+I} folds (Figure 31b) demonstrate that the temperature was not reduced under ductile-brittle transition in the Espoo Granitoid Complex (EGC) and West Uusimaa granulite Complex (WUC). The age of 1804 ± 2 Ma for pegmatitic granite, fragmenting a host rock with pre-existing ductile folds with N-trending axial plane (F_g of Pajunen et al. 2008), corresponding to F_I of this paper, proves that ductile folding with N-trending axial planes predates that age. However, ductile shear structures in the pegmatitic dyke contacts indicate that movements still continued afterwards.

So-called post-tectonic granitic intrusions of a c. 1.8 Ga age group consist of small stocks (indicated by the letter P in Figures 1 and 7) or late pegmatitic granite dykes (cf. Alviola et al. 2001). In Sulkava (Su in Figure 9), post-tectonic granite caused a low-pressure metamorphic contact aureole in a migmatitic garnet-cordierite gneiss (Rastas 1990). These

granites often occur in close association with the N-trending crustal D_I zones, like the Sulkava stock in the Riga Bay-Karelia Zone (RKZ) and the Åva ring intrusion (Lindberg & Eklund 1988) in the Baltic Sea-Bothnian Bay Zone (BBZ). We prefer to relate these intrusions as syn-tectonic to the latest phase of the D_I deformation. Presumably, they formed into patchy dilatational settings during the c. ESE-WNW transpressional D_I regime; however, further structural research is needed for more precise determination of the tectonic setting of these granites.

The late evolution of the D_I zones turned to lower grade processes, which can be seen as a change to more semi-ductile and partitioned deformation in the D_I axial zones. Deformation concentrated into rather narrow fault zones with formation of mica-rich slickenside surfaces and protomylonitic to mylonitic structures. According to Elminen et al. (2008), late movements show steep sinistral east-side-up movement in the Vuosaari-Korso zone. This kind of movement is also evident in the Hyvinkää-Lahti shear/fault zone. These late microstructures, described in detail by Elminen et al. (2008), are at least partly related to post-Svecofennian events, D_P, such as to the rapakivi stage (e.g. Mertanen et al. 2008).

Evolution of the major shear/fault zones of Southern Finland

The Hyvinkää and Mäntsälä-Lahti shear/fault zones characterize the structural pattern in the northern study area, and the Southern Finland, Porkkala-Mäntsälä and Vuosaari-Korso shear/fault zones are important features in analyzing the tectonic evolution in the detail study area (Figures 10 and 41). The high strain zones with the same strike, i.e. the E-trending Hyvinkää and Southern Finland shear/fault zones and the N-NNE-trending Mäntsälä-Lahti and Vuosaari-Korso shear/fault zones, have much in common.

The Hyvinkää shear/fault zone

The Hyvinkää shear/fault zone is a c. 8 km wide complex high-strain zone between the Hyvinkää Gabbroic-volcanic Belt (HGB) and West Uusimaa granulite Complex (WUC). The zone is generally covered by thick overlays of sediments and outcropping is poor. It is composed of strongly sheared rocks (Figure 42a) and slices of heterogeneous granite and supracrustal rocks with intensely folded

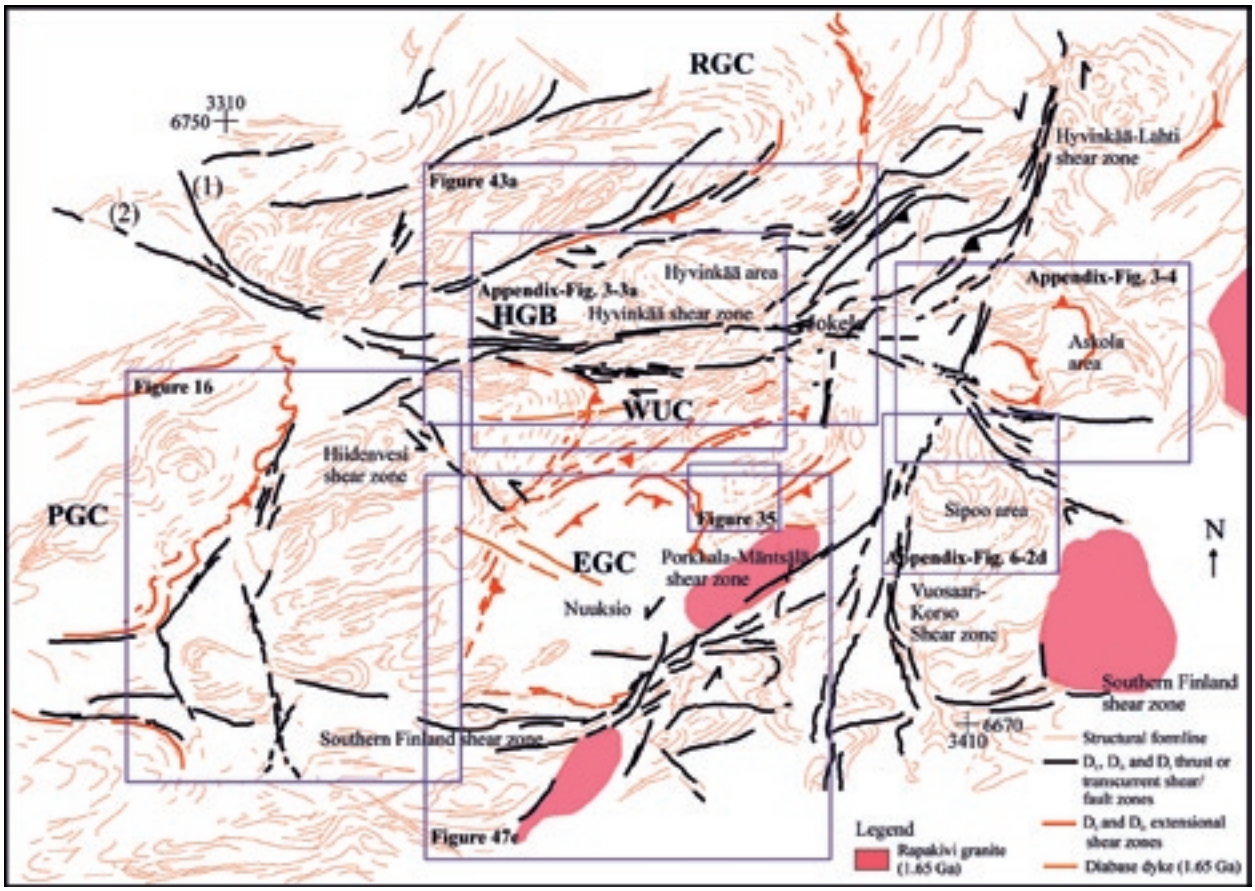

Figure 41. Structural relationships in the Espoo Granitoid granulite Complex (EGC), West Uusimaa granulite Complex (WUC) and Hyvinkää Gabbroic-volcanic Belt (HGB). The areas represented by detailed maps or sketches are shown by boxes. (1) and (2) = NW- and WNW-trending branches of the Hyvinkää shear/fault zone (see text).

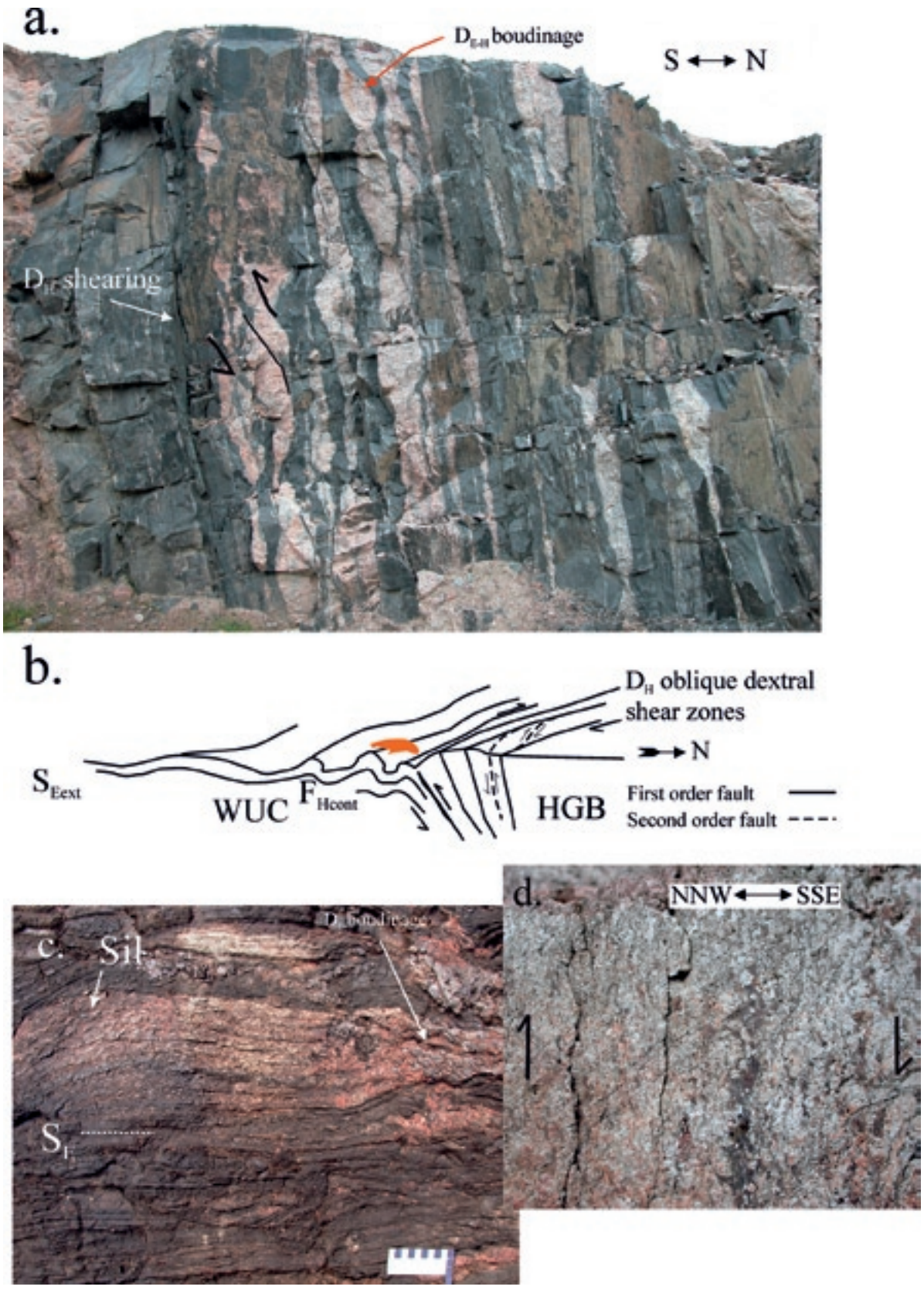

Figure 42. Structures in the polydeformed Hyvinkää shear/fault zone. (a.) A Hyvinkää high strain zone with a strong S_E plane in a steep position. The D_E granite dykes are boudinaged (D_E). Later oblique dextral D_H shearing with N-side-up movement deforms the structure. Width of the area of the figure is c. 6 m. Ylimmäinen, Karkkila (Finnish grid coordinates KKJ2 2534.70E 6715.07N). (b.) A sketch illustrating the $F_H$cont folding of the $S_E$ext planes close to the Hyvinkää shear/fault zone. (c.) S_E foliation with sillimanite in the E-trending mica gneiss related to the Jokela supracrustal association. The outcrop is located in the Hyvinkää shear zone close to the West Uusimaa granulite Complex (WUC), where the gneisses and locally also the granites (see text) show progressive sillimanite growth related to the high-temperature during the deformation. Scale bar is 10 cm in length. Hyvinkää, Kettukallio (Finnish grid coordinates KKJ2 2552.98E 6721.53N). (d.) Protomylonitic granite in the second-order Hyvinkää shear zone; a vertical section showing NW-side-up movement in the dextral oblique shear zone. Width of the area of the figure is c. 1 m. Karkkila, Vaskijärvi (Finnish grid coordinates KKJ2 2518.18E 6717.12N). Photos by M. Pajunen.

internal structures representing the pre-high-strain zone history (Appendix-Fig. 3-2b). The well-preserved Jokela association (Appendix 5) is located in the eastern part of the zone. On the northern edge of the WUC the D_{G+H} interference structures were bent more or less into an E-W-direction against the HGB (Figure 41). Folding with a steep E-trending axial plane (Figure 42b) deformed the $S_E$ext planes (cf. Appendix-Fig. 2-1) close to the zone into a vertical position; further from the zone the $S_E$ext foliation is nearly horizontal and semi-openly refolded by the D_{G+H}.

The first-order structures of Hyvinkää high-strain zone are E-W-trending and refolded/bent by the open D_I structure, like the Hyvinkää-Lahti shear zone. In the west, the Hyvinkää shear/fault zone continues towards the NW; it is divided into branches continuing to Somero and Koski areas ((1) in Figure 41) and, on the other hand, along the lake Painio shear/fault zone, southeast of Somero ((2) in Figure 41). Ductile and sharply-cutting brittle characteristics in the Painio shear/fault zone prove its reactivated evolution. According to geophysical data, the Hyvinkää high-strain zone also has an E-trending extension in the northern side of the Askola dome area (As in Figures 9 and 41), where it is sharply defined, also representing later reactivation of the Hyvinkää zone. Brittle slicken line striations dipping c. 30º to the east on the sheared foliation planes indicate late strike slip movements.

Close to the West Uusimaa granulite Complex (WUC), shearing structures are higher-grade and almost penetratively recrystallized when compared to those to the north of it. In the highest-grade zone in granites (observations only from boulders) and in mica gneisses, sillimanite was formed (Figure 42c) into the sheared foliation plane. Locally, sillimanite-bearing foliation and the folding with E-trending axial planes (Figure 42b) in the WUC are still overprinted by melt patches. These observations indicate that during the deformation, thermal heat flow was high in the vicinity of the hot WUC. We relate the sheared foliation to S_E that corresponds to S_E in the Jokela association (Appendix 5), where the foliation was refolded by later deformation events (Appendix-Fig. 5-3a). The observations suggest that the earliest phase of the evolution of the Hyvinkää shear zone was initiated during the extensional D_E phase (Figure 42a); however, most of the fault rock structures suggest shortening (Figure 42b).

On outcrops, the first-order, E-W-trending shear zones dip steeply (90–80º) to the north, and the second-order zones north of WUC are upright and trend ENE (Figure 42b). Kinematic interpretation of the E-trending first-order zones is based on protomylonitic foliation structures, S-C structures, rotational fragments and drag folds. These steep shear zones show N-side-up dextral oblique reverse movements. There are few observations on the ENE-trending steep second-order shear zones with NNW-side-up dextral oblique reverse movements (Figure 42d). The Hyvinkää gabbro massifs and their surroundings also show a map-scale dextral rotation (Appendix-Fig. 3-3). The E-axial folded structure in Figure 42b concurrent with the shear movements in the high-strain zones suggests a NW-SE transpressional stress field – this type of kinematics characterizes the D_H deformation.

The geophysical model in Figure 43 supports the tectonic interpretation based on field observations. The Hyvinkää high-strain zone forms a belt of tectonic slices narrowing downwards. The structure accompanied with dextral oblique kinematics of the shear zones postulates oblique N-side-up movement of the tectonic slices upon the thrust plane. The interpreted thrust plane, between the WUC and the overlying HGB, dips northwards below the HGB with a dipping angle of c. 20–30º.

Structures in $L_{B/C}$ lineated amphibolitic rock in the Hyvinkää Gabbroic-volcanic Belt (HGB), NE of the Hyvinkää gabbro massif, are schematized in Figure 44a. The amphibolite is cut by pegmatitic granite. Similar pegmatitic granites also cut the Hyvinkää gabbro massifs, supracrustal sequences of the HGB and the Jokela supracrustal association (Appendix-Fig. 5-2). In the internal parts of the HGB, they intruded as sharply-cutting dykes fragmenting a cooled and stabilized crust. We relate these pegmatite granites the D_H granites in the West Uusimaa granulite Complex (WUC) and Espoo Granitoid Complex (EGC). The amphibolite with strong lineation is cut by semi-brittle faults with spacing of several centimetres. The fault planes show slicken line striations that indicate thrusting towards the SSE. Under the microscope (Figure 44b) the rock has a complex pattern of narrow semi-brittle faults cutting the rock. The faults are openly folded by c. E-W contraction. We correlate the faults to oblique thrusting related to the transpressional collision, D_H, in the Hyvinkää high-strain zone and the open folding to the D_I deformation. In general, the transpressional structures (D_H) in the cooled parts of the HGB are semi-brittle to brittle in character (Appendix-Fig. 3-1a).

Summarizing, the formation and kinematics of the high-strain zone between the West Uusimaa granulite Complex (WUC) and Hyvinkää Gabbroic-volcanic Belt (HGB) is related to continuing deformation events. The earliest structures were already formed during the extensional D_E. The strongest shearing structures formed during the crustal

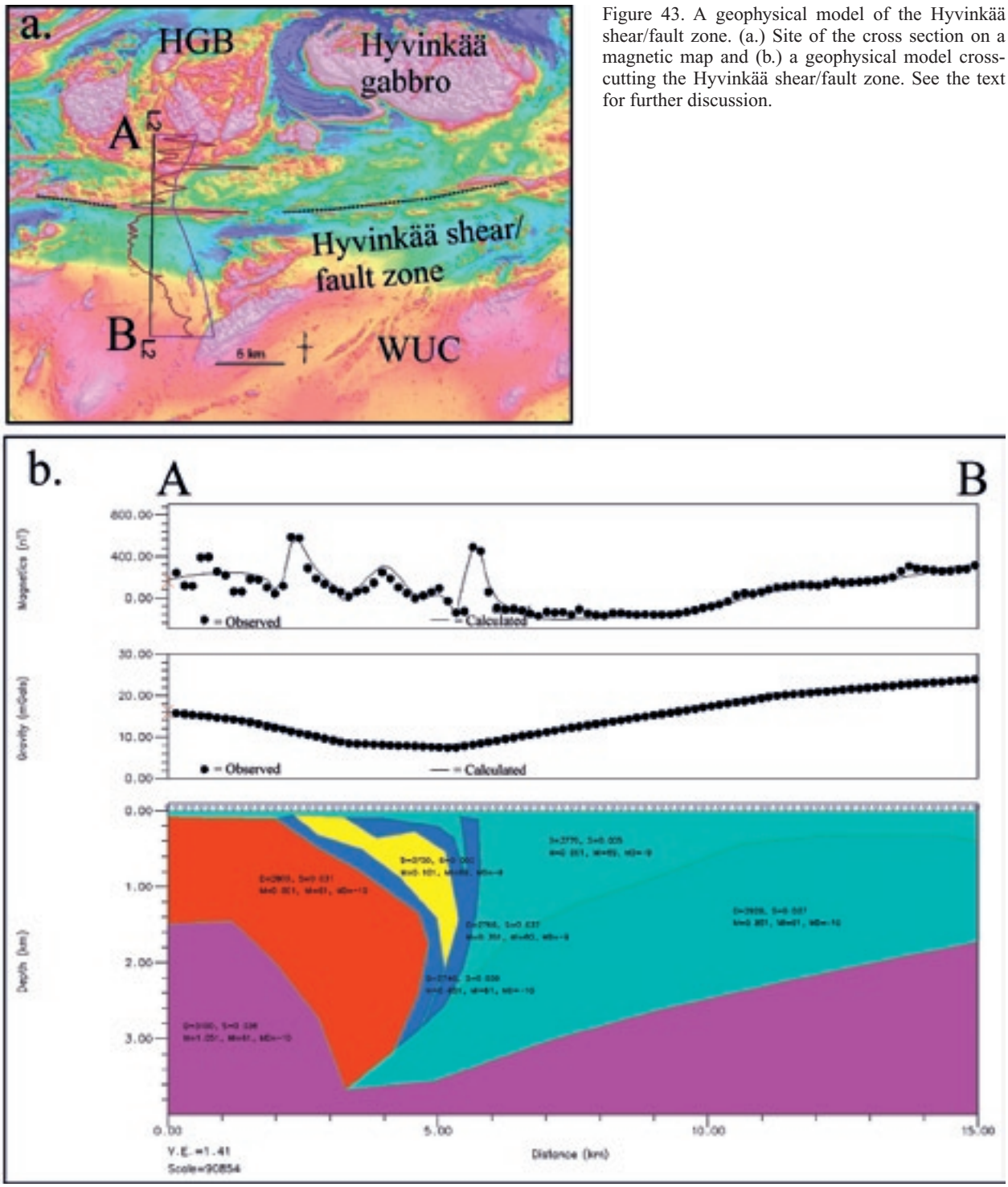

Figure 43. A geophysical model of the Hyvinkää shear/fault zone. (a.) Site of the cross section on a magnetic map and (b.) a geophysical model cross-cutting the Hyvinkää shear/fault zone. See the text for further discussion.

shortening in transpressional deformation D_H. The bends and folds in the boundary zone are a consequence of heterogeneous strain in the border zone during continuing oblique overthrusting of the HGB onto the WUC. The late regional D_I refolded the Hyvinkää zone extensively (Figure 41). During the final stage, movements occurred along E-trending semi-brittle faults due to blocking of the ductile structure under cooling.

The Hyvinkää-Lahti shear/fault zone

The SSW-NNE/SW-NE-trending Hyvinkää-Lahti shear/fault zone is located in the axial zone of D_I (Figures 10 and 41). According to geophysical and tectonic interpretation, using map-scale bends of the earlier structures and the existence of higher-grade rocks in the Askola area, sinistral oblique E-side-up movement occurred in the zone; it is similar

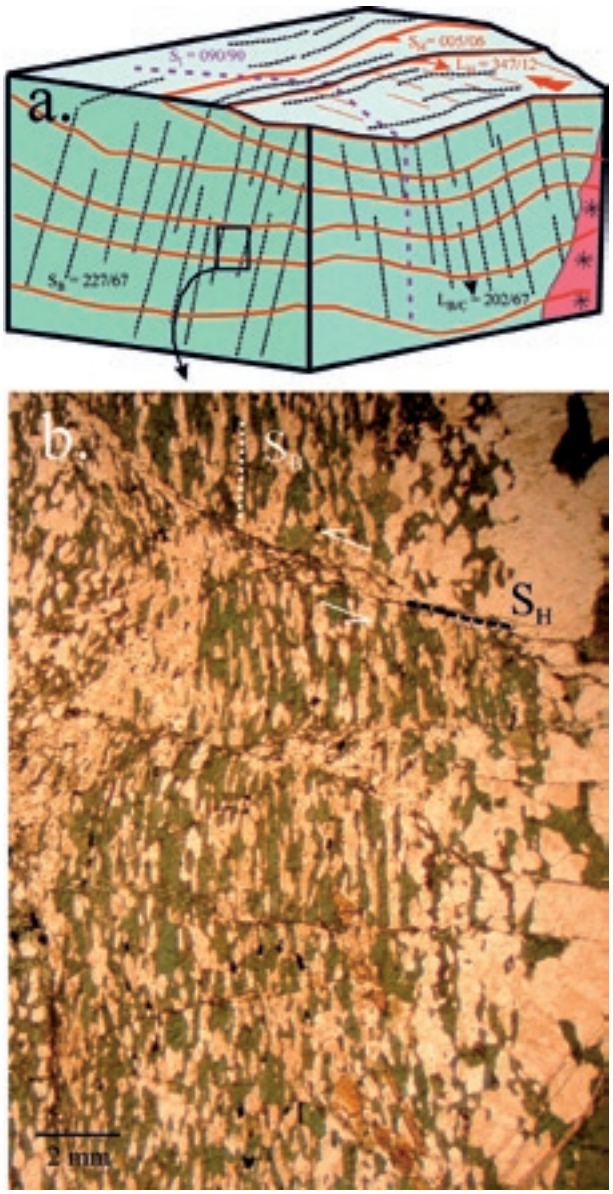

Figure 44. (a.) $L_{B/C}$-lineated amphibolite showing D_I folding of semi-brittle spaced thrust foliation planes, S_H, that were interpreted as a product of oblique c. SSE-thrusting on the northern side of the Hyvinkää gabbro; L_H is slickenline lineation on the S_H planes. The Hyvinkää Gabbroic-volcanic Belt (HGB) was a cooled and competent area during the late D_H event occurring in the granite-dominant units. Thus, the D_H and later structures are brittle and granites sharply cut the HGB (cf. Appendix-Fig. 3-1a). (b.) A microscopic photo of the amphibolite showing semi-brittle fractures. Hirvijärvi, Riihimäki (Finnish grid coordinates KKJ2 2535.92 6729.82N). Photo by M. Pajunen.

to that Vuosaari-Korso zone (cf. Elminen et al. 2008). However, the D_I bends the Hyvinkää shear structures into a NE-NNE direction and this causes complexity in this major crustal zone. On the NW-side of the zone, the magnetic signature of the sliced structure shows a SE-dipping pattern of anomalies. Our tectonic measurements from the area are limited, but in general, the tectonic measurements on the geological map (Kaitaro 1956) show a pattern that predominantly follows the earlier structures, particularly the D_{G+H} pattern. The structures close to the most intense D_I deformation zones are often dipping steeply to the SE, which, together with the magnetic pattern, indicates stacking towards the NW during D_I.

The Hyvinkää-Lahti shear/fault zone, which is parallel to the axial plane of the open semi-ductile crustal bend F_I, continues further north to the Lake Päijänne fracture zone (cf. Sederholm 1932). The differences in characteristics of this D_I zone from the high-T ductile south to low-T brittle north are due to early stabilization of the northern Svecofennian crust.

Southern Finland shear/fault zone

The polyphase E-trending Southern Finland shear/fault zone represents a complex high strain zone (Figure 45a and b), which is faulted/sheared by the late phases of the Porkkala-Mäntsälä zone and extensively folded and faulted by the Vuosaari-Korso D_I deformation zone. The Southern Finland shear/fault zone is composed of several parallel high-strain zones bordering the tectonic units, like those dominated by supracrustal (SVB) and granitic rocks (EGC). The most intense zone in the study area borders the non-migmatitic Pellinki area (Pe in Figure 9) and Vuosaari triangle (Vu in Figure 9) from the granitic units in the north. Elminen et al. (2008) describe in detail the late, ductile to brittle structures and kinematics of the Southern Finland shear/fault zone. Structures in the high-strain gneisses and mylonite gneisses exhibit a steep shear zone with dextral S-side-up oblique reverse movement (Elminen et al. op. cit.). In the stronger zones, intense spaced biotite shear foliation has been generated (Figures 45a and b). However, the metamorphic evidence, well-preserved non-migmatitic volcanic rocks in the Vuosaari triangle versus highly migmatitic rocks just north of the major shear zone, indicates opposite movement in this area. Stretching lineation in the sheared gneisses shows a moderate dip to east, indicating oblique movement.

The Southern Finland shear zone was already initiated during the extensional D_E deformation forming the early border zone between the granitoid and supracrustal belts. The D_G deformation (N-S shortening) intensified close to the zone to form steep southwards-overturned folds (e.g. Figure 28) and reoriented the early phase (D_E) of the E-W-trending zone to a NE-SW trend (Porkkala-Mäntsälä zone). The main structures characterizing the Southern Finland shear zone were generated during the D_H SE-NW transpression. This produced the dextral oblique reverse movements in the steep Southern Finland shear/fault zone. Late reactivation was

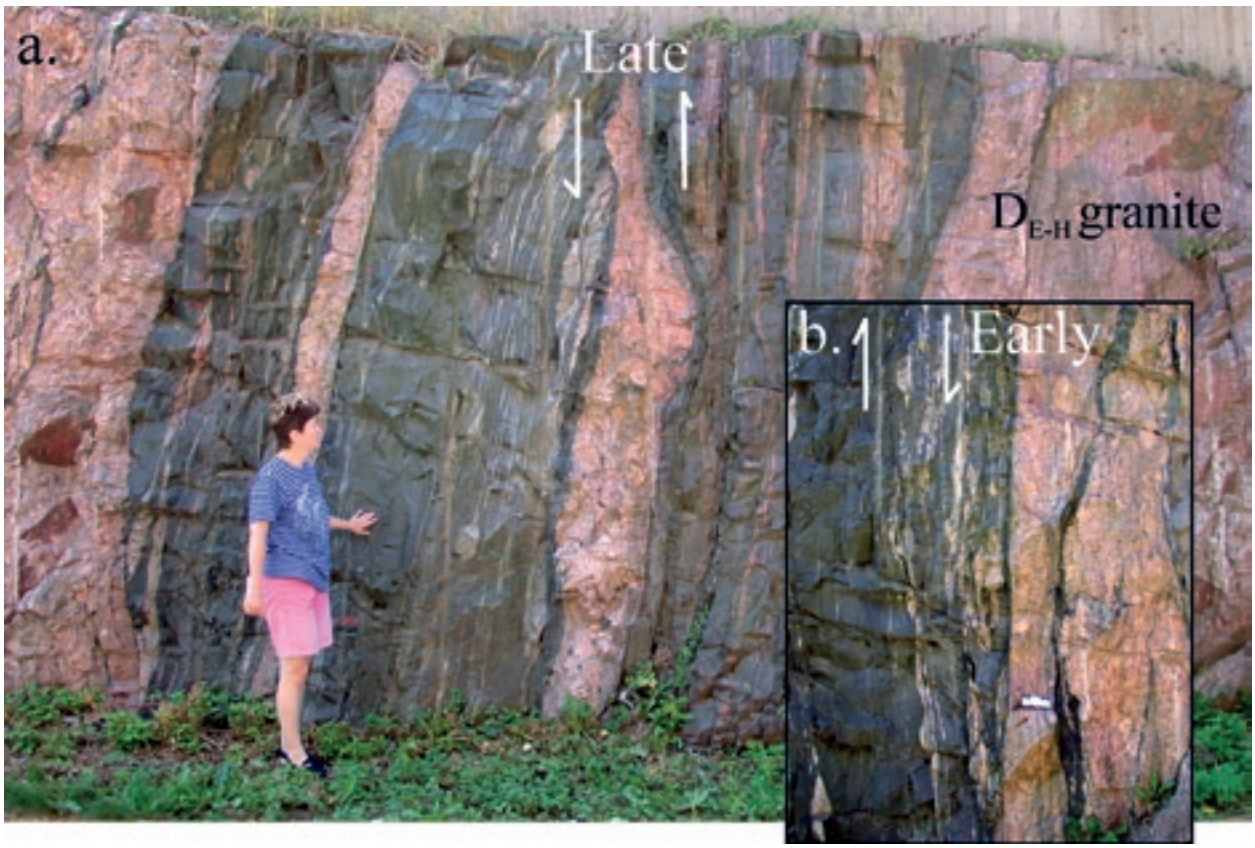

Figure 45. Structures in the Southern Finland shear/fault zone. The outcrop is situated in the strongly deformed and folded area between the Porkkala-Mäntsälä and Vuosaari-Korso zones. The outcrop shows opposite directions of movement on vertical surface: (a.) late movement north-side-up and (b.) early movement south-side-up movements. Scale bar is 15 cm in length. Otaniemi, Espoo (Finnish grid coordinates KKJ2 2545.68E 6674.71N). Photos by M. Pajunen.

common in the Southern Finland shear/fault zone; nearly horizontal slicken line striations on the late E-trending steep fault planes indicate both sinistral and dextral strike-slip movement.

The structures observed in the Southern Finland shear/fault zone are very similar to those in the Hyvinkää shear/fault zone (compare Figures 42a and 45a). Dextral transpressional evolution in the Southern Finland Granitoid Zone (SFGZ) was postulated by Ehlers et al. (1993), but our observations indicate longer history for the zone; the SE-NW transpression only characterizes the latest SFGZ and major shear zone evolution.

Porkkala-Mäntsälä and Vuosaari-Korso shear/fault zones

The polyphase character of the Porkkala-Mäntsälä/(Lahti) shear/fault zone was discussed in early papers, e.g. Härme (1969), and there have been several papers dealing with corresponding NE-trending shear/fault structures further west (compiled by Lindroos et al. 1996). We recommend the name Porkkala-Mäntsälä shear/fault zone because it is connected to the Vuosaari-Korso zone to the south of the E-trending Hyvinkää zone (the name Vuosaari- or Helsinki-Päijänne would better describe the setting of the Vuosaari-Korso zone of this paper; Figures 9 and 10).

The Porkkala-Mäntsälä shear/fault zone steeply cuts the E-W-trending Southern Volcanic-sedimentary Belt (SVB) and Espoo Granitoid Complex (EGC), and also the Southern Finland shear zone. It bends the Southern Finland shear zone into a NE-direction. In the study area the early structures of the Porkkala-Mäntsälä zone are ductile sinistral bending of the earlier structures (Figure 46a) against the Nuuksio granitoid unit. In Figure 46b there is an example of migmatitic tonalitic gneiss in the NE-trending Porkkala-Mäntsälä zone at the Bemböle site in Espoo. Locally, as at the Bemböle site, the steep structures of the originally E-W-trending Southern Finland shear zone were bent into a NE direction, and these old structures oriented the shear movements in the Porkkala-Mäntsälä zone. A NE-trending crenulation cleavage (Figure 46c) and related steep-axial folds with NE-trending axial planes were formed in sinistral strike-slip movement under D_G N-S contraction. On the NW side of the Porkkala-Mäntsälä zone the $S_E$ext and D_G structures were

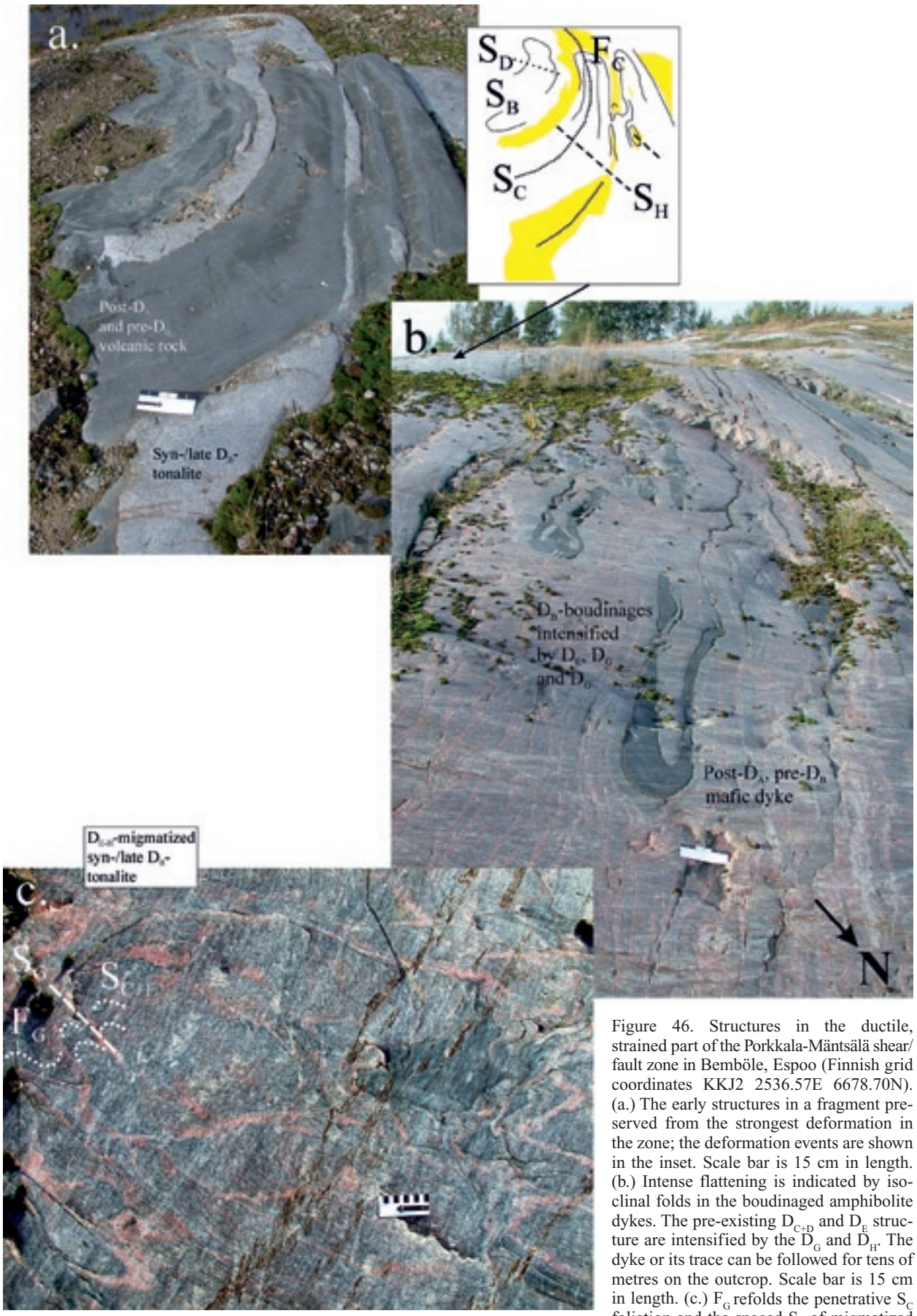

Figure 46. Structures in the ductile, strained part of the Porkkala-Mäntsälä shear/fault zone in Bemböle, Espoo (Finnish grid coordinates KKJ2 2536.57E 6678.70N). (a.) The early structures in a fragment preserved from the strongest deformation in the zone; the deformation events are shown in the inset. Scale bar is 15 cm in length. (b.) Intense flattening is indicated by isoclinal folds in the boudinaged amphibolite dykes. The pre-existing D_{C+D} and D_E structure are intensified by the D_G and D_H. The dyke or its trace can be followed for tens of metres on the outcrop. Scale bar is 15 cm in length. (c.) F_G refolds the penetrative S_C foliation and the spaced S_E of migmatized syn-/late D_B gneissic tonalite. Scale bar is 10 cm in length. Photos by M. Pajunen.

F_H-folded and overturned NW, e.g. in Kauklahti (Figures 19a and d). The F_H with NE-trending axial planes is a consequence of rotation of the stress field into SE-NW-directional transpression during the D_H.

In the high-grade parts of the Espoo Granitoid Complex (EGC) and West Uusimaa granulite Complex, continuing deformation caused intensifying and bending of the earlier D_H structures into a N direction by the D_I, still under high-grade ductile conditions. Sinistral E-side-up shearing (e.g. Figure 31d) occurred along the steep N-directional D_I shear/fault zones, as in the Vuosaari-Korso shear/fault zone. These kinds of sinistral shear zones are also found elsewhere in the study area (Figure 47a). The early stage N-S-trending sinistral shear zones are related to the SE-NW transpression during the D_H; the D_H diabase dykes were intruded into oblique dilatational ($D_H$ext) settings (Figure 40e). During the latest Svecofennian evolution the maximum principal stress rotated from SE-NW into a more easterly direction causing some ductile folding, F_{H+I} (Figure 31b), after which cooling and fading of the Svecofennian deformation caused transformation to more brittle events. Sinistral movements in the Vuosaari-Korso shear zone became brittle and localized in character. In the Porkkala-Mäntsälä fault zone, late movements were dextral (Figure 47b) and they are related to the post-Svecofennian events D_P. Elminen et al. (2008) relate dextral movements to the rapakivi stage.

The tectonic pattern produced by the shear/fault structures, especially D_H and D_I, and the low-angle D_E structures strongly oriented the post-Svecofennian tectonic reactivation and emplacement of the rapakivi intrusions (Figure 47c) in the area.

Structural setting of rapakivi granites – D_P

The rapakivis are divided to different age classes by Haapala et al. (2005). The rapakivi intrusions in the study area belong to the c. 1.67–1.62 Ga age group that forms a c. N-NNE-trending zone from Lithuania to Southern Finland. The intrusions located in a close association with the BBZ are dominated by rapakivis of 1.59–1.54 Ga in age. There are two small 1.65 Ga rapakivi intrusions in the detailed study area, Bodom and Obbnäs, and the Onas and Vyborg rapakivi intrusions are just east of it (Figure 9) (e.g. Vaasjoki 1977a).

The Bodom rapakivi is a NE-trending intrusion on the NW side of the Porkkala-Mäntsälä shear/fault zone. The intrusion is thinner at its northern end; the Svecofennian magnetic anomalies are distinguishable through the rapakivi mass. Its southwestern part forms a round stock without such a magnetic anomaly pattern. According to Kosunen (2004), it represents a younger intrusive phase. The internal structure of the batholith is well seen in the topographic pattern in the rapakivi area. The rapakivi is sharply bordered against the Porkkala-Mäntsälä fault, which drags the SE-border of intrusion under dextral movement D_P. This movement can also be seen in mylonitic shear zones overprinting the early sinistral D_G phase of the zone (Figure 47b). The topography in the Bodom rapakivi area exhibits an arched pattern; in the NE-part of the intrusion the Svecofennian remnants show similar arched forms (Laitala 1967). The magnetic patterns and the arched forms support narrow, sheet-like horizontal intrusions intruded in a laccolith-like manner. Sederholm (1923) argued that the western rapakivis might be sheet-like bodies. Magnetic patterns of the Bodom and Vyborg rapakivi massifs support such a structure. The nearly horizontal $S_{E/H}$ plane characterizing large areas in Nuuksio synform forms an appropriate structure for emplacement of these horizontal rapakivis (Figure 47c). The thickest part of the Bodom intrusion is in the SW. It is interpreted as the site of the intrusion channel, which is located in the intersection point of the Porkkala-Mäntsälä fault, Southern Finland shear zone and the N-trending D_I structure (Figure 47c). The rapakivi-related diabase dykes, especially in the western study area and in the West Uusimaa granulite Complex (WUC), also intruded at least partly into the pre-existing Svecofennian structures. An example is the Hiidenvesi D_F shear zone (Figures 10 and 41), which was hidden below the Espoo Granitoid Complex (EGC), but controls the orientation of the rapakivi-related diabases. Fracturing and jointing (Wennerström et al. 2008) in the dyke direction was also generated in the above-lying Nuuksio granitoid area. Some diabases are very fine-grained, indicating emplacement close to the present erosion level.

The Obbnäs intrusion does not show such a magnetic anomaly pattern as the Bodom intrusion. This is why we suppose it to be thicker and to represent a root section of the rapakivi intrusion corresponding to the SW stock of the Bodom batholith. In principle, its tectonic setting is similar in the intersection of the southern Finland shear zone, Porkkala-Mäntsälä shear/fault zone and D_I deformation zone as was described from Bodom. Airo et al. (2008) noticed gravity lows corresponding to those caused by the described rapakivi intrusions in the intersections of the Vuosaari-Korso and the Porkkala-Mäntsälä zone and further south at the intersection of the southern Finland and the Vuosaari-Korso zones. These anomalies may represent rapakivis that are not exposed on the present erosion level.

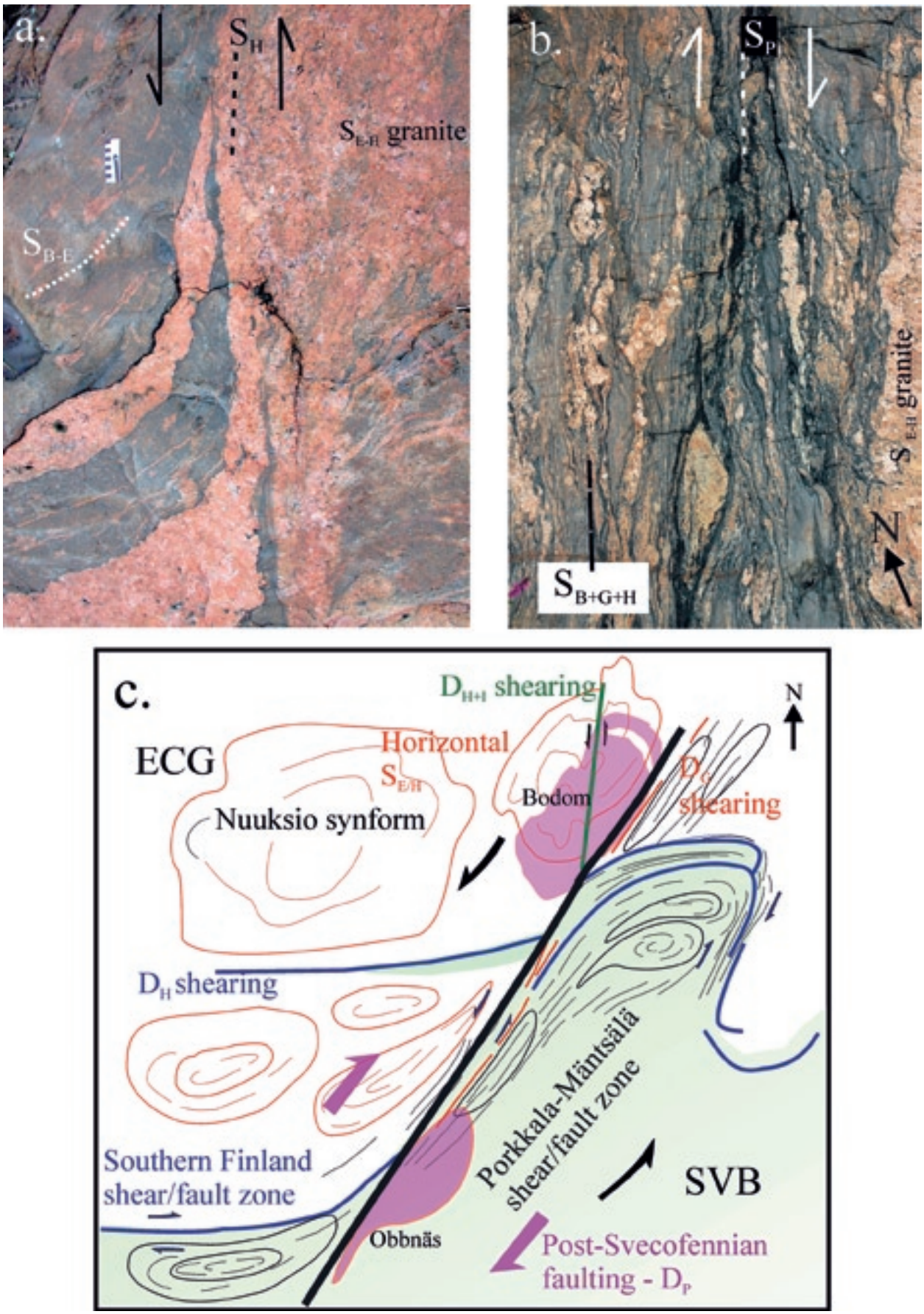

Figure 47. (a.) Sinistral N-trending $D_{H(-I)}$ shearing. Scale bar is 10 cm in length. Kopparnäs, Inkoo (Finnish grid coordinates KKJ2 2514.13E 6659.09N). (b.) Post-Svecofennian dextral D_P faulting on the horizontal surface in the Porkkala-Mäntsälä shear/fault zone. The pre-existing strong D_E is rotated by the D_G into a SW-NE-trend. Width of the area of the figure is c. 70 cm. Porkkala, Kirkkonummi (Finnish grid coordinates KKJ2 2252.10E 6651.87N). (c.) The tectonic structure of the Porkkala-Mäntsälä zone in Espoo and structural setting of the Bodom and Obbnäs rapakivi intrusions. Photos by M. Pajunen.

The Vyborg rapakivi batholith is, according to the magnetic and gravity anomaly pattern, thickest in the western part of the batholith, and the Ahvenisto rapakivi intrusion (5 in Figure 9) is located in the northern extension on this pattern. Both are controlled by the N-trending structure D_1 shown in Figure 8. The magnetic pattern in the Vyborg rapakivi batholith also shows intrusive phases intruded linearly in the ENE direction. It is also evident that the western part of the Vyborg rapakivi represents such an intersection of major crustal fault zones as the Bodom and Obbnäs stocks; according to the magnetic anomaly pattern it thins towards the east from the D_1 zone.

Korja and Heikkinen (1995) described listric fault structures related to the extensional evolution of the rapakivi in Åland. This study shows that the late Svecofennian structures were of great importance for the post-Svecofennian tectonic and magmatic events in controlling where the crust was weakest. The ENE-trending phases in the Vyborg batholith emplaced into the N-trending D_1 zone fit well the dextral kinematic pattern of movements observed in the Porkkala-Mäntsälä zone and in the N-trending major crustal deformation zones, the Baltic Sea-Bothnian Bay Zone (BBZ) and Riga Bay-Karelia Zone (RKZ) (Figure 8). The fault kinematics related to the rapakivi stage indicate c. N-S-directional extension (Elminen et al. 2008) in the study area. Bergman et al. (2006) described dextral transpression in the Storsjö-Edsby Deformation Zone in Sweden. In summary, the emplacement of the rapakivis may be related to dilatational settings during major c. N-trending dextral shearing in transpressional deformation (cf. Bergman et al. 2006), and magma channelling and emplacement were strongly controlled by the late Svecofennian structures, especially the intersections of the major shear/fault zones.

The relations of the latest brittle faults, like the thrust faults shown in Figure 19a, to the Svecofennian structures have not been studied so far; observations of such faults are limited on outcrops due to the weak character of the structures.

TECTONIC EVOLUTION OF THE SVECOFENNIAN DOMAIN IN FINLAND

Hietanen (1975) was the first to compile an evolutionary model based on the modern plate tectonic scheme in Finland. Koistinen (1981) described the structures related to the Svecofennian collision and overthrusting tectonics in the Archaean craton boundary. Korsman et al. (1984) described the tectono-metamorphic discordance between the southern (GMB) and northern (TMB) Svecofennian terranes, and proposed a suture zone between them (Korsman et al. 1988). Based on comprehensive pre-existing data, Lahtinen (1994) presented a model of the accretion history of the Svecofennian orogen suggesting that the Svecofennian domain was produced by complex accretion of several arcs against the Archaean continent. Kilpeläinen (1998) studied the relationships between the tectonic structures and metamorphic evolution in the Vammala Migmatite Belt (VMB) and Tampere Schist Belt (TMB) by analyzing folding patterns of metamorphic isograde surfaces related to different stages of tectonic evolution. He was able to establish the complex pattern of deformation and metamorphism in the deeper crust with concomitant deposition of sediments on the surface in the active collisional orogen. Since then, collision-accretion models have been expanded to include the deep crustal structure (Korsman et al. 1999) and widened to comprehend the whole Fennoscandian Shield (Nironen 1999). Lahtinen et al. (2005) divided Svecofennian evolution into several orogens. The latest models of the crustal structure developed using the reflection seismic data of the Finnish Reflection Experiment, FIRE 2001–2005, are compiled in Kukkonen and Lahtinen (2006).

The Svecofennian structural succession in southernmost Finland has recieved less attention. Laitala (1973a) analyzed the structures in the Pellinki area. Ehlers et al. (1993) divided the deformation in the southern Svecofennian domain into two major crust-forming stages: an early island arc orogen and collision and a later transpressional event responsible for the generation of the Southern Finland Granitoid Zone. Väisänen (2002) compiled the tectono-metamorphic evolution in southwestern Finland concentrating on the granulites in the Turku area; he placed special emphasis on the evolution of the Southern Finland Granitoid Zone and concluded it to be a result of crustal collapse. Pajunen et al. (2002) described the structural evolution in the Helsinki region; this paper is partly a revision of these early results. Skyttä et al. (2006) studied the structural succession and kinematics in Kisko, in the Orijärvi area. They describe the structures in the low-strained steep gneisses in the so-called Kisko Triangle (e.g. Väisänen & Mänttäri 2002; cf. Vetio outcrop, Appendix 4) and in the highly-strained horizontal gneisses outside of the Triangle (cf. Pajunen et al. 2008).

Summary of Svecofennian structural succession and division into geotectonic events

The polyphase structural succession in the southern Svecofennian domain is complicated due to significant rotations of the stress field during the tectonic evolution. The relations of the observed structures appeared to be more complicated because of the contemporaneous formation of structures in contractional and extensional zones during progressive deformation. In the southern study area (1 and 2 in Figure 1) the Svecofennian structures are divided into D_A-D_I phases that can be identified using the overprinting relations of structures, metamorphic events and magmatism on outcrops. The Svecofennian structural succession in the study area (note that due to diachronic evolution the early deformations, D_A-D_D, occurred c. 10 Ma earlier in the north) can be divided into major geotectonic events (E) as follows:

Event 1: D_A deformed the early sedimentary rocks and the volcanogenic rocks of Series I c. 1.9–1.89 Ga ago. Kinematic observations suggest c. N-S compression during D_A causing approximately E-W-trending fold axes of isoclinal, originally recumbent F_A folds. The D_A represents the first major geotectonic Event 1 (E_1), which caused thickening of the early crust under low-temperature conditions.

Event 2: D_B is a crustal flattening phase that deformed the D_A structures under progressive metamorphism, intense magmatism and migmatization. The volcanogenic rocks of Series II were evolved. D_B occurred in the south at c. 1.88–1.87 Ga and is related to crustal extension under rather constant pressure conditions. D_B is regarded as the second major geotectonic Event 2 (E_2), which caused thinning of the E_1 crust.

Event 3: D_C deformed the previous structures during N-S compression to tight F_C folds in amphibolite facies conditions at c. 1.87 Ga ago. The D_C N-S shortening thickened the crust rapidly after E_2 and is separated here as the third major geotectonic Event 3 (E_3). As a result of the Events 1–3, a new Archaean-Svecofennian continental crust was formed.

Event 4: Event 4 (E_4) is linked to the complex structural, magmatic and metamorphic evolution in the new $E_{1–3}$ continental crust. In the south, E_4 is predominantly connected to the evolution of the Southern Finland Granitoid Zone (SFGZ) during the $D_{E\text{-}H}$ deformations. The D_D produced D_{C+D} interferences concurrently with the D_4 block movements in the north. Early E_4 evolution, predominantly D_E that started at 1868 ± 3 Ma, occurred under SW-NE transpression associated with oblique extensional zones of intense intermediate to felsic magmatism. On the erosion surface the oblique extensional pull-apart basins were generated. Transition from SW-NE transpression to SE-NW transpression, during D_H, occurred at c. 1.85–1.84 Ga ago through short steps of varying stress fields – D_G and D_F. The E-W and N-S-trending major high-strain and shear/fault zones played a considerable role during the E_4 transpressional deformations.

Event 5: The latest major Svecofennian geotectonic Event 5 (E_5) is related to the deformation that concentrated in the major N-trending deformation zones, the Riga Bay-Karelia Zone (RKZ) and Transscandinavian Igneous Belt (TIB), and to a lesser extent the Baltic Sea-Bothnian Bay Zone (BBZ). The Southern Finland Granitoid Zone (SFGZ) was deformed in decreasing temperatures under c. ESE-WNW shortening, D_I, to wide-scale folds. At c. 1.8 Ga the crust started to cool, leading to fading of E_5 and the Svecofennian orogeny in Finland.

Table 1 summarizes the observed structures identified in different tectonic units in the southern study area. The structural observations suggest different structural histories in different units and crustal depths. Their occurrence on the recent erosion level is controlled, in addition to the major fault and shear zones, by the wide-scale folding patterns (Figure 11). The following differently deformed and metamorphosed tectonic units can be distinguished:

1. Early high-grade events (E_1 and/or $E_{2–3}$) overprinted by a later high-grade event (E_4) characterizing large areas of the southern Svecofennian domain – exemplified e.g. by Pajunen et al. (2008) by the Västerviken site in Karjalohja.
2. An early weakly-deformed, low-grade event (E_1 and/or $E_{2–3}$) that is later overprinted by an non-migmatitic low-grade (generally amphibolite facies) event (E_4) – exemplified by the Vetio site in Kisko (Appendix-Fig. 4-1).
3. Early low-grade event (E_1 and/or $E_{2–3}$) or late deposition (early E_4) overprinted by later a high-grade event (later E_4) – exemplified by the gneisses of the Upper Tectonic Unit (UTU) (Appendix-Figs. 6-2a–d).
4. Late deposition (early E_4) and a low-grade non-migmatitic (amphibolite facies) late event (later E_4) – exemplified by the rocks of the Jokela supracrustal association (Appendix 5).

The present data are insufficient to map the distribution of these tectono-thermally different units,

Table 1. Observed structures in the geotectonic terranes and tectonic units in the study area.

	SVB	**EGC**	**HGB**		**UTU**	**Jokela supracrustal association**	**WUC (modified from Pajunen et al. 2008)**	**Orijärvi area**
	Supra-crustal rocks	***Grani-toid area***	***Gabbros and supra-crustal rocks***	***Askola dome interiors, supra-crustal rocks***	***Migmatitic garnet-cordierite gneisses rocks***	***Pull-apart basin sedi-ments and volcanic rocks***	***Västerviken outcrop (modi-fied from Pajunen et al. 2008)***	***Vetio outcrop, andalusite-cordierite schist***
Volcanic Series I	X						X	
D_A	X			X			X	
Volcanic Series II	X		X					(?)
Pre-D_B intrusions	X		X				X	
D_B	X		X	X			X	(?)
Syn-/late D_B tonalites	X		X	X			(?)	
D_C	X		X	X			X	
D_D	X		X	?			?	
Cooling	X		X	X			X	X
D_E	X	X	X	X	X	X	X	X
Early/mid-D_E granitoids and dykes		X		X	X		X	
Late D_E gabbros		X					X	
D_F		X					X	
D_G	X	X	X		X	X	X	
D_H	X	X	X		X	X	X	X
D_H granitoids	X	X	X	X	(?)	X	X	
D_I	X	X	X		X	X	X	

but more careful structural mapping and correlation of structural, magmatic and metamorphic events is needed.

The first geotectonic Event 1 (E_1) – early collisions and crustal thickening

The structures of the earliest-observed Svecofennian deformations are not correlative between the major geotectonic terranes like, for example, in the Karelian terrane lying upon the Archaean continent, in the early Svecofennian Pyhäsalmi primitive island arc (Savo Schist Belt, SSB) or in the Southern Volcanic-sedimentary Belt (SVB). Koistinen (1981) interpreted that D_1 in the Karelian terrane, in the Outokumpu area, was related to the regional overthrusting of the Karelian supracrustal sequences and ophiolites upon the Archaean domain; the collision began before 1.90 Ga. Weak pre-D_1 folds were also described, but their tectonic significance was not established (Koistinen 1981).

In the different units of the Svecofennian domain the early structures are quite similar intrafolial folds that in some measurable cases suppose approximately N-S transport (cf. Pajunen et al. 2008) causing crustal thickening. In the southern study area the earliest thickening event (E_1) occurred after the deposition of early volcanic Series I at c. 1.90–1.89 and before Series II 1.88–1.87 Ga ago. We suggest that E_1 was a low-grade, low-angle thrusting event, which had an important effect on the slicing of the earliest primary sequences and the thrusting of rocks from different crustal depths and geotectonic environments close to each other, close to their present-day positions in the $D_{C\text{-}D}$ structures. We also suggest that the accretion of the southern units, the Tonalite Migmatite Belt (TMB) and the Granite Migmatite

Belt (GMB), occurred during the southern D_A. The maximum age of D_1 in the Vammala Migmatite Belt (VMB) is determined as c. 1.91 Ga, which indicates an earlier D_1 evolution when compared to the D_A to the south of it. Kinematic and age determination of the corresponding early structures and references to their ages in the Central Finland Granitoid Complex (CFGC) and Savo Schist Belt (SSB) are lacking.

The earliest structures from the Karelian terrane and southern Finland (SVB) suggest that the early overthrusting or collisions occurred in c. N-NNE compression. The pattern of fragmentation of the Archaean continent indicates that the collision was oblique. The E-W trend of the early structures in the Svecofennian domain suggests that the N-S collision occurred against the Archaean continent with its originally more or less NW-trending shore line (Figure 48). This can also be reconstructed from the enveloping surface of major fold structures, caused by the major block structures further southeast, deforming the Archaean continent (Figure 8). Mantled gneiss domes (Eskola 1949), like the Pitkäranta dome in eastern Russian Karelia and the Kuopio mantled gneiss dome (Brun et al. 1981), were formed close to the collision zone, near the original Archaean-Svecofennian suture. They show ductile folding patterns that formed in the active collision zone, whereas domes further north from the original collision zone, like the Sotkuma dome close to the Karelian terrane-Archaean domain border, are more sliced in character. The distribution of different domes (ductile domes are located in the southern parts and less ductile sliced domes in the northern parts of the N-trending tectonic blocks that were separated from each other by dextral N-trending shear zones) support the early N-S collision. The

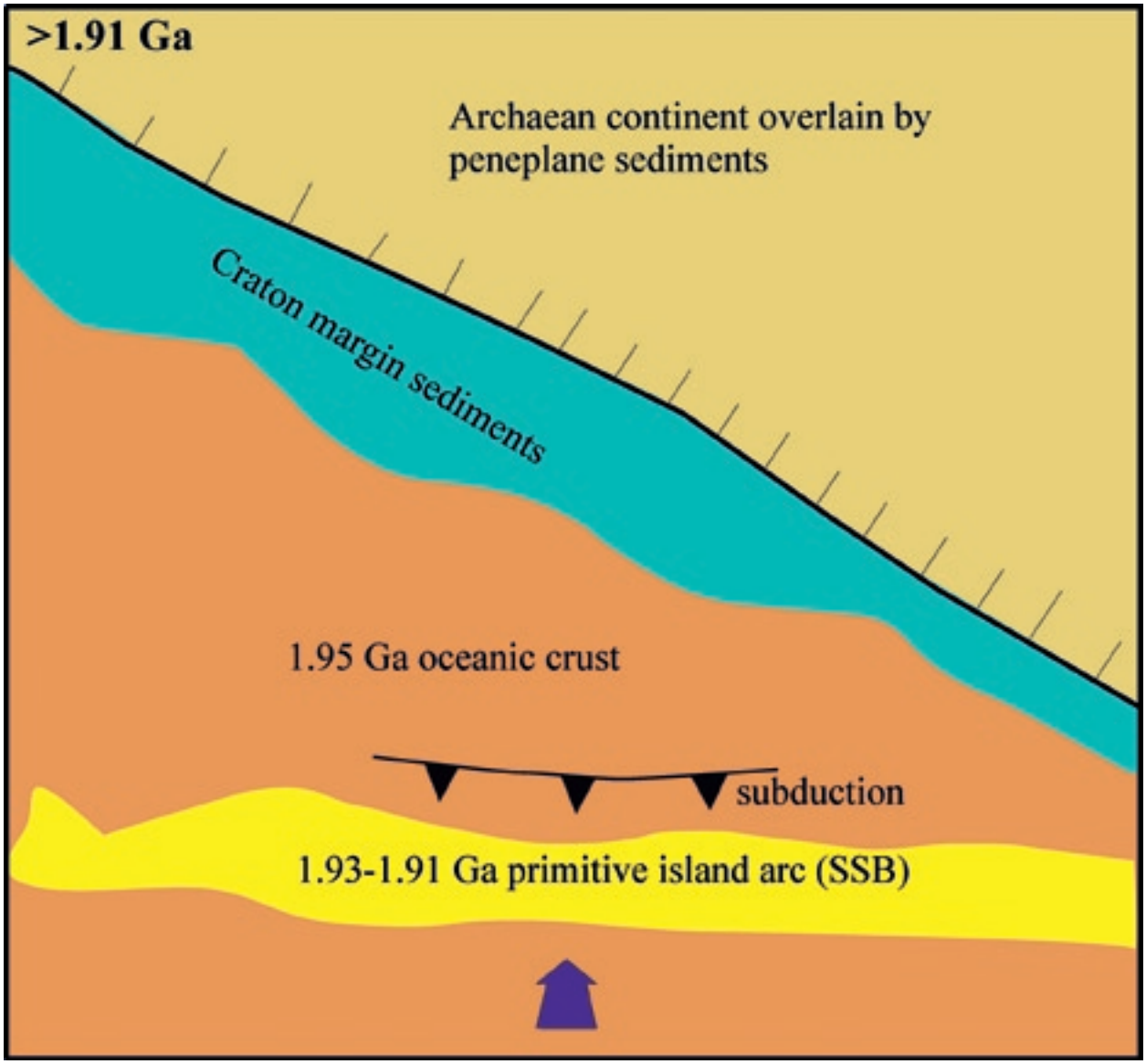

Figure 48. The pre-collisional stage and the generation of the Pyhäsalmi primitive island arc (Savo Schist Belt, SSB) by c. southwards subduction of 1.95 Ga oceanic crust.

early thickening event E_1 of the crust in the southern Svecofennian domain and contemporaneous events in the north are schematized in Figure 49. In the Karelian terrane, the second deformation event D_2 was related to continued collision (Koistinen 1981) and therefore differs markedly in character from the $D_{B/2}$ structures in the southern Svecofennian domain. When E_1 thickening occurred in the south (Granite Migmatite Belt, GMB) the northern terranes (Tonalite Migmatite Belt, TMB) already underwent an extensional event thinning the crust. This supports the idea of diachronic evolution progressing towards the south, and suggests that the N-S collisional event continued during the contemporaneous local extensive events further north.

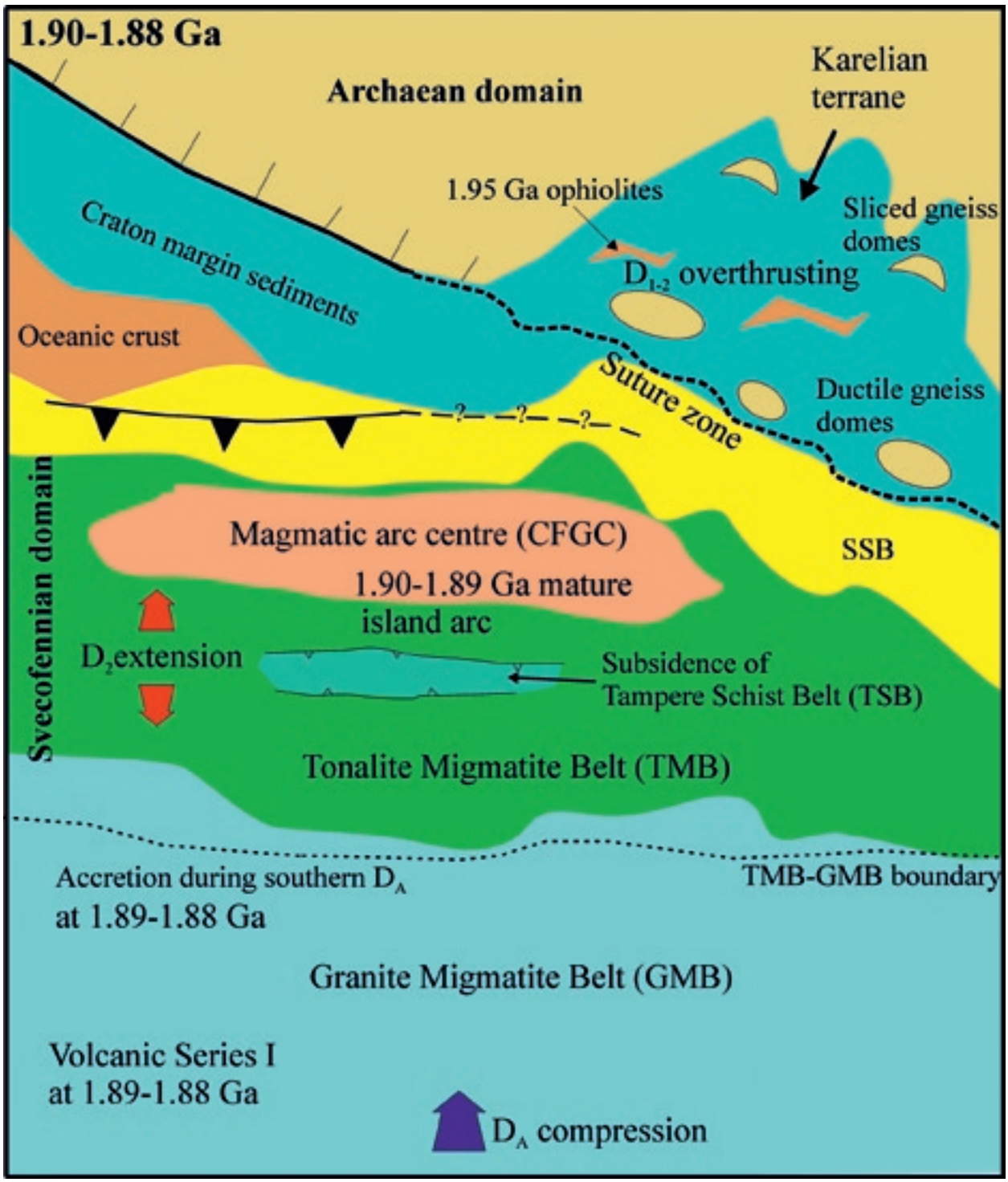

Figure 49. The first geotectonic Event 1 comprises crustal thickening by overthrusting in the southern Svecofennian domain and contemporaneous tectonic events in the north. CFGC = Central Finland Granitoid Complex and SSB = Savo Schist Belt.

The second geotectonic Event 2 (E_2) – collapse of the island arc causing crustal extension

Event 2 appears in the study area as intense vertical shortening of the early D_A structures, early/syn-D_B intrusive rocks and the volcanic Series I. The later volcanic Series II also underwent M_B metamorphism and D_B deformation. Deformation occurred under prograde metamorphic conditions, at low pressures (c. 4–5 kbar, Korsman et al. 1999), and the strain was strong flattening including a rotational shear strain component as indicated by rotated D_B boudinages. The maximum age of E_2 in the study area is fixed by the age of the volcanic sequence of Series II at c. 1.88–1.87 Ga (cf. Väisänen & Mänttäri 2002). The syn-/late D_B tonalites, intruded into the S_B plane of strong D_B flattening and migmatization, are dated at 1.88–1.87 Ga (Appendix 8). Similar ages of "syntectonic granitoids" and neosomes are common in southernmost Finland (Hopgood et al. 1983, Huhma 1986, Vaasjoki & Sakko 1988, Nironen 1999, Mouri et al. 1999, Väisänen et al. 2002 and Skyttä et al. 2006).

We propose that D_B occurred in the arc environment (back arc basin environment of Väisänen & Mänttäri 2002) that was already thickened by collision during the E_1 event. The later volcanic Series II represents an intra-arc extensional volcanism into the upper crust. The increased heat flow caused increased production of tonalitic magmas during the latest phases of the extensional E_2. The S_C is dominantly the first strong penetrative foliation in the wider intrusions (e.g. Hindsby), but intrusion into S_B planes (Figure 20a) indicates their close association with the D_B. In the earlier or deeper-level D_B granitoids (cf. Skyttä et al. 2006 and Pajunen et al. 2008), and in the pre-D_B gabbroic-tonalitic rocks, amphibolite facies S_B foliation generally developed. A possible explanation for the extensional E_2 with the characteristic low-pressure prograde metamorphism, intensive migmatization and contemporaneous upper crustal volcanism, is the increased heat flow generated by upwelling of the lithosphere and sinking of the oceanic slab into the mantle, as modelled by Platt and England (1993). This extension caused subsidence in the upper crust and the low-grade, non-migmatitic rocks (Vuosaari triangle and Vetio, Appendix 4; cf. Kisko Triangle in Skyttä et al. 2006) underwent their first metamorphism.

The E_2 affected the whole area of the Granite Migmatite Belt (GMB), Hyvinkää Gabbroic-volcanic Belt (HGB) and Hämeenlinna Volcanic Belt (HVB). In the northern terranes, such as in the Vammala Migmatite Belt (VMB), D_2 is a similar strong, prograde flattening deformation to that in the GMB (Koistinen et al. 1996, Pietikäinen 1994, Kilpeläinen 1998 and Pajunen et al. 2001a), but dated by magmatic rocks to c. 1.89–1.88 Ga (compiled in Korsman et al. 1999). "Syntectonic" magmas of this age also characterize major parts of the Central Finland Granitoid Complex (CFGC) (Nironen 2003). The ages are on average c. 10 Ma older in the northern terranes, like the Tonalite Migmatite Belt (TMB) (e.g. Huhma 1986, Vaasjoki & Sakko 1988 and Nironen 1989), than in the GMB, again proving the diachronic character of the Svecofennian orogeny. This suggests that the collapse structure caused by mantle upwelling began in the north and was migrating towards the south c. 10 Ma later. The structural observations indicate the co-existence of the geotectonic units already after D_A. The Tampere Schist Belt (TSB) began to subside during the northern D_2 extension correspondingly to the southern non-migmatitic units such as the Vuosaari triangle and Vetio (Appendix 4, cf. the Kisko Triangle, Skyttä et al. 2006).

Event 2 and corresponding structural characteristics in the southern Svecofennian domain are illustrated in Figure 50. The extensional evolution, D_B, in the south was coeval with the contractional structures D_3 in the north. This supports the conclusion of overall N-S compression and localized extension. This is why the extensional E_2 rapidly turned to the compressional event E_3.

The third geotectonic Event 3 (E_3) – collision due to N-S compression

In the study area the E_2 extension was soon followed, or concomitantly affected, by the N-S shortening E_3, which deformed the supracrustal series and the early magmatic rocks into tight, often northwards overturned folds with originally c. E-W-trending steep axial planes related to the D_C. In the study area the D_C structures are best preserved in the Southern Volcanic-sedimentary Belt (SVB). In the Espoo Granitoid Complex (EGC) the D_C structures are often difficult to identify because of the strong later deformations, metamorphism and magmatism. The observations on mineral growth in relation to the structural succession suggest that the temperature peak was already achieved during the extensional E_2, but was still high, as can be concluded from the amphibolite facies S_C as the first foliation in the syn-/late D_B tonalites. The ductile folding character also establishes the evolution as closely following E_2. The age determinations indicate that the compressional E_3 evolution rapidly followed the formations of the later volcanic Series II and syn-/late D_B tonalites. The E_3 ended in the study area certainly

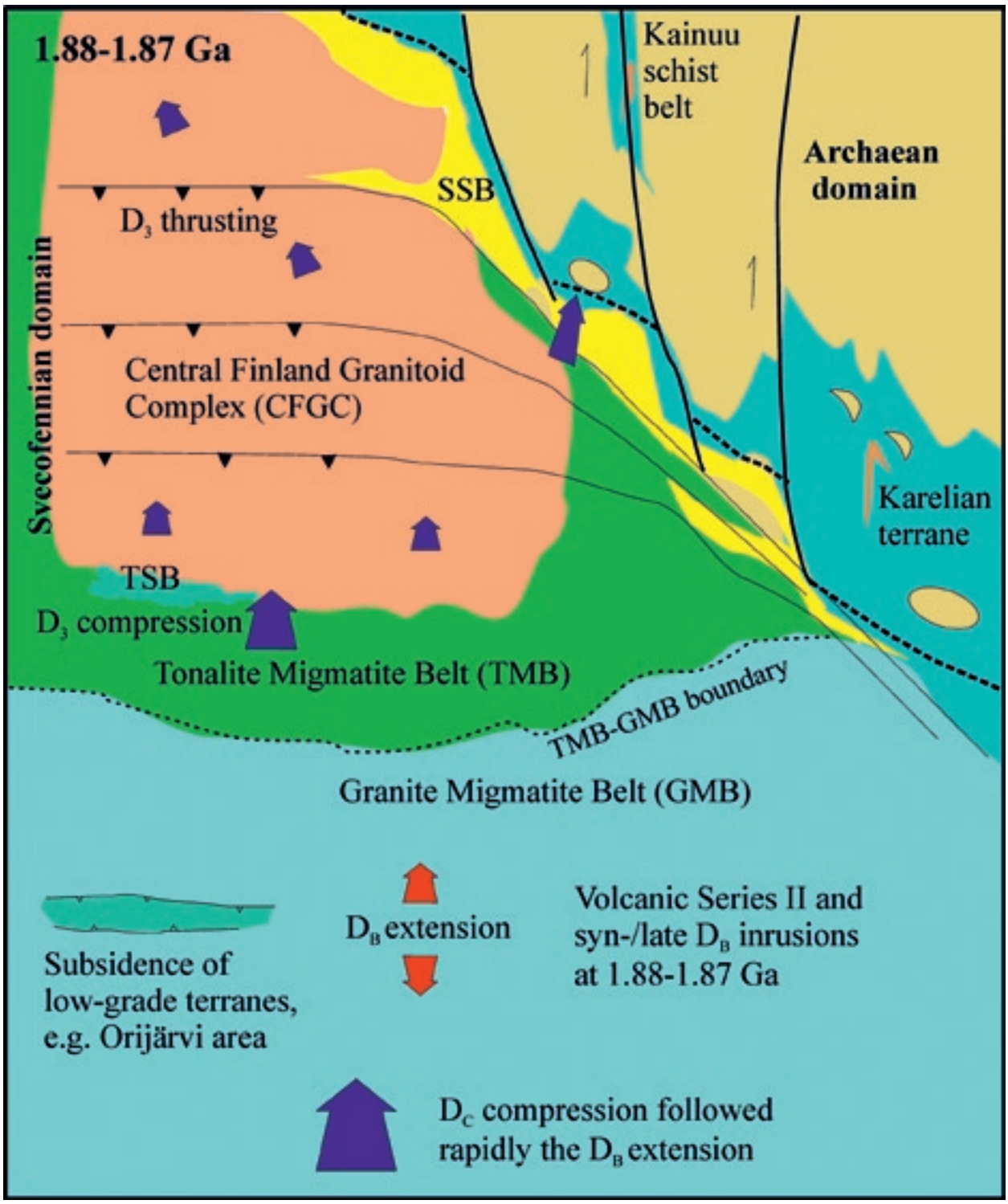

Figure 50. The second geotectonic Event 2 caused crustal thinning in the southern Svecofennian domain and contemporaneous overthrusting and thickening of the crust in the north. TSB = Tampere Schist Belt.

before the first D_E intrusion at 1868 ± 3 Ma (Hakkila, Appendix 8): it also cuts the D_D structures. The northern D_4, simultaneously with the D_D in the south, fixes the age of the major geotectonic E_3 at 1.88–1.87 Ga, i.e. closely to the age of E_2.

We interpret that E_3 was continued northward collision against the northern terranes. The structural relations in the southern Svecofennian domain are illustrated in Figures 50 and 51. In central Finland, D_3 is an overthrusting deformation with low-angle thrust planes dipping towards the southeast (cf. Sorjonen-Ward 2006). The Tampere Schist Belt (TSB) is located in the E-W-trending electric conductive zone between the Vammala Migmatite Belt

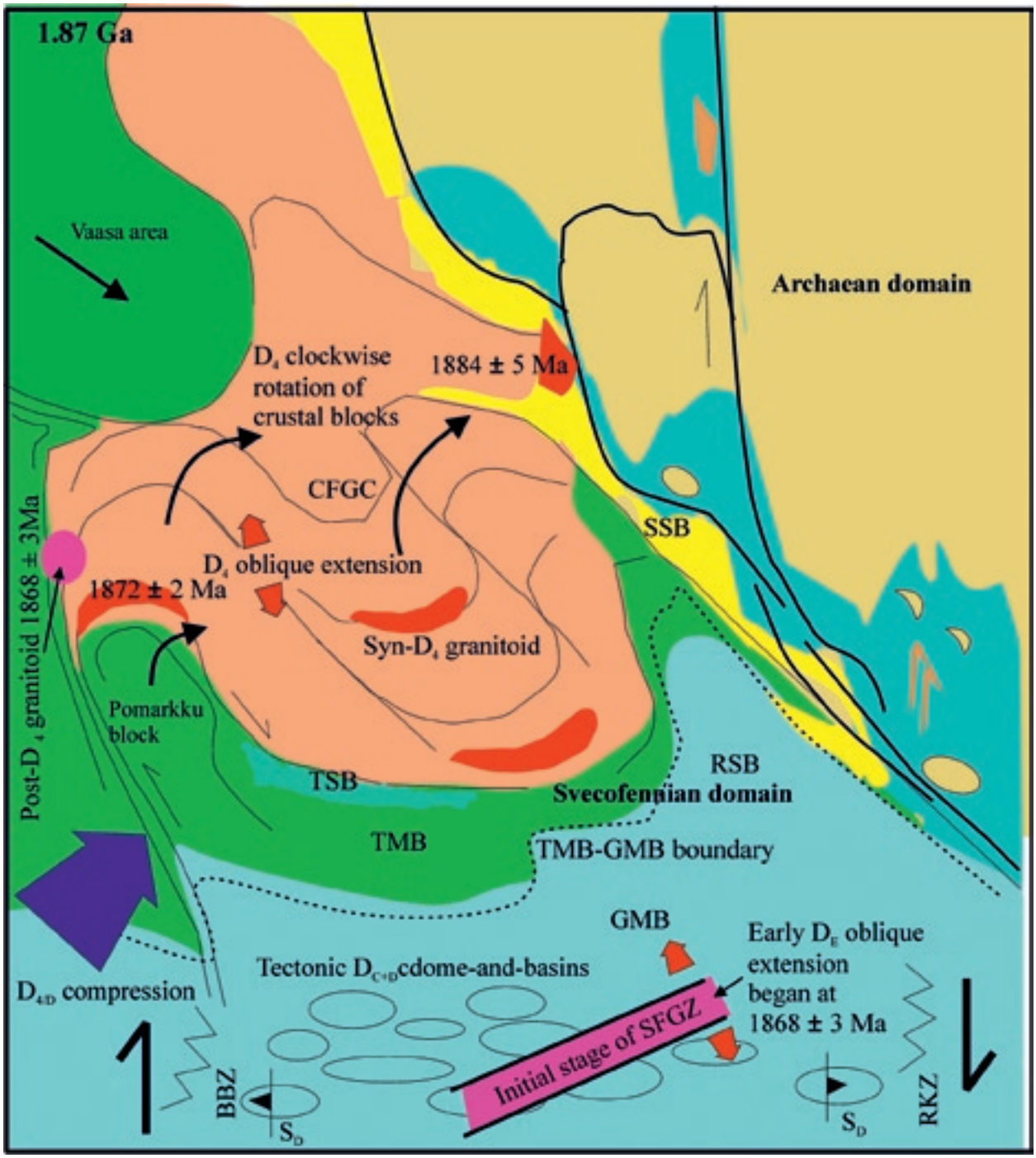

Figure 51. Relations between the northern D_4 and the southern D_D deformations and the beginning of the fourth major geotectonic Event 4 – the beginning of evolution of the Southern Finland Granitoid Zone. Abbreviations: SSB = Savo Schist Belt, RSB = Rantasalmi-Sulkava area, TMB = Tonalite Migmatite Belt, GMB Granite Migmatite Belt, TSB = Tampere Schist Belt, SFGZ = Southern Finland Granitoid Zone, CFGC = Central Finland Granitoid Complex, BBZ = Baltic Sea-Bothnian Bay Zone and RKZ = Riga Bay-Karelia Zone.

(VMB) and the Central Finland Granitoid Complex (CFGC) (Korja 1990); the zone dips beneath the CFGC and is regarded as a suture zone along which the conductive schists of accretionary prism of the VMB were pushed below the CFGC (e.g. Lahtinen 1994, Kilpeläinen 1998 and Korsman et al. 1999). In the model presented here the zone is in a corresponding setting to the D_3 zones in the northern margin of the Pomarkku block (Appendix 7 and Appendix-Fig. 7-1c). It can be interpreted as a crustal-scale thrust zone related to E_3, presumably reactivating the E_2 extensional zones.

The strong crustal slicing and northwestwards stacked structure in the Central Finland Granitoid

Complex (CFGC) may be due to the competent character of the CFGC when compared to the sediment-dominant units. We relate the major 1.89–1.88 Ga (Vaasjoki & Sakko 1988) granitoid pulse in the CFGC to the generation of a magmatic complex in the central arc that developed beside/upon or collided against the 1.93–1.91 Ga old primitive island arc (Savo Schist Belt, SSB). Anyhow, at present the contact between the CFGC and SSB is a tectonic zone that is characterized by strong granite magmatism, granitization and shearing (Pajunen 1986 and Pääjärvi 1991) and by a gravity low (Korhonen et al. 2002b), predominantly syn-D_3. The CFGC does not show such a D_2 flattening as the supracrustal units of the Tonalite Migmatite Belt (TMB), again supporting its more competent character – extensional deformation mainly concentrated in zones. The D_3 in the north is slightly older than D_C in south; the D_3 is about the age range of the southern D_B. Hence, E_3 also becomes diachronic younger towards the south; at the time of thrusting in the north the southern crust underwent the extensional collapse E_2.

Due to large differences in competencies between the Archaean continent and the active Svecofennian crust, deformation developed to dextral shearing along the NW- and N-trending shear zones along Archaean border zone (Figure 50). The Archaean continent fragmented to c. N-S-trending slices that slid dextrally towards north along with some rotation of the blocks. Movements partly occurred along pre-existing c. N-S-trending zones of weakness, for example, the structures related to the early break-up of the Archaean continent, the Early Proterozoic c. N-S-trending diabase dykes or the Siilinjärvi carbonatite occurrence (Korsman et al. 1997). Korsman et al. (1999) explained the preservation of thick crust in eastern Finland as a consequence of continued compression preventing thinning that in the southern and western Svecofennian domain is predominantly related to the extensional E_2. Indeed, the Archaean region did not undergo the extensional E_2, but the crust was thickening by oblique collision at that time. The extensional collapse was caused by the subsidence of the oceanic slab and upwelling of mantle. This did not occur in the Archaean area, which supports subduction away from the Archaean terrane. The late extensional structures, the D_E-D_H, did not notably affect the Archaean continent, with the exception of the easternmost Southern Finland Granitoid Zone or Central Lapland granitoid area, where the crust is thinner. These are the main reasons for the thick crust in eastern Finland.

After the major geotectonic Events 1–3 the Svecofennian arcs were accreted to the Archaean continent forming a new continental environment.

The fourth geotectonic Event 4 (E_4) – evolution of the Southern Finland Granitoid Zone

The fourth geotectonic event, E_4 (D_D-D_H), occurred in the new continental crust (Archaean and accreted Svecofennian) and is predominantly linked to the evolution of the Southern Finland Granitoid Zone (SFGZ) (D_E-D_H). E_4 shows a complicated history; the tectonic evolution of the SFGZ exhibits significant rotations of the stress field accompanied by enormous magma production.

Ductile F_D folds in the south refolded the earlier structures under decreased temperatures after $E_{2–3}$ and produced the map- to outcrop-scale D_{C+D} dome-and-basin interferences, preserved well in the Southern Finland Volcanic-sedimentary Belt (SVB). The c. 1.88–1.87 Ga age of D_D is linked to the northern syn-D_4 granitoids (Appendix 7) emplaced into the D_4 oblique extensional zones under NE-SW transpression in between the major N-trending deformation zones, e.g. the Baltic Sea-Bothnian zone (BBZ) and the Riga Bay-Karelia zone (RKZ) (Figure 8). The F_D folds in the south are results of this transpressional deformation.

The transpressional $D_{D/4}$ evolution shows similar diachronic progression towards the southwest and south as occurred during the earlier geotectonic E_2 and E_3. D_4 terminated in the Savo Schist Belt (SSB) at 1884 ± 5 Ma (Hölttä 1988) and in the western Tonalite Migmatite Belt (TMB) at 1868 ± 3 Ma (Lehtonen et al. 2005). In the north, the D_3 thrust planes (Figure 50) were deformed in the D_4 to arched structures and blocks that were bordered by c. NW-SE-trending shear zones/faults and were rotated clockwise; Figure 51 summarizes the results of the rotational deformation of the blocks. The Pomarkku block (Appendix 7) is a typical result of this transpression. The migmatitic Vaasa area (Va in Figure 9), which in the south is bordered by the Vittinki shear/fault zone (Figure 10), continues to the Swedish coast. According to Rutland et al. (2004), it was transported from the west on its present setting. We agree with the eastward movement of the unit and relate it to the deformation D_4 in the north; movements occurred still later during the short-lasting D_F E-W contraction. Similar block structures characterize the western parts of the Archaean craton. Further east, in Russia, the structure changes to open folding, as can be interpreted from the magnetic data (Figure 8). The N- and NW-trending, mainly dextral shear zones (e.g. Talvitie 1971) of the Ladoga-Bothnian Bay zone mark the present border zone between the Archaean and Svecofennian domains; the original Archaean-Svecofennian suture zone nowadays occurs as deformed pieces in

the southern borders of N-trending tectonic slices (Figure 50).

The termination of D_4 deformation and stabilization of the crust at 1868 ± 3 Ma (Lehtonen et al. 2005) in the north caused a jump of the major deformation towards the south into the area of the Southern Finland Granitoid Zone (SFGZ). The early evolution of the SFGZ is linked to the emplacement of the first dated early D_E tonalite at 1868 ± 3 Ma (Appendix 8). The southern Svecofennian domain cooled and became more competent after D_D. It was susceptible to oblique SE extension along the E-ENE-trending zones under the overall SW-NE transpression between the active major N-trending deformation zones, the Baltic Sea-Bothnian zone (BBZ), the Riga Bay-Karelia zone (RKZ) and Transscandinavian Igneous Belt (TIB). Thus, the earliest deformation in the SFGZ, the D_E, is characterized by similar SW-NE transpression to that which occurred during the $D_{D/4}$.

The earliest structures in the Southern Finland Granitoid Zone (SFGZ) are related to oblique extension in the ENE-trending zone. At greater crustal depths, nearly horizontal the extensional $S_E$ext shear foliation developed. Oblique contractional structures like the $S_E$cont, produced by the progressive SW-NE transpression, appear more intensely in the early D_E magmatic rocks than in the later ones. The early D_E magmatism is represented by the garnet-bearing early D_E tonalites, microtonalite dykes and wider tonalitic to granodioritic intrusions at 1.87–1.86 Ga. Most microtonalites intruded into upper parts of the cooled crust, but some dykes and most of the tonalitic-granodioritic rocks were intruded into the high-grade ductile environment at greater depth. In eastern Finland, corresponding microtonalites are 1.86–1.85 Ga old (Huhma 1981). Continued extensional evolution in the SFGZ led to the enlargement of intermediate magma production and an increase in the metamorphic grade. The second major migmatization phase after E_2 evolved and the granulitic rocks of West Uusimaa Complex (WUC) were generated into the middle and, due to the high thermal gradient (cf. Korsman et al. 1999), even into the upper crust. The pyroxene tonalite from the WUC at 1860 ± 5 Ma (Appendix 8) predates the penetrative horizontal $S_E$ext characterizing the high-T areas of the SFGZ. The later metamorphic 1841 ± 4 Ma zircon phase and 1837 ± 3 Ma monazites in tonalites (Appendix 8) suggest continuing high heat flow. Channels also opened for deeper-derived mafic magmas that culminate the oblique extensional evolution in the SFGZ; the late D_E gabbro is dated at 1841 ± 7 Ma (Appendix 8).

In the upper crust the SE extension was more zoned and was characterized by faulting and shearing. The Jokela supracrustal association, and corresponding rocks in the southern Svecofennian domain (yellow triangles in Figure 9), started their deposition with high-energy clastic sediments, quartzites and conglomerates (Appendix 5); corresponding associations also exist in Sweden. Sedimentation basins developed in between the active N-trending transcurrent shear zones, the Baltic Sea-Bothnian Bay zone (BBZ) and the Riga Bay-Karelia zone (RKZ), as oblique extensional pull-apart basins under the overall SW-NE transpression. Similar quartzites in Sweden suggest oblique extensional pull-apart-basins between the BBZ and the Transscandinavian Igneous Belt (TIB) (or unknown zones even further west, nowadays destroyed, for example, due to opening of the Iapetus Sea or the Caledonian orogeny). The subsidence of the Jokela supracrustal association proceeded with rapid steps as evidenced by the sharp change from high-energy clastic sandstone to mica gneiss, referring to more peaceful deeper-water sedimentation. The volcanic rocks within the Jokela association can be related to the increased deep-derived mafic or the intermediate magma production in the lower crustal levels during the D_E. This assumption of the genetic relations between the Jokela volcanogenic rocks and the deeper crustal intrusives is based on correlation of their structural successions, and requires further establishment, e.g. by geochemical methods.

In the study area, there are only scarce signatures of the E-W contradictional D_F that appears as a zoned fold deformation with N-trending axial planes in eastern Finland at c. 1.86–1.85 Ga ago (cf. Koistinen 1981). The deformation was concomitant with the early D_E in the south. The sinistral Hiidenvesi shear zone is linked to that stage. The related fold deformation has not been identified in the SFGZ. The D_F in eastern Finland is related to the transport of a large central Finland block shown in Figure 8 towards the east. The northern border of the block is the sinistral E-W-trending shear zone at the level of the northern end of the Bothnian Bay. In the south the bordering shearing occurred along the dextral E-W-trending Hyvinkää, Hämeenlinna and Tampere shear zones. The stress was released into these zones and no significant folding corresponding to the F_F (F_4 Koistinen et al. 1996) occurred to the south of the zones. The 1.85 Ga dilatational fluid activity causing strong metasomatic alterations in shear zones in the Archaean domain (Pajunen & Poutiainen 1999) and felsic granitoids of that age (compiled in Pajunen & Poutiainen op. cit.) in eastern Finland can be related to this deformation. Near the craton boundary, some NW-SE-trending shear zones show a sinistral sense of movement (e.g. D_c in Pajunen 1986) and NE-SW-trending shear zones are

dextral, like the Auho fault cutting the Kainuu schist belt (Kärki 1995); their formation or reactivation can be related to the E-W contraction. The D_F was localized in the northern part of the Svecofennian domain and the E-W stress field thus reflects these local conditions.

In the study area the large-scale F_G folds and the sinistral shearing along the Porkkala-Mäntsälä shear zone indicate a short transitional period of N-S contraction, before the stress field rotated into a SE-NW trend. Corresponding major shear zones in the c. SE-NW and also SW-NE directions characterize the crustal structure in the southwestern archipelago, where the beginning of the SE-NW shear zone is dated at c. 1.85 Ga (Torvela et al. 2008), and further south in the Baltic region (Figure 8). Such a wide-scale F_G folding related to the D_G also deforms the northern terranes, e.g. the Tonalite Migmatite Belt (TMB).

Rotation of the stress field from SW-NE affecting through S-N during the early E_4 to SE-NW during the late E_4 occurred rapidly at c. 1.84 Ga ago. The rotation indicates the start of the D_H deformation, the latest major evolutionary phase of the Southern Finland Granitoid Zone (SFGZ). The 1.83 Ga pegmatitic granitic dykes cutting the syn-/late D_B tonalite (Appendix 8) indicate the beginning of the D_H granitic pulse in the marginal area of the Espoo Granitoid Complex (ECG). The dyke-intrusive relations provide evidence that the crust stabilized and cooled for c. 40 Ma. Corresponding cooling stages are identified between early/mid-D_E microtonalites and syn-/late D_B tonalites, and Sederholm (1927) described a tectono-thermal gap between magma pulses in the Hanko-Inkoo area. However, in places, such as in the northern EGC or West Uusimaa granulite Complex (WUC), compositionally varying magmatic activity continued in a ductile state practically throughout the E_4 evolution. Hence, the contemporaneous igneous rocks show different characteristics depending on the thermal state of their emplacement environment.

The SE-NW transpression occurred in between the active E-W-trending Southern Finland and Hyvinkää shear zones. Ehlers et al. (1993) related the evolution of the Southern Finland Granite Zone (SFGZ) to SE-NW transpression, but the observations of this study demonstrate that the SFGZ evolution was a more complex and longer-lasting process. Transpression caused oblique contractional folding $F_H$cont, forming the regional-scale D_{G+H} dome-and-basin interferences. The simultaneous oblique extension $D_H$ext caused strong vertical shortening, felsic magmatism and increased heat flow, causing a new pulse of migmatization. Huge amounts of granodioritic to granitic magmas were produced between 1.85–1.82 Ga, dated by Kurhila et al. (2005) from the Espoo Granitoid Complex (EGC). The age of migmatization ranges between 1.82–1.81 Ga (Korsman et al. 1984, 1988, 1999 and Väisänen et al. 2004). This migmatization also occurred in the D_E granitoids. Differences in competencies, due to variations in thermal state and magmatic activity, caused variations in local deformation patterns. In the cooled areas no significant deformation occurred, whereas strong magmatism and deformation occurred in the areas nearby; e.g. Espoo Granitoid Complex (EGC) or the West Uusimaa Complex (WUC) as compared to the Southern Volcanic-sedimentary Belt (SVB). In the cooled parts of the crust outside the most active D_H extensional zones, medium-grained to pegmatitic granite dykes emplaced.

NW-SE transpression suggests c. E-directional dilatation or NW-N oblique extension between the E-W-trending dextral major shear zones. The granitic igneous activity during the late $Event_4$ was scattered and concentrated in spots (Figure 38); spot-like dilatation centred during the late E_4 is supported by kinematic observations on the varying directions of dilatation in the surroundings of the Nuuksio granitoid area. The contractional $F_H$cont folds openly deform even the latest identified granite pulses in the study area, presuming that NW-SE transpression acted very late in the SFGZ evolution. The latest Svecofennian rocks in the study area are <1.8 Ga diabase dykes intruded into c. E- or N-trending dilatation zones in the Southern Volcanic-sedimentary Belt (SVB). The amphibolite facies diabase dykes locally show contractional $F_H$cont and high temperature assimilation structures, indicating their hot emplacement environment. They are related kinematically to the D_H SE-NW-transpression, very close to the transition to E_5; their age is within the error limits the same as that of the latest dated F_I granite dykes (E_5) in the area (c.f. Pajunen et al. 2008).

The evolution of southern Finland and the Hyvinkää shear/fault zones shows a polyphase history that began during the early SE-NW extensional E_4. It continued during the oblique dextral movements causing clockwise rotation of the competent blocks, like the Hyvinkää gabbros, during the latest E_4 SE-NW transpression. The transpression also caused the oblique overthrusting of the Hyvinkää Gabbroic-volcanic Belt (HGB) upon the high-grade West Uusimaa Complex (WUC). The tectonic-metamorphic observations from the Jokela supracrustal association, the pull-apart basin that started its evolution during the early E_4 NE-SW transpression, reveal that a series of contractional structures formed under varying stress fields during the $E_{4–5}$ evolution (D_F-D_I). During the latest E_4, pegmatitic granite dykes intruded it.

Close to the border zone of the Archaean continent, dextral movements of crustal N-trending blocks characterize the oblique collisional structures formed during the E_3 event. During the continuing oblique collision under SW-NE transpression the E_3 the shear zones remained active and dextral movements continued. During the early E_4 evolution the northern Svecofennian crust in central Finland was deformed to form NW-trending crustal slices and blocks that rotated clockwise and transported eastwards. Correspondingly, the crustal blocks already formed during the E_3 were transported dextrally towards north; these blocks also show some rotation. The eastwards transport of the central Finland block during D_F E-W contraction exhibits a local event. During the late E_4 evolution, oblique extension zones represented by the Southern Finland Granitoid Zone were formed between the crustal-scale N-trending the Baltic Sea-Bothnian Bay Zone (BBZ), Riga Bay-Karelia Zone (RKZ) and Transscandinavian Igneous Belt (TIB). The evolution of the BBZ was predominantly related to the early E_4 SW-NE transpression. The TIB show a strong dextral component of movement, which is not the case with the RKZ; therefore, the E_4 granitic areas are much larger in the west than close the RKZ.

Magmatic rocks or thermal events at c. 1.87–1.84 Ga characterize the N-trending zones (e.g. Huhma 1981, Neuvonen et al. 1981, Pajunen & Poutiainen 1999, Koistinen et al. 2001 and Högdahl et al. 2004). Some observations of late movements and cordierite alteration in shear zones in central Finland, e.g. in Hallaperä sulphide ore in Kiuruvesi (Pajunen 1988) or close to the N-trending high-strain zone in the Haukivuori area (Ha in Figure 9), are very similar to the 1.85 Ga metasomatic zones in the Archaean continent (Pajunen & Poutiainen 1999), and also indicate crustal reactivation in the Savo Schist Belt (SSB) during the E_4. In eastern Finland, granitoids related to E_4 are concentrated in a zone from the Maarianvaara granite in eastern Finland to the Kainuu schist belt and to the north, central Lapland. The central Lapland granite complex shows similar characteristics to the Southern Finland Granitoid Zone (SFGZ), but it was developed into Archaean crust similarly to the easternmost parts of the SFGZ in southeastern Finland (cf. Huhma 1981). We suggest that the evolution of these c. 1.86–1.80 Ga granitoid terranes is of similar origin during the E_4. The 1.80 Ga granites in the Kajaani area (Korsman et al. 1997) can also be related to the E_4 evolution.

The $E_{3–4}$ evolutions produced a complex structural pattern of rotated and moved crustal blocks. A continuous oblique collision model that was produced predominantly under SW-NE transpression can explain the structures. Local variations in the stress field are due to continuing deformation that rotated originally extensional areas to contractional; e.g. the early E_4 oblique SE extension (D_E) in the Southern Finland Granitoid Zone rotated to SE-NW transpression (D_H) that caused shortening of the originally extensional zones. All this may occur by clockwise rotation of the zone itself under overall SW-NE transpression. Similarly, the complex rotational block patterns in central and eastern Finland can be explained by a continuous SW-NE transpression that caused the escape of crustal blocks towards the east and north.

Tectonic evolution and kinematics during the E_4-E_5 evolution in the area of the Southern Finland Granitoid Zone are summarized in Figure 52.

The geotectonic Event 5 (E_5) – evolution following the Southern Finland Granitoid Zone

The major N-trending D_I deformation zones the Transscandinavian Igneous Belt (TIB), Baltic Sea-Bothnian Bay Zone (BBZ) and the Riga Bay Karelia Zone (RKZ) provide evidence of a long-lasting history. Their latest structures deform the Southern Finland Granitoid Zone (SFGZ) and the E-W-trending Hyvinkää and Southern Finland shear/fault zones and are linked to a new geotectonic Event 5 (E_5). The stress field was c. ESE-E trending during the E_5. In the detailed study area the effects of the E_5 are seen in the structural evolution of the Vuosaari-Korso shear/fault zone.

The distribution of the remnants of the Jokela association and related rocks (Figure 9), and the older non-migmatitic areas like the Vuosaari triangle (Vu in Figure 9) and the Orijärvi area (Kisko Triangle of Skyttä et al. 2006 and the Vetio outcrop in Appendix 4) are strongly controlled by the intersections of the major E-W-trending and the N-trending D_I shear zones. The isoclinal F_I folds (Figure 31b) in the axial area in the northern Espoo Granitoid Complex (EGC) demonstrate that the temperature was not reduced under the ductile-brittle boundary. The monazite age of 1804 ± 2 Ma is suggested to represent the age of pegmatitic granite (Pajunen et al. 2008) that cuts the ductile F_I folding (F_g in Pajunen et al. op. cit.). Ductile shearing structures close to dyke contacts indicate ductile movements that are still continuing (Pajunen et al. op. cit.). The bedrock north of the Southern Finland Granitoid Zone (SFGZ) was stabilized at c. 1.87 Ga ago and the D_I structures there are brittle, as in the Päijänne fracture zone. The fracture pattern described by Sederholm (1932b) is in good agreement with the E-W shortening during the D_I.

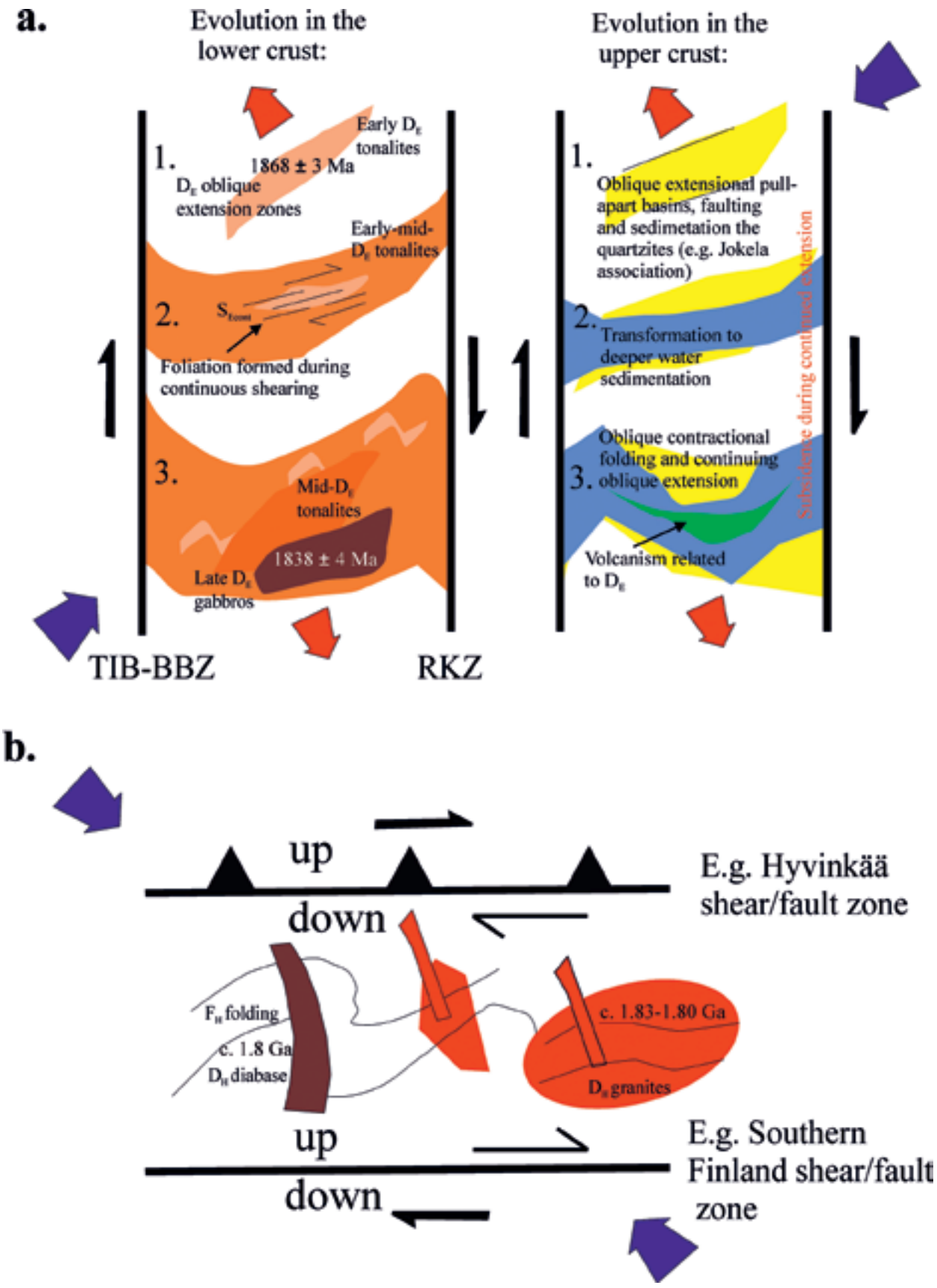

Figure 52. Schematic model of the evolution of Event 4 in (a.) during the oblique extension (D_E) under SW-NE transpression – in the lower crust on the left and in the erosion level on the right and (b.) during the (D_H) SE-NW transpression. E_4 includes the generations of the Southern Finland Granitoid Zone and the E_4 pull-apart basins.

So-called post-orogenic 1.8 Ga group granitic intrusions, locally showing low-pressure contact metamorphic aureoles (Rastas 1990), are small stocks or ring intrusions (Lindberg & Eklund 1988) that are often located in close association with the D_I zones. The latest Svecofennian rocks in the study area are diabase dykes dated at c. 1.8 Ga in the Southern Volcanic-sedimentary Belt (SVB). They are connected according to their kinematics to the E_4 event (D_H). The diabase age is within the error limits the same as the F_I granite (cf. Pajunen et al. 2008). The structural relations suggest that the jump from E_4 to E_5 involved only small rotation of the stress field. This and the structural relationships of the late magmatic rocks suggest that E_4 and E_5 are not strongly differentiated in their kinematics or in time.

The late stages of the E_5 deformation turned to lower-grade processes, which can be seen in a change of the shear structures to semi-ductile. In the latest stage, deformation concentrated into rather narrow zones with sinistral east-side-up movement and the formation of mica-rich slicken side surfaces and protomylonitic to mylonitic structures (Elminen et al. 2008). These late microstructures are predominantly related to post-Svecofennian events such as to the rapakivi stage (e.g. Mertanen et al. 2008). Kinematics of this kind are also evident in the Hyvinkää-Lahti shear/fault zone. The Svecofennian shear/fault zones controlled the movements in post-Svecofennian times and the intersections of the Svecofennian shear/fault zones effectively channelled the rapakivi granite magmatism. Figure 53a shows the occurrences of the rapakivi granites in the Fennoscandian Shield. The structures that have been active during the E_5, like the Baltic Sea-Bothnian Bay Zone (BBZ) and Riga Bay-Karelia Zone (RKZ), strongly control the present setting of the rapakivi intrusions in Finland and Sweden. However, only preliminary results are currently available on the relations between the later structures such as brittle thrust faults (e.g. Pajunen et al. 2001a, Elminen et al. 2008 and Wennerström et al. 2008) and the Svecofennian structural framework.

In Estonia, late ages of metamorphic minerals, monazite and garnet (Puura et al. 2004), may indicate a diachronic jump of tectono-thermal processes towards the south, and that the Svecofennian orogeny continued with a new evolutionary step. Open warps with E-trending axial planes post-dating the D_I structures (Figure 11) and sinistral movements along sharp faults deforming the Southern Finland Granitoid Zone suggest c. N-S contraction. The age and regional context of this deformation is not known.

The Svecofennian orogeny – the result of oblique collision characterized by escape tectonics

There are several determinations of zircons and sphenes preceding the Svecofennian orogeny in metasedimentary rocks (e.g. Huhma et al. 1991, Lahtinen et al. 2002 and Rutland et al. 2004). The existence of these ages and Sm-Nd data from the Central Finland Granitoid Complex granitoids (Lahtinen & Huhma 1997) are proposed as evidence of pre-existing continental crust, such as microcontinents (e.g. Lahtinen et al. 2005) or pre-Svecofennian metamorphism and deformation (e.g. Rutland et al 2004). Such old inherited zircons also occur in the igneous rocks in the study area, for example the inherited 3.3 Ga Archaean zircons in the Hakkila early D_E tonalite (Appendix 8). There are several possible source provenances for these old minerals or crustal geochemical components preceding the Svecofennian orogeny in the Svecofennian domain: 1) the Archaean continent; 2) an unknown removed continent formed by the break-up of the earlier Archaean (the removed continent may include crustal components of ages not identified in the Fennoscandian Shield, except the detrital zircons); 3) sedimentary sequences overlying the Archaean + Early Proterozoic (?) supercontinent before the break-up; 4) magmatism related to break-up of the supercontinent; 5) continental craton margin sedimentary sequences and 6) the 1.93–1.91 Ga Svecofennian primitive island arc sediments and volcanism. The old zircons are met widely, even in the most mature parts of the island arc, which is not expected in mature arcs initiated in the oceanic environment. In the tectonic model presented in this paper, the early sediments were formed from very variable sources and they were already mixed with volcanic sequences during the earliest collisional stages of the Svecofennian orogen. The continuing evolution that turned to transpressional collision that caused strong magmatism and remelting of the early associations, including the very heterogeneous set of the old minerals like zircons. This suggests that the evolution of the mature Svecofennian island arc and following collapse (E_2) occurred close to the Archaean continent, and no hidden microcontinents are needed to explain the pre-Svecofennian detrital zircons or crustal components.

After the early stages of the Svecofennian collision, $E_{1–3}$, the formation of tectonic block structures characterizes the orogeny. The main deformation migrated towards the south and southwest during diachronic transpression, which caused the movement of crustal blocks towards the north and east with accompanying rotation of the blocks. This deformation predominantly occurred in the newly-

formed continental crust. The deformation pattern is very similar to that in the continental crust formed by the extrusion/escape tectonics in the Himalayas (Tapponier et el. 1982). The escape tectonics model explains the regional patterns of extensional, contractional and strike-slip terranes formed in the continent-continent collision of the Indian plate against the Asian continent. According to Jacobs and Thomas (2004), a lateral escape tectonics model explains the tectonic movements of crustal blocks in the southern Neo-Proterozoic-early-Proterozoic Antarctic orogen. In the Svecofennian collision such an indenter described from the Himalayas, the Indian plate, is not known, and the main intender for the long-lasting transpression remains open. A possible interpretation is that the main intender causing the Svecofennian transpressional structures has been somewhere in the south-southeast, but at present is hidden (removed?) due to the SE-NW-trending Tornquist zone (cf. Shomali et al. 2006) bordering the Fennoscandian Shield in the southwest. This type of escape tectonics model explains the present co-existence of different crustal blocks close to each other in the present-day tectonic constitution. Thus, the model of several orogens between microcontinents (e.g. Lahtinen et al. 2005) can be explained by one continued oblique Svecofennian orogen. A simplified escape tectonics model for the oblique collisional Svecofennian orogeny in Finland is presented in Figure 53b.

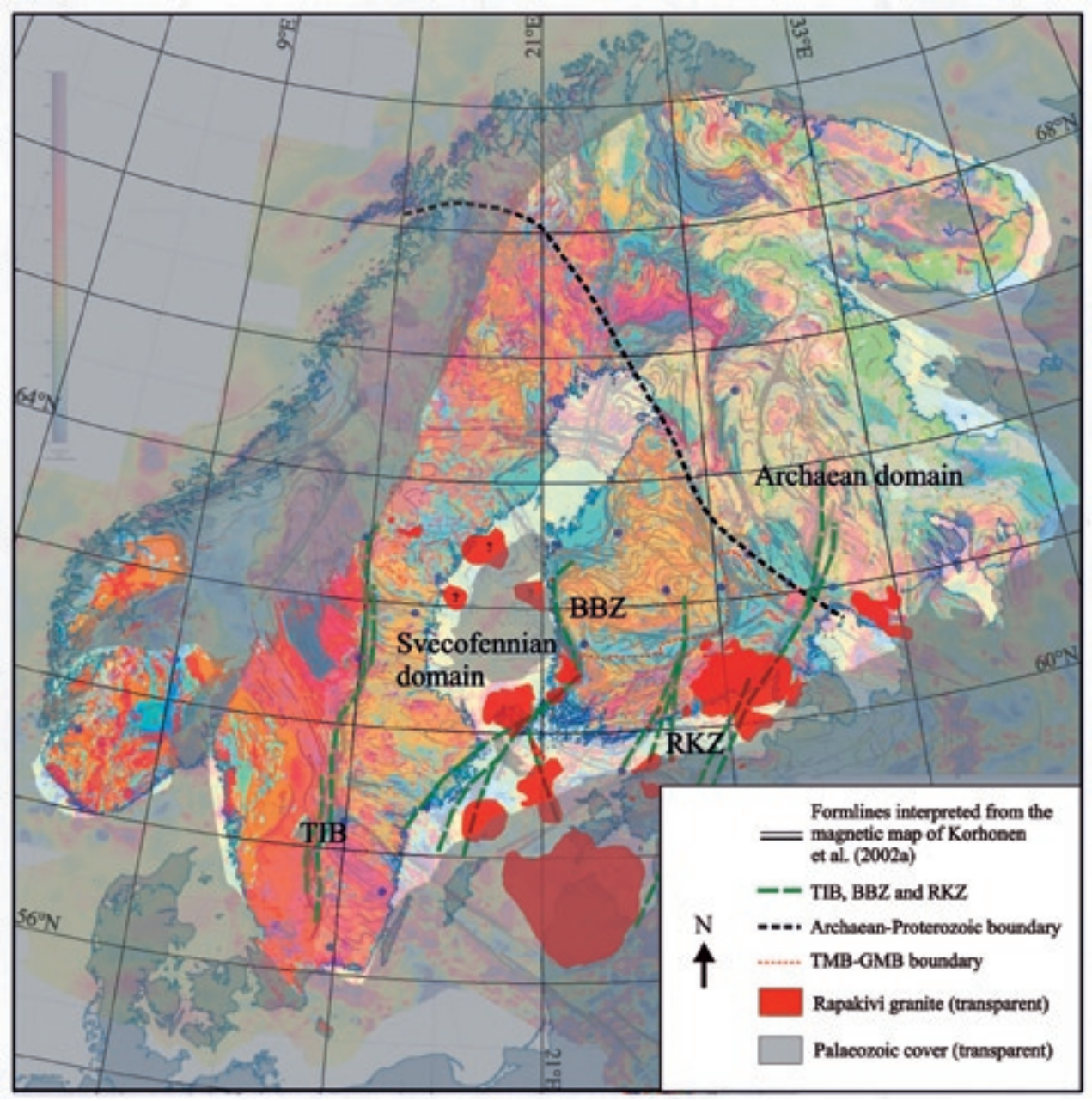

Figure 53. (a.) Tectonic structural formlines on the magnetic map of Korhonen et al. (2002b); the magnetic map is overlain by the transparent lithological map of Koistinen et al. (2001). Locations of the rapakivi granites in the major crustal deformation zones (TIB = Transscandinavian Igneous Belt, BBZ = Baltic Sea-Bothnian Bay Zone and RKZ = Riga Bay-Karelia Zone) are indicated.

CONCLUDING REMARKS

A new model of Svecofennian tectonic evolution in southern Finland is presented, and some suggestions for the wider context of this model are also given. The model is based on observations of structural successions in the field and on regional correlations of structures described in previous studies. The successions were dated using structurally-fixed samples by SIMS and TIMS methods and by correlations with published age data. The data were collected in several projects of the Geological Survey of Finland in the Helsinki region and in the Pori area. The main conclusions and suggestions for the forthcoming studies and applied research are summarized as follows:

Results of the study:

1. Svecofennian structural evolution at 1.9–1.8 Ga in southern Finland was complex, showing successive major structures of the D_A-D_1 deformations, and the evolution was divided into major geotectonic Events 1–5 ($E_{1–5}$).

2. E_1 was the early Svecofennian c. N-S collisional event in the island arc and against the Archaean continent. E_2 is related to the collapse of the island arc. E_3 represents continuing N-S collision; during $E_{1–3}$ a new continental crust was formed.

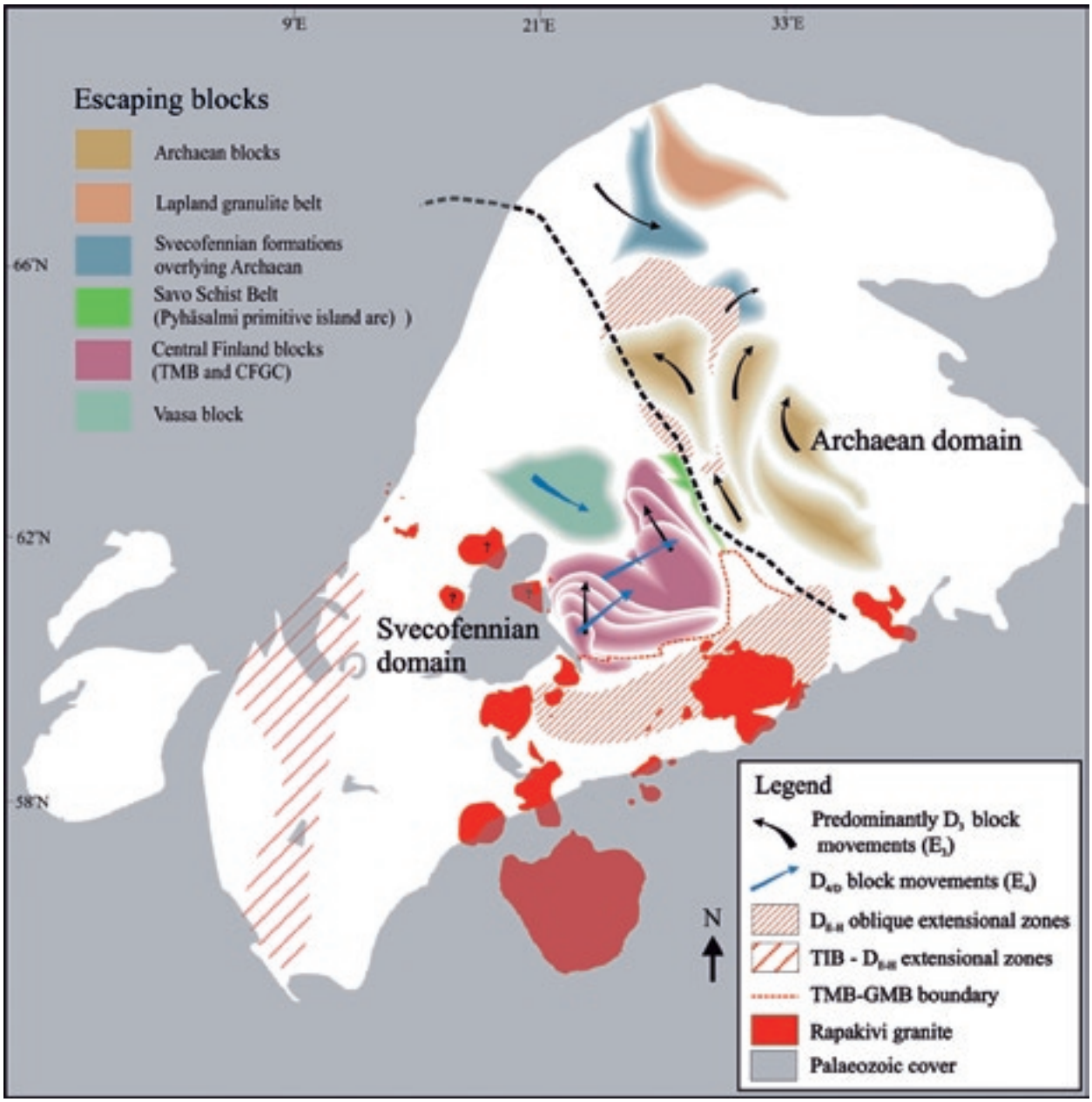

Figure 53. (b.) The escape tectonics model of the Svecofennian orogeny. The major extensional, contractional terranes and movements and rotations of the blocks are indicated. Base map © National Land Survey of Finland, permit No. 13/MML/08.

E_4 includes a complex SW-NE transpressional evolution, showing local variations of the stress directions, in the $E_{1–3}$-generated continental crust, resulting in strong fragmentation and rotation of crustal blocks. The transpressional Southern Finland Granitoid Zone and pull-apart basins were developed. E_5 post-dates the main Southern Finland Granitoid Zone evolution and led to fading of the Svecofennian evolution in Southern Finland.

3. The tectonic evolution was diachronic, becoming younger towards the south and southwest; structural succession in the north occurred c. 10 Ma earlier than in the south.

4. The Svecofennian orogeny represents one oblique collision of the growing and active Svecofennian island arc complex against the Archaean continent. The new continental crust, formed during the early evolution $E_{1–3}$, was followed by a complex transpressional E_4 characterized by escape tectonics. A complex pattern of contractional, transcurrent fault and extensional terranes developed. The transpressional evolution of the Svecofennian orogeny took c. 70 Ma and, in the present tectonic constitution, the kinematically different terranes form a complex structure of rotated and migrated crustal blocks.

5. The thick crust in eastern Finland is a result of continuous collision that partly prevented thinning. The area did not undergo the E_2 collapse, such as thinning the crust in the Svecofennian domain. Instead, it was at that time under contractional and transpressional thickening. This tectonic pattern supports the idea of southwards subduction in which the Svecofennian island arc complex formed.

6. The mature portions of the Svecofennian island arc formed close to the Archaean continent, and mixing of early sediments and volcanic sequences of Series I occurred during the earliest collisional stage E_1. Remelting and mixing of the early components was extensive during the later evolution $E_{2–4}$. The later volcanism of Series II is related to the collapse stage E_2 of the arc.

7. The pre-existing structures in the Archaean crust, such as the inclined shoreline with respect to the colliding arc or early zones of weakness in the Archaean crust, controlled the tectonic pattern formed by the escape tectonics, especially close to the Archaean border zone. The primary suture zone is fragmented into pieces and exhibits at present, if preserved at all, on the southern edges of the N-S-trending Archaean blocks. In the present constitution the Archaean-Svecofennian border is predominantly tectonic in character.

8. The Southern Finland Granitoid Zone had a long evolution during E_4. The evolution of the Central Lapland granitoid complex was corresponding but occurred in Archaean crust. The granitoid terranes represent the major extensional zones determined by the E_4 SW-NE transpressional escape tectonics model. The Baltic Sea-Bothnian Bay Zone, Transscandinavian Igneous Belt and Riga Bay-Karelia Zone represent the contractional transcurrent zones, and the areas between the extensional and transcurrent terranes are characterized by strike-slip tectonics and block structures, like large areas in Central Finland. According to our interpretation, the Baltic Sea-Bothnian Bay Zone stabilized earlier than the Transscandinavian Igneous Belt. The E_4 movements were less significant in the Riga Bay-Karelia Zone. Recent constitution of these terranes suggests that the major transcurrent zone was migrating toward west during E_4. This is the reason for the wider occurrence of E_4 magmatism in the west than in the east.

9. The high-T/low-p metamorphism in the Svecofennian domain is predominantly related to extensional stages of the orogeny, especially during the E_2 collapse and E_4 oblique extensional events.

10. Even though the Svecofennian orogeny shows a continuing character with magmatic and metamorphic events covering the whole time frame, there are several tectono-thermal discordances of a more local character. This is why some tectonic units show earlier stabilization than their neighbouring ones. The Southern Finland Granitoid Zone and the northern terranes, e.g. the Tonalitic Migmatite Belt, provide examples. There are also more local discordances, as described from the study area. These differently-stabilized units show different later histories, which is important when comparing the evolution of the later semi-brittle to brittle structures in them. In the areas showing late Svecofennian high-T evolution the brittle evolution started in places c. 70 Ma later than in the earlier stabilized units.

11. Post-Svecofennian structures are effectively controlled by the Svecofennian orogeny. For example, the channelling and emplacement of the rapakivi intrusions in the study area show significant relations to the mid-late Svecofennian structures. Reactivation of the Svecofennian shear zones during the late Svecofennian or post-Svecofennian brittle regime was important. The present setting of the rapakivi occurrence is strongly controlled by the major N-S-trending transpressional transcurrent zones.

Further suggestions and remarks:

12. The presented tectonic model set a new basic for tectonic characterization of the Svecofennian domain.

13. The complex model of collision and escape tectonics has to be taken in to account when examining the plate tectonic constructions. Rotation and transport of the crustal blocks should be considered when interpreting, for example, the paleomagnetic orientations for continental constructions.

14. The evolution model presented here gives new possibilities to consider the genesis of ores and especially their later remobilization. There are examples of the remobilization and formation of new ore constituents during the mid-late Svecofennian evolution. Semi-brittle to brittle evolutionary stages also vary in time and kinematics in different geotectonic units. This variation should be taken in to account when prospecting and studying the mineralizations related to tectonic processes.

15. This study is part of a larger programme of research organized by the Geological Survey of Finland that is attempting to acquire basic geological information for helping and advising societies in their various activities, for example, such as construction, planning, ground water prospecting and nature protecting. This work concentrates on the ductile stages of crustal evolution and attempts to set the framework for identifying tectonic terranes showing different histories. The most important structures for various applications developed during the semi-brittle to brittle stages of crustal evolution. As noted above, the occurrence brittle stages varies in time and place due to the complexity of the Svecofennian orogeny and due to the different timing of discordances during the orogeny. Therefore, the brittle structures, such as faulting and jointing patterns, should be analyzed with these variations in minds.

16. Several problems remained unsolved or need further research. For example:

    a. The earliest stages of the Svecofennian collision E_1 vary from place to place. For example, note the differences between $D_{1–2}$ in the Archaean domain and D_A in southernmost part of the Svecofennian domain. The oblique collision suggests a complex process with transpressional structures even during the earliest stages, but no information is currently available. Whether early local contractional zones, e.g. early subduction zones, or extensional zones were related to E_1 remains open with the pre-existing data. Such early oblique tectonics could explain the complex variations in the characters of the earliest supracrustal sequences.
    b. The direction of the southwards-migrating E_2 collapse zone is not known with certainly. The occurrence of mafic magmatism related to it, like that of Hyvinkää, supposes a c. ESE-trending zone. Further study is also needed to establish the ages of this mafic magmatism in the southernmost part of the Svecofennian domain.
    c. There are no ages for the microtonalite phase related to the early E_4 in the southern Svecofennian domain, and the relationship between late migmatization and magmatism during the late E_4 needs further establishment. Kinematic observations on the spot-like oblique extension during the D_H are based on rather limited data so far. The tectonic setting of so-called post-orogenic granites has not entirely been studied.
    d. The connections between volcanism in the E_4 pull-apart basins and the contemporaneous magmatism needs further establishment.

17. Studies on relationships between the brittle structures, faults and joints, with respect to the structures controlled by the Svecofennian orogeny are presently taking their first steps in Finland and require a considerable input in the near future.

ACKNOWLEDGEMENTS

This study is compilation of several projects of the Geological Survey of Finland; the results were mainly produced in the project "Construction potential modelling of bedrock in urban areas" carried out in 1999–2002 in the Helsinki area. We thank the Technological Agencies of Finland (TEKES), Helsinki, Espoo and Vantaa cities and the private companies Viatek Ltd and Rockplan Ltd for their financial support in this project.

Kalevi Korsman and Tapio Koistinen have been very keen on the developments of this research, and have helped us during the work in many different ways. They both read the early version of the manuscript and suggested several important aspects to touch on more carefully. We are grateful to them for their kind and supporting help. Our great thanks to Nicklas Nordbäck, who helped us in detailed and regional mapping. Matti Karhunen, Leena Järvinen and Marita Niemelä are thanked for rock crushing, mineral separation and laboratory assistance, and Andrej Wennström and Jouko Pääkkönen for preparing the thin sections.

We want to thank the official reviewers of the early version of the paper, Carl Ehlers and Karin Högdahl, for their suggestions for major revisions to improve the paper. Kerstin Saalmann reviewed this late version of the manuscript, which includes a lot of new data, and suggested several corrections; we thank her for her great help. This paper is a Nordsims publication # 206. The ion microprobe facility in Stockholm (Nordsims) is operated under an agreement between the joint Nordic research councils (NOS-N), the Geological Survey of Finland and the Swedish Museum of Natural History. The personnel of the NORDSIM laboratory, Martin Whitehouse, Lev Ilyinsky and Bodil Kajrup, are thanked.

Our greatest thanks to Roy Siddall for checking the English of the manuscript.

We are also grateful to many persons not named for their help during this process and hope that this co-operation will continue in the future during the more demanding stages of the forthcoming research work.

REFERENCES

Airo, M.-L. 1999. Aeromagnetic and petrophysical investigations applied to tectonic analysis in the northern Fennoscandian Shield. Geological Survey of Finland, Report of Investigation 145. 51 p.

Airo, M.-L., Elminen, T., Mertanen, S., Niemelä, R., Pajunen, M., Wasenius, P. & Wennerström, M. 2008. Aerogeophysical approach to ductile and brittle structures in the densely populated urban Helsinki area, southern Finland. In: Pajunen, M. (ed.) Tectonic evolution of the Svecofennian crust in southern Finland – a basis for characterizing bedrock technical properties. Geological Survey of Finland, Special Paper 47, 283–308.

Alviola, R., Mänttäri, I., Mäkitie, H. & Vaasjoki, M. 2001. Svecofennian rare-element granitic pegmatites of the Ostrobothnia region, western Finland: their metamorphic environment and time of intrusion. In: Mäkitie, H. (ed.) Svecofennian granitic pegmatites (1.86–1.79 Ga) and quartz monzonite (1.87 Ga), and their metamorphic environment in the Seinäjoki region, western Finland. Geological Survey of Finland, Special Paper 30, 9–29.

Bergman, S., Sjöström, H. & Högdahl, K. 2006. Transpressive shear related to arc magmatism: The Paleoproterozoic Storsjön-Edsbyn Deformation Zone central Sweden. Tectonics 25, 1–16.

Bleeker, W. & Westra, L. 1987. The evolution of Mustio gneiss dome, Svecofennides of SW Finland. Precambrian Research 36, 227–240.

Brun, J. P., Gapais, D. & Le Theoff, B. 1981. The mantled gneiss domes of Kuopio (Finland): interfering diabirs. Tectonophysics 74, 283–304.

Edelman, N. & Jaanus-Järkkälä, M. 1983. A plate tectonic interpretation of the Precambrian of the Archipelago of southwestern Finland. Geological Survey of Finland, Bulletin 325. 33 p.

Ehlers, C. & Lindroos, A. 1990. Early Proterozoic Svecofennian volcanism and associated plutonism in Enklinge, SW Finland. Precambrian Research 47, 307–318.

Ehlers, C., Lindroos, A. & Selonen, O. 1993. The late Svecofennian granite-migmatite zone of southern Finland – a belt of transpressive deformation and granite emplacement. Precambrian Research 64, 295–309.

Ekdahl, E. 1993. Early Proterozoic Karelian and Svecofennian formations and the evolution of the Raahe-Ladoga ore zone, based on the Pielavesi area, Central Finland. Geological Survey of Finland, Bulletin 373. 137 p.

Elminen, T., Airo, M.-L., Niemelä, R., Pajunen, M., Vaarma, M., Wasenius, P. & Wennerström, M. 2008. Fault structures in the Helsinki Area, southern Finland. In: Pajunen, M. (ed.) Tectonic evolution of the Svecofennian crust in southern Finland – a basis for characterizing bedrock technical properties. Geological Survey of Finland, Special Paper 47, 185–213.

Elo, S., Pirttijärvi, M. & Eskelinen, J. 2007. "Maankuoren anomaalisten massojen vaikutus kallioperän yläosan jännitystilaan Suomessa". In: Kaila, K. & Korja, T. (eds.) XXIII Geofysiikan Päivät, Oulu, 23.–24.05.2007. Oulu: Geofysiikan Seura, 35–39. (in Finnish)

Eskola, P. 1914. On the petrology of the Orijärvi region in southwestern Finland. Bulletin de la Commission Géologique de Finlande 40. 277 p.

Eskola, P. 1915. Om sambandet mellan kemisk och mineralogisk sammansättning hos Orijärvi traktens metamorfa bergarter. Summary of the contents: On the Relations between the Chemical and Mineralogical Composition in the Metamorphic Rocks of the Orijärvi Region. Bulletin de la Commission Géologique de Finlande 44, 1–107. Summary, 109–145.

Eskola, P. 1949. The problem of mantled gneiss domes. J. Geol. London 104, 461–476.

Eskola, P. 1954. Ein Lamprophyrgang in Helsinki und die Lamprophyrprobleme. Tschermak's Mineralogische und Petrographische Mitteilungen 3, 4, 1–4, 329–337.

Gaál, G. & Gorbatschew, R. 1987. An outline of the Precambrian evolution of the Baltic Shield. Precambrian Research 35, 15–52.

Grad, M. & Luosto, U. 1992. Fracturing of the crystalline uppermost crust beneath the SVEKA profile in Central Finland. Geophysica 28, 53–66.

Haapala, I., Rämö, T. & Frindt, S. 2005. Comparison of Proterozoic and Phanerozoic rift-related basaltic-granitic magmatism. Lithos 80, 1–32.

Hakkarainen, G. 1994. Geology and geochemistry of the Hämeenlinna-Somero Volcanic Belt, southwestern Finland: a Paleoproterozoic island arc. In: Nironen, M. & Kähkönen, Y. (eds.) Geochemistry of Proterozoic supracrustal rocks in Finland. IGCP Project 179 Stratigraphic methods as applied to the Proterozoic record and IGCP Project 217 Proterozoic geochemistry. Geological Survey of Finland, Special Paper 19, 85–100.

Härme, M. 1953. Karkkila. Geological Map of Finland 1:100 000, Pre-Quaternary Rocks, Sheet 2042. Geological Survey of Finland.

Härme, M. 1965. On the potassium migmatites of South Finland. Bulletin de la Commission Géologique de Finlande 219. 43 p.

Härme, M. 1969. Kerava. Geological Map of Finland 1:100 000, Pre-Quaternary Rocks, Sheet 2043. Geological Survey of Finland.

Härme, M. 1978. Pre-Quaternary Rocks of the Kerava and Riihimäki Map-Sheet area. Geological Map of Finland 1:100 000, Explanation to the Maps of Pre-Quaternery Rocks, Sheets 2043 and 2044. Geologinen tutkimuslaitos. 51 p. (in Finnish with English summary).

Heeremans, M. 1997. Silicic magmatism and continental lithosphere thinning; Inferences from field studies and numerical modelling of the Oslo Graben and the anorogenic crustal evolution of southern Finland. Publication no. 970122. Netherlands Research School of Sedimentary Geology. 197 p.

Hietanen, A. 1975. Generation of potassium-poor magmas in the northern Sierra Nevada and the Svecofennian of Finland. J. Res. U.S. Geol. Surv. 3, 631–645.

Högdahl, K., Andersson, U. & Eklund, O. (eds.) 2004. The Transscandinavian Igneous Belt (TIB) in Sweden: a review of its character and evolution. Geological Survey of Finland, Special Paper 37. 125 p.

Holdsworth, R. E., Strachan, R. A. & Dewey, J. F. (eds.) 1998. Continental transpressional and transtensional tectonics. London: Geological Society, Special Publications 135. 360 p.

Hölttä, P. 1988. Metamorphic zones and the evolution of granulite grade metamorphism in the early Proterozoic Pielavesi area, central Finland. Geological Survey of Finland, Bulletin 344. 50 p.

Hölttä, P. & Pajunen, M. 1988. The Pielavesi-Kiuruvesi area. In: Pajunen, M. (ed.) Project No. 235 "Metamorphism and geodynamics" excursion in Finland 15.6.–19.6.1988. Geological Survey of Finland, Guide 21, 13–18.

Hölttä, P., Lahti, S. & Pajunen, M. 1988. The Vaaraslahti pyroxene granitoid intrusion. In: Pajunen, M. (ed.) Project No. 235 "Metamorphism and geodynamics" excursion in Finland 15.6.–19.6.1988. Geological Survey of Finland, Guide 21, 19–22.

Hölttä, P., Huhma, H., Mänttäri, I. & Paavola, J. 2000. P-T-t development of Archaean granulites in Varpaisjärvi, central Finland. II. Dating of high-grade metamorphism with the U-Pb and Sm-Nd methods. Lithos 50 (1–3), 121–136.

Hopgood, A. M. 1980. Polyphase fold analysis of gneisses and migmatites. Transactions of the Royal Society of Edinburgh: Earth Sciences 71, 55–68.

Hopgood, A. M. 1984. Structural evolution of Svecokarelian migmatites, southern Finland: a study of Proterozoic crustal development. Transactions of the Royal Society of Edinburgh: Earth Sciences 74, 229–264.

Hopgood, A. M. 1999. Determination of structural successions in migmatites and gneisses. Dordrecht: Kluwer Academic. 346 p.

Hopgood, A. M., Bowes, D. R. & Addison, J. 1976. Structural development of migmatites near Skåldö, southwest Finland. Geologische Rundschau 67, 313–330.

Hopgood, A., Bowes, D., Kouvo, O. & Halliday, A. 1983. U-Pb and Rb-Sr isotopic study of polyphase deformed migmatites in the Svecokarelides, southern Finland. In: Atherton, M. & Gribble, C. (eds.) Migmatites, melting and metamorphism. Nantwich: Shiva, 80–92.

Huhma, A. 1981. Youngest Precambrian dyke rocks in North Karelia, East Finland. Bulletin of the Geological Society of Finland 53, 67–82.

Huhma, H. 1986. Sm-Nd, U-Pb and Pb-Pb isotopic evidence for the origin of the Early Proterozoic Svecokarelian crust in Finland. Geological Survey of Finland, Bulletin 337. 48 p.

Huhma, H., Claesson, S., Kinny, P. D. & Williams, I. S. 1991. The growth of Early Proterozoic crust: new evidence from Svecofennian detrital zircons. Terra Nova 3 (2), 175–178.

Jacobs, J. & Thomas, R. J. 2004. Himalayan-type indenter-escape tectonics model for the southern part of the late Neoproterozoic-early Porterozoic East-African-Antarctic orogen. Geology 32 (8), 721–724.

Kähkönen, Y. 1987. Geochemistry and tectonomagmatic affinities of the metavolcanic rocks of the early Proterozoic Tampere schist belt, southern Finland. Precambrian Research 35, 295–311.

Kähkönen, Y. 1989. Geochemistry and petrology of the metavolcanic rocks of the early Proterozoic Tampere Schist Belt, southern Finland. Geological Survey of Finland, Bulletin 345. 107 p.

Kähkönen, Y., Huhma, H. & Aro, K. 1989. U-Pb zircon ages and Rb-Sr whole rock isotope studies of Early Proterozoic volcanic and plutonic rocks near Tampere, southern Finland. Precambrian Research 45, 27–43.

Kaitaro, S. 1956. Riihimäki. Geological Map of Finland 1:100 000, Pre-Quaternary Rocks, Sheet 2044. Geological Survey of Finland.

Kärki, A. 1995. Palaeoproterozoic shear Tectonics in the Central Fennoscandian Shield, Finland. Department of Geosciences and Astronomy, University of Oulu, Res. Terrae Ser. A vol 10.

Kearey, P. & Vine, F. J. 1996. Global tectonics. London: Blackwell Science Ltd. 333 p.

Kilpeläinen, T. 1988. Evolution of deformation and metamorphism as a function of time in the Rantasalmi-Sulkava area, southeastern Finland. In: Korsman, K. (ed.) Tectono-metamorphic evolution of the Raahe-Ladoga zone. Geological Survey of Finland. Bulletin 343, 77–87.

Kilpeläinen, T. 1998. Evolution and 3D modelling of structural and metamorphic patterns of the Palaeoproterozoic crust in the Tampere-Vammala area, southern Finland. Geological Survey of Finland, Bulletin 397. 124 p.

Kilpeläinen, T. 2007. Elämänjärven hiertovyöhyke – loiva-asentoinen makrorakenne Keski-Suomen granitoidikompleksin ja Savon vyöhykkeen rajalla. Geologi 59, 35–38

Kilpeläinen, T. & Rastas, J. 1990. Etelä-Suomen leptiittijakson tektonis-metamorfisesta kehityksestä. University of Turku, Institute of Geology and Mineralogy, Publication No 21. 37 p. (in Finnish).

Kohonen, J., Pihlaja, P., Kujala, H. & Marmo, J. 1993. Sedimentation of the Jotnian Satakunta sandstone, western Finland. Geological Survey of Finland, Bulletin, 369. 24 p.

Koistinen, T. 1981. Structural evolution of an early Proterozoic stratabound Cu-Co-Zn deposit, Outokumpu, Finland. Transactions of the Royal Society of Edinburgh: Earth Sciences 72, 115–158.

Koistinen, T. 1992. Lyhyt kuvaus Tammisaaren karttaalueen kallioperästä. Suomen geologinen kartta 1:100 000, tilapäiskarttojen selitykset lehti 214. Geological Survey of Finland. 47 p. (in Finnish).

Koistinen, T., Klein, V., Koppelmaa, H., Korsman, K., Lahtinen, R., Nironen, M., Puura, V., Saltykova, T., Tikhomirov, S. & Yanovskiy, A. 1996. Paleoproterozoic Svecofennian orogenic belt in the surroundings of the Gulf of Finland. In: Koistinen, T. J. (ed.) Explanation to the map of Precambrian basement of the Gulf of Finland and surrounding area 1:1 million. Geological Survey of Finland, Special Paper 21, 21–57.

Koistinen, T., Stephens, M. B., Bogatchev, V., Nordgulen, Ø., Wennerström, M. & Korhonen, J. (comp.) 2001. Geological map of the Fennoscandian Shield, scale 1:2 000 000. Geological Survey of Finland, Special Maps 48.

Kontinen, A. 1987. An early Proterozoic ophiolite – the Jormua mafic-ultramafic complex, north-eastern Finland. Precambrian Research 35, 313–341.

Kontinen, A., Paavola, J. & Lukkarinen, H. 1992. K-Ar ages of hornblende and biotite from Late Archaean rocks of eastern Finland – interpretation and discussion of tectonic implications. Geological Survey of Finland, Bulletin 365. 31 p.

Korhonen, J. V., Aaro, S., All, T., Nevanlinna, H., Skilbrei, J. R., Säävuori, H., Vaher, R., Zhdanova, L. & Koistinen, T. (comp.) 2002a. Magnetic anomaly map of the Fennoscandian Shield: DGRF–65 anomaly of total field. Anomaly continued upwards to 500 m above ground: scale 1:2 000 000. Geological Survey of Finland, Special Maps 54.

Korhonen, J. V., Aaro, S., All, T., Elo, S., Haller, L. Å., Kääriäinen, J., Kulinich, A., Skilbrei, J. R., Solheim, D., Säävuori, H., Vaher, R., Zhdanova, L. & Koistinen, T. (comp.) 2002b. Bouguer anomaly map of the Fennoscandian Shield: IGSN 71 gravity system, GRS80 normal gravity formula. Bouguer density 2670 kg/m³, terrain correction applied. Anomaly continued upwards to 500 m above ground: scale 1:2 000 000. Geological Survey of Finland, Special Maps 53.

Korja, A., Korja, T., Luosto, U. & Heikkinen, P. 1993. Seismic and geoelectric evidence for collisional and extensional events in the Fennoscandian Shield – implications for Precambrian crustal evolution. Tectonophysics 219, 129–152.

Korja, A. & Heikkinen, P. 1995. Proterozoic extensional tectonics of central Fennoscandian Shield: results from the Baltic and Bothnian echoes from the Lithosphere experiment. Tectonics 14, 504–517.

Korja, A. & Heikkinen, P. 2005. The accretionary orogen – insight from BABEL profiles. Precambrian Research 136, 241–268.

Korja, T. 1990. Electrical conductivity of the lithosphere. Magnetotelluric studies in the Fennoscandian Shield, Finland. Acta Univ. Oulu, v. A215. 55 p.

Korsman, K. 1977. Progressive metamorphism of the metapelites in the Rantasalmi-Sulkava area, southeastern Finland. Geological Survey of Finland, Bulletin 290. 82 p.

Korsman, K., Hölttä, P., Hautala, T. & Wasenius, P. 1984. Metamorphism as an indicator of evolution and structure of the crust in Eastern Finland. Geological Survey of Finland, Bulletin 328. 40 p.

Korsman, K. & Kilpeläinen, T. 1986. Relationship between zonal metamorphism and deformation in the Rantasalmi-Sulkava area, southeastern Finland. In: Korsman, K. (ed.) Development of deformation,

metamorphism and metamorphic blocks in eastern and southern Finland. Geological Survey of Finland, Bulletin 339, 33–42.

Korsman, K., Niemelä, R. & Wasenius, P. 1988. Multistage evolution of the Proterozoic crust in the Savo schist belt, Eastern Finland. Geological Survey of Finland, Bulletin 343, 89–96.

Korsman, K., Koistinen, T., Kohonen, J., Wennerström, M., Ekdahl, E., Honkamo, M., Idman, H. & Pekkala, Y. (eds.) 1997. Bedrock map of Finland 1:1 000 000. Geological Survey of Finland, Special Maps 37.

Korsman, K., Korja, T., Pajunen, M. & Virransalo, P. 1999. The GGT/SVEKA transect: structure and evolution of the continental crust in the Paleoproterozoic Svecofennian orogen in Finland. International Geology Review 41, 287–333.

Korsman, K. & Lestinen, P. (eds.) 2002. Raahe-Laatokka – symposio. Kuopio 20.–21.3.2001. Laajat abstraktit. Geological Survey of Finland, unpublished report K 21.42/2002/1. 121 p. (in Finnish)

Kosunen, P. 2004. Petrogenesis of mid-Proterozoic A-type granites: Case studies from Fennoscandia (Finland) and Laurentia (New Mexico). PhD thesis, University of Helsinki, Department of Geology. 21 p.

Kousa, J., Marttila, E. & Vaasjoki, M. 1994. Petrology, geochemistry and dating of Paleoproterozoic metavolcanic rocks in the Pyhäjärvi area, central Finland. In: Nironen, M. & Kähkönen, Y. (eds.) Geochemistry of Proterozoic supracrustal rocks in Finland. IGCP Project 179 Stratigraphic methods as applied to the Proterozoic record and IGCP Project 217 Proterozoic geochemistry. Geological Survey of Finland, Special Paper 19, 7–27.

Krogh, T. E. 1973. A low-contamination method for hydrothermal decomposition of U and Pb for isotopic age determinations. Geochimica et Cosmochimica Acta 37, 485–494.

Krogh, T. E. 1982. Improved accuracy of U-Pb zircon ages by the creation of more concordant systems using an air abrasion technique. Geochimica et Cosmochimica Acta 46, 637–649.

Kuivamäki, A., Vuorela, P. & Paananen, M. 1998. Indications of postglacial and recent bedrock movements in Finland and Russian Karelia. Nuclear Waste Disposal Research, Geological Survey of Finland, Report YST–99. 92 p.

Kukkonen, I. & Lahtinen, R. (eds.) 2006. Finnish Reflection Experiment FIRE 2001–2005. Geological Survey of Finland, Special Paper 43, 247 p.

Kurhila, M., Vaasjoki, M., Mänttäri, I., Rämö, T. & Nironen, M. 2005. U-Pb ages and Nd isotope characteristics of the lateorogenic, migmatizing microcline granites in southwestern Finland. Bulletin of the Geological Society of Finland 77 (2), 105–128.

Lahtinen, R. 1994. Crustal evolution of the Svecofennian and Karelian domains during 2.1–1.79 Ga, with special emphasis on the geochemistry and origin of 1.93–1.91 Ga gneissic tonalites and associated supracrustal rocks in the Rautalampi area, central Finland. Geological Survey of Finland, Bulletin 378. 128 p.

Lahtinen, R. & Huhma, H. 1997. Isotopic and geochemical constraints on the evolution of the 1.93–1.79 Ga Svecofennian crust and mantle in Finland. Precambrian Research 82, 13–34.

Lahtinen, R., Huhma, H. & Kousa, J. 2002. Contrasting source components of the Paleoproterozoic Svecofennian metasediments : detrital zircon U-Pb, Sm-Nd and geochemical data. Precambrian Research 116 (1–2), 81–109.

Lahtinen, R., Korja, A. & Nironen, M. 2005. Paleoproterozoic tectonic evolution. In: Lehtinen, M., Nurmi, P. A. & Rämö, O. T. (eds.) Precambrian Geology of Finland. Key to the Evolution of the Fennoscandian Shield. Amsterdam: Elsevier Science B.V., 481–531.

Laitakari, I. & Simonen, A. 1962. Lapinjärvi. Geological Map of Finland 1:100 000, Pre-Quaternary Rocks, Sheet 3022. Geological Survey of Finland.

Laitakari, I. & Simonen, A. 1963. Pre-Quaternary Rocks of the Lapinjärvi Map-Sheet area. Geological Map of Finland 1:100 000, Explanation to the Maps of Pre-Quaternery Rocks, Sheet 3022. Geological Survey of Finland. 48 p. (with English summary).

Laitala, M. 1960. Siuntio. Geological Map of Finland 1:100 000, Pre-Quaternary Rocks, Sheet 2032. Geological Survey of Finland.

Laitala, M. 1961. Pre-Quaternary Rocks of the Siuntio Map-Sheet area. Geological Map of Finland 1:100 000, Explanation to the Maps of Pre-Quaternery Rocks, Sheet 2032. Geological Survey of Finland. 32p. (with English summary).

Laitala, M. 1964. Porvoo. Geological Map of Finland 1:100 000, Pre-Quaternary Rocks, Sheet 2021. Geological Survey of Finland.

Laitala, M. 1965. Pellinki. Geological Map of Finland 1:100 000, Pre-Quaternary Rocks, Sheet 2012. Geological Survey of Finland.

Laitala, M. 1967. Helsinki. Geological Map of Finland 1:100 000, Pre-Quaternary Rocks, Sheet 2034. Geological Survey of Finland.

Laitala, M. 1973a. On the Precambrian bedrock and its structure in the Pellinge region, South Finland. Geological Survey of Finland, Bulletin 264. 76 p.

Laitala, M. 1973b. Jussarö. Geological Map of Finland 1:100 000, Pre-Quaternary Rocks, Sheet 2013. Geological Survey of Finland.

Laitala, M. 1984. Pre-Quaternary Rocks of the Pellinki and Porvoo Map-Sheet areas. Geological Map of Finland 1:100 000, Explanation to the Maps of Pre-Quaternery Rocks, Sheets 3012 and 3021. Geological Survey of Finland. 53 p. (with English summary).

Laitala, M. 1991. Pre-Quaternary rocks of Helsinki Map-Sheet area. Geological Map of Finland 1:100 000, Explanation to the Maps of Pre-Quaternery Rocks, Sheet 2034. Geological Survey of Finland. 47 p. (with English summary).

Laitala, M. 1994. Lohja. Geological Map of Finland 1:100 000, Pre-Quaternary Rocks, Sheet 2041. Geological Survey of Finland.

Latvalahti, U. 1979. Cu-Zn-Pb ores in the Aijala-Orijärvi area, Southwest Finland. Economic Geology 75, 1035–1059.

Lehijärvi, M. 1961. Kärkölä. Geological Map of Finland 1:100 000, Pre-Quaternary Rocks, Sheet 2133. Geological Survey of Finland.

Lehijärvi, M. 1964. Lahti. Geological Map of Finland 1:100 000, Pre-Quaternary Rocks, Sheet 3111. Geological Survey of Finland.

Lehtonen, M. I., Kujala, H., Kärkkäinen, N., Lehtonen, A., Mäkitie, H., Mänttäri, I., Virransalo, P. & Vuokko, J. 2005. Etelä-Pohjanmaan liuskealueen kallioperä. Summary: Pre-Quaternary rocks of the South Ostrobothnian Schist Belt area. Geological Survey of Finland, Report of Investigation 158. 155 p.

Lindberg, B. & Eklund, O. 1988. Interactions between basaltic and granitic magmas in a Svecofennian postorogenic granitoid intrusion, Åland, southwest Finland. Lithos, 22, 13–23.

Lindroos, A., Romer, R. L., Ehlers, C. & Alviola, R. 1996. Late-orogenic Svecofennian deformation in SW Finland constrained by pegmatite emplacement ages. Terra Nova 8 (6), 567–574.

Ludwig, K. R. 2001. Isoplot/Ex rev. 2.49. A geochronological toolkit for Microsoft Excel. Berkeley Geochronology Center.

Ludwig, K. R. 2001. PbDat 1.21 for MS-dos: A computer program for IMB-PC Compatibles for processing raw Pb-U-Th isotope data. Version 1.07.

Ludwig, K. R. 2003. Isoplot/Ex 3. A geochronological toolkit for Microsoft Excel. Berkeley Geochronology Center, Special publication No. 4.

Luosto, U., Lanne, E., Korhonen, H., Guterch, A., Grad, M., Materzok, R. & Perchuk, E. 1984. Deep structure of the Earth's crust on the Sveka profile in central Finland. Ann. Geophys. 2, 559–570.

Luosto, U., Tiira, T., Korhonen, H., Azbel, I., Burmin, V., Buyanov, A., Kosminskaya, I., Ionkis, V. & Sharov, V. 1990. Crust and upper mantle structure along the DSS Baltic profile in SE Finland: Gephys. Jour. Int., 101, 89–110.

Mäkitie, H. & Lahti, S. I. 2001. The fayalite-augite quartz monzonite (1.87 Ga) of Luopa, western Finland, and its contact aureole. In: Mäkitie, H. (ed.) Svecofennian granitic pegmatites (1.86–1.79 Ga) and quartz monzonite (1.87 Ga), and their metamorphic environment in the Seinäjoki region, western Finland. Geological Survey of Finland, Special Paper 30, 61–98.

Marrett, R. & Peacock, D. C. P. 1999. Stress and strain. Journal of Structural Geology 21, 1057–1063.

Mertanen, S. 2001. Sekudääriset remanenssit kallioperän geologisten prosessien ilmentäjänä. In: Airo, M.-L. & Mertanen, S. (eds.) XX Geofysiikan päivät Helsingissä 15.–16.5.2001. Geofysiikan Seura, Geophysical Society of Finland, 129–134. (in Finnish)

Mertanen, S., Pajunen, M. & Elminen, T. 2001. Applying palaeomagnetic method for dating young geological events. In: Autio, S. (ed.) Geological Survey of Finland, Special Paper 31, 123–129.

Mertanen, S., Pajunen, M. & Elminen, T. 2004. Multiple remagnetization events of shear zones in southern Finland. In: Mertanen, S. (ed.) Supercontinents, remagnetizations and geomagnetic modelling. 5th Nordic Paleomagnetic Workshop, Suitia-Helsinki, Finland, September 25–30, 2004, 39–44.

Mertanen, S., Airo, M.-L., Elminen, T., Niemelä, R., Pajunen, M., Wasenius, P. & Wennerström, M. 2008. Paleomagnetic evidence for Mesoproterozoic – Paleozoic reactivation of the Paleoproterozoic crust in southern Finland**.** In: Pajunen, M. (ed.) Tectonic evolution of the Svecofennian crust in southern Finland – a basis for characterizing bedrock technical properties. Geological Survey of Finland, Special Paper 47, 215–252.

Mikkola, T. 1955. Origin of ultrabasics in the Orijärvi region. Extrait des Comptes Rendus de la Société géologigue de Finlande N:o XXVIII, 39–51.

Mouri, H., Korsman, K. & Huhma, H. 1999. Tectonometamorphic evolution and timing of the melting processes in the Svecofennian tonalite-trondhjemite migmatite belt: An example from Luopioinen, Tampere area, southern Finland. Bulletin of the Geological Society of Finland 71, 31–56.

Murphy, M. A. 2002. Orogen-parallel extension as expressed by the development of gneiss domes: an example from the Himalaya. 2002 Denver Annual Meeting (October 27–30, 2002), Session No 50, Thermal and Mechanical Significance of Gneiss Domes in the Evolution of Orogens, Paper No. 50–4, Geological Society of America. http://gsa.confex.com/gsa/2002AM/finalprogram/abstract_42867.htm.

Neuvonen, K. J. 1954. Forssa. Geological Map of Finland 1:100 000, Pre-Quaternary Rocks, Sheet 2113. Geological Survey of Finland.

Neuvonen, K. J., Korsman, K., Kouvo, O. & Paavola, J. 1981. Paleomagnetism and age relations of the rocks in the Main Sulphide Ore Belt in central Finland. Bulletin of the Geological Society of Finland 53 (2), 109–133.

Nironen, **M. 1989**. Emplacement and structural setting of granitoids in the early Proterozoic Tampere and Savo Schist Belts, Finland – implications for contrasting crustal evolution. Geological Survey of Finland, Bulletin 346. 83 p.

Nironen, **M. 1997**. The Svecofennian Orogen: a tectonic model. Precambrian Research 86 (1–2), 21–44.

Nironen, M. 1999. Structural and magmatic evolution in the Loimaa area, southwestern Finland. Bulletin of the Geological Society of Finland 71, 57–71.

Nironen, M. 2003. Keski-Suomen granitoidikompleksi, Karttaselitys. English summary: Central Finland Garnitoid Complex – Explanation to a map. Geological Survey of Finland, Report of Investigation 157. 45 p.

Nironen, M. & Lahtinen, R. 2006. Late Svecofennian sedimentary-volcanic association at Pyhäntaka. Bulletin of the Geological Society of Finland, Special Issue 1, 109.

Nurmi, P. & Haapala, I. 1986. The Proterozoic granitoids of Finland; granite types, metallogeny and related crustal evolution. Bulletin of the Geological Society of Finland 58, 241–261.

Pääjärvi, A. 1991. Pre-Quaternary Rocks of the Vesanto Map-Sheet area. Geological Map of Finland 1:100 000, Explanation to the Maps of Pre-Quaternery Rocks,

Sheet 3313. Geological Survey of Finland. 64 p. (with English summary).

Pajunen, M. 1986. Deformation analysis of cataclastic structures and faults in the Tervo area, central Finland. Geological Survey of Finland, Bulletin 339, 16–31.

Pajunen, M. 1988. Tectono-metamorphic evolution of the Hallaperä pyrrhotite-pyrite ore deposit, Central Finland. Geological Survey of Finland, Bulletin 343, 51–76.

Pajunen, M. & Poutiainen, M. 1999. Palaeoproterozoic prograde metasomatic-metamorphic overprint zones in Archaean tonalitic gneisses, eastern Finland. Bulletin of the Geological Society of Finland 71, 73–132.

Pajunen, M., Airo, M.-L., Wennerström, M., Niemelä, R. & Wasenius, P. 2001a. Preliminary report: The "Shear zone research and rock engineering" project, Pori area, south-western Finland. Geological Survey of Finland, Special Paper 31, 7–16.

Pajunen, M., Elminen, T., Airo, M.-L. & Wennerström, M. 2001b. Structural evolution of bedrock as a key to rock mechanical properties. In: Rock Mechanics. A Challence for Society. Proceeding of Regional Symposium EUROCK 2001. Rotterdam: A. A. Balkema, 143–148.

Pajunen, M., Airo, M.-L., Elminen, T., Niemelä, R., Vaarma, M., Wasenius, P. & Wennerström, M. 2002. Kallioperän rakennettavuusmalli taajamiin. Menetelmänkehitys ja ohjeistus. Geological Survey of Finland, unpublished report K 21.42/2002/5. 95 s. (in Finnish).

Pajunen, M., Elminen, T., Airo, M.-L. & Wennerström, M. 2004. Structural evolution of Svecofennian crust in southern Finland. The 26th Nordic Geological Winter Meeting, January 6th–9th 2004, Uppsala Sweden. GFF 126, (1), 32–33.

Pajunen, M., Hopgood, A., Huhma, H. & Koistinen, T. 2008. Integrated structural succession and age constraints on a Svecofennian key outcrop in Västerviken, southern Finland. In: Pajunen, M. (ed.) Tectonic evolution of the Svecofennian crust in southern Finland – a basis for characterizing bedrock technical properties. Geological Survey of Finland, Special Paper 47, 161–184.

Parras, K. 1958. On the charnockites in the light of highly metamorphic rock complex in Southwestern Finland. Bulletin de la Commission Géologique de Finlande 181. 137 p.

Patchett, P. J., Kouvo, O., Hedge, C. E. & Tatsumoto, M. 1981. Evolution of continental crust and mantle heterogeneity: evidence from Hf isotopes. Contributions to Mineralogy and Petrology 78 (3), 279–297.

Patchett, J. & Kouvo, O. 1986. Origin of continental crust of 1.9–1.7 Ga age: Nd isotopes and U-Pb zircon ages in the Svecokarelian terrain of South Finland. Contributions to Mineralogy and Petrology 92 (1), 1–12.

Pietikäinen, K. 1994. The geology of the Paleoproterozoic Pori shear zone, southwestern Finland, with special reference to the evolution of veined gneisses from tonalitic protoliths. PhD thesis, Michigan Technological University. 130 p.

Peltonen, P., Mänttäri, I., Huhma, H. & Whitehouse, M. J. 2006. Multi-stage origin of the lower crust of the Karelian craton from 3.5 to 1.7 Ga based on isotopic ages of kimberlite-derived mafic granulite xenoliths. Precambrian Research 147, 107–123.

Pihlaja, P. & Kujala, H. 2005. Kankaanpää. Geological Map of Finland 1:100 000, Pre-Quaternary Rocks, Sheet 1144. Geological Survey of Finland.

Platt, J. P. & England, P. C. 1993. Convective removal of lithosphere beneath mountain belts: Thermal and mechanical consequences. American Journal of Sciences 293, 307–336.

Ploegsma, M. & Westra, L. 1990. The Early Proterozoic Orijärvi triangle (southwest Finland): a key area of the tectonic evolution of the Svecofennides. Precambrian Research 47, 51–69.

Puura, V., Hints, R., Huhma, H., Klein, V., Konsa, M., Kuldkepp, R., Mänttäri, I. & Soesoo, A. 2004. Svecofennian metamorphic zones in the basement of Estonia. Proceedings of the Estonian academy of Sciences 53, 3, 190–209.

Rämö, O. T. 1991. Petrogenesis of the Proterozoic rapakivi granites and related basic rocks of southeastern Fennoscandia: Nd and Pb isotopic and general geochemical constraints. Geological Survey of Finland, Bulletin 355. 161 p.

Rämö, O. T., Kurhila, M., Nironen, M., Mänttäri, I. & Elliot, B. A. 2004. Nd isotope variation in the lateorogenic microcline granites and their synorogenic country rock granitoids in southern Finland. The 26th Nordic Geological Winter Meeting, January 6th–9th 2004, Uppsala, Sweden. GFF 126, (1), 34.

Ramsay, J. G. & Huber, M. I. 1983. The techniques of modern structural geology, volume 1: Strain Analysis. 307 p.

Rastas, J. 1990. Savonlinnan Pihlajaveden intruusiobreksiasta. Pro gradu-tutkielma, Turun yliopisto. 72 p. (in Finnish).

Reinikainen, J. 2001. Petrogenesis of Paleoproterozoic marbles in the Svecofennian Domain, Finland. Geological Survey of Finland, Report of Investigation 154. 84 p.

Ruotoistenmäki, T. 1996. A schematic model of the plate tectonic evolution of Finnish bedrock. Geological Survey of Finland, Report of Investigation 133. 23 p.

Rutland, R. W. R., Williams, I. S. & Korsman, K. 2004. Pre–1.91 Ga deformation and metamorphism in the Paleoproterozoic Vammala Migmatite Belt, southern Finland, and implications for Svecofennian tectonics. Bulletin of the Geological Society of Finland 76, 93–140.

Saalmann, K., Tessensohn, F., Piepjohn, K, von Gosen, W. & Mayr, U. 2005. Structure of Plaeogene sediments in east Ellesmere Island: Constraints on Eureken tectonic evolution and implications for Nares Strait problem. Tectonophysics 406, 81–113.

Salli, I. 1955. Suomusjärvi. Geological Map of Finland 1:100 000, Pre-Quaternary Rocks, Sheet 2023. Geological Survey of Finland.

Saltikoff, B., Tontti, M. & Puustinen, K. (comp.) 2002. Metallogenic map of Finland 1:1 000 000. Geological Survey of Finland.

Scheinin, B. & Korsman, K. 2007. Jakob Johannes Sederholm. Geolog, humanist och sanninggsökare (Jakob Johannes Sederholm. A geologist, humanist and a seeker after truth). Bidrag till kännedom av Finlands natur of folk 170. Helsinki: Finska Vetenskaps-Societen – Suomen Tiedeseura – Finnish Society of Science and Letters. 95 p.

Schreurs, J. & Westra, L. 1986. The thermotectonic evolution of a Proteozoic, low pressure, granulite dome, West Uusimaa, SW Finland. Contributions to Mineralogy and Petrology 93, 236–250.

Sederholm, J. J. 1907. Om granit och gneis, deras uppkomst, uppträdande och utbredning inom urberget i Fennoskandia. Bulletin de la Commission Géologique de Finlande 23 u. Fennia 26 (2). 90 p. English summary of the contents: On granite and gneiss, their origin, relations and occurrence in the pre-cambrian complex of Fenno-Scandia. 20 p.

Sederholm, J. J. 1923. On migmatites and associated pre-Cambrian rocks of southwestern Finland. Part 1. The Pellinge region. Bulletin de la Commission Géologique de Finlande 58. 153 p.

Sederholm, J. J. 1926. On migmatites and associated pre-Cambrian rocks of southwestern Finland. II. The region around the Barösundsfjärd W. of Helsingfors and neighbouring areas. Bulletin de la Commission Géologique de Finlande, 77. 143 p.

Sederholm, J. J. 1927. Precambrian of Fennoscandia with special reference to Finland. Bull. Geol. Soc. Amer. vol. 38, 1927, 13–836.

Sederholm, J. J. 1931. On the Sub-Bothnian unconformity and on Archaean rocks formed by secular weathering. Bulletin de la Commission Géologique de Finlande 95, 1–79.

Sederholm, J. J. 1932a. On the geology of Fennoscandia with special reference to the Pre-Cambrian. Explanatory notes to accompany a General geological map of Fennoscandia. Bulletin de la Commission Géologique de Finlande 98. 30 p.

Sederholm, J. J. 1932b. Über die Bodenkonfugurationen des Päijänne-Sees. Bulletin de la Commission Géologique de Finlande 100. 23 p.

Sederholm, J. J. 1967. Selected Works; Granites and migmatites. Edinburgh-London: Oliver & Boyd. 608 p.

Shomali, H. Z., Roberts, R. G., Pedersen, L. B. & the TOR Working Group 2006. Lithospheric structure on the Tornquist Zone resolved by nonlinear P and S teleseismic tomography along the TOR array. Tectonophysics 416, 133–149.

Simonen, A. 1949. Hämeenlinna. Geological Map of Finland 1:100 000, Pre-Quaternary Rocks, Sheet 2131. Geological Survey of Finland.

Simonen, A. 1955. Somero. Geological Map of Finland 1:100 000, Pre-Quaternary Rocks, Sheet 2024. Geological Survey of Finland.

Simonen, A. 1956. Pre-Quaternary rocks of the Somero Map-Sheet area. Geological Map of Finland 1:100 000, Explanation to the Maps of Pre-Quaternary Rocks, Sheet 2024. Geological Survey of Finland. 31 p. (with English summary).

Simonen, A. 1965. Karhula. Geological Map of Finland 1:100 000, Pre-Quaternary Rocks, Sheet 3024. Geological Survey of Finland.

Simonen, A. 1987. Pre-Quaternary Rocks of Map-Sheet areas of the rapakivi massif in SE Finland. Geological Map of Finland 1:100 000, Explanation to the Maps of Pre-Quaternery Rocks, Sheets 3023+3014, 3024, 3041, 3042, 3044, 3113, 3131, 3133. Geological Survey of Finland. 49 p. (with English summary).

Simonen, A. & Lehijärvi, M. 1963. Kouvola. Geological Map of Finland 1:100 000, Pre-Quaternary Rocks, Sheet 3113. Geological Survey of Finland.

Simonen, A. & Laitala, M. 1970. Kotka. Geological Map of Finland 1:100 000, Pre-Quaternary Rocks, Sheets 3023+3014. Geological Survey of Finland.

Skyttä, P., Väisänen, M. & Mänttäri, M. 2006. U-Pb zircon SIMS dating of deformation in the Orijärvi area, southern Finland. Bulletin of the Geological Society of Finland, Special Issue 1, 184.

Sorjonen-Ward, P. 2006. Geological and structural framework and preliminary interpretation of the FIRE 3 and FIRE 3A reflection seismic profiles, central Finland. Geological Survey of Finland, Special Paper 43, 105–159.

Stacey, J. S. & Kramers, J. D. 1975. Approximation of terrestrial lead isotope evolution by a two-stage model. Earth and Planetary Science Letters, 26, 207–221.

Stephansson, O., Särkkä, P. & Myrvang, A. 1986. State of stress in Fennoscandia. Proc. Int. Symp. on Rock Stress Measurements, Stockholm (Stephansson, O. ed). Luleå: Centek Publishers, 21–32.

Suominen, V. 1988. Radiometric ages on zircons from a cogenetic gabbro and plagioclase porphyrite suite in Hyvinkää, southern Finland. Bulletin of the Geological Society of Finland 60 (2), 135–140.

Suominen, V. 1991. The chronostratigraphy of southwestern Finland with special reference to Postjotnian and Subjotnian diabases. Geological Survey of Finland, Bulletin 356. 100 p.

Suominen, V. 1997. Smectite alteration in a lamprophyre dyke; a case study. GFF 119, 149–150.

Talvitie, J. 1971. Seismotectonics of the Kuopio region, Finland. Bulletin de la Commission Géologique de Finlande 248. 41 p.

Tapponier, P., Peltzer, G., Le Dain, A.Y., Armijo, R. & Cobbing, P. 1982. Propagating extrusion tectonics in Asia: new insights from simple experiments with plasticine. Geology 10, 611–616.

Torvela, T., Mänttäri, I. & Hermansson, T. 2008. Timing of deformation phases within the South Finland shear zone, SW Finland. Precambrian Research 160, 277–298.

Tuisku, P. & Laajoki, K. 1990. Metamorphic and structural evolution of the Early Proterozoic Puolankajärvi formation, Finland – II. The pressure-temperature-deformation-composition path. J. Metamorphic Geol. 8, 375–391.

Tuominen, H. V. 1957. The structure of an Archean area: Orijärvi, Finland. Bulletin de la Commission Géologique de Finlande 177, 1–31.

Vaasjoki, M. 1977a. Rapakivi granites and other postorogenic rocks in Finland: their age and the lead isotopic composition of certain associated galena mineralizations. Geological Survey of Finland, Bulletin 294. 64 p.

Vaasjoki, M. 1977b. Phanerozoic resetting of U- Pb ages in some South-Finnish uraninites. In: ECOG V. Fifth European Colloquium of Geochronology, Cosmochronology and Isotope Geology, Pisa, September 5.10.1977. 2 p.

Vaasjoki, **M. 1995.** Rengon Rouvinmäen kvartsimontsodioriitti: uusi posttektoninen granitoidi. Summary: The Rouvinmäki quartzmonzodiorite at Renko: a new posttectonic granitoid. Geologi 47 (6), 79–81.

Vaasjoki, M. & Sakko, M. 1988. The evolution of the Raahe-Ladoga zone in Finland: isotopic constraints. In: Korsman, K. (ed.) Tectono-metamorphic evolution of the Raahe-Ladoga zone. Geological Survey of Finland, Bulletin 343, 7–32.

Väisänen, M. 2002. Tectonic evolution of the palaeoproterozoic Svecofennian orogen in Southwestern Finland. Annales Universitatis Turkuensis, A II, 154. 143 p.

Väisänen, M. & Hölttä, P. 1999. Structural and metamorphic evolution of the Turku migmatite complex, southwestern Finland. Bulletin of the Geological Society of Finland 71, 177–218.

Väisänen, M. & Mänttäri, I. 2002. 1.90–1.88 Ga back arc basin in the Orijärvi area, SW Finland. Bulletin of the Geological Society of Finland 74, 185–214.

Väisänen, M., Mänttäri, I. & Hölttä, P. 2002. Svecofennian magmatic and metamorphic evolution in southern Finland as revealed by U-Pb zircon SIMS geochronology. Precambrian Research 116, 111–127.

Väisänen, M., Andersson, U. B., Huhma, H. & Mouri, H. 2004. Age of late Svecofennian regional metamorphism in southern Finland and south-central Sweden. The 26th Nordic Geological Winter Meeting, 6.–9.1.2004, Uppsala, Sweden, abstract volume. GFF 126, 40.

Wegmann, C. E. 1928. Über die Tektonik der jüngeren Faltung in Ostfinnland. Fennia 50, 1–22.

Wennerström, M., Airo, M.-L., Elminen, T., Niemelä, R., Pajunen, M., Vaarma, M. & Wasenius, P. 2008. Orientation and properties of jointing in Helsinki area, southern Finland. In: Pajunen, M. (ed.) Tectonic evolution of the Svecofennian crust in southern Finland – a basis for characterizing bedrock technical properties. Geological Survey of Finland, Special Paper 47, 253–282.

Whitehouse, M. J., Claesson, S., Sunde, T. & Vestin, J. 1997. Ion microprobe U-Pb zircon geochronology and correlation of Archaean gneisses from the Lewisian complex of Gruinard Bay, northwestern Scotland. Geochimica et Cosmochimica Acta, 61, 4429–4438.

Whitehouse, M. J., Kamber, B. & Moorbath, S. 1999. Age significance of U-Th-Pb zircon data from early Archaean rocks of west Greenland – a reassessment based on combined ion-microprobe and imaging studies. Chemical Geology, 160, 201–224.

Wiedenbeck, M., Allé, P., Corfu, F., Griffin, W. L., Meier, M., Oberli, F., von Quadt, A., Roddick, J. C. & Spiegeln, W. 1995. Three natural zircon standards for U-Th-Pb, Lu-Hf, trace element and REE analysis. Geostandards Newsletter, 19, 1–23.

Zhang, J., Ding, L., Zhong, D. & Zhou, Y. 2000. Orogen-parallel extension in Himalaya: Is it the indicator of collapse or the product in process of compressive uplift? Chinese Science Bulletin 45, 2, 114–119.

APPENDICES

Appendix 1. Structural relationships in the Tonalite Migmatite Belt

The Tampere Schist Belt (TSB), Vammala Migmatite Belt (VMB) and Hämeenlinna Volcanic Belt (HVB) form a key area for the correlations of the early tectonic history of the Tonalite Migmatite Belt (TMB) and Granite Migmatite Belt (GMB) (Figure 9). Their tectono-metamorphic evolution has been under intense research (e.g. Korsman et al. 1984, Pietikäinen 1994, Koistinen et al. 1996, Kilpeläinen 1998, Korsman et al. 1999, Nironen 1999, Pajunen et al. 2001a and Rutland et al. 2004) since the early studies published in several papers by Sederholm (e.g. 1931).

The earliest tectonic D_1 structures are identified from sedimentary and volcanic rocks. S_1 is nearly bedding-parallel, weak, penetrative foliation, and F_1 folds (Appendix-Fig. 1-1a) are strongly strained and flame-hinged (Appendix-Figs. 1-1a and b). In the strongly migmatitic areas, such as the Vammala Migmatite Belt (VMB), S_1 is preserved in competent felsic rocks; in metapelitic rocks it is represented by an internal biotite foliation in the early potassium feldspar porphyroblasts (Kilpeläinen 1998 and Nironen 1999). Corresponding F_1 folds (Appendix-Fig. 1-1b) also exist further south in the Eurajoki area to the SW of Pori, close the TMB-GMB border. According to Kilpeläinen (1998), the D_1 structures are absent in the lower-grade Tampere Schist Belt (TSB). He concluded that in the deeper part of the crust, represented by the VMB, metamorphism and deformation began earlier. Rutland et al. (2004) supposed time discordance between the TSB and VMB. The stacked northern border zone of the Granite Migmatite Belt (GMB) and the Hämeenlinna Volcanic Belt (HVB) (Figures 9 and 10) show isoclinal F_1 folding with sharp hinges in non-migmatitic andalusite-bearing metapelites (Appendix-Fig. 1-1a). Thus, the early structural succession of the HVB differs from that of the low-grade TSB. Instead, it resembles the early D_A structures (the volcanic Series I) in the detail study area, e.g. in the Southern Volcanic-Sedimentary Belt (SVB).

In the Tampere Schist Belt (TSB) the age of volcanism is c. 1.90–1.89 Ga (Kähkönen et al. 1989). The youngest age of detrital zircons in metaturbidites in the TSB is c. 1.91 Ga (Huhma et al. 1991); the metaturbidite age determines the maximum age of D_1 (Kilpeläinen 1998). This presupposes, however, that sediments of the Vammala Migmatite Belt (VMB) and Tampere Schist Belt (TSB) represent the same supracrustal sequence.

Progressive metamorphism and partial melting of rocks, concurrently with deformation D_2, penetratively modified the Vammala Migmatite Belt (VMB). In the turbiditic metasediments the early migmatite neosomes are trondhjemitic in composition. Strong vertical shortening is indicated by originally recumbent isoclinal to tight F_2 folds with strong mineral growth in the axial planes, S_2, and by intense boudinage of competent layers. The S_2 was originally horizontal. Koistinen et al. (1996) described chocolate tablet boudinage of competent layers of sedimentary rocks; this suggests flattening strain. Often the deformation was strong, causing gneissic to mylonite gneissic structures and shearing/transposition along the fold limbs. In the most intensive high-strain zones, schollen migmatites developed (e.g. Pietikäinen 1994). Their boudinaged fragments contain preserved fragments of early F_2 folds indicating effective deformation during the progression of D_2. The schollen migmatitic mica gneiss from Eurajoki, with fragments including F_2 folds (Appendix-Fig. 1-1c), is similar to those in the Pori study area. In contrast to this, such schollen migmatites do not occur in the southernmost part of the GMB. The metamorphic peak indicating high heat flow over wide areas was achieved under a rather constant pressure of c. 5 kbar (Korsman et al. 1999). Mouri et al. (1999) determined from Luopioinen in the Vammala Migmatite Belt (VMB) peak metamorphic conditions of 700–750 ºC at 4–5 kbar and $aH_2O = 0.4–0.7$, which was followed by decompressional cooling. Vertical flattening strain, in addition to high heat flow under rather constant pressure over wide areas (up to now no evidence or relics of progressive high-pressure assemblages have been found), indicates an extensional tectono-thermal event during D_2. It is very similar to the D_B in the southern study area.

In the Vammala Migmatite Belt (VMB) D_3 structures, formed due to N-S shortening, deformed the originally horizontal D_{1+2} structures, the schollen migmatites included, to a more or less upright position by F_3 folding (e.g. Pietikäinen 1994, Koistinen et al. 1996, Kilpeläinen 1998, Korsman et al 1999, Nironen 1999 and Pajunen et al. 2001a). The D_2 isotherms along with the D_3 ones form a complicated interference pattern with decreasing metamorphic grade towards the north to the Tampere Schist Belt (TSB) (Kilpeläinen 1998).

Due to the complex tectonic pattern in the Tonalite Migmatite Belt – Granite Migmatite Belt border zone described by Kilpeläinen (1998), it is difficult to bind the intrusive events to a certain deformation phase. The continuing character of magmatism (see the main text) further complicates this approach. According to

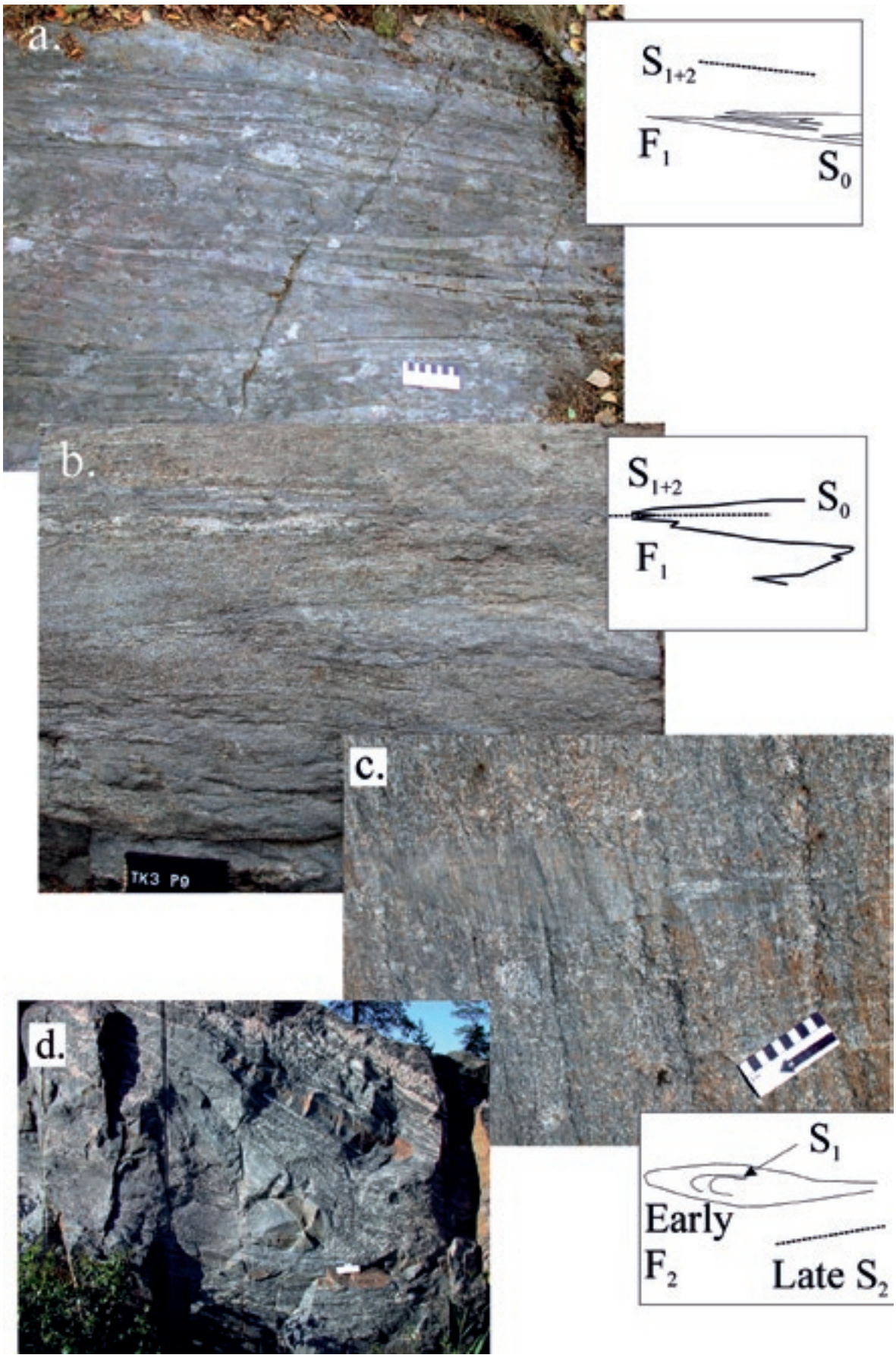

Appendix-Fig. 1-1. (a.) F_1 fold in mica schist. Scale bar is 10 cm in length. Taljala, Kalvola (Finnish grid coordinates KKJ2 2503.04E 6777.70N). (b.) F_1 fold in mica gneiss. Scale bar is 10 cm in length .Olkiluoto, Eurajoki (Finnish grid coordinates KKJ1 1525.57E 6792.75N). (c.) A fragment showing early F_2 fold ($+F_1$?) surrounded by the late S_2 in schollen migmatitic mica gneiss. Scale bar is 10 cm in length. Olkiluoto, Eurajoki (Finnish grid coordinates KKJ1 1524.28E 6792.20N). (d.) Northwestwards-overturned folding deforms strongly-sheared migmatite foliation corresponding the S_E and F_H relationships in the detailed study area. Scale bar is 15 cm in length. Heikkilä, Eurajoki (Finnish grid coordinates KKJ1 1530.31E 6789.19N). Photos by M. Pajunen.

Nironen (1989), the weakly-deformed Hämeenkyrö D_2 tonalite intrusion in the TSB is 1885 ± 2 Ma in age, while the sphene age is 1864 ± 1 Ma; the corresponding Värmälä intrusion has an age of 1878 ± 3 Ma. The metamorphosed Järvenpää quartz diorite in the Vammala Migmatite Belt (VMB) has an age of 1881 ± 4 Ma and is D_{2+3} deformed; it was interpreted as syn-D_2 by Kilpeläinen (op. cit.). Further south, in the Granite Migmatite Belt, the syn-D_3 Pöytyä granodiorite in the Hämeenlinna Volcanic Belt (HVB) is dated at 1870 ± 12 Ma, representing the main intrusive phase, and at 1869 ± 8 Ma for a porphyritic phase (Nironen 1999). These results mean that D_3 started about 10 Ma later or it continued longer in the southern Granitic Migmatite Belt (GMB) than in the Vammala Migmatite Belt (VMB). The emplacement of the Värmälä and Pöytyä intrusions are concomitant with the syn-/late D_B tonalites in the southern Espoo Granitoid Complex (EGC). The observations from the Vammala Migmatite Belt (VMB) and Hämeenlinna Volcanic Belt (HVB) suggest their co-existence during D_2, and suppose that D_1 was the major collisional/overthrusting phase juxtaposing the units.

Plutonic clasts in the Veittijärvi intraformational conglomerate, in Ylöjärvi in the Tampere Schist Belt (TSB), show typical synkinematic ages of 1.89–1.88 Ga (Nironen 1989). This means that the Tampere Schist Belt (TSB) underwent deformation that formed the basin for the deposition of the conglomerate and related sediments after that age. According to Kilpeläinen (op. cit.), D_2 in the VMB is c. 1.88 Ga old. The extensional D_2 evolution was able to form sedimentary basins with rapid deposition of the supracrustal sequences of the TSB. The conglomerate clasts foliated moderately during continuing subsidence and heating under D_2 extension. Extensional D_2 process explains the subsidence of the schists of TSB from the upper crustal levels next to the high-grade gneisses, the absence of D_1 from TSB schists and the progressive increase in metamorphic grade towards south from the non-migmatitic rocks of the TSB to the migmatites of the VMB (cf. Kilpeläinen 1988 and Korsman et al. 1999). Corresponding subsidence of much later sedimentary-volcanic sequences of the Jokela supracrustal association into a higher-grade environment is described in Appendix 5. The Haukivuori conglomerate with 1885 ± 6 Ma old plutonic clasts is located in the Rantasalmi-Sulkava area (RSB), which is overthrusted upon the southern part of Savo Schist Belt (SSB) (Korsman et al. 1988). Korsman et al. (op. cit.) related the conglomerate to the evolution of the tectono-metamorphic discordance between the northern the SSB and southern RSB. The northern part of SSB was eroding simultaneously with a high-temperature metamorphic event in the southern unit. Thus, the overthrusting is younger than 1885 Ma; intrusion of 1836 ± 20 Ma lamprophyre dykes (Neuvonen et al. 1981) sharply cut the SSB, but they are metamorphosed in the RSB (K. Korsman pers. comm. 2006).

The young ages, e.g. the sphene age in Hämeenkyrö, indicates that the later deformations and heating effectively acted as far north as the Tampere Schist Belt (TSB). The ages are compatible with ages of the D_E thermal evolution in the study area, e.g. in the Espoo Granitoid Complex (EGC) and West Uusimaa granulite Complex (WUC). The late structures, such as shearing and fragmentation of the early D_B neosome, in migmatitic mica gneiss from Eurajoki (Appendix-Fig. 1-1d) are similar to the D_E-D_H structures in the detailed study area. This suggests that D_E and D_H deformations occurred quite similarly in southwestern Finland (Eurajoki). The wide-scale F_I folding (Figure 11) bends the Granite Migmatite Belt (GMB) towards the north in southwestern Finland and in the southwestern archipelago (Figure 9).

Appendix 2. West Uusimaa granulite Complex characteristics

The traditional granulite-facies West Uusimaa granulite Complex (WUC) (Eskola 1914, 1915, Tuominen 1957 and Parras 1958) forms a complex structure exposed between amphibolite-facies units and granitoid complexes. Väisänen and Hölttä (1999) described corresponding granulites from the Turku area (Figures 9 and 10). The granulites are gneissic orthopyroxene-bearing granitoids, often tonalitic, migmatitic garnet-cordierite gneisses and variable pyroxene-bearing felsic, intermediate and basic gneisses (Parras 1958). Principally, the supracrustal rocks represent high-T/low-p variants of the lower-grade sequences further south in the Southern Volcanic-sedimentary Belt (SVB), such as in the Orijärvi area (e.g. Eskola 1914, 1915, Parras 1958, Schreurs & Westra 1986 and Kilpeläinen & Rastas 1990). Our field observations are from the northeastern part of the WUC between the border zone of the Hyvinkää Gabbroic-volcanic Belt (HGB) and the Espoo Granitoid Complex (EGC).

The contact of the WUC with the overlying EGC is characterized by shearing described in detail from Klaukkala (Figure 35). The contact is a low-angle extensional shear zone with top-to-SE movement; the deformation is related the D_E extension. The border with the Perniö Granitoid Complex (PGC), interpreted using the magnetic maps and tectonic observations, is a similar low-angle zone dipping SE; the zone was deformed by the F_{G-H} interference folding, thus, evidencing its pre-D_{G-H} generation (Figure 16). The sharp Kisko fault (Figures 10 and 16) was oriented by this old structure. In the north the WUC is bordered against the Hyvinkää Gabbroic-volcanic Belt (HGB) along the complex Hyvinkää shear/fault zone (Figures 9 and 10), and the D_H structures were bent due to progressive SE-NW D_H transpression into a E-W direction in the vicinity of the shear/fault zone. In the east the Vuosaari-Korso shear/fault zone cuts the WUC; only small areas of corresponding high-grade rocks are exposed in antiformal structures in the Sipoo area. A small granulitic window is also exposed in the Nuuksio (Nu in Figure 9) granite area.

The West Uusimaa granulite Complex (WUC) forms a wide antiformal fold interference dome (Figure 11) showing a complex internal tectonic pattern (Figure 41); granulites in Turku are situated in a corresponding tectonic dome setting (Figure 9 and 11). The westernmost part of the WUC is characterized by dome-and-basin interferences, c. 8 km in diameter with ENE-trending high-strain zones between the dome-and-basin chains (Figures 16 and 41). The structural pattern is exposed between the Orijärvi area and the NW-trending Hiidenvesi shear zone (Figure 10). We interpret these as reflections of $D_{G+H\pm I}$ interferences (cf. D_{3+4} interferences by Kilpeläinen & Rastas 1990) corresponding to the structure described from the Askola area (Appendix-Fig. 3-4).

The northeastern parts of the West Uusimaa granulite Complex (WUC) comprise large areas that show a simple tectonic geometry with exceptionally well-developed straight foliation (Appendix-Fig. 2-1). The foliation is nearly horizontal and is deformed into open $F_{G+H\pm I}$ fold interferences. Between the horizontal areas are complexly folded units; their forms are determined by the $F_{G+H\pm I}$ interferences (Figure 41). The borders between the complexly-deformed horizontal tectonic units and the units showing the straight foliation are low-angle, extensional D_E shear zones. Our interpretation is that the straight foliation was formed during a penetrative extensional D_E event under granulite facies conditions; large-scale crustal shearing under granulite-facies conditions produced a granoblastic microstructure in the one- or two-pyroxene rocks. In the upper crustal levels and lower temperatures the ductile deformation was more zoned, and close to the erosion level sharp faults occur (cf. Figure 4). Carbonate was often precipitated into extensional fractures or along the foliation planes of the pyroxene-gneisses. Some carbonate was precipitated still later, as indicated by the c. 10-m-wide fracture-controlled impure carbonate filling in the Porkkala-Mäntsälä zone (Hämeenkylä, Vantaa, Finnish grid coordinates KKJ2 2544.61E 6684.73N). These carbonates are products of remobilization of the primary sedimentary and volcanic carbonates that are typical in the corresponding lower-grade units (Southern Volcanic-sedimentary Belt, SVB), and of possible additive CO_2 influx that, according to Schreurs & Westra (1986), caused the granulite metamorphism. Those parts of the crust that were not deformed penetratively by the D_E show the complex preserved pattern formed during the pre-existing D_{A-D} tectonic history.

The granulite-facies rocks occur in a c. E-ENE-trending zone. In the east it continues below the Askola area (As in Figure 9), where this hot crustal “slice” caused the ductility of the overlying crust during their deformation into D_{G+H+I} dome-and-basins corresponding to those in the western WUC. This interpretation is supported by the pattern of the upwards-continued magnetic field that represents the deeper and wider magnetic anomalies of the crust (Figure 12a). The anomaly pattern characteristic for the WUC continues east to the western parts of the Vyborg rapakivi batholith (1 in Figure 1), up to the crustal-scale N-trending Riga Bay-Karelia Zone (RKZ) (Figures 8 and 10). This zone shows the lowest magnetic and gravity anomalies, indicating the deepest extension of the Vyborg rapakivi granite in the zone.

Appendix-Fig. 2-1. Well-developed and straight S_E-foliated pyroxene-bearing felsic gneiss in the West Uusimaa granulite Complex (WUC). Compass is 12 cm in length. Röykkä, Nurmijärvi (Finnish grid coordinates KKJ2 2534.02E 6715.41N). Photo by N. Nordbäck.

The orthopyroxene-bearing tonalite (charnockite) from Lohja, Maikkala that was preserved "untouched" in the D_E penetrative shearing, was dated by conventional U-Pb at 1860 ± 4 Ma based on zircon and 1837 ± 3 Ma based on monazite. The U-Pb zircon ages obtained with SIMS from the same sample give a concordia age of 1862 ± 4 Ma for the rock (Appendix 8). The penetrative D_E shearing sharply cuts the tonalite areas. Therefore, the intrusion age of the tonalite determines that the major penetrative horizontal D_E deformation occurred later than c. 1.86 Ga. The age is similar to those obtained from corresponding pyroxene granitoids from Kakskerta, near Turku, and from Houtskär, from the Turku archipelago (Suominen 1991).

Granulite mineral assemblages formed during progressive metamorphism are often later affected by retrograde metamorphism; decomposition of pyroxenes to clinoamphibole is typical, for example in the northern Espoo Granitoid Complex (EGC). The Maikkala tonalite also contains metamorphic mineral assemblages suggesting later high-temperature metamorphism, presumably represented by the monazite and homogeneous core ages of c. 1.84–1.83 Ga (Appendix 8). The c. 1.82 Ga ages of migmatite neosomes in granulitic metapelites (Väisänen et al. 2004) indicate a continued high-T event. According to our observations, these late granitic neosomes are related to the evolution of D_H, which is also characterized by large amounts of granitic melt elsewhere. Locally, particularly in the areas of lower metamorphic grade, there was a cooling stage between the events. At deeper crustal depths, high heat flow was more continuous from the early-D_E tonalites at 1.86 Ga to the D_H phases evolving at c. 1.83–1.81 Ga. The temperature remained quite high, because granitic melts, like the 1804 ± 2 Ma pegmatitic granite dykes (Pajunen et al. 2008), still intruded the latest-identified Svecofennian D_I folds.

Appendix 3. Structural relationships in Hyvinkää Gabbroic-volcanic Belt

The structurally-complex Hyvinkää Gabbroic-Volcanic Belt (HGB) is located between the Hyvinkää shear/fault zone and strong shear zones bordering it in the north to the Renko area (Figures 9 and 41). The NNE-trending Hyvinkää-Lahti shear/fault zone divides the HGB into Hyvinkää (Hy in Figure 9) and Askola (As in Figure 9) areas. Large c. 1.88 Ga old (Patchett et al. 1981) layered gabbro massifs surrounded by supracrustal sequences characterize the Hyvinkää-part of the HGB. The Askola area is characterized by roundish dome-and-basin structures; gabbroic-volcanic rock associations are squeezed between the domes.

Setting of gabbros of the Hyvinkää Gabbroic-volcanic Belt

The central parts of the gabbroic massifs are weakly deformed (Appendix-Fig. 3-1a), but their border zones are strongly deformed and show ductile shearing, and locally the gabbros are semi-brittley faulted. Volcanic rocks and mica gneisses that surround the gabbros locally show primary structures such as bedding, fragmentary (Appendix-Fig. 3-2a), agglomerate and pillow lava structures. The paragneisses often show a complex polyphase deformation that is very similar to that described from the Espoo Granitoid Complex (EGC) and Southern Volcanic-sedimentary Belt (SVB), like the D_{C-D} dome-and-basin structure shown in Appendix-Fig. 3-2b, but no F_A fold observations currently exist. In the supracrustal rocks, especially in amphibolites, a lineation dips steeply E or SE (Appendix-Fig. 3-2c); correspondingly to that described from the SVB (Figure 14e).

Often the primary magmatic layers of the Hyvinkää gabbro are folded to an upright position. Open folds with NW-trending steep axial planes of the magmatic layers indicate ductile deformation even in the well-preserved parts. The recent setting of magmatic layers becomes evident as variation in the magnetic anomaly pattern (Appendix-Fig. 3-3a). At the southwestern end of the Hyvinkää gabbro massif a folded "tail" of deformed layered mafic rock (Appendix-Figs. 3-3 and 3-1b and c) is interpreted as a layered gabbro that thins and dies out towards the attenuated NE-end of the western massif. The western massif has a corresponding tail in its NE-part, and there are drag folds in the SE and NE corner of the western massif – the structures indicate their dextral rotation. The folded "tail" shows a fold axis paralleling the lineation observed in the amphibolites elsewhere in the HGB (Appendix-Fig. 3-2c). We interpret this as $L_{B/C}$, corresponding to $L_{A+B/C}$ of the Southern Volcanic-sedimentary Belt (SVB).

The supracrustal sequences, intensely folded between the gabbros, exhibit corresponding dextral rotation drags. The "tail" structures suggest D_B boudinage that was later refolded by D_C and rotated during continuing deformations. The volcanic belt between the major gabbro bodies forms D_{C+D} dome-and-basin structures that were subsequently bent by later deformations (Appendix-Fig. 3-2b). The structures suggest that the gabbros represented originally widespread layered massifs that were fragmented and boudinaged during D_B flattening, and were folded by D_{C+D} and dextrally rotated by D_H. The interpretation is supported by the folded pattern of occurrence of gabbroic "fragments" in the Granite Migmatite Belt (GMB) (Figures 7 and Appendix-Fig. 3-3). The structural evolution of the gabbros is summarized in Appendix-Fig. 3-3b; the complexly folded gabbros represent originally nearly horizontal magma bodies and their exposure is determined by the late wide-scale folding phases D_G, D_H and D_I. In the Askola area (see below), gabbroic rocks are sometimes preserved as remnants in metamorphic amphibolites; therefore, it is likely that gabbros were originally more widespread than can be estimated from the map shown in Appendix-Fig. 3-4.

The gabbro massifs are cut by straight NE-trending structures that were formed by dextral movement. Some linear ESE- and SE-trending structures also occur. In the Hyvinkää massif NW-trending structures also cut the massif: they are parallel to the axes of open-folding $F_H$cont. On an outcrop, in the interior of the Hyvinkää massif, semi-brittle faulting and granite-filled fractures show an en échelon pattern, suggesting competent behavior of the gabbros during the NW-SE-directional shortening. These structures coincide with the clockwise rotation and dextral movements along the E-W-trending shear zones, and the overall SE-NW transpression during the D_H deformation.

Dome structures in the Askola area of the Hyvinkää Gabbroic-volcanic Belt

The Askola area (As in Figure 9) of the Hyvinkää Gabbroic-volcanic Belt (HGB) is separated from the Hyvinkää area (Hy in Figure 9) by the sinistral Hyvinkää-Lahti shear/fault zone (Figures 10 and 41), which is related to the N-NNE-trending D_I deformation; the shear/fault zone is located in the northern continuation of the Vuosaari-Korso shear/fault zone (Figures 10 and 41). The axial plane of the open semi-ductile crustal

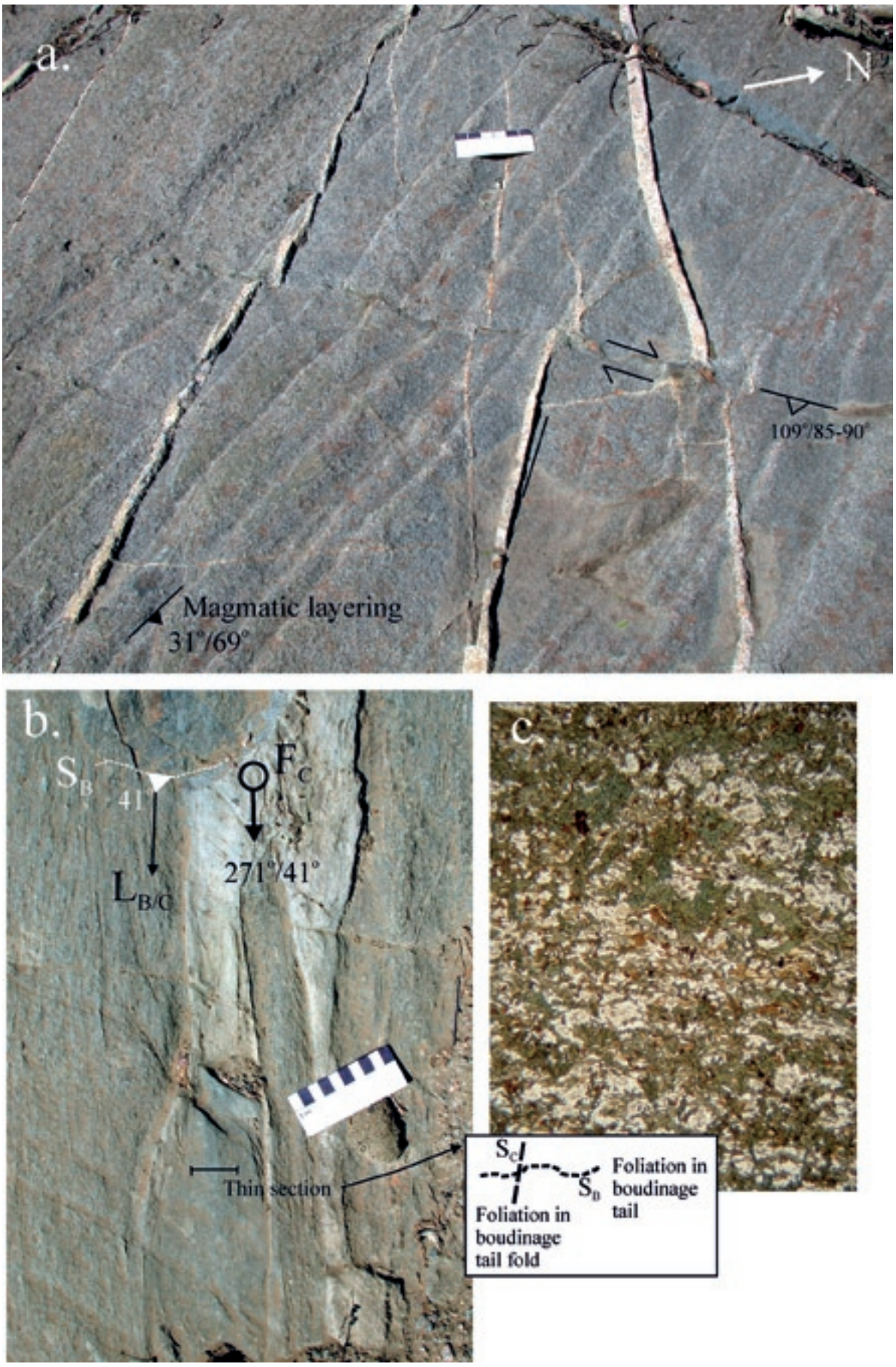

Appendix-Fig. 3-1. (a.) Layered Hyvinkää gabbro is cut by granite dykes and semi-brittle faults. Scale bar is 15 cm in length. Lähdemäki, Hyvinkää (Finnish grid coordinates KKJ2 2535.59E 6723.69N). (b.) Detail from the folded tail in the SE-side of the Hyvinkää gabbro and (c.) a microphoto from the fold. The new mineral growth in the folded tail indicates medium-grade metamorphic conditions. Scale bar is 10 cm in length in (b.). Rantalanhaka, Hyvinkää (Finnish grid coordinates KKJ2 2534.50E 6722.85N). Photos by M. Pajunen.

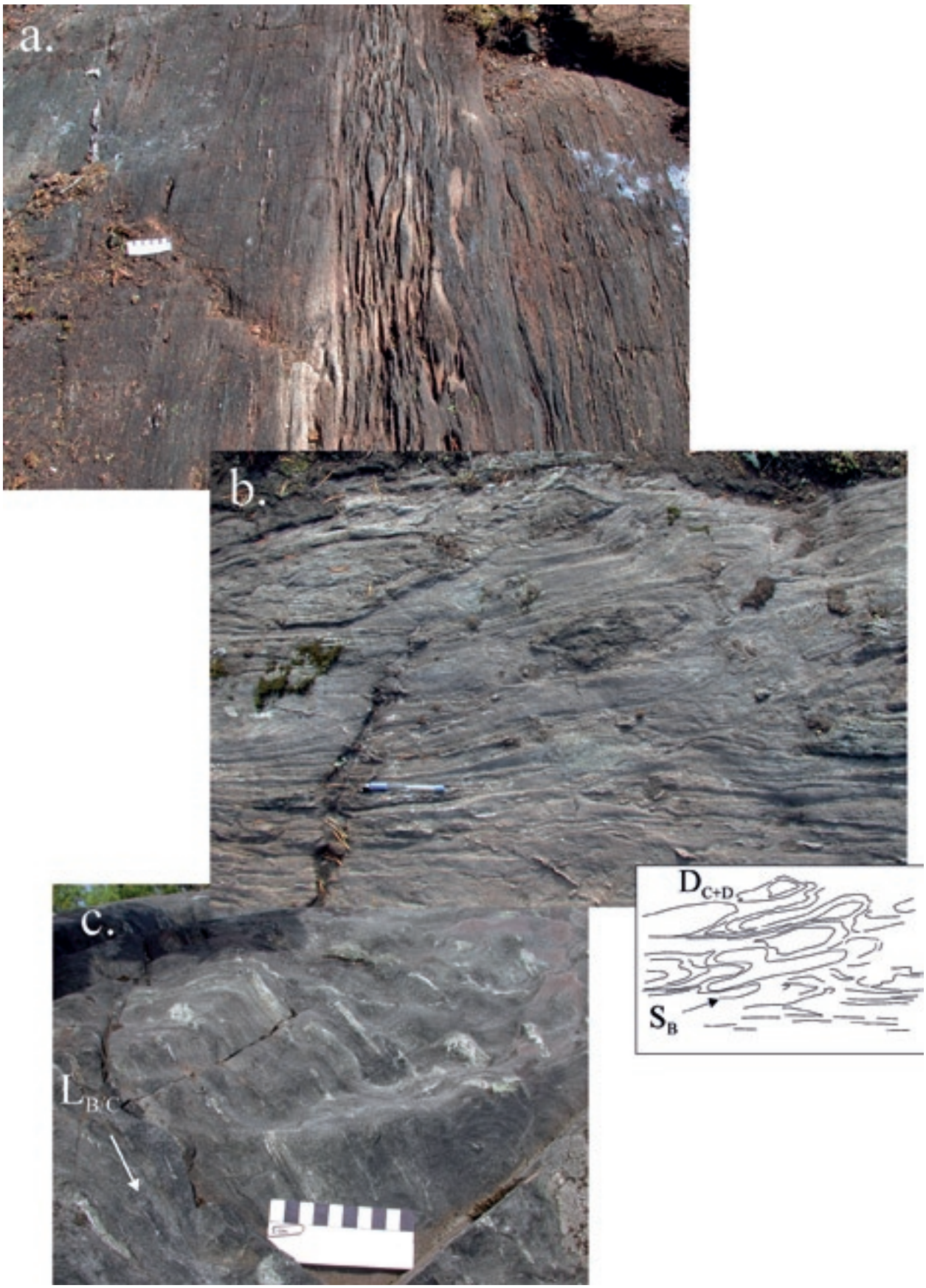

Appendix-Fig. 3-2. (a.) Mafic, partly fragmentary volcanic rock in the Hyvinkää Gabbroic-volcanic Belt (HGB). Scale bar is 10 cm in length. Konnunsuonmäki, Hyvinkää (Finnish grid coordinates KKJ2 2528.20E 6723.31N). (b.) D_{C-D} dome-and-basin structure in non-migmatitic mica gneiss in the border zone of the Hyvinkää Gabbroic-volcanic Belt (HGB) and the West Uusimaa granulite Complex (WUC). Pencil is 14 cm in length. Karhulampi, Hyvinkää (Finnish grid coordinates KKJ2 2537.04E 6714.43N). (c.) Strong lineation ($L_{B/C}$) in amphibolite in the HGB. Scale bar is 10 cm in length. Palosenkallio, Hyvinkää (Finnish grid coordinates KKJ2 2542.97E 6718.08N. Photos by M. Pajunen.

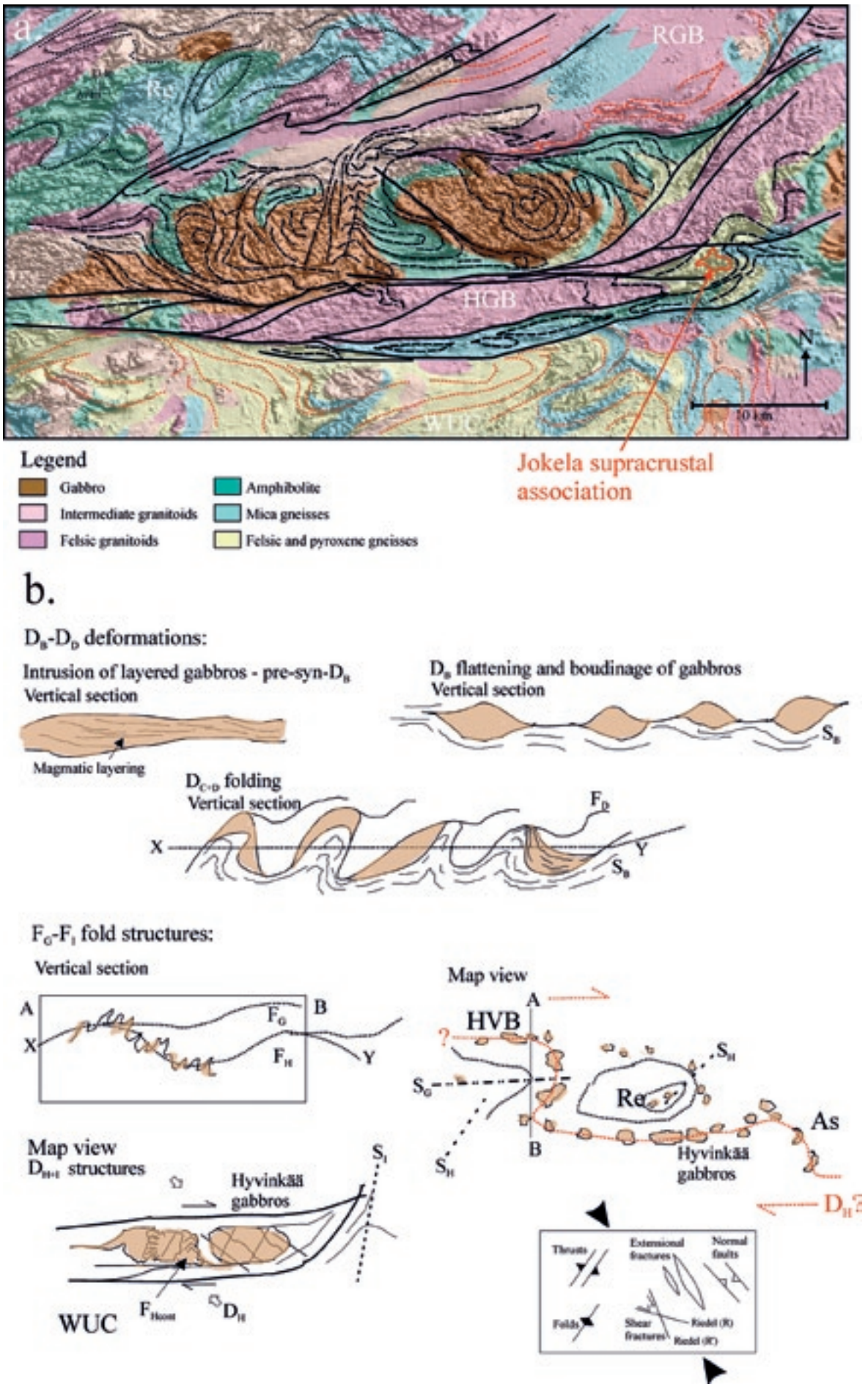

Appendix-Fig. 3-3. (a.) Tectonic structure of the Hyvinkää gabbro and (b.) schematic model of its tectonic evolution on a combined magnetic (shadowing) and lithological (colours) map. The location of the Jokela supracrustal association (Jo) is shown.

bend F_I parallels the Hyvinkää-Lahti shear/fault zone, which further north changes in character to the Lake Päijänne fracture pattern already described by Sederholm (1932b) (Figure 10).

The Askola area differs structurally from the western part of the Hyvinkää Gabbroic-Volcanic Belt (HGB). It shows systematic dome-and-basin structures with zones of gabbros and amphibolites and lesser mica gneisses squeezed between the dome structures (Figure 9 and Appendix-Fig. 3-4). The internal parts of the domes are composed of granodioritic to tonalitic intrusives and migmatitic garnet-cordierite gneisses. The structural pattern of the foliations, shown in Appendix-Fig. 3-4, suggests that the lower tectonic slices of crust are exposed in the dome windows and the rocks of the upper tectonic slice, typical rocks of the HGB, are compressed between the domes (Appendix-Fig. 3-4).

Migmatitic mica gneisses in the Onkimaa dome centre provide evidence of several folding generations prior to the formation of the open rounded dome structure. Isoclinal early flame-crested folds (F_A) underwent additional flattening with contemporaneous granitic melting during D_B (Appendix-Fig. 3-5). Isoclinal folds (F_C) with steep NE-trending axial planes refold these structures. The early D_{C-D} dome-and-basin interference structures typical in the southern units, like in the Southern Finland Sedimentary-volcanic Belt (SVB), are not identified here (due to restricted observations by us).

Intermediate microtonalite dykes (observed up to 0.5 m wide) cut the structures, suggesting a cooling stage after the $D_{A-C-(D)}$ and a new pulse of magmatism. We relate the dykes to the D_E (see main text). A model shown in Figure 4 can explain the contrasts between the steeply and gently dipping foliations in the dome interior contra margin settings. The borders of the internal dome and overlying rocks were interpreted as an extensional D_E shear structure corresponding to that described from the Espoo Granitoid Complex (EGC) in Klaukkala (Figure 35). The open fold structure F_I with NW-SE-trending axial planes deforms the strong S_{A-B} foliation, appearing as macro-crenulation on the outcrop (Appendix-Fig. 3-5). It also deforms the microtonalite dykes. This folding has map-scale amplitude. Although some overprinting occurred due to shearing along eastern low-angle border faults of the Onkimaa dome, it is evident that the folds are related to dome formation. This is supported by a similar NW-trending fold pattern in the overlying tectonic slice

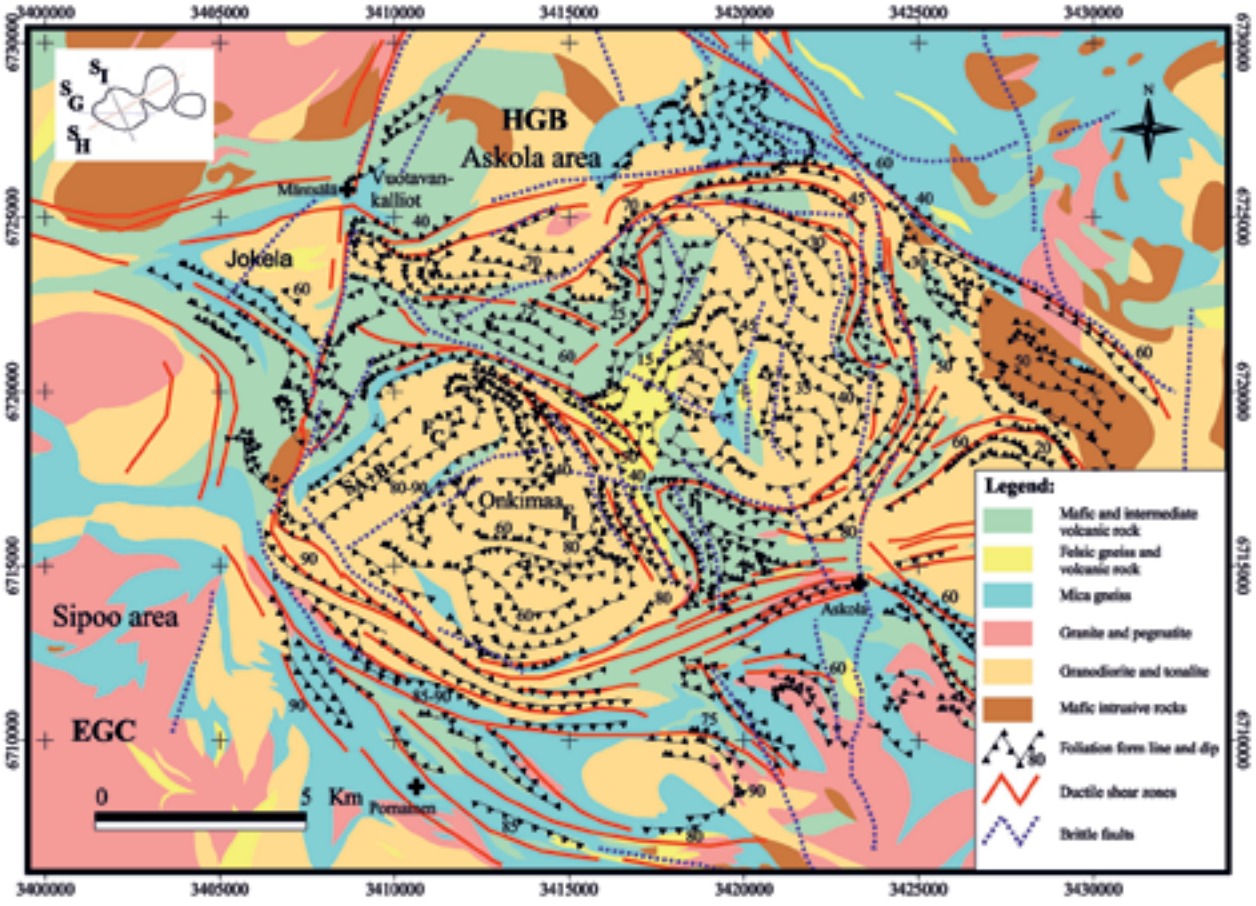

Appendix-Fig. 3-4. Tectonic structure in the Askola dome-and-basin area. (Finnish grid coordinates KKJ3).

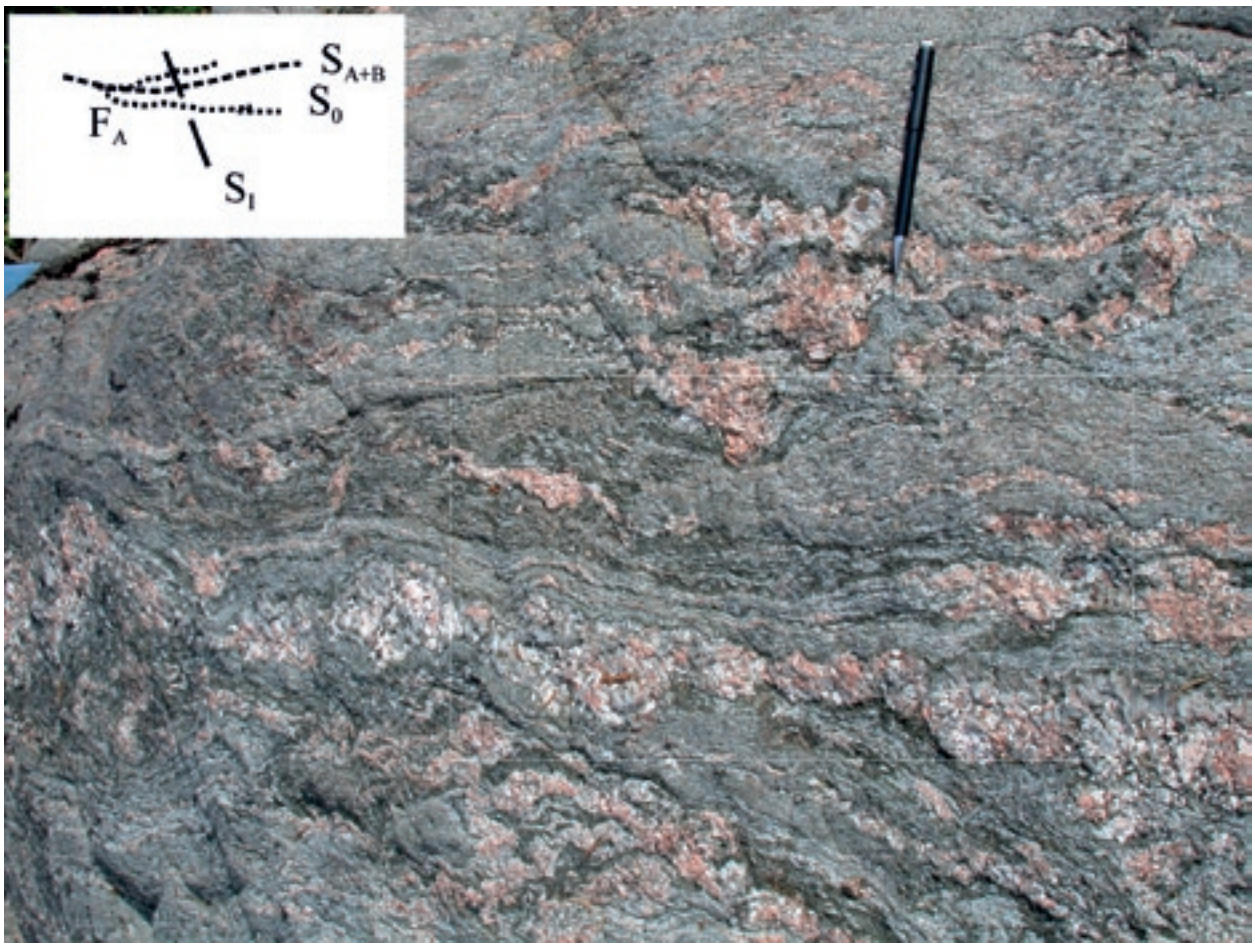

Appendix-Fig. 3-5. F_A folding intensified and migmatized by D_B and refolded by F_I in migmatitic garnet-bearing mica gneiss inside the Onkimaa dome. Pencil is 14 cm in length. Palosenkallio, Pornainen (Finnish grid coordinates KKJ2 2756.81E 6716.42N). Photo by M. Pajunen

that was compressed between the domes to the northwest of Askola. The dome series suggests a complex fold interference pattern formed during D_{G+H+I} (Appendix-Fig. 3-4).

The structural pattern is fragmented by predominantly N-trending brittle faults that partly follow the ductile shear zones; observations further west in the Sipoo area suggest late (post-Svecofennian) low-angle overthrust faults with east-side-up movement.

The relations of the Onkimaa granodiorite in the northern part of the dome have not been studied here, but structurally (e.g. strongly foliated and showing a complex pattern of shear bands) it is quite similar to the tonalites in the Sipoo area, e.g. the Hindsby tonalite (main text). The cutting intermediate microtonalite dykes are also quite similar and we can suppose that the dome windows represent antiforms of the same tectonic slice exposed in the eastern Espoo Granitoid Complex (EGC) in Sipoo (Si in Figure 9). The Askola area is bordered to the southwest and south along steep strong shear zones against the Sipoo area.

Appendix 4. Structural succession in non-migmatitic Orijärvi area

The lower amphibolite facies Orijärvi area (Or in Figure 9) have been extensively studied since the detailed metamorphic studies of Eskola (1914 and 1915) because of its ore potential (e.g. Latvalahti 1979) and scientific value (e.g. Eskola ops. cit., Tuominen 1957, Schreurs & Westra 1986, Ploegsma & Westra 1990, Kilpeläinen & Rastas 1990, Skyttä et al. 2006 and Pajunen et al. 2008). In the Orijärvi area the primary structures of supracrustal rocks are well preserved. The Zn-Cu-Pb ores associated with altered rocks, such as coarse-grained cordierite-anthophyllite rocks (Eskola 1914 and 1915), skarn-iron ores, iron formations (e.g. Eskola 1914, Latvalahti 1979 and Saltikoff et al. 2002) and carbonate rock horizons (Bleeker & Westra 1987 and Reinikainen 2001) in the Orijärvi area indicate a shallow-water deposition. According to Lahtinen et al. (2002), the depositional age of mica gneisses in Orijärvi belongs to the Svecofennian age group of c. 1.9 Ga. Väisänen & Mänttäri (2002) proposed a back-arc basin origin for the volcanogenic rocks. Volcanic rocks are divided into two series according to their structural relationships (the early Series I and the later Series II; see main text) and to their geochemical characteristics and ages (cf. Väisänen & Mänttäri 2002). The 1998 ± 2 Ma Orijärvi granodiorite was interpreted as syngenetic with the early volcanic sequence (Väisänen & Mänttäri 2002). The gabbroic associations described by Hopgood et al. (1976 and 1983) and Hopgood (1984) from the Jussarö-Skåldö area (Ju in Figure 9) are also related to the early volcanism.

The Orijärvi area is characterized by F_G folds with E-trending axial planes and nearly horizontal axes (Figure 16). In the central part of the area the axial planes are openly warped, but folding intensified to tight in the N-trending deformation zone in the east (reactivated by ductile Jyly shearing); we have interpreted this N-trending zone as a D_I structure by comparing it to the structures in the Vuosaari-Korso zone in the Espoo Granitoid Complex, EGC (Figure 11). The minimum age of D_I folding can be estimated with pegmatitic granite at c. 1.804 ± 2 Ga (I_g granitoid in Pajunen et al. 2008). The D_H folds with NE-trending axial planes that characterize the West Uusimaa granulite Complex (WUC) and the Espoo Granitoid Complex (EGC) as large-scale folds can also be seen on outcrops as gentle to open, sometimes north-westwards overturned folds; they form complex dome-and-basin structures with F_G and F_I. In the high-grade areas some granitic melt fraction intruded into the S_H axial planes (Figures 29 and 30a), or a new mineral foliation formed in the D_E granitoids. The D_H folding is the main structure seen in the *Vetio outcrop* (site shown in Figure 16) at Kisko, in the Orijärvi area (Appendix-Fig. 4-1). The outcrop illustrates well the principal features of metamorphic mineral growth and deformation in the lower-grade mica schists. Granitoids related to D_E are absent from this lower-grade outcrop.

The mica schist shows well-preserved primary layering S_0, which gives a good reference point for analyzing the structural succession on the Vetio outcrop. Large, long andalusite$_1$ porphyroblasts have crystallized sub-parallel to primary layering. Andalusite contains an early foliation parallel to the bedding S_0. The foliation is preserved as fine-grained internal S_i biotite foliation; locally, the same foliation is also preserved in the pressure shadows of andalusite. The andalusite growth resembles that of the Tampere Schist Belt (TSB) (cf. Kilpeläinen 1998) and the Rantasalmi-Sulkava area (RSB) (Korsman 1977 and Korsman & Kilpeläinen 1986). The early cordierite$_1$, possibly formed by breakdown of chlorite, overgrew S_0 and the nearly bedding-parallel foliation; it was penetratively retrogressed to pinite. The foliation, sub-parallel to S_0, indicates nearly horizontal generation of this early foliation. An intermediate dyke including recrystallized (grains are entirely mortar-textured or on grain rims) plagioclase laths has also intruded into the direction of S_0. The dyke has weak dyke-parallel foliation and was folded by F_H; the most intense penetrative biotite foliation is S_H.

D_H deforms the early foliation, andalusite$_1$ and cordierite$_1$ porphyroblasts, and the penetrative S_H biotite foliation curves around the porphyroblasts. Idioblastic andalusite$_2$ grew onto the edges of andalusite$_1$ and overgrows the S_H foliation. The increased temperature is shown by fibrolitic sillimanite that was crystallized in S_H foliation plane, especially close to the andalusite grains in the intensely D_H-deformed parts of the rock. Cordierite$_2$ grew as syntectonic poikiloblasts, and its latest phase is idioblastic and overgrew S_H. On the outcrop scale the large cordierite porphyroblasts were aligned in the S_H planes. The early generation of quartz veins was formed into dilatational fractures during the early D_H into the S_H direction. The veins were deformed to become pinch-and-swell-structured and folded during the continuing D_H. Late idioblastic garnet poikiloblasts overgrow S_H. Late muscovite porphyroblasts overgrow all the described structures and indicate a late potassium-rich fluid infiltration. This is also supported by some late alteration on the edges of cordierite$_2$.

The occurrence of retrograde phases (e.g. in cordierite$_1$) predating D_H and the existence of low-temperature quartz$_1$ veins suggests a cooling stage between the early andalusite-cordierite deformation and later

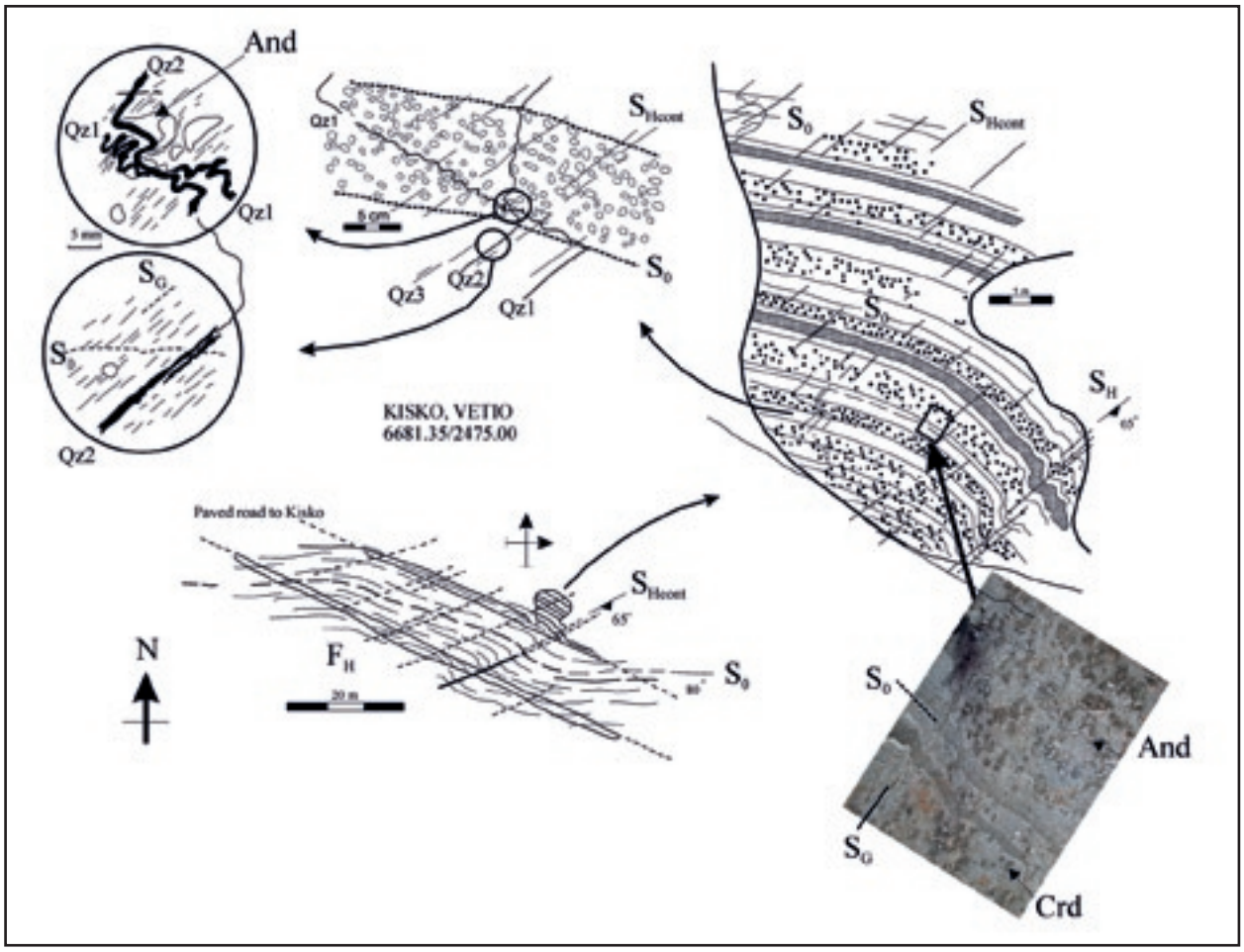

Appendix-Fig. 4-1. Detailed structures of andalusite-cordierite-bearing mica schist (photo; width of the area of the figure is c. 0.5 m) in the Orijärvi area. Vetio, Kisko (Finnish grid coordinates KKJ2 2475.00E 6681.35N). Primary drawing by T. Koistinen reinterpreted here. Photo by M. Pajunen.

D_H with peak metamorphism in the sillimanite stability field. Thus, the bedding-parallel dykes may be correlative with the pre-D_B volcanogenic dykes that are boudinaged and S_H foliated, e.g. in Rövaren (Figure 40a). The foliation in the early andalusite$_1$ and cordierite$_1$ resembles that observed in the early K-feldspar porphyroblasts of the mica gneisses in the upper tectonic slices of the Hyvinkää Gabbroic-volcanic Belt (HGB), but we have no observations on relics of early andalusite from them, even though primary layering is often well preserved. No pseudomorphs of the early andalusite have been found in the higher-grade gneisses, either.

Appendix 5. Jokela supracrustal association

The supracrustal Jokela association (Figure 9 and Appendix-Fig. 3-4) is situated at the eastern end of the Hyvinkää shear/fault zone, in the intersection with the Hyvinkää-Lahti shear/fault zone. It stands out from its surroundings as a highly magnetized synformal association between branches of the Hyvinkää shear/fault zone. Scattered quartzite exposures also occur outside of the coherent Jokela formation.

The association is composed of polydeformed supracrustal rocks showing primary depositional structures, which, however, are often destroyed by penetrative shearing or transposition. The reddish to grey quartzite, e.g. in the Jokela open pit (Appendix-Fig. 5-1a), shows primary layering and beds are locally laminated and cross-bedded. The rock is fractured and foliated with flattened quartz surrounded by weakly recrystallized fine-grained grains. Minor phases, tourmaline, magnetite and sillimanite formed by breakdown reaction of muscovite, refer to some clay content in the quartzite. The quartzite is in close association with less mature feldspathic arenites and intraformational conglomerates. The sedimentary structure of the conglomerate, with clasts of up to 2–3 cm scattered in a sandy matrix, is still identifiable after deformation (Appendix-Fig. 5-1b). The only observed contact of quartzite against non-mature sediments is primarily depositional and only weakly tectonic (Appendix-Fig. 5-1c). The succession also contains calcareous interlayers, and in places the rock is penetratively silicified and tourmalinized due to later fluidization events. Intermediate clinoamphibole-bearing volcanogenic gneisses, presumably tuffitic in origin, and bedding-parallel, weakly plagioclase porphyritic mafic dykes are in close association with the sediments (Appendix-Fig. 5-2a). Locally, they occur as interlayers in impure sediments (Appendix-Fig. 5-4c); such interlayers are not met in quartzite. Pegmatitic granites intrude the supracrustal association. It locally contains fragments of complexly-folded quartzite (Appendix-Fig. 5-3d) that is strongly assimilated into granite (Appendix-Fig. 5-3c). However, the granite dyke sharply cuts the volcanogenic rock, which does not show such complex folding as in quartzite, indicating that the volcanogenic series post-dates the quartzite accumulation. The volcanogenic rocks are mostly associated with the less mature sediments, suggesting that the impure sedimentation was also later than the deposition of the quartzite. The pelitic layers with sillimanite (Appendix-Fig. 5-3a) show feldspar porphyroblasts and some melting, and display a simpler folding pattern than quartzite (Appendix-Fig. 5-3d). The lithology and primary structures suggest that the deposition of quartzite and its associates occurred in a sub-aquatic, high-energy environment accompanied by volcanic activity. Transition from clastic sediments, quartzites, conglomerates and arenites to calcareous sedimentary rocks (Appendix-Fig. 5-3b) and pelitic gneisses refers to the change in deposition to a tranquil deeper-water environment.

In Tiirismaa the detrital zircon population of 1.87–1.86 Ga indicates the maximum age of deposition of the quartzite (Lahtinen et al. 2002). According to the close resemblance to Tiirismaa in lithology, metamorphism and tectonic setting, we conclude that the Jokela association also represents a young deposition and volcanism. It is a good fixing point for structural analysis of the post-sedimentation (post–1.87–1.86 Ga) evolution.

The outcrop in Mäntsälä, Jokela, at the Kettukallio site in Appendix-Fig. 5-2 exemplifies the tectono-metamorphic history of the association. The strongest penetrative structure on outcrops is a spaced biotite foliation; we relate it to D_E based on the combination of the information from surrounding areas and on the age data. Early quartz veins precede the main foliation S_E. Under the microscope, an openly-folded internal biotite foliation, S_{i1}, exists in the early K-feldspar$_1$ porphyroblasts. A penetrative schistosity S_{i2} in the axial plane of the open folds also appears as a weak biotite growth in the pressure shadows of K-feldpar$_1$ porphyroblasts (Appendix-Fig. 5-4a). This kind of pre-D_E foliation also exists in the gneisses of so-called Upper Tectonic Unit, UTU (cf. Appendix 6). We are not able to relate the early foliations, S_{i1} and S_{i2}, to the structural successions described from the other units. The earliest fold structure deforming the primary layering and lamination, S_0, are isoclinal, round-hinged intrafolial folds (Appendix-Fig. 5-2b). The polyphase folding in the quartzite fragment (Appendix-Fig. 5-3d) does not show the intense S_E foliation, and we suppose the folding to be related to the early, low-T evolution of the sedimentary-volcanic pile.

The spaced biotite foliation S_E deforms the weak penetrative S_{i2} biotite foliation. S_E curves around the K-feldspar$_1$ porphyroblasts. Early granitic melts with K-feldspar$_2$, on the one hand, cut the S_E foliation; on the other hand, S_E curves around the melt patches (Appendix-Fig. 5-4a). On the outcrop these melt patches are S_E-parallel, boudinaged granite veins, considered to be syntectonic with D_E. The D_E is characterized by intense boudinage of competent layers (Appendix-Figs. 5–2a and 5–4c). C. 50% shortening during D_E can roughly be estimated from bent primary layers surrounding a rotated, pre-early D_E, extensional quartz vein (Appendix-Fig. 5-4b). Isoclinal intrafolial folds parallel to bedding in quartzite that show a very weak axial

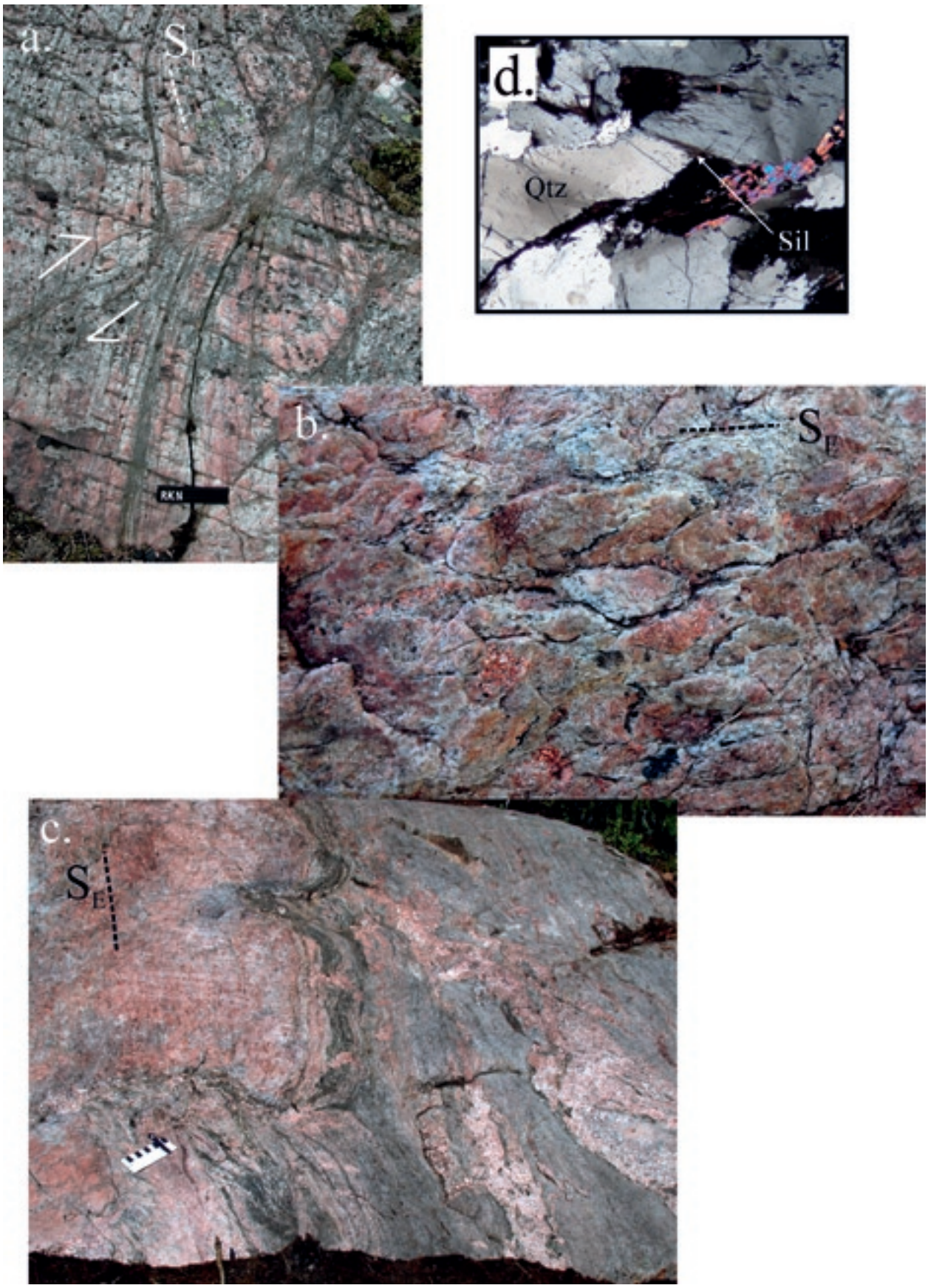

Appendix-Fig. 5-1. (a.) D_E deformed and sheared quartzite of the Jokela supracrustal association; microphoto in (d.). Scale bar is 12 cm in length in (a.). Junninkallio, Hyvinkää (Finnish grid coordinates KKJ2 2554.34E 6721.44N). (b.) Intraformational conglomerate of the Jokela supracrustal association. Width of the area of the figure is c. 0.5 m. Junninkallio NE, Hyvinkää (Finnish grid coordinates KKJ2 2554.70E 6721.70N). (c.) Primary depositional contact between Jokela quartzite and mica gneiss. Scale bar is 10 cm in length. (d.) Microphoto of Jokela quartzite; Qtz = quartz and Sil = sillimanite. Width of the area of the figure is c. 3 mm. Junninkallio, Hyvinkää (Finnish grid coordinates KKJ2 2554.76E 6721.73N). Photo (a.) by R. Niemelä and photos (b.)-(d.) by M. Pajunen.

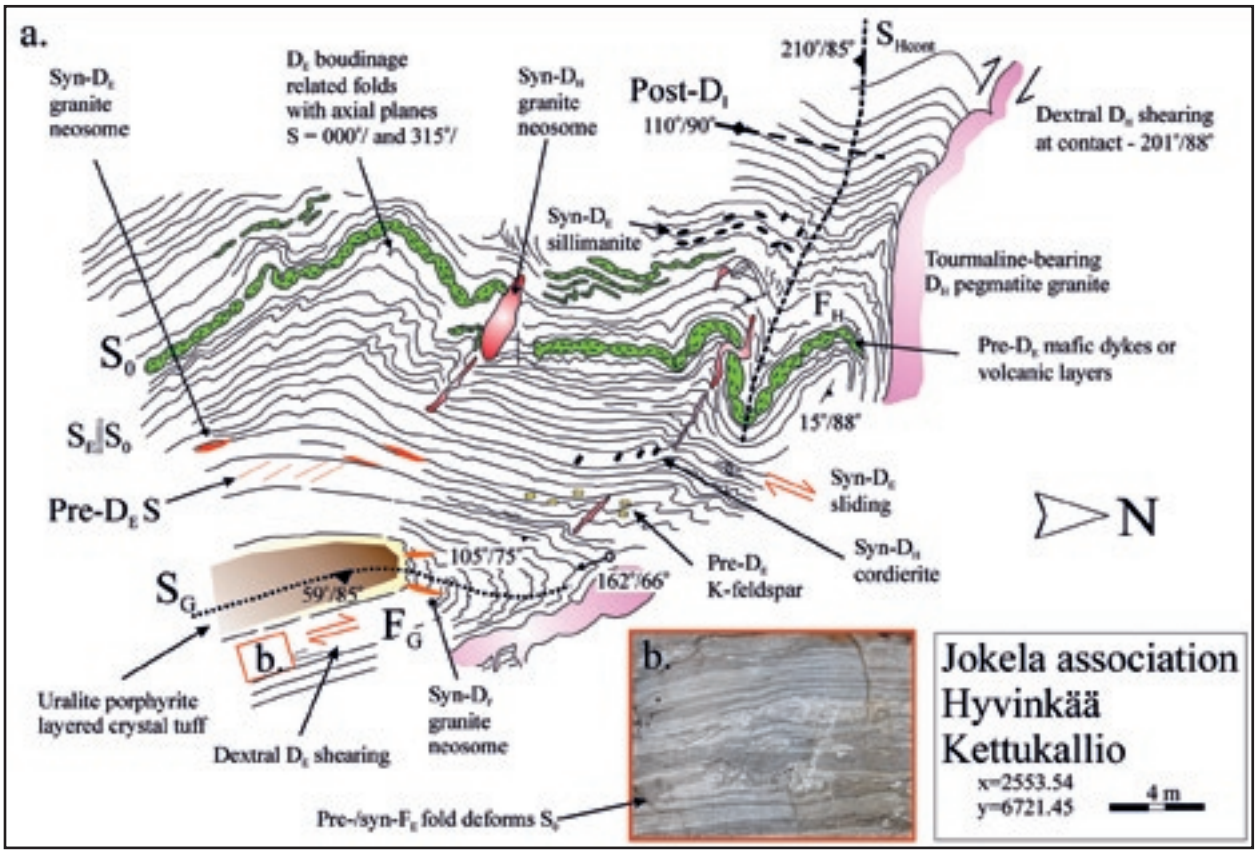

Appendix-Fig. 5-2. (a.) Detailed structures of the Jokela supracrustal association on the Kettukallio key outcrop in Hyvinkää (Finnish grid coordinates KKJ2 2553.54E 6721.45N). (b.) Pre-/syn-D_E folds deforming S_0 layering at Kettukallio. Width of the area of the figure is c. 0.5 m. Photo by M. Pajunen.

plane foliation are related to D_E (Appendix-Fig. 5-2a and b). In the pelitic sillimanite gneiss, sillimanite predominantly grew in the S_E plane (Appendix-Fig. 5-3a). An increase in temperature caused instability of biotite-sillimanite paragenesis, forming cordierite and melt. It is plausible that the early K-feldspar$_1$ was formed due to the breakdown of early muscovite.

The S_0 and S_E are folded by tight F_G with c. N-trending axial planes (Appendix-Figs. 5-2 and 5-4d). The S_G is a macro-crenulation with some granitic segregation in the foliation planes. The D_G synform structure in Appendix-Fig. 5-2a dips moderately towards the south, but no reliable observation of the top direction of bedding has been made. Dextral, tight F_H folds with NNW-trending axial planes refold the earlier structures (Appendix-Fig. 5-4b); S_H foliation is weak. In the pelitic layers, cordierite and some granitic melt was formed in the S_H plane; this indicates peak metamorphism during F_H folding. The intrusion of the pegmatitic granite dykes occurred during or after D_H. In places the previous structures are almost totally assimilated into granite (Appendix-Fig. 5-3c). The whole outcrop was openly refolded by c. E-W contraction during D_I, which also caused dextral sliding along the granite contact. Localized dextral folds deforming the axial plane granite of D_H or S_{0+E} may belong to D_I. The pegmatitic granite dykes show the same position in the structural sequence as the 1.8 Ga pegmatitic granite dyke described by Pajunen et al. (2008). When correlating the directions of structures to the surrounding areas, the D_{G-H} structures were rotated c. 90º anticlockwise. This rotation is considered to be caused by the D_I deformation; the Jokela association is located in close association with the strong F_I axial zone (Figure 11).

The tectono-metamorphic evolution in Jokela shows a one-stage prograde metamorphic event in the sillimanite and cordierite stability fields under low-pressure amphibolite facies conditions. It corresponds to that described from the Upper Tectonic Unit (Appendix 6), even though metamorphic mineral parageneses there indicate a higher grade. In the southern Svecofennian domain, corresponding supracrustal associations (yellow triangles in Figures 9) have undergone a similar tectonic-metamorphic evolution; they are closely associated with major crustal high-strain zones, especially their intersections, such as between the

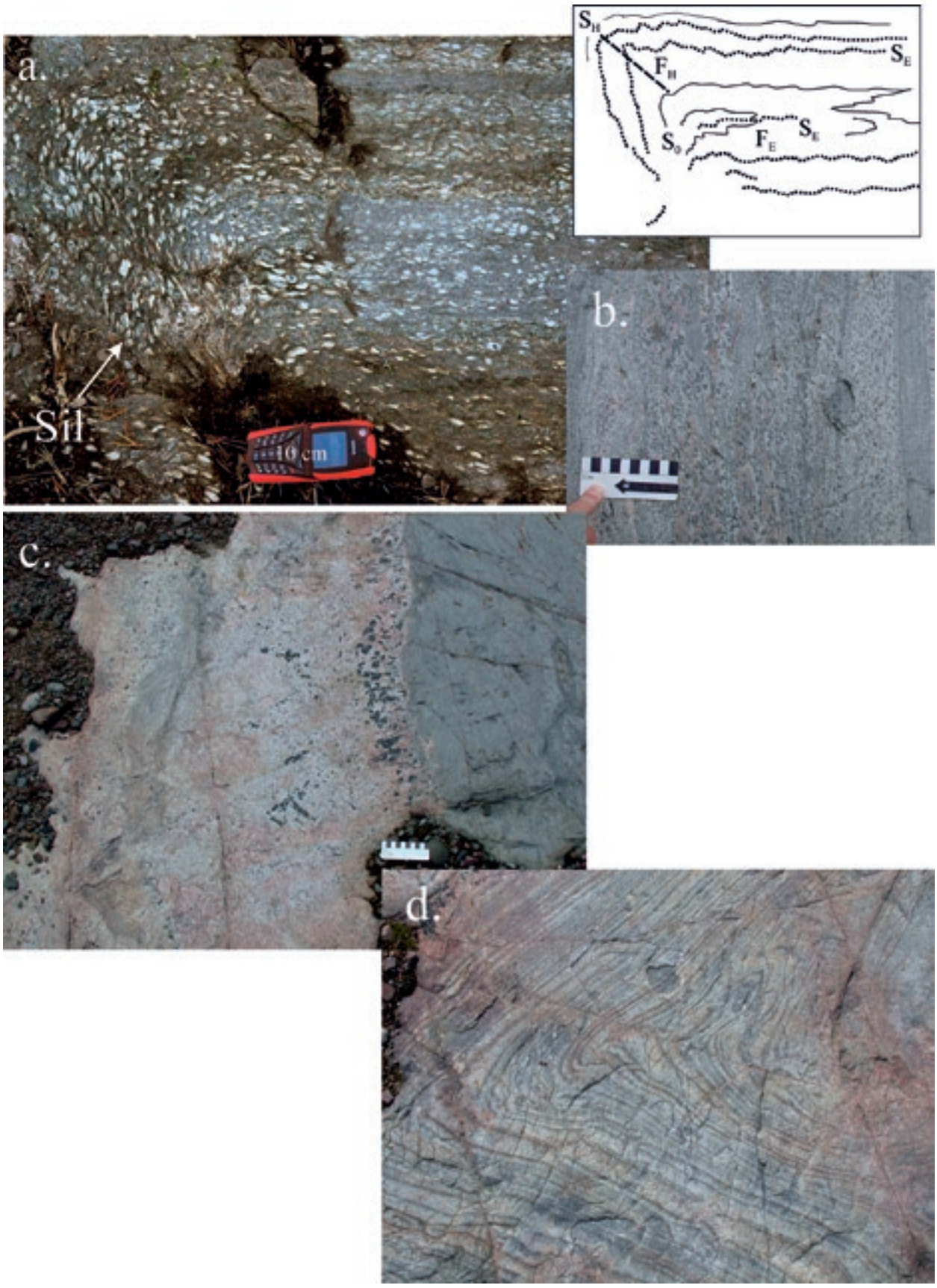

Appendix-Fig. 5-3. (a.) Sillimanite-bearing mica schist in the Jokela supracrustal association. Junninkallio NE, Hyvinkää (Finnish grid coordinates KKJ2 2554.80E 6721.62N). (b.) Calcareous sediment within the Jokela supracrustal association. Scale bar is 10 cm in length. (c.) Jokela quartzite as a strongly assimilated fragment in the D_G pegmatitic granite dyke, which sharply cuts the volcanic rock of the same association. The relations with granite provide evidence that the quartzite predates the volcanic rock. Scale bar is 10 cm in length. (d.) A better-preserved part of the same quartzite as in the fragment shown in (c.). Polyphase folding of the primary layering, S_0, predates the pegmatitic granite related to the D_H. Width of the area of the figure is c. 1 m. Figures (b-d.) = Latostenmaanmäki, Hyvinkää (Finnish grid coordinates KKJ2 2554.83E 6722.63). Photos by M. Pajunen.

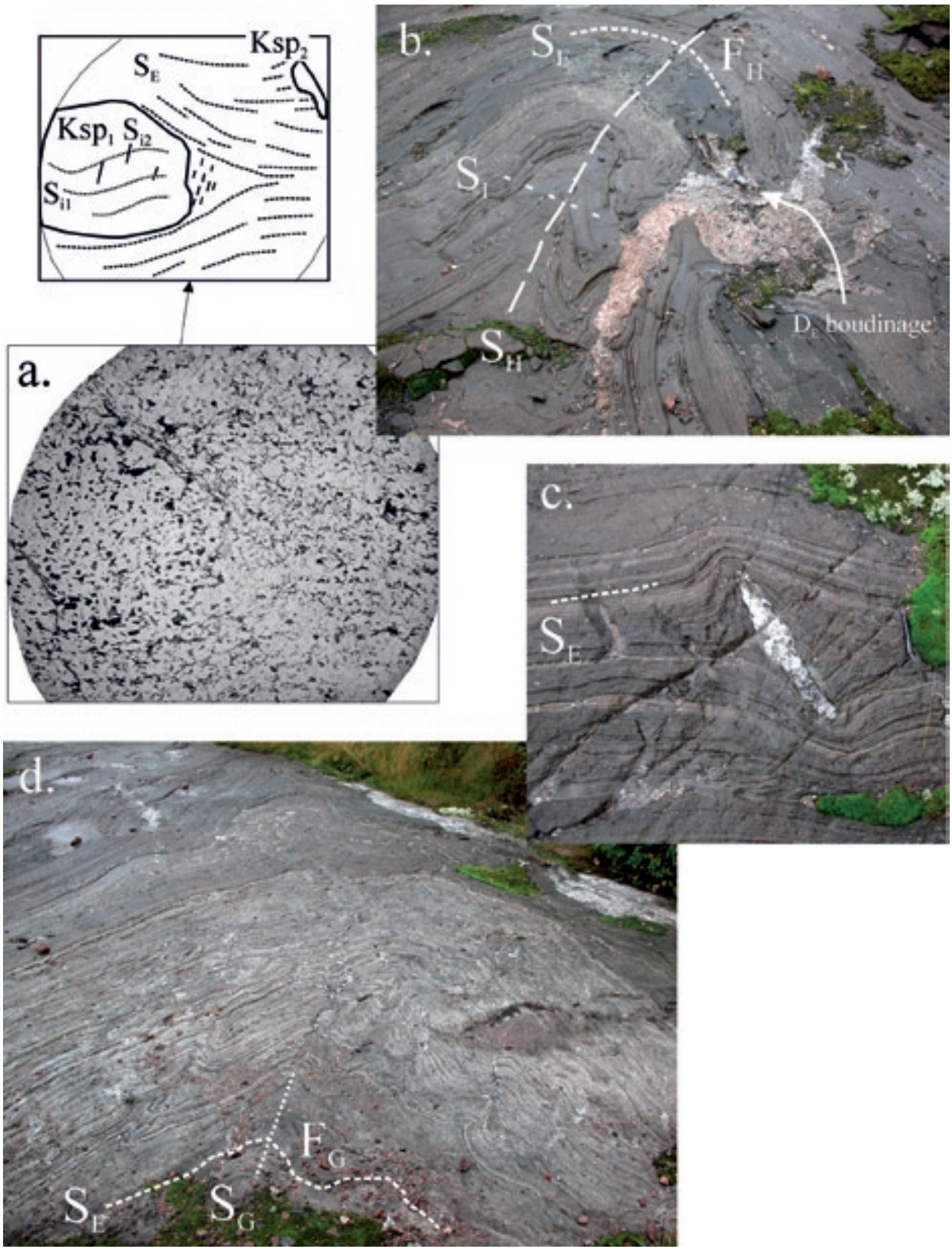

Appendix-Fig. 5-4. Detailed structures on the Kettukallio key outcrop. Kettukallio, Hyvinkää (Finnish grid coordinates KKJ2 2553.54E 6721.45N). (a.) A microphoto showing the early internal foliation structures, S_{i1} and S_{i2}, in potassium feldspar, Ksp_1, and their relations with S_E and syn-D_E neosome, Ksp_2. Width of the area of the figure is c.10mm. (b.) An S_E boudinage structure refolded by F_H. Width of the area of the figure is c. 1.5 m. (c.) A pre-D_E quartz vein surrounded by the bent S_E indicating c. 50% vertical shortening; some shear had occurred, as indicated by rotation of the quartz vein. Width of the area of the figure is c. 0.5 m. (d.) An F_G fold in felsic gneiss (impure sediment). Width of the area of the figure is c. 2 m. Photos by M. Pajunen.

Hyvinkää, Southern Finland or Hämeenlinna high-strain/shear zones and the major D_I axial zones. Simonen (1987; also in Korsman et al. 1997) related the origin of supracrustal sedimentary-volcanic rocks of the Taalikkala inclusion in Vyborg rapakivi at Lappeenranta (Ta in Figure 8) to the rapakivi stage. We re-examined the samples collected during the regional mapping of GTK (Simonen 1987), because Simonen (op. cit.) described depositional discordance between the arkosic sediments overlain by volcanic sequences and Svecofennian granitoid of unknown age. According to the tectonic-metamorphic correlation the rocks correspond to the one-stage association in Jokela. Unfortunately, we were not able to re-investigate the depositional relationships in the field but, if the discordance observation is correct, further studies on the Taalikkala "roof pendant" could be helpful in understanding the stratigraphic position and depositional environment of these rocks.

Nironen and Lahtinen (2006) suggested an extensional rift-related shallow basin for the formation of the corresponding Pyhäntaka formation. Corresponding quartzites also exists in Sweden. The evolution from the D_D to $D_{E\text{-}H}$ and finally to D_I shows a very continued character. We suggest a rapid evolution of the supracrustal association and a tectonically-active, high-energy depositional environment as indicated by the intraformational conglomerates within the quartzite beds. We suggest that the depositional evolution of the whole Jokela sequence was related to the oblique dilatational events during the SW-NE transpression in the $D_{(D\text{-})E}$ and SE-NW transpression in the D_H. The process was accompanied by crustal thinning and high heath flow, which culminated c. 1.85–1.84 Ga ago. Contractional $D_E$cont and $D_H$cont caused rapid folding during the progressive deformation. Extension caused upper crustal subsidence with rapid evolution of basins for sedimentation of high-energy sedimentary sequences. Quartzites were originally rather thin formations, which were thickened by the complex deformation multiplying the thickness of the quartzite sequence. These sediments were already folded when the later-stage volcanic sequences were generated (Appendix-Figs. 5-3c and d). The rapid subsidence was stepwise, which is evidenced by a rapid change from quartzite to impure sediment sedimentation (Appendix-Fig. 5-1c).

Pull-apart basins form restricted structures in transcurrent zones appropriate for the rapid accumulation of thick sediment deposits and contemporaneous volcanism (e.g. Kearey & Vine 1996 and Saalmann et al. 2005). Such basins form during continuous tectonic evolution. In the study area they were related to thinning of the crust and increased the heat flow that may be related to the magmatic rocks of D_E in the deeper crustal levels. Suitable structures bordering such pull-apart basins include major crustal structures, like the E-W-trending Hämeenlinna, Hyvinkää and the southern Finland shear zones showing complex deformation histories. This large, originally ESE-trending pull-apart basin was formed between the major crustal deformation zones of the Riga Bay-Karelia Zone (RKZ) and Baltic Sea-Bothnian Bay Zone (BBZ), or the Transscandinavian Igneous Belt (TIB) (Figure 8).

Appendix 6. Structural characteristics of high-grade gneisses of the Upper Tectonic Unit (UTU) of the southern Svecofennian domain

The rocks of the Hyvinkää Gabbroic-volcanic Belt (HGB) are squeezed between the large-scale D_{G+H+I} dome-and-basin structures in the Askola area. The volcanic and closely related sedimentary rocks of the HGB show structures that were already formed during the early stages of the Svecofennian orogeny; they show at least the D_B structures. However, there are also high-grade migmatitic metapelitic gneisses that do not show signatures of these early deformations in the study area, for example the Jokela supracrustal association. Structural evolutions of these rocks are exemplified from the Vuotavankalliot site in Mäntsälä (HGB) and the Matinojankallio site in Sipoo (EGC) (Appendix-Fig. 3-4).

Garnet-cordierite gneiss (Appendix-Fig. 6-1a) in the Vuotavankalliot site in Mäntsälä (Appendix-Fig. 3-4), to the north of the Askola dome area, is located within the gabbroic and volcanic rocks in the vicinity of the Hyvinkää-Lahti shear zone. The migmatitic gneiss is characterized by a spaced biotite foliation that overprints an earlier weak penetrative biotite foliation. The gneiss shows open to tight folds with NNE-trending axial planes, which deform both foliations and also the garnet- and cordierite-bearing melt patches in the gneiss. According to correlation with neighbouring areas, these folds are related to the F_I folds. Early K-feldspar$_1$ that was formed by progressive metamorphism (by breakdown of muscovite?) includes two biotite generations, inclined towards each other, as an internal S_i structure. The later foliation represents the main spaced foliation in the gneiss. During progressive metamorphism, biotite and sillimanite became unstable; cordierite$_1$ with sillimanite and spinel inclusions and K-feldspar$_2$ (Appendix-Fig. 6-1b) were formed. The cordierite$_1$ crystallized in the direction of the spaced foliation, which, however, curves around the porphyroblasts. Large melt patches including fresh cordierite$_2$, without sillimanite inclusions, garnet and a new K-feldspar$_2$ are also surrounded by the spaced cleavage, but their development continued after the active phase of that deformation because melt patches partly overgrow it. The K-felspar$_1$ is slightly altered to sericite (K-felspar$_2$ is not altered). The macro-crenulation in Appendix-Fig. 6-1a refolds all the structures described (Appendix-Fig. 6-1c) and is related to D_I according to the orientation of the axial plane in a NNE direction. It shows a high-T and ductile character. The latest deformation is a semi-brittle shearing, which occurred in the andalusite stability field as indicated by small andalusite grains in these seams.

In general, the tectonic evolution of these gneisses is simpler than that described from migmatitic mica gneisses of the Southern Volcanic-sedimentary Belt (SVB) or the Espoo Granitoid Complex (EGC). The rock experienced only one important migmatization phase related to its continuous progressive mineral growth history, whereas several observations indicate at least two migmatization events occurring widely in the southern Svecofennian (cf. Pajunen et al. 2008 and Figures 22 and 36). We have not identified D_C and D_D fold patterns from the Vuotavankalliot gneiss. Often the spaced S_E foliation parallels S_0 referring to horizontal event. Due to correlation with neighbouring areas like the Espoo Granitoid Complex (EGC) and West Uusimaa Complex (WUC), we relate the spaced foliation, the strongest foliation in the rock, to the extensional deformation D_E. This interpretation is supported by progressive high-T/low-p metamorphism accompanied by granitic melts. There is only one weak deformation predating the D_E; it has not been established whether it represents the early D_E or very weak deformation during the earliest stages (e.g. D_B?) of crustal evolution, because the deposition age of the rock is not known. The original position of D_E structures was generally nearly horizontal; the steep position of D_E before F_I folding indicates folding events (D_{G-H}) between the D_E and D_I.

In Sipoo, at the Matinojankallio site, migmatitic garnet-cordierite gneisses (Appendix-Figs. 6–2b and c) are in close association with a syn-/late D_B tonalite (Appendix-Fig. 6-2a). Unfortunately, their contact was not exposed during mapping. The outcrop is located in the folded E-trending synformal structure. According to tectonic interpretation, the synform is overlying the high-grade tonalitic rocks exposed in an antiformal setting in the west (Appendix-Fig. 6-2d), in northern Sipoo (Si in Figure 9). Intermediate microtonalite dykes cut the tonalite and migmatitic gneiss and the rocks show a major tight folding phase with E-trending axial planes. The dyke contacts of the tonalite indicate intrusion into cooled rock with indistinct altered chilled margins (Appendix-Fig. 6-2a); the structures and relationships between the dyke and tonalite are quite similar to those described before, e.g. at Hindsby (Figure 24). A wide altered zone surrounds the dyke in the mica gneiss (Appendix-Fig. 6-2b) and its composition changes close to the dyke borders to garnet-rich. In the mica gneiss the wall rock-dyke reactions were strong and are interpreted to have resulted in intrusion into a lower-grade and more reactive rock.

The tectonic succession in mica gneiss (Appendix-Fig. 6-2c) resembles that in Vuotavankalliot (above). The mica gneiss has rather well preserved primary bedding and a strong prograde mineral foliation parallel

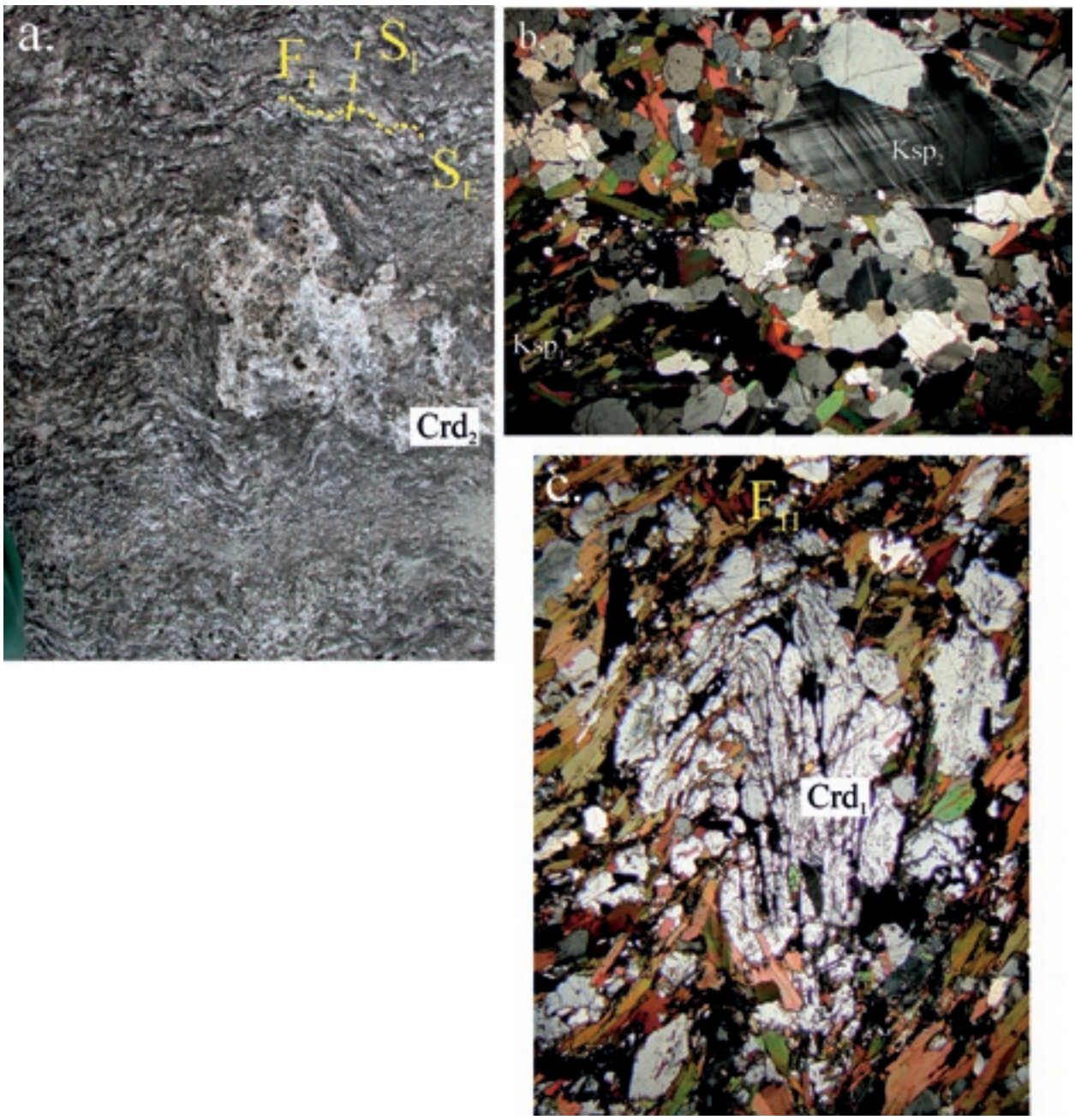

Appendix-Fig. 6-1. (a.) F_I folds in S_E foliated garnet-cordierite gneiss from the Upper Tectonic Unit (UTU). Width of the area of the figure is c. 0.5 m. (b.) and (c.) show the microstructures of the gneiss; see text for details. Crd = cordierite and Ksp = potassium feldspar. Width of the area of the figure is (b.) is c. 4 mm and (c.) is c. 3 mm. Vuotavankalliot, Mäntsälä (Finnish grid coordinates KKJ2 2569.22E 6736.67N)). Photos by M. Pajunen.

to it. We relate the main foliation to the D_E deformation. The intermediate dyke intruded nearly parallel to the bedding planes, but the alteration zone surrounding the dyke overprints S_0. The dyke has a S_E penetrative mineral foliation. Thus, we interpret the dyke to be intruded during early D_E. The main foliation S_E intensified during a continuing temperature increase that also caused progressive migmatization. Only one prograde migmatization pulse finally producing garnet-bearing melt can be detected. At least three post-D_E fold generations occurred. We relate the folds with E-trending axial planes to D_G, which was refolded by F_H forming the D_{G+H} synform; the synform was openly bent by later F_I folding with NNW-trending axial planes. Migmatization began to develop in the S_E planes and achieved its peak during D_H; the coarse melt fractions were intruded into the S_H axial planes. The contact between the tonalite and gneiss must be in this case tectonic and formed pre-/early D_E.

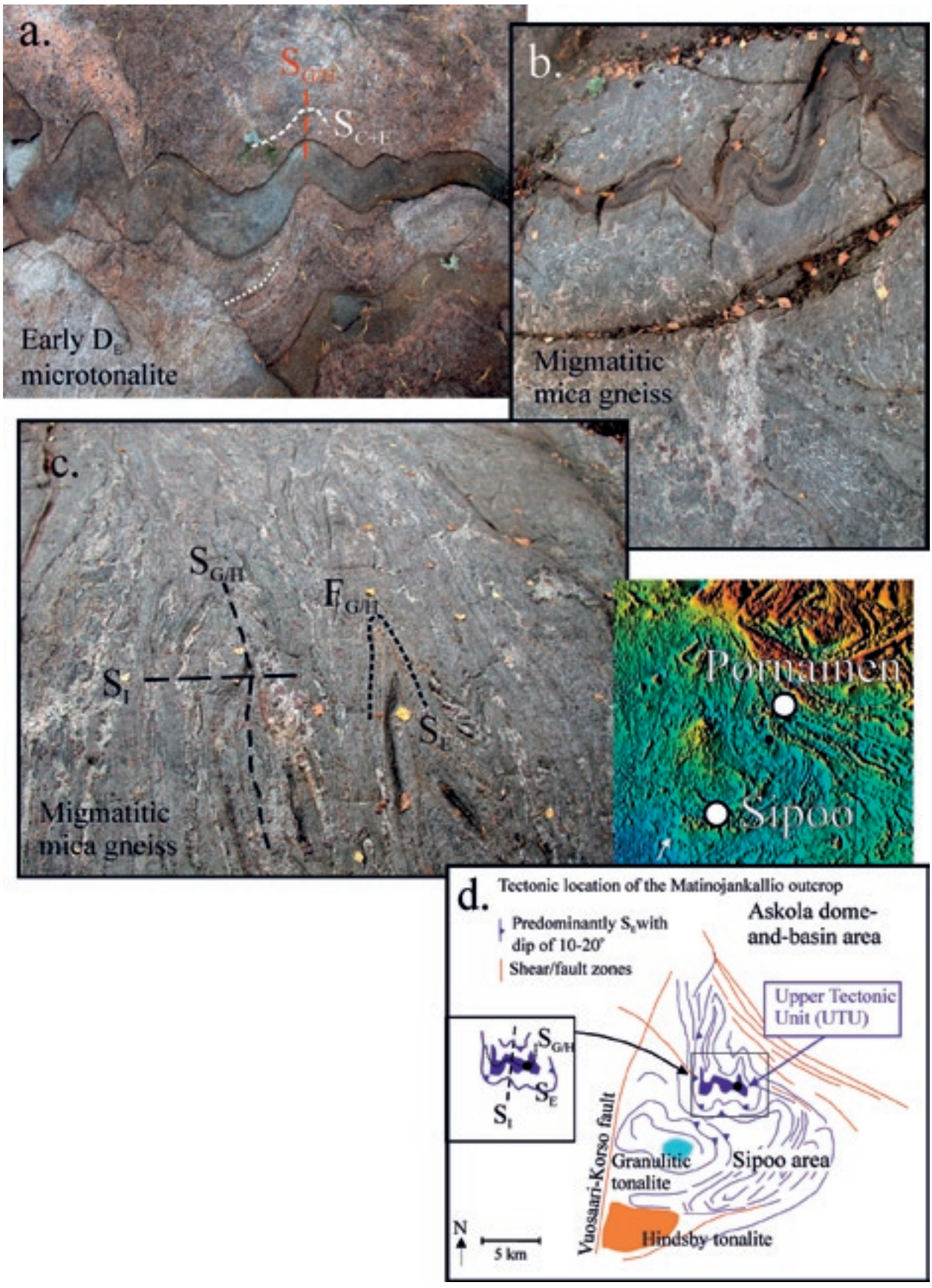

Appendix-Fig. 6-2. (a.) An intermediate D_E microtonalite dyke cutting the syn-/late D_B tonalite. Width of the area of the figure is c. 1.5 m. (b.) The same dyke is cutting the migmatitic garnet-bearing mica gneiss (Upper Tectonic Unit, UTU), showing a wide alteration rim and garnet-bearing contact zone; width of the area of the figure is c. 1.5 m. The folding pattern in the outcrop (c.) is interpreted from the tectonic data and aeromagnetic map (inset) as a part of regional tectonic pattern in (d.). Width of the area of the figure is c. 2 m. Matinojankallio, Sipoo (Finnish grid coordinates KKJ2 2572.72E 6703.64N). Photos by M. Pajunen.

In summary, these high-grade gneisses show only one strong metamorphic event, without signs of pre-existing coarse-grained andalusite-metamorphism that characterizes the Vetio outcrop in the Orijärvi area (Appendix 4). The early tectonic history of these gneisses occurred in upper crustal level low-grade conditions and the peak of the progressive high-grade metamorphism was achieved during the late Svecofennian period. Tectonically, these mica gneisses are located in the large-scale F_{G+H+I} synforms. However, the high-grade mica gneisses in the D_{G+H+I} antiformal settings show a two-stage metamorphic character with two neosome phases (e.g. Pajunen et al. 2008). We include these gneisses into so-called Uppet Tectonic Unit (UTU). The UTU tectonic succession is very similar to that observed in the Jokela association (Appendix 5), which has a young deposition age. The age of the deposition of the mica gneisses is not known. The similarity to the Jokela association may support their coherent origins. This interpretation suggests that the late deep-water sediments were more widespread than was previously known, and these mica gneisses thus represent the later stage of the pull-apart basin sedimentation described from Jokela (Appendix 5).

Appendix 7. Pomarkku block – key to the generation of stacked structures in central and eastern Finland

The tectonic setting of the Pomarkku block in the Pori area (Po in Figure 9; cf. Pietikäinen 1994 and Pajunen et al. 2001a), bordered by high-strain zones, is of key importance in analyzing the development of the NW-stacking and block structures of Central Finland; the Central Finland Granitoid Complex (CFGC) and the Savo Schist Belt (SSB). Similar characteristics can also be found in the geometries of the N-directional blocks in the Archaean domain (Figure 8).

The internal structure of the Pomarkku block is characterized by F_3 folding with E-trending axial planes (naming after Pajunen et al. 2001a) that deforms the subhorizontal D_2 structures. In the tonalite-dominant parts the F_3 folds are generally open with a weak upright S_3 foliation/crenulation. S_2 and S_3 intersection forms approximately horizontal, E-W-trending intersection lineation $L_{2/3}$. In the central part of the Pomarkku block, southwards-overturned F_3 folds indicate overthrusting towards the south along c. E-W trending shear zones (Pajunen et al. 2001a). At the southwestern edge of the Pomarkku block the D_3 structures are bent and crosscut by the steep 1–2 km wide Kynsikangas shear zone (Appendix-Fig. 7-1a) that turns from a NW to a N trend near the Bothnian coast. Rotation of porphyroblasts, drag folds and a strong horizontal stretching lineation (Appendix-Fig. 7-1b) in the amphibolite facies protomylonitic to mylonitic rocks indicate sinistral strike-slip movement (Pietikäinen 1994 and Pajunen et al. 2001a); Pajunen et al. (op. cit.) named the shearing phase as $D_{3\text{-late}}$. The Kynsikangas structure shows less prominent recrystallization and neomineralization than the earlier D_3 shear structures trending WNW in the Pori area, southwest of Kynsikangas. The zone shows polyphase deformation; it was still reactivated during the 1.5–1.6 Ga rapakivi granite event and the formation of the Satakunta sandstone basin. In the E-W-trending northern edge of the Pomarkku block the observations on drag folds and lineations dipping NE (cf. Pihlaja & Kujala 2005) indicate ductile sinistral oblique reverse top-to-SW movement. At the eastern margin of the Pomarkku block the E-W-trending D_3 structures are bent into the direction of the NW-trending Kankaanpää shear zone. This eastwards-bulging eastern border of the Pomarkku block (Appendix-Fig. 7-1c) shows drag folds and a moderate lineation plunging c. NE (Pajunen et al. 2001a), as well as oblique dextral movement in the zone.

The age of block forming deformation can be fixed by the quartz monzonites to north of the Pori area. The granitoid set into an arched structure, imitating the form of the northern edge of the Pomarkku block, (Figures 9 and Appendix-Fig. 7-1c) was dated at 1872 ± 2 Ma (Mäkitie & Lahti 2001); it is penetrating the earlier structure, but showing some signatures of deformation in the zone. However, the practically non-deformed Härkmeri quartz-monzonite dated at 1868 ± 3 Ma (Lehtonen et al. 2005) is cutting the Kynsikangas structure and causes a metamorphic contact aureole upon regional metamorphic parageneses, and fixes the end of the major deformation in the Tonalite Migmatite Belt (TMB). This intrusive, marking the end of the deformation in the north, gives approximately the same age as is obtained from the garnet-bearing tonalites that originated in the Southern Finland Granitoid Zone in the south, in the Espoo Granitoid Complex (EGC) (see the main text). Using structural and age correlation with the detailed study area we relate the strongest ductile phase shearing in the Kynsikangas zone to D_D deformation, D_4 in the north in the following ($D_{3\text{-late}}$ of Pajunen et al. 2001a), which appears in the south as ductile folding with N-trending axial planes forming the D_{C+D} dome-and-basin structures. The sinistral sliding along the Kynsikangas and concomitant overthrusting of the Central Finland Granitoid Complex (CFGC) upon the Pomarkku block at its northern and eastern edges indicate c. SW-NE shortening during the D_D. Sinistral strike-slip movement in the Kynsikangas zone and sinistral oblique dip-slip movement at the northern edge and dextral oblique movement in the Kankaanpää zone refer to clockwise rotation of the Pomarkku block (Appendix-Fig. 7-1c). The model of clockwise rotation during dextral transpression along the major N-trending deformation zones, the Baltic Sea-Bothnian Bay Zone (BBZ) and Riga Bay-Karelia Zone (RKZ) (Figure 8) explains the tectonic development of the Pomarkku Block. It also accounts for the SW-trending dextral movement causing the bulbous structure of the Pomarkku block and the boudinage-like structures (B in Appendix-Fig. 7-1c) in the western side of the N-trending part of the Kynsikangas zone. The arched, 1872 ± 2 Ma intrusion was intruded into oblique dilatational settings during this transpressional deformation $D_{4/D}$.

Later movements were more concentrated in zones. To the south of the Pomarkku block, local zones of symmetrical to dextral asymmetrical folds with N-S-trending axial planes show some shearing in the axial direction (F_4 of Pajunen et al. 2001a). Correlation of these sporadic folds is uncertain: they may represent the F_D, F_F or even the F_I folds. Open warps with N-S-trending axial planes, deforming the described structures and causing ovoidal interference structures, were named by Pajunen et al. (2001a) as F_x; this interference pattern is similar to the $D_{F\text{-}H}$ structures in the detailed study area. The final products of faulting,

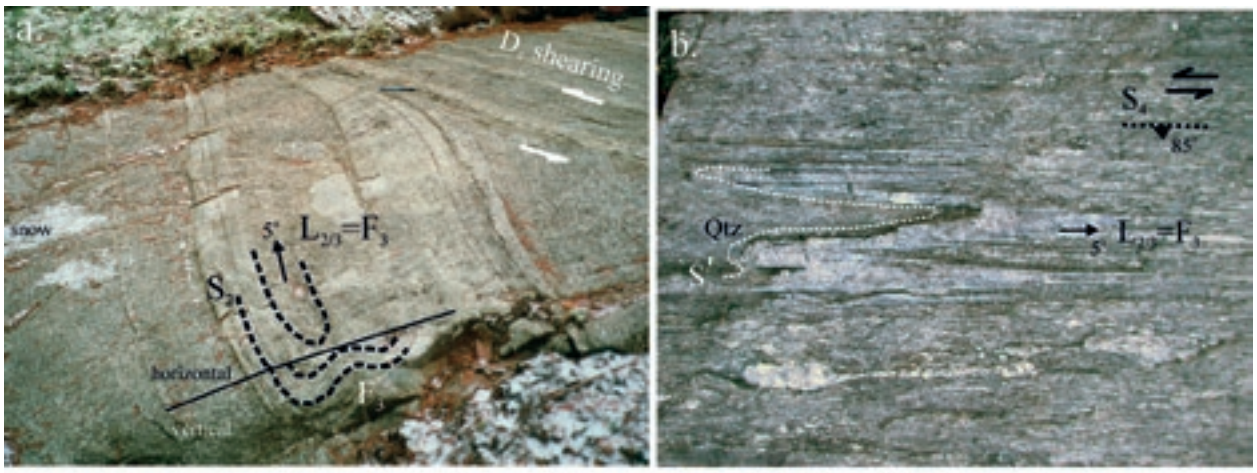

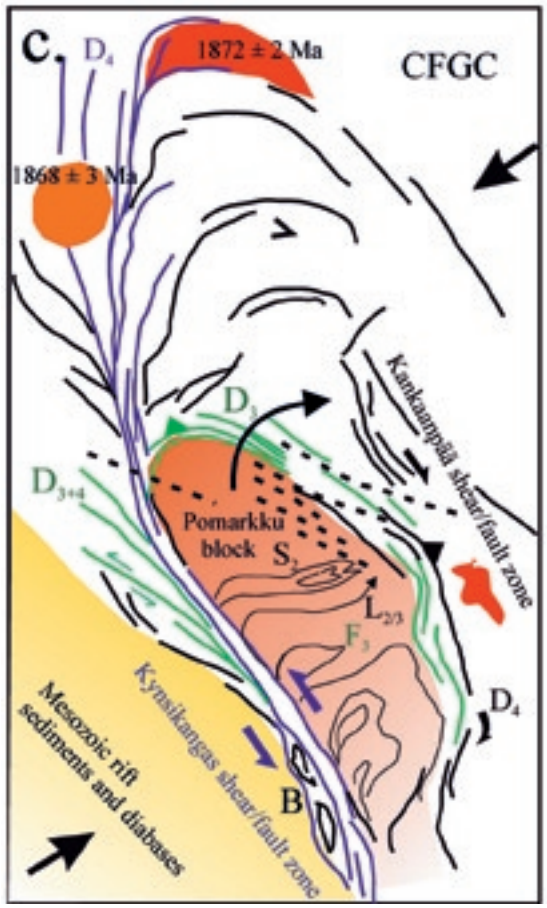

Appendix-Fig. 7-1. (a.) Sinistral shearing bends the pre-existing structure, e.g. F_3, into the direction of the Kynsikangas shear/fault zone. Pencil is 14 cm in length. (b.) Strong stretching lineation in the direction of the zone. Width of the area of the figure is c. 0.5 m. Levanpelto, Kullaa (Finnish grid coordinates KKJ1 1566.89E 6809.60N). (c.) A schematic model of the generation of the Pomarkku block in a SW-NE transpressional event that caused clockwise rotation of the Pomarkku block. The 1872 ± 2 Ma granitoid (Mäkitie & Lahti 2001) shows signatures of deformation in the Kynsikangas structure, but the 1868 ± 3 Ma granitoid (Lehtonen et al. 2005) cuts it. Photos by M. Pajunen.

especially close to the sandstone basin, are brittle pseudotachylites that sometimes have "vesicle" microstructures (Pajunen et al. 2001a).

Correlations with central and eastern Finland

The Archaean-Svecofennian border is characterized by major crustal NW- and N-trending shear zones of the Ladoga-Bothnia Bay zone (e.g. Talvitie 1971 and Korsman & Lestinen 2002). The major NW-trending zone is determined as a linear gravity low (Korhonen et al. 2002b) caused by shearing, granitization and granite magmatism (e.g. Pajunen 1986 and Pääjärvi 1991). The zone shows polyphase cataclastic characteristics. NW-trending zones are generally ductile dextral shear zones (e.g.Talvitie 1971); sometimes they also show sinistral strike-slip movement (D_c in Pajunen 1986). N-trending semi-ductile east-side-up dextral oblique shear/fault zones (D_d in Pajunen 1986) overprint the NW-trending shear zones. These NW- and N-trending shear zones overprint shear zones dipping with a low angle towards the SE (see also Kilpeläinen

2007) and cause the nearly-horizontal sliced structure that characterizes the Central Finland Granitoid Complex (CFGC) and the Savo Schist Belt (SSB). This structure is well defined in the magnetic anomaly pattern, especially near the Archaean-Proterozoic suture zone, but become less evident in the central parts of the CFGC. This stacked structure is also supported by the tectonic pattern of supracrustal remnants in the granitoid unit; the WNW-trend of the western extensions of the SSB, for example in the Rautalampi district (Ra in Figure 9) and in the Pyhäsalmi area towards the west, which are bent by the $D_{4/D}$ deformation.

The stacked and sheared structures in the Central Finland Granitoid Complex (CFGC) and further east show similarities to the structure of the Pomarkku block. The NW-trending dextral shearing structures can be explained by more N-S-oriented shortening than in the west, but the stress field later turned close to a NE-SW direction, as indicated by the dextral N-S faults (D_d of Pajunen 1986). The more brittle character of the N-S faults in Central Finland with respect to that in the west indicates earlier cooling and stabilization in Central Finland. We suppose that the NW-stacked, low-angle structure was formed by overthrusting towards the north during the collisional event corresponding to the D_3 deformation in the Pomarkku Block; the NW-trending shear zones could have formed contemporaneously. Lahtinen and Huhma (1997) separated two different magmatic series due to their Sm-Nd characteristics: the earlier, ca 1.888 Ga old granitoids show more primitive characteristics, whereas the later pulse show signatures from re-melted pre-existing crust. The later granitoids in the CFGC follow the arced structures: the post-/late orogenic granitic intrusion in Figure 9 (see also Nironen 2003). We proposed their emplacement into oblique dilatation zones related to the overall SW-NE-trending $D_{4/D}$ transpression. They were intruded especially into the E-W-trending, originally contractional low-angle zones (D_C) that turned to extensional during the later evolution ($D_{4/D}$). These granitoids were effectively destroying the earlier low-angle SE-dipping features of the CFGC. The collisional stage in areas close to the Archaean-Proterozoic boundary zone had already proceeded far before the intrusion of 1884 ± 5 Ma orthopyroxene-bearing granitoids (Hölttä 1988), because their contact cut the regional metamorphic parageneses and contractional F_3 folding (Hölttä et al. 1988 and Korsman et al. 1999); these granitoids represent the end of the main thermal events near the craton boundary. However, in western Finland, corresponding orthopyroxene-bearing granitoids have ages of 1871 ± 2 to 1868 ± 3 Ma. As noted, the later magma phase determines the major stacking and folding structures in this area, and indicates c. 10–15 Ma later stabilization with respect to the craton boundary. According to Koistinen (1981), the N-trending D_3, labelled later as syn-D_4 (Koistinen et al. 1996) (D_F of this paper), was dated in eastern Finland with the syn-D_4 Maarianvaara granite at c. 1857 ± 8 Ma old (Huhma 1986). The development of these structures, and magma and metasomatic pulses in these times (cf. Pajunen & Poutiainen 1999) establishes the continuality of deformation and heat flow. However, in the northern units it was more divided and local at this stage.

Appendix 8. Multigrain TIMS U-Pb isotopic dating of zircon and monazite, and SIMS dating of zircon

SAMPLES

Samples A1738 Staffas (syn-/late D_B tonalite, Hindsby intrusion; SIMS), A1676 Bollstad (syn-/late D_B tonalite; TIMS & SIMS), A1785 Hakkila (early D_E garnet-bearing tonalite), A1784 Hyrylä (early D_E garnet-bearing tonalite/granite), A1335 Maikkala (pyroxene-bearing tonalite, charnockite), A1745 Jyskelä (late D_E gabbro; TIMS & SIMS), A1677 Bollstad (D_H pegmatitic granite; TIMS) and A1678 Kopparnäs (D_H diabase; TIMS & SIMS). The Samples were collected in the project "Construction potential modeling of bedrock in urban areas" during 1999–2002, except for the sample A1335 Maikkala, which was collected by K. Korsman (unpublished report by H. Huhma 3.2.94/GSF/Petrological Department/Isotope Geology Division); the original data have been recalculated here.

ANALYTICAL METHODS

The digestion of zircon and extraction of U and Pb for TIMS isotopic age determinations mainly follows the procedure described by Krogh (1973). ^{235}U–^{208}Pb (zircon) or ^{235}U–^{206}Pb (monazite) spiked and non-spiked isotopic ratios were measured using a VG Sector 54 TIMS (Thermal Ionization multicollector Mass Spectrometer). The measured lead and uranium isotopic ratios were normalized to the accepted ratios of SRM 981 and U500 standards. The U-Pb age calculations were done using the PbDat-program (Ludwig 1991) and the fitting of the discordia lines using the Isoplot/Ex program (Ludwig 2001). Further information is given in App-Table 1.

For ion microprobe dating (NORDSIM Project#: N04-FI–12), the selected zircon grains were mounted in epoxy, polished, and coated with gold. The ion microprobe U-Pb analyses were carried out using the Nordic Cameca IMS 1270 at the Swedish Museum of Natural History, Stockholm, Sweden. The spot-diameter for the 4nA primary O_2^- ion beam was c. 25 µm and oxygen flooding in the sample chamber was used to increase the production of Pb^+ ions. Three counting blocks, each including four cycles of the Zr, Pb, Th, and U species of interest, were measured from each spot. The mass resolution (M/ΔM) was 5400 (10%). The raw data were calibrated against a zircon standard (91500; Wiedenbeck et al. 1995) and corrected for background at mass 204.2 and modern common lead (T = 0; Stacey and Kramers 1975). For the detailed analytical procedure see Whitehouse et al. (1997 and 1999). The plotting of the U-Pb data and calculating of the concordia and intercept ages were performed using the Isoplot/Ex 3 program (Ludwig 2003). The data-point error ellipses in the concordia diagrams are 2 sigma. All the errors in age results are 2 sigma and calculated ignoring the decay constant errors. The results are compiled in App-Table 2.

SAMPLES, ZIRCON DESCRIPTIONS AND U-PB AGE RESULTS

A1738 Staffas, Sipoo – syn-/late D_B tonalite

Finnish grid coordinates KKJ2 2568.79E 6694.48N
SIMS, zircon, NORDSIM sample number n1660, mount number M561 (large grains)

Sample information

Sample A1738 from Staffas in Sipoo, from the wide and homogeneous Hindsby intrusion (Figures 24 and 25), was analyzed to establish the isotopic age of the typical, structurally-fixed syn-/late D_B tonalite intrusion. The tectonic antiformal setting of the Hindsby intrusion is presented in Appendix-Fig. 6-2d, and the details of its structural evolution are discussed in the main text. The tonalite is metamorphosed with the main mineral assemblage plagioclase, quartz, biotite with minor garnet and pyroxene. Pyroxene is decomposed to clinoamphibole, and biotite is locally chloritized.

App-Table 1. Multigrain TIMS U-Pb isotopic data on zircons and monazites. Samples A1676 Bollstad tonalite, A1335 Maikkala charnockite, A1745 Jyskelä gabbro, A1677 Bollstad pegmatite and A1678 Kopparnäs diabase.

Sample information	Sample	U	Pb	$^{206}Pb/^{204}Pb$	$^{208}Pb/^{206}Pb$	ISOTOPIC RATIOS[1]							APPARENT AGES / Ma±2 sigma		
Analysed mineral and fraction	weight/mg	ppm		measured	radiogenic	$^{206}Pb/^{238}U$	2SE%	$^{207}Pb/^{235}U$	2SE%	$^{207}Pb/^{206}Pb$	2SE%	Rho[2]	$^{206}Pb/^{238}U$	$^{207}Pb/^{235}U$	$^{207}Pb/^{206}Pb$
A1676 Bollstad tonalite															
A) Zircon d>4.3 g cm–3, >75µm, short prismatic, l:w=2.5–5, light coloured, abraded 7h	0.61	299	91	3994	0.06	0.2969	0.65	4.619	0.65	0.1128	0.15	0.97	1676	1753	1846±3
B) Zircon d>4.3 g cm–3, >75µm, short prismatic, l:w=2.5–5, light coloured	0.55	479	137	1516	0.06	0.2755	0.65	4.264	0.65	0.1123	0.15	0.97	1569	1687	1837±3
C) Zircon d>4.3 g cm–3, <75µm, short prismatic, l:w=2.5–5, light coloured, abraded 6h	0.49	473	145	5293	0.05	0.3027	0.65	4.708	0.65	0.1128	0.15	0.97	1705	1769	1845±3
D) Zircon d>4.3 g cm–3, <75µm, short prismatic, l:w=2.5–5, light coloured	0.41	530	156	1641	0.05	0.2855	0.65	4.436	0.65	0.1127	0.15	0.97	1619	1719	1843±3
E) Monazite: fine-grained, oval-shaped, abraded 1/4 h	0.17	3506	4788	21173	3.68	0.3291	0.95	5.072	0.96	0.1118	0.15	0.99	1834	1832	1829±3
A1335 Maikkala charnockite[3]															
A) Zircon d: 4.3–4.5 g cm^{-3}, >75 µm, abraded	7.6	541	169	9660	0.05	0.3117	0.65	4.863	0.65	0.1131	0.15	0.97	1749	1795	1850±3
B) Zircon d: 4.3–4.5 g cm–3	6.3	498	159	10250	0.05	0.3195	0.65	4.988	0.65	0.1133	0.15	0.97	1787	1817	1852±3
C) Zircon d: 4.2–4.3 g cm–3	8.1	626	196	7001	0.05	0.3103	0.65	4.824	0.65	0.1128	0.15	0.97	1742	1789	1844±3
D) Zircon d: 4.3–4.5g cm–3, < 75 µm, abraded 5h	6.7	534	171	7622	0.05	0.3182	0.65	4.972	0.65	0.1133	0.15	0.97	1781	1814	1853±3
F) Zircon d: 4.3–4.5 g cm–3, >75 µm, abraded	6.7	536	168	10447	0.05	0.3125	0.65	4.878	0.65	0.1132	0.15	0.97	1753	1798	1851±3
G) Zircon d: 4.0–4.2 g cm–3, >75 µm	7.8	905	242	3613	0.06	0.2645	0.65	4.061	0.65	0.1114	0.15	0.97	1512	1646	1821±3
E) Monazite	1.9	896	5207	10811	19.44	0.3258	0.65	5.045	0.65	0.1123	0.15	0.97	1818	1826	1837±3
A1745 Jyskelä gabbro															
A) Zircon d>4.2 g cm^{-3}, >75 µm, brown, tranparent, subhedral-anhedral, elongated, abraded 8 h	0.42	951	330	8990	0.13	0.3223	0.65	4.984	0.65	0.1122	0.15	1	1801	1817	1835±3
B) Zircon d>4.2 g cm^{-3}, <75 µm, brown, tranparent, subhedral-anhedral, elongated, abraded 1 h	0.32	830	285	5291	0.13	0.3180	0.65	4.896	0.65	0.1117	0.15	1	1780	1802	1827±3
C) Zircon d: 4.2–4.0 g cm^{-3}, >75 µm, brown, tranparent, subhedral-anhedral, elongated, abraded 8 h	0.35	1393	464	4181	0.12	0.3120	0.65	4.793	0.65	0.1114	0.15	1	1750	1784	1823±3
D) Zircon d: 4.2–4.0 g cm^{-3}, <75 µm, brown, tranparent, subhedral-anhedral, elongated, abraded 1 h	0.40	1340	447	4392	0.12	0.3109	0.65	4.778	0.65	0.1114	0.15	1	1745	1781	1823±3

Sample information Analysed mineral and fraction	Sample weight/mg	U ppm	Pb ppm	$^{206}Pb/^{204}Pb$ measured	$^{208}Pb/^{206}Pb$ radiogenic	ISOTOPIC RATIOS[1]							APPARENT AGES / Ma±2 sigma		
						$^{206}Pb/^{238}U$	2SE%	$^{207}Pb/^{235}U$	2SE%	$^{207}Pb/^{206}Pb$	2SE%	Rho[2]	$^{206}Pb/^{238}U$	$^{207}Pb/^{235}U$	$^{207}Pb/^{206}Pb$
A1677 Bollstad pegmatite															
A) Zircon d: 4.0–3.8 g cm–3, >150 µm, prismatic, dark brown, abraded 21h	0.48	3693	951	7952	0.01	0.2648	0.65	3.990	0.65	0.1093	0.15	0.97	1514	1632	1789±3
B) Zircon d: 4.0–3.8 g cm–3, 150–75 µm, prismatic,dark brown, abraded 18h	0.42	3443	882	9011	0.01	0.2642	0.65	3.987	0.65	0.1094	0.15	0.97	1512	1632	1790±3
C) Zircon d: 4.0–3.8 g cm–3, <75 µm, prismatic,dark brown, abraded 12h	0.52	3721	964	4324	0.01	0.2651	0.65	4.003	0.65	0.1095	0.15	0.97	1516	1635	1792±3
D) Zircon d>4.0g cm–3, >75 µm, prismatic,dark brown, abraded 4h	0.17	5116	1305	4711	0.01	0.2612	0.65	3.935	0.65	0.1093	0.15	0.97	1496	1621	1788±3
E) Zircon d>4.0g cm–3, >75 µm, prismatic, dark brown	0.24	3249	832	2561	0.02	0.2585	0.65	3.889	0.65	0.1091	0.15	0.97	1482	1611	1785±3
F) Zircon d: 4.0–3.8 g cm–3, <75 µm, prismatic,dark brown	0.42	3255	820	1750	0.02	0.2516	0.65	3.781	0.65	0.1090	0.15	0.97	1447	1589	1782±3
G) Monazite: coarse-grained, euhedral-subhedral, abraded 1/4 h	0.22	6273	1.07 %	47968	4.87	0.3298	0.97	5.081	0.97	0.1117	0.06	0.99	1838	1833	1828±1
A1678 Kopparnäs diabase															
A) Zircon d>4.0 g cm–3, <75 µm, elongated, bright, light coloured, abraded 4h	0.48	443	144	2188	0.14	0.2956	0.65	4.508	0.65	0.1106	0.15	1	1669	1733	1810±3
B) Zircon d>4.0 g cm–3, <75 µm, elongated, bright, light coloured, abraded 3h	0.07	614	204	1283	0.13	0.3006	0.65	4.602	0.65	0.1110	0.15	1	1694	1750	1816±3
C) Zircon d>4.0 g cm–3, >75 µm, elongated, bright, light coloured, abraded 3h	0.05	511	180	634	0.15	0.3027	0.65	4.632	0.65	0.1110	0.15	1	1705	1755	1816±3

[1] Isotopic ratios corrected for fractionation, blank (30–50 pg), and age related common lead (Stacey and Kramers, 1975; $^{206}Pb/^{204}Pb$±0.2; $^{207}Pb/^{204}Pb$±0.1; $^{208}Pb/^{204}Pb$±0.2). [2] Rho=Error correlation between $^{207}Pb/^{235}U$ and $^{206}Pb/^{238}U$ ratios. [3] Analyses by H.Huhma; blank 0.5 ng.

App-Table 2. SIMS U-Pb isotopic data on zircons. Samples from Uusimaa area, southern Finland.

Sample/ spot #	Spot site on zircon, zircon type	$^{207}Pb/^{206}Pb$	±s	$^{207}Pb/^{235}U$	±s	$^{206}Pb/^{238}U$	±s	$^{207}Pb/^{206}Pb$	±s %	$^{207}Pb/^{235}U$	±s %	$^{206}Pb/^{238}U$	±s %	r	Disc. % 2s lim.	[U] ppm	[Th] ppm	[Pb] ppm	Th/U meas	$^{206}Pb/^{204}Pb$ measured
A1738 Staffas tonalite (n1660)																				
n1660-01a	quite homog, long prismatic	1879	4	1892	12	1904	22	0.1149	0.2	5.445	1.3	0.3436	1.3	0.99		1453	282	585	0.19	1.79E+05
n1660-02a	weakly zoned, short prismatic	1836	3	1842	11	1847	21	0.1122	0.2	5.134	1.3	0.3317	1.3	0.99		832	54	312	0.06	2.98E+04
n1660-03a	quite homog, long prismatic	1832	4	1835	12	1838	21	0.1120	0.2	5.096	1.4	0.3300	1.3	0.98		522	29	194	0.06	8.54E+03
n1660-04a	weakly zoned, short prismatic, healthy	1797	4	1802	11	1807	21	0.1098	0.2	4.898	1.3	0.3234	1.3	0.99		719	105	268	0.15	1.35E+05
n1660-05a	zoned, short prismatic	1851	6	1842	12	1834	21	0.1132	0.3	5.134	1.4	0.3291	1.3	0.97		401	47	151	0.12	7.21E+03
n1660-06a	weakly zoned, short prismatic	1839	8	1854	12	1867	22	0.1124	0.5	5.207	1.4	0.3358	1.3	0.94		486	70	188	0.14	1.04E+03
n1660-07a	quite homog(dark), prismatic (incl. secondary zr phase)	1849	5	1843	12	1839	21	0.1130	0.3	5.144	1.4	0.3301	1.3	0.98		549	57	207	0.10	3.69E+03
n1660-08a	*zoned, prismatic*	*1851*	*19*	*1808*	*15*	*1771*	*21*	*0.1132*	*1.1*	*4.934*	*1.7*	*0.3161*	*1.3*	*0.78*		*614*	*71*	*222*	*0.12*	*8.25E+02*
n1660-09a	quite homog, pale outer domain, short prismatic	1806	6	1824	12	1839	21	0.1104	0.3	5.025	1.4	0.3300	1.3	0.97		484	73	184	0.15	1.94E+03
n1660-09b	*dark inner domain, short prismatic*	*1927*	*32*	*1897*	*19*	*1870*	*22*	*0.1180*	*1.8*	*5.478*	*2.2*	*0.3365*	*1.3*	*0.60*		*81*	*28*	*33*	*0.34*	*4.39E+02*
n1660-10a	quite homog., prismatc	1851	5	1856	12	1860	21	0.1132	0.3	5.221	1.4	0.3345	1.3	0.98		422	47	162	0.11	7.24E+04
n1660-11a	quite homog, pale outer domain, prismatic	1867	7	1845	12	1825	21	0.1142	0.4	5.152	1.4	0.3271	1.3	0.96		693	78	260	0.11	1.05E+03
n1660-11b	dark, zoned inner domain (dark), prismatic	1960	9	1947	13	1935	22	0.1202	0.5	5.804	1.4	0.3501	1.3	0.93		145	68	63	0.47	9.28E+03
n1660-12a	weakly zoned, prismatic	1868	5	1864	12	1861	21	0.1143	0.3	5.272	1.4	0.3347	1.3	0.98		438	31	167	0.07	6.69E+04
n1660-13a	*quite homog, pale tip domain, prismatic*	*1864*	*21*	*1885*	*16*	*1904*	*24*	*0.1140*	*1.2*	*5.399*	*1.9*	*0.3436*	*1.4*	*0.78*		*547*	*30*	*210*	*0.05*	*2.71E+02*
n1660-13b	*quite homog, dark inner domain, prismatic*	*1866*	*11*	*1844*	*12*	*1825*	*21*	*0.1141*	*0.6*	*5.148*	*1.5*	*0.3272*	*1.3*	*0.91*		*425*	*52*	*158*	*0.12*	*4.56E+02*
n1660-14a	quite homog, prismatic	1880	4	1886	12	1891	22	0.1150	0.2	5.405	1.3	0.3409	1.3	0.99		940	188	377	0.20	6.89E+04
n1660-15a	zoned, prismatic	1838	5	1830	12	1823	21	0.1124	0.3	5.065	1.4	0.3269	1.3	0.98		450	47	168	0.10	9.78E+03
n1660-16a	weakly zoned, prismatic	1865	3	1921	12	1973	23	0.1141	0.2	5.631	1.3	0.3581	1.3	0.99	3.8	1561	119	634	0.08	2.48E+05
n1660-17a	*zoned (hit on fracture), prismatic*	*1802*	*18*	*1631*	*14*	*1502*	*18*	*0.1101*	*1.0*	*3.985*	*1.7*	*0.2624*	*1.3*	*0.80*	*-13.4*	*180*	*36*	*55*	*0.20*	*4.00E+02*
n1660-18a	*weakly zoned, dark, prismatic*	*1838*	*17*	*1808*	*14*	*1782*	*21*	*0.1123*	*0.9*	*4.933*	*1.6*	*0.3185*	*1.3*	*0.82*		*382*	*39*	*138*	*0.10*	*4.13E+02*
A1784 Hyrylä granite dyke (n1661)																				
n1661-01a	quite homog, short prismatic	1852	7	1849	12	1847	21	0.1132	0.4	5.179	1.4	0.3317	1.3	0.96		381	227	162	0.60	3.21E+04
n1661-02a	quite homog, prismatic	1862	5	1860	12	1859	22	0.1138	0.3	5.247	1.4	0.3343	1.3	0.98		314	94	126	0.30	6.37E+04
n1661-03a	quite homog, prismatic	1864	6	1852	12	1841	21	0.1140	0.3	5.194	1.4	0.3306	1.3	0.97		275	124	113	0.45	1.90E+05
n1661-04a	homog pale outer domain/rim, prismatic	1860	4	1771	11	1696	20	0.1137	0.2	4.720	1.3	0.3009	1.3	0.99	-7.4	1423	261	500	0.18	6.72E+03
n1661-04b	quite homog dark inner domain/core, prismatic	1921	7	1852	12	1791	21	0.1176	0.4	5.194	1.4	0.3202	1.3	0.96	-4.8	210	60	80	0.28	1.00E+04
n1661-05a	quite homog, prismatic	1863	4	1867	12	1871	22	0.1139	0.2	5.289	1.3	0.3367	1.3	0.99		524	289	224	0.55	5.58E+04
n1661-06a	homog, long prismatic	1865	5	1864	12	1864	22	0.1141	0.3	5.272	1.4	0.3352	1.3	0.98		438	229	185	0.52	6.74E+04
n1661-07a	homog darker inner domain, stubby rounded grain with paler outer domain	1840	7	1846	12	1851	22	0.1125	0.4	5.158	1.4	0.3326	1.3	0.96		189	129	82	0.68	4.23E+04
n1661-08a	homog darker inner domain, stubby rounded grain with paler outer domain	1857	8	1852	12	1848	21	0.1136	0.4	5.197	1.4	0.3319	1.3	0.95		243	78	97	0.32	1.12E+05
n1661-09a	homog darker inner domain, stubby rounded grain with paler outer domain	1861	6	1861	12	1861	22	0.1138	0.4	5.253	1.4	0.3347	1.3	0.97		266	113	110	0.43	1.04E+05
n1661-10a	quite homog dark, short prismatic	1854	6	1859	14	1864	27	0.1134	0.3	5.241	1.7	0.3353	1.6	0.98		291	179	126	0.62	2.54E+04
n1661-11a	quite homog dark, long prismatic	1857	5	1846	14	1836	26	0.1136	0.3	5.160	1.7	0.3295	1.6	0.98		606	242	245	0.40	4.71E+03
n1661-12a	weakly zoned dark, prismatic	1944	9	1932	15	1921	27	0.1192	0.5	5.706	1.7	0.3472	1.6	0.95		155	88	69	0.57	5.88E+03
n1661-13a	quite homog dark, prismatic	1852	6	1808	14	1770	25	0.1132	0.4	4.933	1.7	0.3160	1.6	0.98	-1.5	421	198	166	0.47	5.23E+03
n1661-14a	weakly zoned dark, prismatic	1861	4	1855	14	1849	26	0.1138	0.2	5.213	1.6	0.3323	1.6	0.99		537	316	229	0.59	9.69E+04
n1661-15a	homog, round grain	1872	6	1870	14	1869	27	0.1145	0.3	5.308	1.7	0.3363	1.6	0.98		257	90	105	0.35	8.88E+04
n1661-16a	homog paler outer domain, short prismatic	1862	3	1888	14	1912	27	0.1139	0.1	5.420	1.6	0.3452	1.6	1.00		1595	132	635	0.08	5.84E+04
n1661-16b	homog darker inner domain, short prismatic	1975	4	2025	15	2074	29	0.1213	0.2	6.345	1.6	0.3794	1.6	0.99	2.2	560	330	279	0.59	1.37E+04

Sample/ spot #	Spot site on zircon, zircon type	$^{207}Pb/^{206}Pb$	±s	$^{207}Pb/^{235}U$	±s	$^{206}Pb/^{238}U$	±s	$^{207}Pb/^{206}Pb$	±s %	$^{207}Pb/^{235}U$	±s %	$^{206}Pb/^{238}U$	±s %	r	Disc. % 2s lim.	[U] ppm	[Th] ppm	[Pb] ppm	Th/U meas	$^{206}Pb/^{204}Pb$ measured
A1785 Hakkila tonalite (n1662)																				
n1662-01c	*homog pale rim, stubby grain*	*1545*	*113*	*722*	*34*	*487*	*7*	*0.0958*	*6.3*	*1.036*	*6.4*	*0.0784*	*1.5*	*0.23*	*-36.0*	*2798*	*532*	*249*	*0.19*	*6.54E+02*
n1662-01b	homog darker inner domain/core, stubby grain quite homog dark inner domain,	1878	8	1900	12	1920	22	0.1149	0.4	5.497	1.4	0.3469	1.3	0.95		222	58	92	0.26	4.23E+03
n1662-02a	stubby grain (+thin outer rim)	3298	4	3275	13	3237	34	0.2686	0.2	24.164	1.3	0.6524	1.3	0.98		184	107	172	0.58	1.94E+05
n1662-03a	homog outer rim, stubby grain	1863	4	1811	11	1767	21	0.1139	0.2	4.953	1.3	0.3154	1.3	0.99	-3.2	944	31	335	0.03	7.07E+03
n1662-03b	homog paler inner domain, stubby grain	1871	3	1867	11	1864	21	0.1144	0.2	5.291	1.3	0.3353	1.3	0.99		1075	111	412	0.10	1.44E+05
n1662-04a	homogenized?, long crystal	1848	5	1827	12	1808	21	0.1130	0.3	5.043	1.4	0.3238	1.3	0.98		646	300	259	0.46	2.75E+03
n1662-05a	zoned, long crystal	1869	7	1849	12	1831	21	0.1143	0.4	5.176	1.4	0.3285	1.3	0.96		209	108	87	0.52	1.87E+04
n1662-06a	zoned, long crystal	1873	5	1865	12	1858	22	0.1145	0.3	5.275	1.4	0.3340	1.3	0.98		412	166	170	0.40	1.48E+05
n1662-07a	zoned, long crystal	1865	5	1851	12	1838	21	0.1140	0.3	5.188	1.3	0.3300	1.3	0.98		412	34	155	0.08	9.71E+04
n1662-08a	zoned, long crystal	1860	6	1832	12	1808	21	0.1137	0.3	5.075	1.4	0.3237	1.3	0.97	-0.2	576	185	226	0.32	1.22E+04
n1662-09a	zoned, long crystal	1870	4	1877	14	1883	27	0.1144	0.2	5.348	1.6	0.3392	1.6	0.99		587	55	227	0.09	6.81E+04
n1662-10a	zoned, long crystal	1872	4	1869	14	1865	27	0.1145	0.2	5.299	1.6	0.3356	1.6	0.99		736	447	319	0.61	6.28E+04
n1662-11a	zoned, long crystal	1864	6	1874	14	1883	27	0.1140	0.3	5.329	1.7	0.3391	1.6	0.98		302	81	122	0.27	2.07E+04
n1662-12a	zoned, long crystal	1870	3	1878	14	1884	27	0.1144	0.2	5.355	1.6	0.3395	1.6	1.00		1216	18	462	0.01	1.60E+05
n1662-13a	quite homog, long crystal	1869	4	1872	14	1875	27	0.1143	0.2	5.321	1.6	0.3377	1.6	0.99		819	668	374	0.82	9.63E+04
n1662-14a	quite homog, long crystal	1858	5	1866	14	1873	27	0.1136	0.3	5.282	1.6	0.3372	1.6	0.99		847	37	322	0.04	3.86E+04
n1662-15a	zoned, long crystal	1871	4	1881	14	1891	27	0.1144	0.2	5.378	1.6	0.3409	1.6	0.99		681	489	307	0.72	1.42E+05
A1335 Maikkala charnockite (n1663)																				
n1663-01a	weakly zoned (dark domain), long prismatic	1853	11	1860	13	1867	22	0.1133	0.6	5.247	1.5	0.3359	1.3	0.90		224	46	88	0.21	2.65E+03
n1663-01b	weakly zoned (pale domain), long prismatic	1862	5	1859	12	1857	21	0.1139	0.3	5.240	1.4	0.3338	1.3	0.98		544	84	210	0.15	3.62E+04
n1663-02a	weakly zoned, long prismatic	1865	6	1855	12	1845	21	0.1141	0.3	5.212	1.4	0.3314	1.3	0.97		279	63	109	0.23	5.95E+04
n1663-03a	quite homog, long prismatic	1861	4	1856	12	1852	21	0.1138	0.2	5.221	1.3	0.3328	1.3	0.98		485	28	182	0.06	1.94E+04
n1663-04a	weakly zoned, short prismatic	1867	4	1855	12	1845	21	0.1142	0.2	5.217	1.3	0.3313	1.3	0.99		531	88	204	0.17	8.50E+04
n1663-05a	zoned, long prismatic	1860	9	1821	12	1788	21	0.1137	0.5	5.011	1.4	0.3196	1.3	0.93	-1.0	100	18	37	0.18	3.12E+04
n1663-06a	zoned, short prismatic	1870	6	1871	12	1871	22	0.1144	0.4	5.312	1.4	0.3368	1.3	0.97		295	82	119	0.28	7.16E+04
n1663-07a	homogenized, pale core, prismatic	1830	3	1813	11	1797	21	0.1119	0.2	4.960	1.3	0.3215	1.3	0.99		1239	32	444	0.03	7.20E+03
n1663-07b	darker tip domain	1859	4	1862	12	1864	21	0.1137	0.2	5.256	1.3	0.3353	1.3	0.98		530	147	212	0.28	1.12E+04
n1663-08a	zoned, short prismatic	1864	7	1853	12	1843	21	0.1140	0.4	5.201	1.4	0.3310	1.3	0.96		228	46	88	0.20	3.88E+04
A1676 Bollstad tonalite (n1665)																				
n1665-01a	*quite homog, dark inner domain, prismatic*	*1856*	*94*	*1776*	*48*	*1708*	*25*	*0.1135*	*5.4*	*4.748*	*5.6*	*0.3035*	*1.6*	*0.29*		*284*	*34*	*98*	*0.12*	*2.72E+02*
n1665-02a	zoned, short prismatic	1857	7	1894	15	1928	27	0.1135	0.4	5.459	1.7	0.3487	1.6	0.97	0.5	191	39	78	0.20	3.80E+04
n1665-03a	quite homog, dark inner domain, short prismatic	1858	10	1857	15	1856	27	0.1136	0.5	5.226	1.7	0.3337	1.6	0.95		173	70	71	0.40	8.90E+03
n1665-04a	weakly zoned, short prismatic	1888	9	1873	15	1860	27	0.1155	0.5	5.328	1.7	0.3345	1.6	0.95		137	52	56	0.38	1.26E+05
n1665-05a	zoned, short prismatic	1879	7	1886	15	1892	27	0.1150	0.4	5.406	1.7	0.3410	1.6	0.97		202	76	84	0.38	3.09E+04
n1665-08a	quite homog, dark, short prismatic	1874	11	1867	15	1862	27	0.1146	0.6	5.290	1.8	0.3348	1.7	0.94		120	43	49	0.36	4.69E+03
n1665-06a	pale inner domain/core	1868	7	1815	14	1769	25	0.1142	0.4	4.973	1.7	0.3157	1.6	0.97	-2.5	340	159	133	0.47	4.34E+03
n1665-07a	weakly zoned, short prismatic	1879	7	1883	15	1886	27	0.1149	0.4	5.386	1.7	0.3399	1.6	0.97		195	78	82	0.40	1.23E+04
A1745 Jyskelä gabbro (n1666)																				
n1666-01a	quite homog	1836	3	1834	14	1832	26	0.1123	0.2	5.087	1.6	0.3286	1.6	0.99		1097	223	422	0.20	3.90E+04
n1666-02a	quite homog	1830	4	1816	14	1803	26	0.1119	0.2	4.979	1.7	0.3228	1.6	0.99		466	133	180	0.28	1.00E+05
n1666-03a	quite homog	1847	4	1832	14	1818	26	0.1129	0.2	5.073	1.6	0.3258	1.6	0.99		669	186	260	0.28	1.07E+05
n1666-04a	quite homog	1841	2	1834	14	1828	26	0.1125	0.1	5.089	1.6	0.3280	1.6	1.00		1622	1282	711	0.79	2.05E+05
n1666-05a	quite homog	1824	6	1815	14	1807	26	0.1115	0.3	4.975	1.7	0.3236	1.6	0.98		287	46	108	0.16	3.00E+04
n1666-06a	quite homog	1838	3	1837	14	1837	26	0.1123	0.1	5.106	1.6	0.3296	1.6	1.00		1540	164	581	0.11	2.18E+05
n1666-07a	quite homog	1821	10	1766	15	1721	25	0.1113	0.5	4.695	1.7	0.3059	1.6	0.95	-2.3	270	48	96	0.18	3.38E+03

Sample/ spot #	Spot site on zircon, zircon type	$^{207}Pb/^{206}Pb$	±s	$^{207}Pb/^{235}U$	±s	$^{206}Pb/^{238}U$	±s	$^{207}Pb/^{206}Pb$	±s %	$^{207}Pb/^{235}U$	±s %	$^{206}Pb/^{238}U$	±s %	r	Disc. % 2s lim.	[U] ppm	[Th] ppm	[Pb] ppm	Th/U meas	$^{206}Pb/^{204}Pb$ measured
A1678 Kopparnäs diabase (n1664)																				
n1664-01a	homog, elongated formless large grain	1827	3	1840	11	1851	21	0.1117	0.2	5.122	1.3	0.3326	1.3	0.99		1497	137	566	0.09	1.98E+05
n1664-02a	homog, long prismatic large crystal	1832	3	1842	11	1851	21	0.1120	0.2	5.135	1.3	0.3325	1.3	0.99		1144	123	434	0.11	1.08E+05
n1664-03a	homog, long prismatic large crystal	1833	3	1846	11	1859	21	0.1120	0.2	5.162	1.3	0.3342	1.3	0.99		1041	77	394	0.07	1.68E+05
n1664-04a	homog, short large grain	1831	2	1862	11	1890	22	0.1119	0.1	5.258	1.3	0.3407	1.3	1.00	0.9	1981	170	766	0.09	1.33E+05
n1664-05a	homog, short large grain	1831	6	1847	12	1861	21	0.1120	0.3	5.166	1.4	0.3347	1.3	0.97		592	85	228	0.14	6.01E+04
n1664-06a	homog, round bright	1832	3	1854	14	1873	27	0.1120	0.2	5.206	1.6	0.3371	1.6	0.99		868	131	338	0.15	8.13E+04
n1664-07a	homog, round bright	1831	8	1834	15	1836	26	0.1119	0.5	5.086	1.7	0.3296	1.6	0.96		163	95	69	0.58	2.80E+04
n1664-08a	homog, round bright	1830	3	1843	14	1854	26	0.1118	0.2	5.140	1.6	0.3333	1.6	0.99		746	98	286	0.13	1.33E+05
n1664-09a	quite homog, dark, prismatic	1680	22	998	13	717	11	0.1030	1.2	1.672	2.0	0.1177	1.6	0.81	-54.0	215	81	31	0.37	9.16E+02
n1664-10a	dark tip, prismatic	1752	11	1511	14	1345	20	0.1072	0.6	3.429	1.7	0.2320	1.6	0.94	-22.1	240	243	81	1.01	2.88E+03
n1664-11a	quite homog, dark, elongated	1832	9	1819	14	1808	26	0.1120	0.5	5.000	1.7	0.3238	1.6	0.96		177	133	76	0.75	1.05E+04
n1664-12a	weakly zoned, prismatic	1845	2	1867	14	1886	27	0.1128	0.1	5.287	1.6	0.3399	1.6	1.00		1977	73	755	0.04	2.05E+04
n1664-13a	weakly zoned, long prismatic	1819	6	1836	14	1851	26	0.1112	0.4	5.101	1.7	0.3327	1.6	0.98		258	130	108	0.50	1.49E+04
n1664-14a	quite homog, elongated	1838	5	1844	14	1850	26	0.1124	0.3	5.150	1.7	0.3324	1.6	0.99		793	113	304	0.14	2.77E+03
n1664-15a	*quite homog, dark, prismatic(fractured)*	*1773*	*26*	*1693*	*18*	*1629*	*24*	*0.1084*	*1.4*	*4.299*	*2.2*	*0.2875*	*1.6*	*0.76*	*-1.9*	*188*	*129*	*70*	*0.69*	*3.66E+02*
n1664-16a	quite homog, dark, prismatic(fractured)	1795	17	1700	16	1624	24	0.1098	0.9	4.334	1.9	0.2864	1.6	0.87	-5.6	137	133	52	0.97	8.95E+02
n1664-17a	*dark outer domain, prismatic(fractured)*	*1699*	*83*	*1258*	*36*	*1017*	*15*	*0.1041*	*4.6*	*2.453*	*4.9*	*0.1708*	*1.6*	*0.34*	*-21.0*	*309*	*76*	*62*	*0.25*	*1.73E+02*

All errors are at 1 sigma level. Degree of discordance is calculated at the closest 2 sigma limit. Rejected data are indicated in italics.

*) Internal structure of the dated zircon domains on BSE-images: zoned = magmatic compositional zoning (oscillatory, banded, etc.); homog= quite homogeneous zircon domain.

Zircon description

The tonalite sample A1738 Staffas has a homogeneous zircon population. The grain-size differences are also quite small. The zircon is mostly pale brown, transparent to translucent, and prismatic with a length to width ratio of 3–5.

SIMS U-Pb age results

From the Staffas tonalite we dated 21 zircon domains and rejected six analyses because of the low $^{206}Pb/^{204}Pb$ ratios (App-Table. 2). In BSE images the zircons show mostly either weak zoning and/or homogeneous internal structure and frequent fractures. The U-Pb data are mostly concordant and show a wide range of ages (Appendix-Fig. 8-1a).

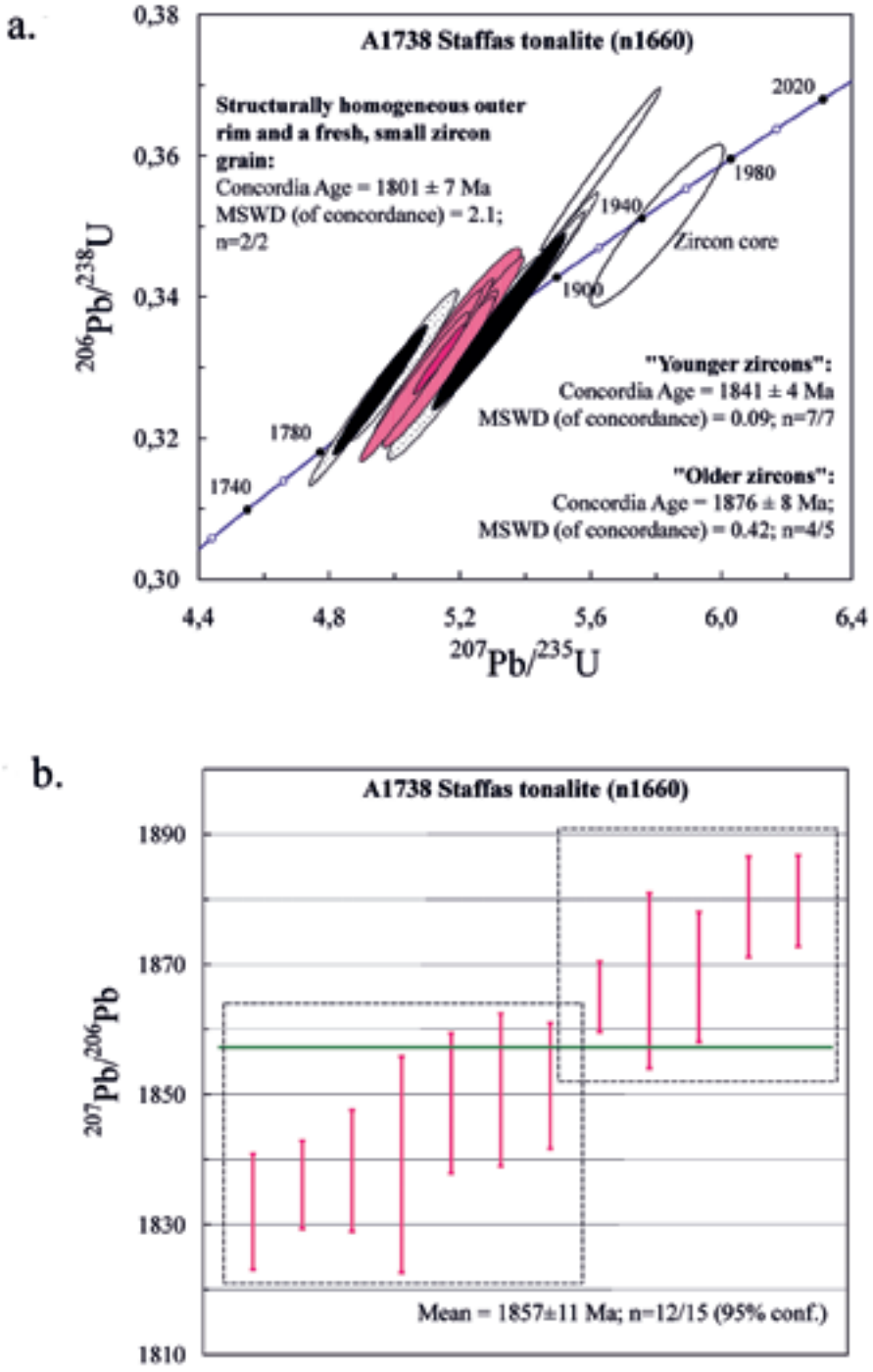

Appendix-Fig. 8-1. Ion microprobe age data on zircons; sample A1738 Staffas tonalite. A) Concordia plot. B) Weighted average of $^{207}Pb/^{206}Pb$ ages. The two youngest and the oldest data points are not shown in figure.

The oldest age of 1.96 Ga was measured from a BSE-darker core domain (11b) that is surrounded by younger zircon phase (1.87 Ga) (Appendix-Fig. 2). Additionally it has a thin rim growth on the other end of the grain (Appendix-Fig. 8-2a). A BSE-pale, homogeneous rim domain of zircon 09 has a $^{207}Pb/^{206}Pb$ age of 1.81 Ga. Its BSE-darker core has a clearly older age (ca. 1.93 Ga) but the analysis was rejected because of high common lead content. A 1.80 Ga age was measured from a small, euhedral, and weakly zoned zircon with an anomalous outlook. Thus, it is unsure if it is contamination from rock-crushing or mineral separation processes. The other possibility is that it is from some tiny vein connected with metamorphism. The concordia age for the two young zircons is 1801 ± 7 Ma (Appendix-Fig. 8-1a).

The majority of the U-Pb data plot between 1880 Ma and 1840 Ma. The weighted average of the $^{207}Pb/^{206}Pb$ ages is 1857±11 Ma (Appendix-Fig. 8-1b). However, the data seem to form two separate age populations (Appendix-Fig. 8-1a) although evidence from the dated zircon domains is totally absent. Younger and older ages have been dated both from BSE-darker domains with weak internal structure and internally quite homogeneous domains. The concordia ages for the two apparent age groups are 1841 ± 4 Ma (n=7/7) and 1876 ± 8 Ma (n=4/5) (Fig. 3a). Based on field evidence, the older age of ~1.88–1.87 Ga is considered as better alternative for the tonalite age and then, the ~1.84 Ga zircon may indicate metamorphism related lead loss.

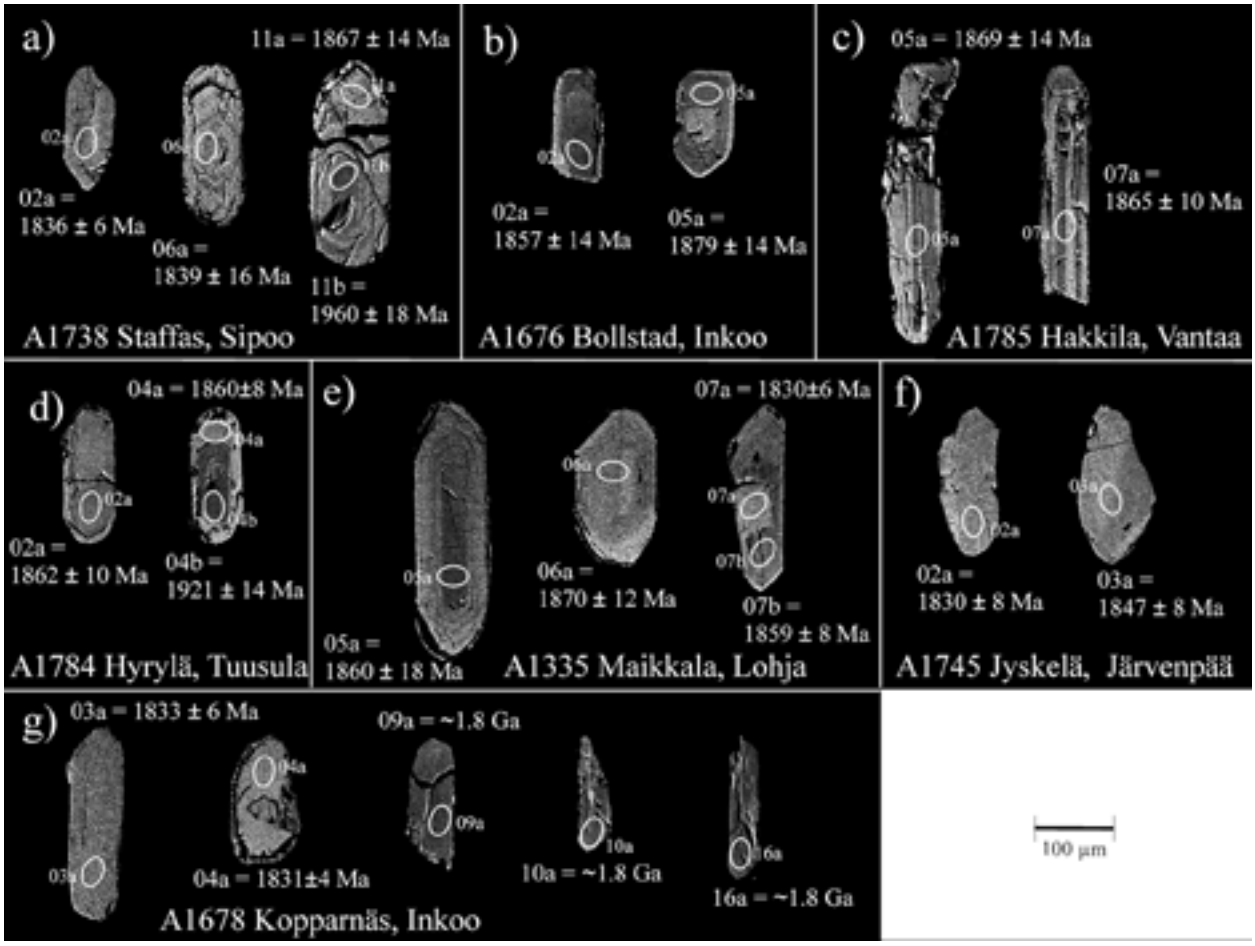

Appendix-Fig. 8-2. Selected BSE images of zircons: a) A1738 Staffas, syn-/late D_B tonalite – Hindsby intrusion; b) A1676 Bollstad, syn-/late D_B tonalite; c) A1785 Hakkila, early D_E garnet-bearing tonalite; d) A1784 Hyrylä, early D_E garnet-bearing tonalite; e) A1335 Maikkala, pyroxene-bearing tonalite, charnockite; f) A1745 Jyskelä, late D_E gabbro; A1678 Kopparnäs, D_H diabase.

A1676 Bollstad 1, Inkoo – syn-/late DB tonalite

Finnish grid coordinates KKJ2 2497.78E 6662.16N
TIMS, zircon and monazite
SIMS, zircon, NORDSIM sample number n1665, mount number M562 (small grains)

Sample information

The sample A1676 Bollstad from Inkoo was taken to establish the age of a tonalite that was intruded by granitic pegmatite dykes (sample A1677 Bollstad 2) that structurally evidences the beginning of the D_H extensional deformation in the Inkoo area. The tonalite is strongly deformed by D_H and shows new progression overprinting the early magmatic structure. The dated tonalite, with the main mineral composition plagioclase, biotite, quartz, is shown in Figure 39. The purpose was to determine the length of the discordance that is evident based on structure (cf. Sederholm 1926 and Pajunen et al. 2008).

Zircon and monazite descriptions

The sample included very fine-grained, pale yellow, ellipsoidal to round monazite without developed crystal faces. Zircon population is quite homogeneous and fine-grained (<75 µm). Typically zircon is brownish, translucent and prismatic or shorter, partly without crystal faces. More ellipsoidal and rounded, bright, possibly metamorphic zircon also exists (not included in the TIMS analysis).

TIMS U-Pb age result

The TIMS age was analyzed from rather fine-grained, reddish and long zircon grains. The Pb/U ratios scatter evenly on the regression line, giving the upper intercept age of 1855 ± 6 Ma (n=4; MSWD=1.7). The concordant monazite age of 1829 ± 3 Ma was obtained by TIMS. The TIMS U-Pb data are shown in App-Table 1 and Appendix-Fig. 8-3.

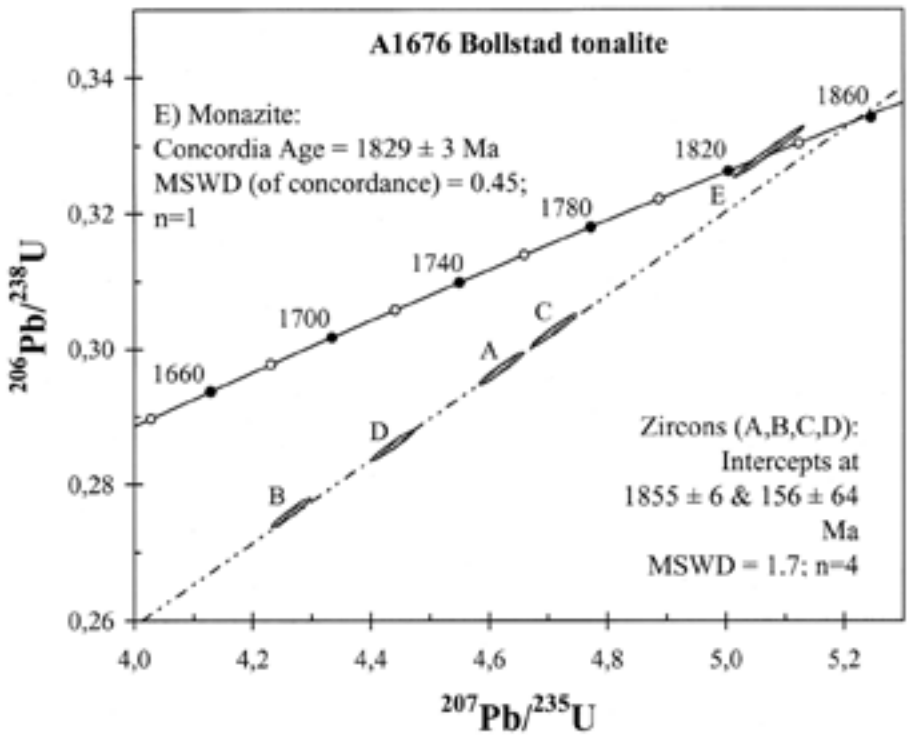

Appendix-Fig. 8-3. A concordia plot for TIMS U-Pb data on zircon and monazite; sample A1676 Bollstad tonalite (see also App-Table 1), Inkoo.

SIMS U-Pb age results

From the tonalite sample A1676 Bollstad 1, only eight dates were determined (App-Table 2), and one of these was rejected because of the high common lead content. Zircon is mostly quite stubby, shows only a weak internal structure and frequently has a very thin BSE-pale rim around it (Appendix-Fig. 8-2b).

All data plot in a cluster on a concordia diagram (Appendix-Fig. 8-4). A concodia age of 1873 ± 7 Ma for six of the seven data points can be calculated. The slightly discordant data (06a) are from an internally homogeneous core.

1873 ± 7 Ma is an unambiguous age for the syn-/late D_B tonalite. Although no direct age data are available, the thin BSE-pale rims are suggested to represent metamorphic zircon growth at 1.83 Ga, which is defined by the monazite from the rock. The TIMS U-Pb age of 1855 ± 6 Ma is slightly younger than that from the ion microprobe analyses. It is considered that the upper intercept defined by the discordant data has shifted slightly down because of 1.83 Ga metamorphism.

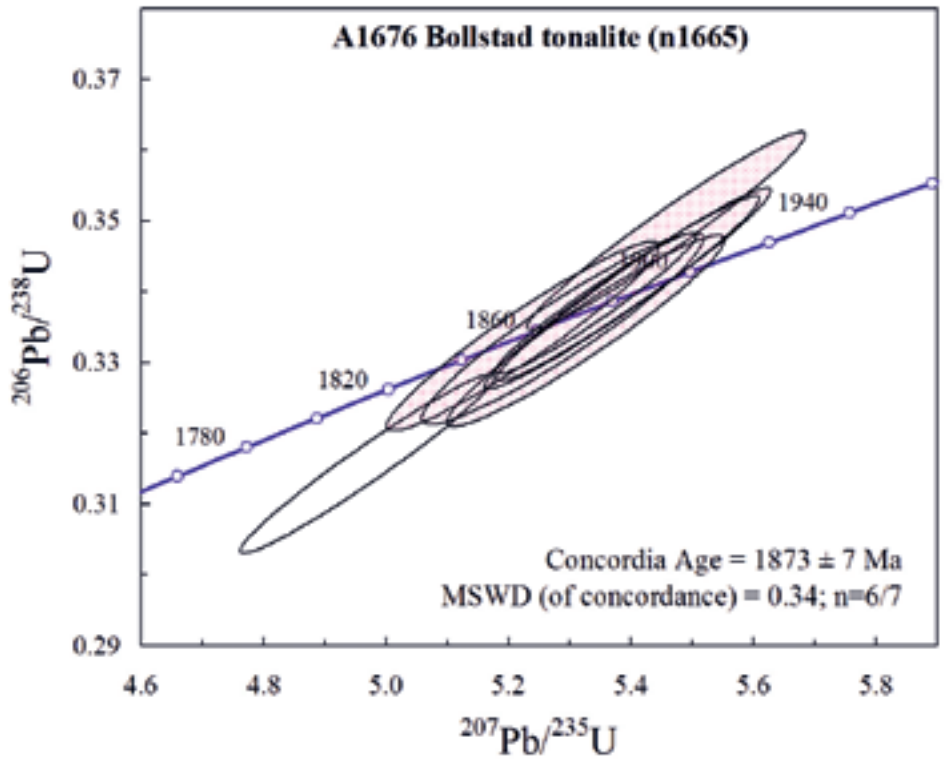

Appendix-Fig. 8-4. A concordia plot for SIMS U-Pb data on zircons; sample A1676 Bollstad tonalite, Inkoo.

A1785 Hakkila, Vantaa – an early D_E garnet-bearing tonalite dyke

Finnish grid coordinates KKJ2 2560.63E 6687.710
SIMS, zircon, NORDSIM sample number n1662, mount number M561 (large grains) and M562 (small grains)

Sample information

The sample A1785 Hakkila from Vantaa, a garnet-bearing tonalite dyke (Figure 29), represents a tonalitic magma event that cuts the early deformation phases, especially the tectonic D_{C+D} dome-and-basin structures. It is strongly metamorphosed and migmatized by the D_H granitic neosomes. According to structural analysis it is related to the early phase of the D_E magmatism. The age was determined to establish the start of the D_E evolution in the detailed study area. The sample location is shown in Figure 13 with the rectangle indicating the site of the tonalite in Figure 29.

Zircon description

The zircon population in tonalite sample A1785 Hakkila is quite homogeneous. It mainly consists of very long, pale brownish, transparent to translucent, principally quite tabular crystals. In addition to these, more brownish, short stubby grains with or without clear crystal faces also exist.

U-Pb age results

A total of 17 zircon domains were dated using an ion microprobe (App-Table 2). One data point (n1662–01c) was rejected, as its $^{206}Pb/^{204}Pb$ ratio was very low. The long zircon crystals mainly showing clear zoning determine the age for the tonalite; 11 of 12 analyses yield a concordia age of 1868 ± 3 Ma (Appendix-Fig. 8-5). Only one apparently younger data (n1662–04a) from an internally-homogenized domain was not included in the tonalite age calculation. The BSE images of typical analyzed zircons are presented in Appendix-Fig. 8-2c.

Only four domains were dated from the stubby zircons. An inner domain/core of one grain shows an extremely old age of 3.30 Ga. The other three ages from internally structureless inner and outer domains (cores and rims?) plot in the same cluster with the age data from the long magmatic crystals. As these zircons are considered as inherited ones, their U-Pb system must have been homogenized during the tonalite intrusion. The age of 1868 ± 3 Ma is interpreted as the intrusion age of the Hakkila early D_E garnet-bearing tonalite dyke.

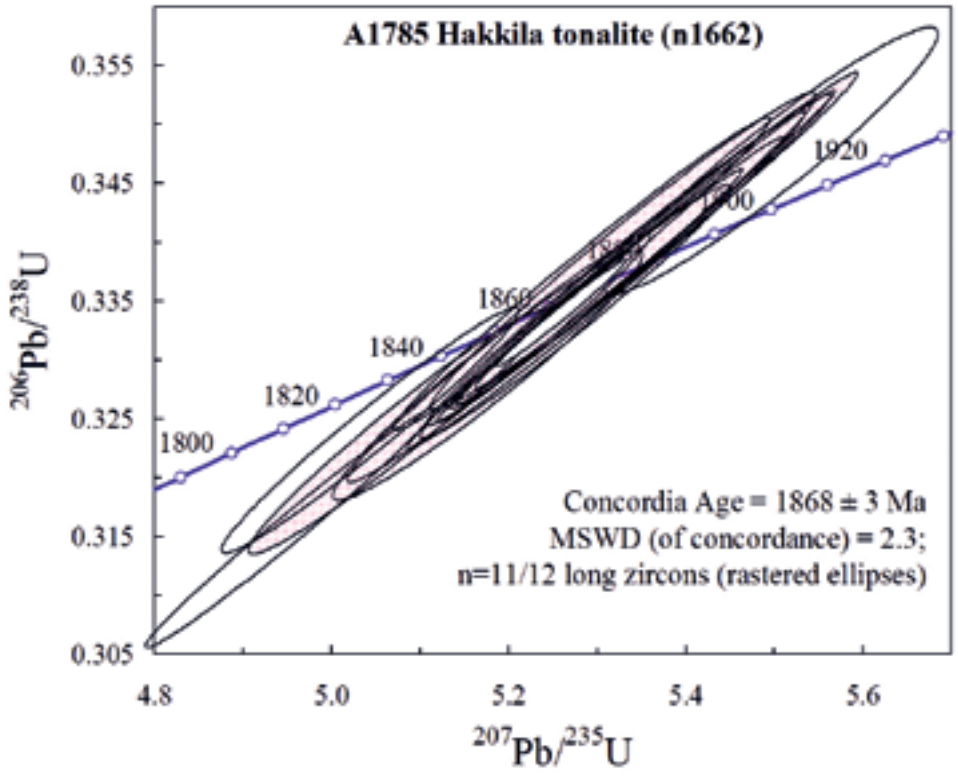

Appendix-Fig. 8-5. A concordia plot for SIMS U-Pb data on zircons; sample A1785 Hakkila tonalite, Vantaa.

A1784 Hyrylä, Tuusula – early D_E garnet-bearing tonalite dyke

Finnish grid coordinates KKJ2 2557.23E 6697.25N
SIMS, zircon, NORDSIM sample number n1661, mount number M561 (large grains) and M562 (small grains)

Sample information

The sample A1784 Hyrylä from Tuusula is a structurally similar tonalitic dyke (Figure 30a) to the Hakkila dyke, but it cuts slightly more deformed gneissic country rock. According to structural analysis it is also early D_E intrusive dyke that close by also forms larger intrusions showing lamination related to extensional SE-opening during emplacement (Figures 30b ad c). The dyke age was proposed to establish the age for the extensional opening phase.

Zircon description

The granitic dyke A1784 Hyrylä contains only a tiny amount of zircon. The population is heterogeneous, consisting of long and short prismatic crystals, very bright, equidimensional crystals as well as oval grains without crystal faces. The majority of the grains are transparent to translucent. It is also possible that all the zircons are inherited ones.

SIMS U-Pb age results

Eighteen zircon domains were dated using an ion microprobe (App-Table 2). Of these, four were dated from internally-homogeneous, stubby, round zircons and the rest from prismatic grains that do not show clear magmatic zoning but have quite homogeneous internal structures in BSE images. No correlation between the U and Th concentrations and zircon types existed (see App-Table 2).

The U-Pb data from the majority (10/14) of the prismatic zircons plot in a cluster defining a concordia age of 1860 ± 3 Ma (Appendix-Fig. 8-6). Three of the prismatic zircons are certainly inherited, showing a discordia age of c. 1.95 Ga. Two of these were measured from inner domains enveloped by younger rim phases (n1661–04b, n1661–16b). However, in the BSE images (Appendix-Fig. 8-2d), the inner darker older domains and the pale younger domains do not have any clear boundaries. It is thus suggested that the outer domains of the grains have suffered homogenization of their U-Pb system.

The rounded, stubby grains considered as metamorphic zircons give the same age as the prismatic crystals. The concordia age for these is 1858±7 Ma (Appendix-Fig. 8-6). These zircons can be considered initially as inherited ones.

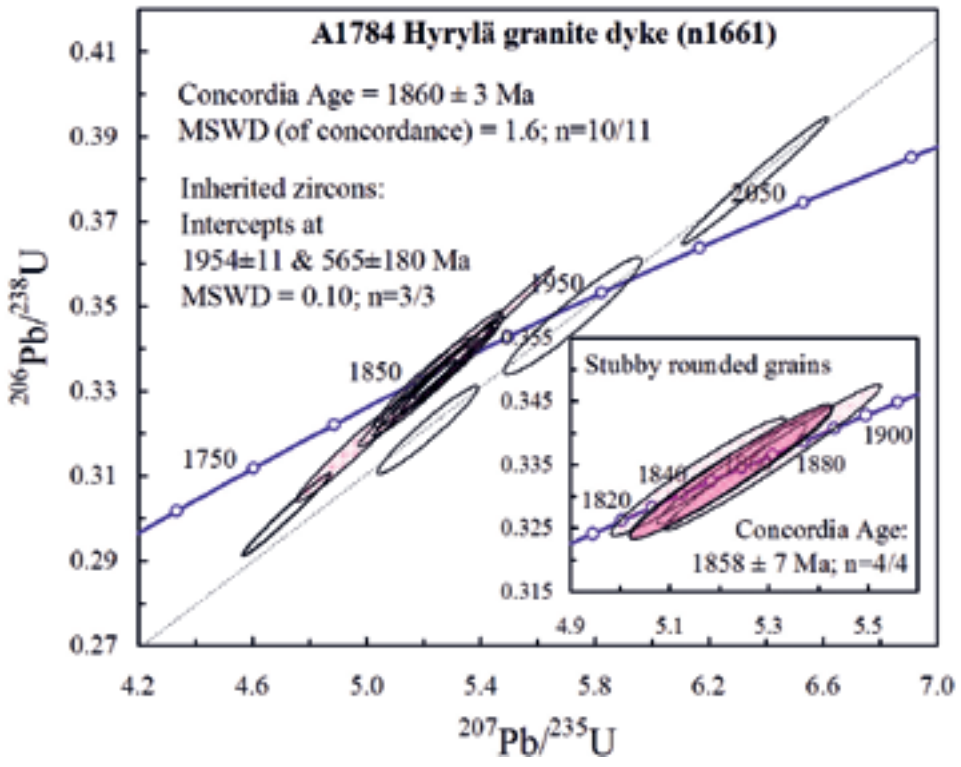

Appendix-Fig. 8-6. A concordia plot for SIMS U-Pb data on zircons; sample A1784 Hyrylä granite dyke, Tuusula.

A1335 Maikkala, Lohja – mid-D_E pyroxene-bearing tonalite, charnockite

Finnish grid coordinates KKJ2 2500.50E 6690.60N
TIMS, zircon and monazite
NORDSIM, zircon, mount number n1663, large grains = M561
SIMS, zircon, NORDSIM sample number n1663, mount number M561 (large grains)

Sample information

K. Korsman originally gathered this sample for dating the tectono-metamorphic evolution of the granulites in the West Uusimaa granulite Complex; the TIMS analysis was carried out by H. Huhma. The sample A1335 Maikkala from Lohja represents a high-grade tonalitic rock (charnockite) form. It is pyroxene-bearing, medium-grained, rather homogeneous rock and represents a rock preserved from the penetrative D_E deformation in the granulite area. Thus, in addition to the intrusion age for the tonalite it also established the upper limit for the penetrative extensional D_E deformation age.

Monazite and zircon descriptions

The sample included enough monazite for two fractions for TIMS. It included a lot of homogeneously pale brownish, translucent zircon varying from very long or shorter (length-width ratio = 3–7) prismatic grains to short, roundish grains. The zircon grains are zonal with well-developed crystal-faces referring to their magmatic origin. Only a few clear cores still having crystal structures preserved were detected.

TIMS U-Pb age result and zircon description

Six fractions of zircon were analyzed by TIMS. The U-Pb data (App-Table 1) give an upper intercept age of 1860 ± 5 Ma (Appendix-Fig. 8-7), predominantly based on the light fraction. The age is regarded as the magmatic age. A concordant monazite age of 1837 ± 3 Ma is interpreted as metamorphic (App-Table 1).

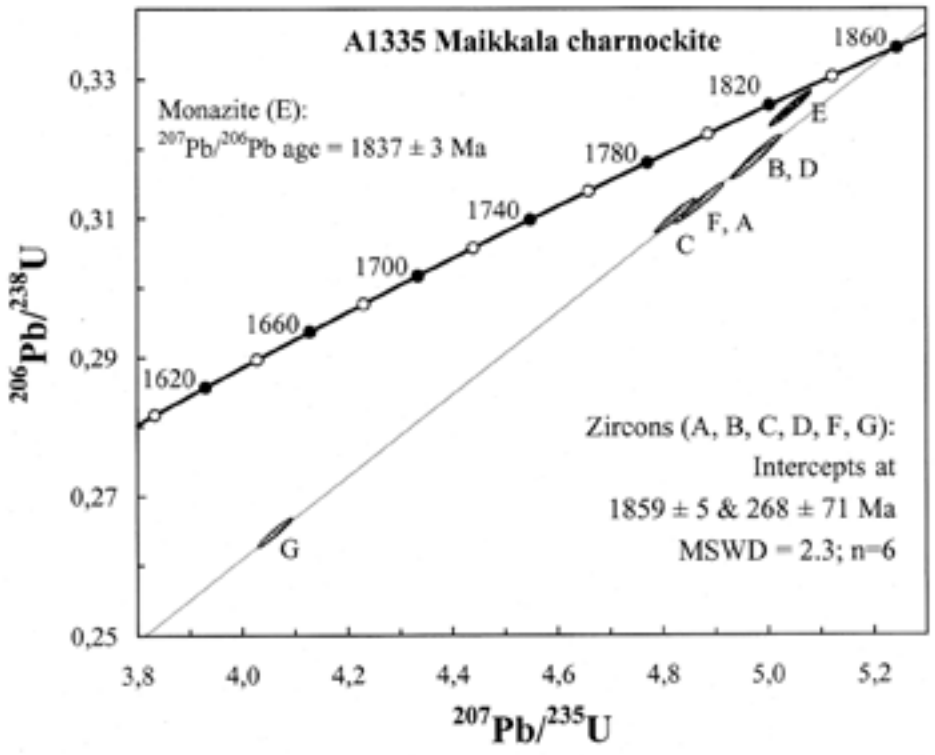

Appendix-Fig. 8-7. A concordia plot for TIMS U-Pb data on zircon and monazite; sample A1335 Maikkala pyroxene-tonalite (charnockite), Lohja.

U-Pb age results

From the charnockite sample A1335 from Maikkala, a total of ten zircon domains were dated using an ion microprobe (App-Table 2). All the data are concordant and nine of them define a concordia age of 1862 ± 4 Ma for the rock (Appendix-Fig. 8-8). All these were dated from magmatically-zoned zircons. A slightly younger age of c. 1.83 Ga is from a BSE-pale, homogeneous, low Th/U core domain (07a) with a 1.86 Ga BSE-darker main phase of the zircon (07b) (Appendix-Fig. 8-2e).

The TIMS U-Pb age and ion microprobe age are consistent. The homogenized core of the zircon 07 gives the same metamorphic age as the monazite. It thus seems probable that the previously metamict core was healed during the metamorphism.

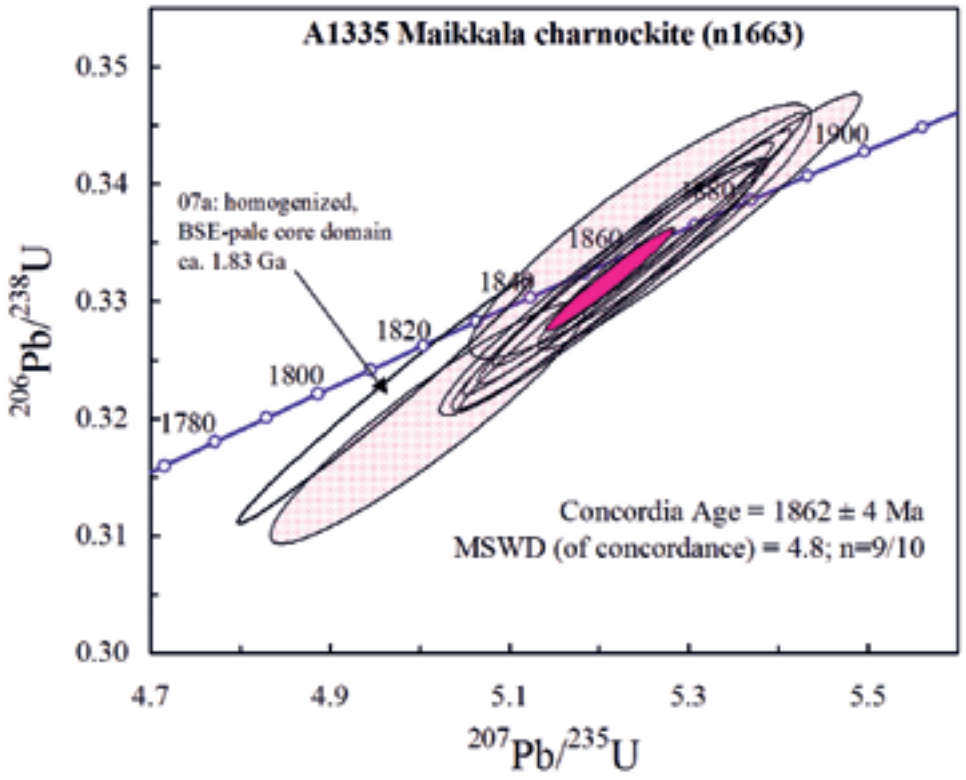

Appendix-Fig. 8-8. A concordia plot for SIMS U-Pb data on zircons; sample A1335 Maikkala pyroxene-bearing tonalite (charnockite), Lohja.

A1745 Jyskelä, Järvenpää – D_E gabbro

Finnish grid coordinates KKJ2 2562.56E 6711.55N
TIMS, zircon
SIMS, zircon, NORDSIM sample number n1666, mount number M562 (small grains)

Sample information

The gabbroic rocks are rare in the central parts of the granitoid-dominant units like the Espoo Granitoid Complex (EGC); the sample A1745 Jyskelä from Järvenpää is a gabbro from such an area. It was emplaced according to structural analysis into a low-angle structure that is interpreted as extensional S_E foliation exemplified in Figure 34b and c. The gabbro's structural setting is illustrated in Figure34a and its relations to the later D_H granites are shown in Figure 34d.

TIMS U-Pb age result and zircon description

The A1745 Jyskelä gabbro was dated using the conventional U-Pb method (App-Table 1). The four analyzed fractions give an upper intercept age of 1841 ± 7 Ma (MSWD=1.2) for the gabbro (Appendix-Fig. 8-9). The zircons in sample are quite odd-looking (EDS: Zr, Si, O). They are dark brown, transparent to translucent, elongated, and often flat with only rare crystal faces. Actually, the margins can be quite shapeless. However, dark brown zircons are quite usual in mafic igneous rocks.

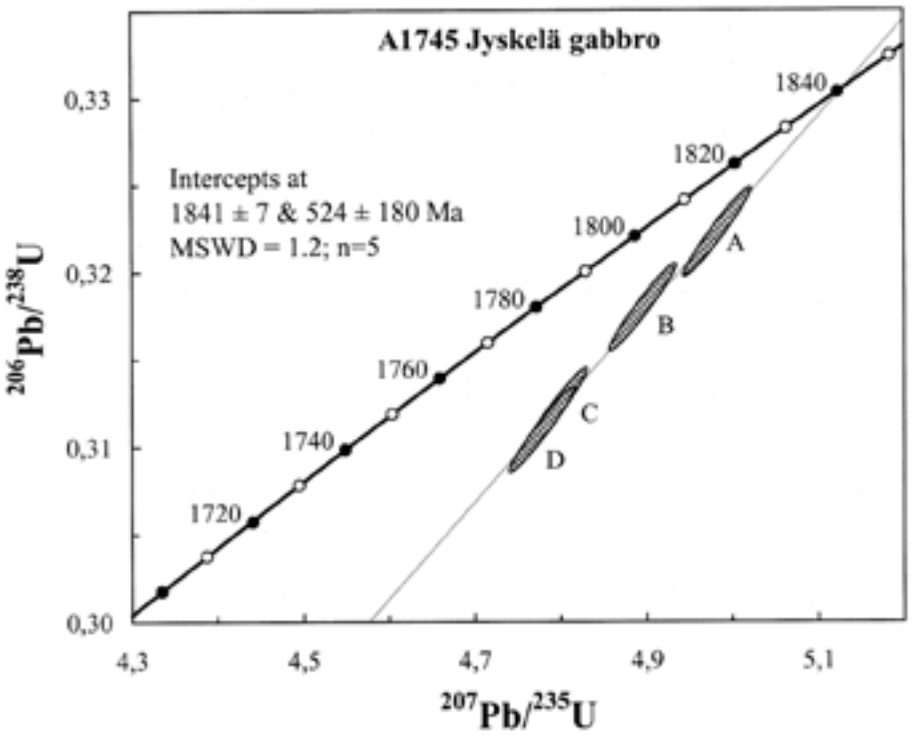

Appendix-Fig. 8-9. A concordia plot for TIMS U-Pb data on zircons; sample A1745 Jyskelä gabbro, Mäntsälä.

SIMS U-Pb age results

From the A1745 Jyskelä gabbro, seven zircon domains were dated using an ion microprobe (App-Table 2). The zircons show no clear zoning and some domains show tiny BSE-white heavy spots (phase separation?) (Appendix-Fig. 8-2f). The dated zircon domains are all unaltered, preferably dark in BSE images. The six concordant U-Pb analyses give an unambiguous age of 1838 ± 4 Ma (Appendix-Fig. 8-10) for the gabbro. This age is identical within the error limits with the conventional U-Pb age of 1841 ± 7 Ma.

A1677 Bollstad 2, Inkoo –D_H pegmatitic granite

Finnish grid coordinates KKJ2 2497.78E 6662.16N
TIMS, zircon and monazite

Sample information

The pegmatitic granite, sample A1677 Bollstad 2 from Inkoo, represents a D_H granite dyke that was emplaced into a cooled syn-/late D_B tonalite (sample A1676 Bollstad 1). The D_H granites characterize the Southern Finland Granitoid Zone (SFGZ). The dyke was originally set into an upright position, but due to continued flattening and heating it deformed into isoclinal folds. The structural relationships of the

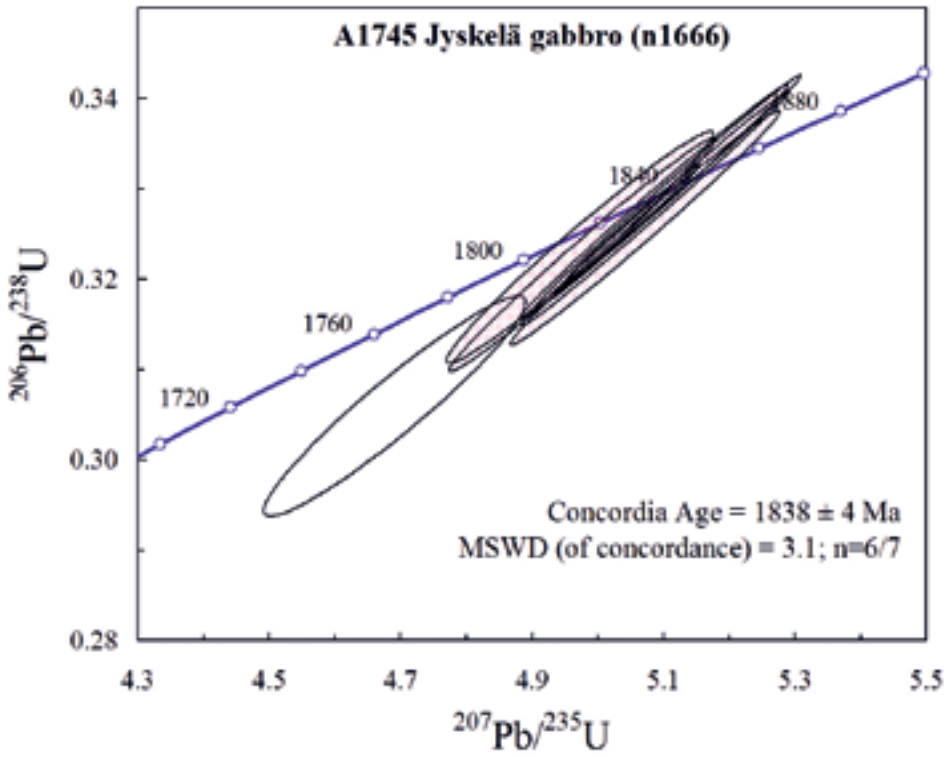

Appendix-Fig. 8-10. A concordia plot for SIMS U-Pb age data on zircons; sample A1745 Jyskelä gabbro, Mäntsälä.

dyke are illustrated in Figure 39. The age of the dyke establishes the beginning of the D_H phase in the Inkoo area.

Monazite and zircon descriptions

The sample included much brownish orange, pigmented (Fe?) monazite, and some bright yellow crystals with well-developed crystal face. Monazite is coarse-grained, referring to its magmatic origin. There are only a few mixed-like zircons in the density fraction >4.2 g/cm^3. The fraction 4.2–4.0 g/cm^3 had enough zircon for only a few age determination fractions. The majority of the prismatic (length-width ratio = 2.5–5) zircons are very light, <4.0 gcm^{-3}, dark brownish and metamict in character. These zircons are typical for pegmatite granites.

TIMS U-Pb age results

Monazite gives a concordant $^{207}Pb/^{206}Pb$ age of 1828 ± 1 Ma; the age taking into account the concodancy is 1828 ± 3 Ma (Appendix-Fig. 8-11). The age is exactly consistent with the monazite age from the Bollstad tonalite (sample A1676 Bollstad 1).

Six fractions of zircon were analyzed (App-Table 1). The zircons were light and high in uranium, and the analyze points scattered far from the concordia. The upper intercept age for zircons gives an age of 1817 ± 15 (MSWD = 1.6 (n = 6) (Figure Appendix-Fig. 8-11). Even though the error is large it can be assumed that the zircon is not much older than the monazite in the rock. When combined with the monazite analyses the value describing the quality of regression is 1.1 (MSWD). Because it is close to 1, are the zircon and monazite quite similar in age.

The age of monazite is interpreted to represent the pegmatitic granite dyke age. The dyke emplacement establishes the initiation of the late D_H granite event in the border zone of the most intense granitoid areas, such as the Espoo Granitoid Complex (EGC).

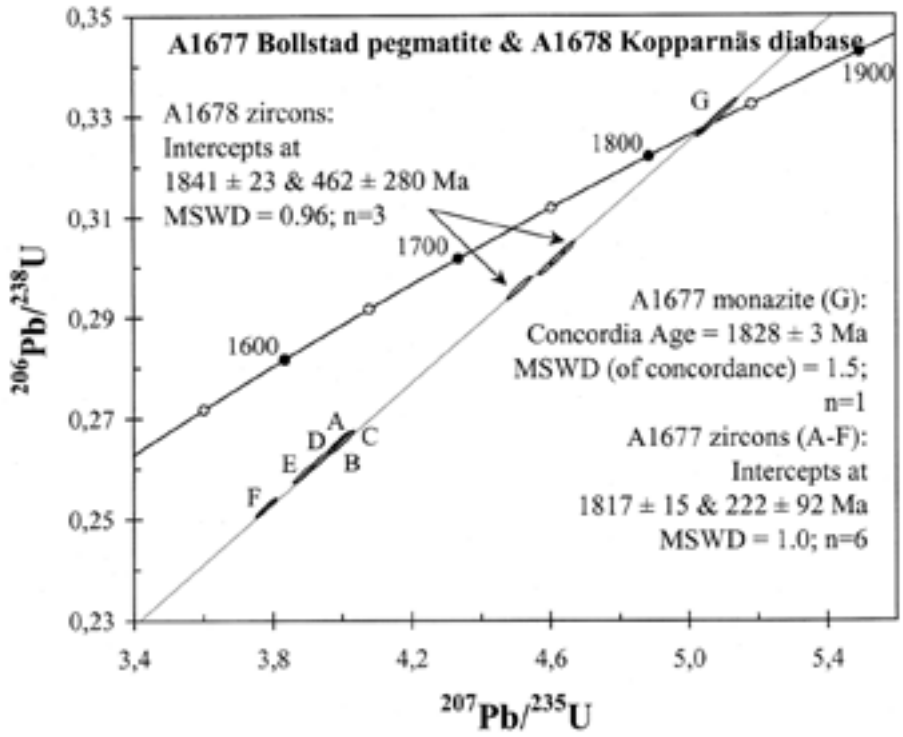

Appendix-Fig. 8-11. A concordia plot for TIMS U-Pb data on zircon and monazite; sample A1677 Bollstad pegmatite granite, Inkoo; sample A1678 Kopparnäs diabase, Inkoo.

A1678 Kopparnäs diabase

Finnish grid coordinates KKJ2 2514.13E 6659.09N
TIMS, zircon
SIMS, zircon, NORDSIM sample number n1664, mount number M561 (large grains) and M562 (small grains)

TIMS U-Pb age result and zircon description

From the A1678 Kopparnäs diabase, three zircon fractions have previously been dated using TIMS (App-Table 1). For the analyses, only extremely fine-grained, pale, transparent, and elongated zircons, which do not often show clear crystal faces, were selected. The larger grains were not dated as it is extremely implausible that a very fine-grained rock contains large or medium-sized co-magmatic zircons. In addition to these fine-grained dated zircons the sample contains large, dark brown and pale zircons with mixed shapes. As the zircon amount in the sample is very small and the quality is rather heterogeneous, it could be considered that all the zircons are inherited.

The age results (App-Table 1) are highly discordant and give an upper intercept age of 1841 ± 23 Ma (MSWD=0.96; n=3) (Appendix-Fig. 8-11). However, it should be kept in mind that three point isochrones defined by highly discordant data are certainly doubtful. The data points plot on the same discordia line with the highly discordant zircon data from Bollstad pegmatite.

For ion microprobe dating, various zircon types were selected: the large grains are mostly turbid to translucent, long and short crystals and the majority of the smaller zircons are brownish, transparent to translucent, long and short grains as well as roundish ones.

SIMS U-Pb age results

From diabase sample A1678 Kopparnäs, a total of 17 zircon domains were dated using an ion microprobe (App-Table 2). Two of these were rejected because of high common lead contents. Twelve analyses plot in a tight cluster on a concordia diagram (Appendix-Fig. 8-12). Eleven of the 12 confirm an age of 1831 ± 3

Ma for these zircons, which include large and small euhedral to round grains with mainly homogeneous internal structures.

Three small, brownish, long BSE-dark zircon grains (9a, 10a, and 16a) show younger $^{207}Pb/^{206}Pb$ ages with an upper intercept age of 1784 ± 24 Ma (the two rejected data with low $^{206}Pb/^{204}Pb$ (15a and 17a) from a similar zircon type would also plot on the same discordia line) (Appendix-Fig. 8-2g). These zircons also have the lowest U contents in the data.

In our opinion the maximum age for the diabase preferably is determined according to those 1.78 Ga small, long, brownish, low-U grains, as a very fine-grained mafic rock normally does not include much co-magmatic zircon. Thus, the c. 1.83Ga zircons are all inherited.

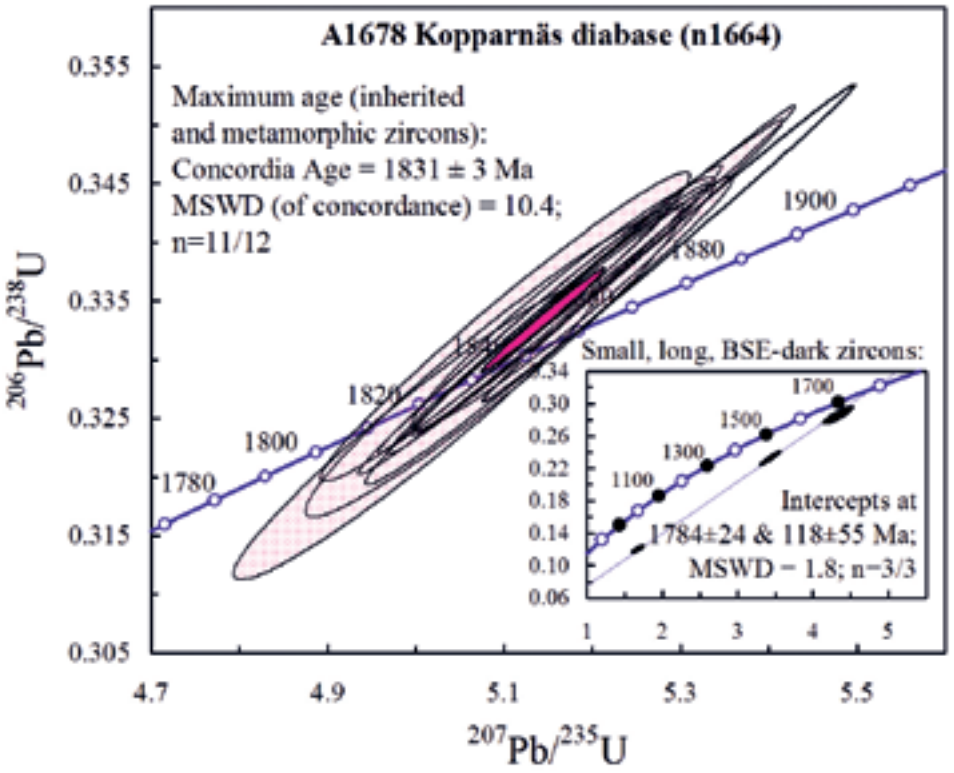

Appendix-Fig. 8-12. A concordia plot for SIMS U-Pb data on zircons; sample A1678 Kopparnäs diabase, Inkoo.

SUMMARY

The ages of rocks discussed in the main text are summarized in App-Table 3.

App-Table 3. Summary of the age results (see Appendix 8 for further information).

Sample name **Rock type**	**Anal. no.**	**TIMS U-Pb age results**	**NORDSIM U-Pb age results**
A1785 HAKKILA TONALITE	n1662	-	1868 ± 3 Ma (n=11/12; concordia age)
A1784 HYRYLÄ GRANITE DYKE	n1661	-	1860 ± 3 Ma (n=10/11; concordia age) Metamorphic ages 1858 ± 7 Ma; n=4/4; Inherited ~1.95 Ga
A1738 STAFFAS TONALITE	n1660	-	AVE=1857 ± 11 Ma (n=12) "Younger?" 1841 ± 4 Ma (n=7/7) "Older?" 1876 ± 8 Ma (n=4/5) Metamorhic zircon phases 1801±7 Ma (n=2/2)
A1745 JYSKELÄ GABBRO	n1666	1841 ± 7 Ma / zircon	1838 ± 4 Ma (n=6/7)
A1678 KOPPARNÄS DIABASE	n1664	1841 ± 23 Ma (n=3) Three highly discordant fractions / tiny zircons). Fractions plot on a discordia line with the pegmatite zircons from Bollstad	1831 ± 3 Ma (n=11/12) inherited grains 1784 ± 24 Ma (n=3/3) a few small grains. This age is considered as maximum age for the Kopparnäs diabase.
A1676 BOLLSTAD TONALITE	n1665	1855 ± 6 Ma / zircon (n=4) 1829 ± 3 Ma / monazite (n=1)	1873 ± 7 Ma (n=6/7)
A1677 BOLLSTAD PEGMATITIC GRANITE		1828 ± 3 Ma / monazite ~1.82 Ga / zircon (n=6) Highly discordant zircon U-Pb data	
A1335 MAIKKALA PYROXENE-TONALITE (CHARNOCKITE)	n1663	1860 ± 5 Ma / zircon 1837 ± 3 Ma / monazite	1862 ± 4 Ma (n=9/10) ~1.83 Ga metamorphic zircon phase (n=1)

Appendix 9. Tectono-metamorphic evolution of the Svecofennian domain in the study area is compiled in App-Table 4.

App-Table 4. Summary of the tectonic evolution of the Svecofennian domain in southern Finland. Abbreviations: VMB = Vammala Migmatite Belt, SVB = Southern Finland Volcanic-Sedimentary Belt, EGC = Espoo Granitoid Complex, HGB = Hyvinkää Gabbroic-volcanic Belt, WUC = West Uusimaa granulite Complex, GMB = Granitic Migmatite Belt, TMB Tonalite Migmatite Belt, SFGZ = Southern Finland Granitoid Zone, BBZ = Baltic Sea-Bothnian Bay Zone, RKZ = Riga Bay Karelia Zone and TIB = Transscandinavian Igneous Belt.

MAJOR GEOTECTONIC EVENT	DEFORMATION PHASE	AGE (Ga)	LITHOLOGY	RELATIONSHIPS OF STRUCTURES AND METAMORPHISM	STRESS FIELD	GEOTECTONIC INTERPRETATION	DISCUSSION AND APPLICATIONAL ASPECTS
SVECOFENNIAN EVENTS							
	EARLY SEDIMENTATION AND VOLCANISM						
Pre-E_1	**Pre-D_A**	1.95- (?)	Ultramafic and mafic rocks (e.g. cortlandites in VMB)[1]; psammitic-dominant metasedimentary rocks[1]			Early ocean floor magmatism?	Similar psammitic metasediments locally occur in the GMB
		1.9-1.89	Series I volcanism: mafic-intermediate-felsic volcanic rocks[2] in the SVB and EGC; Orijärvi granodiorite(2); there are also other early granitoids in the SVB (e.g. Algersö granodiorite in Föglö(5)), but their relations to volcanism are not known	Early volcanic and sedimentary sequences are folded by F_A; structures in Orijärvi granodiorite not known		Island arc volcanism and magmatism	In the SVB and EGC mafic-intermediate dykes cut the S_A of the early sedimentary-vocanic sequences; two volcanic series can be distinguished on a structural basis
		1.9	Psammitic-pelitic metaturbiditic metasedimentary rocks, sulphide and iron ore formations, calcaraeous rocks and limestones in the SVB	F_A-folded limestone in Kalkkiranta Sipoo is in association with F_A-folded volcanogenic felsic gneisses		Limestones, sulphide ores and iron formations indicate a low-water environment; metapsammitic and metapelitic sediments deposited in deep water environment	Psammitic-pelitic sedimentary rocks occur in close association with the pre-D_A felsic gneisses (volcanic rocks) and shallow water sediments due to later deformations (especially D_A)
	EARLY COLLISIONAL EVENT BETWEEN THE ARCHAEAN CONTINENT AND SVECOFENNIAN ISLAND ARC						
E_1	**D_A**	ca. 1.9-1.88		Isoclinal, often rootless folds, and weak penetrative foliation, probably major thrust faults	C. N-S contraction according to F_A observations	Early crustal thickening (possibly in island arc environment)	Strong rearrangement of rocks from different geotectonic environments close to each other; a change from lithostratigraphy to tectonic stratigraphy; relations of D_A to the D_1 in the northern terranes is not determined
	COLLAPSE OF ISLAND ARC AND LATER SEDIMENTATION AND VOLCANISM						
E_2	**Post-D_A and pre-/early syn-D_B**	1.88-1.87[2]	Series II volcanism: mafic to intermediate early/syn-D_B volcanism and mafic to intermediate dykes	The earliest identified structure S_B ; no F_A folds detected; mafic dykes cut the S_A		Possible intra-arc volcanism	Related to collapse and sinking of oceanic slap into the mantle
	Pre-/early syn-D_B	1.88-1.87[3]	Gabbroic-tonalitic association in the SVB and gabbros in the HGB	Strongly S_B-foliated and boudinaged - relationships with D_A in the volcanic series not known		Possible intra-arc magmatism syngenetic to the intra-arc volcanic rocks	Mafic rocks are sometimes suggested as synvolcanic with the early volcanic sequences[3]; further study is needed to determine their structural relationships
	D_B		Throndhjemitic to granitic migmatization	Isoclinal (to tight) recumbent folding with strong penetrative foliation, lineation weak - intersection between $S_{(A)+B/C}$, boudinage of competent layers with local shearing, prograde metamorphism to medium- to high-grade conditions	Strong vertical shortening due to crustal extension	Extensional event related to collapse of the island arc due to sinking of the oceanic slap into the mantle	Subduction is interpreted to be away from the Archeaen craton; the distribution of the gabbroic rocks in the HGB and HVB (App-Fig. 3-3b) estimates approximately SSW-NNE minimum principal stress; becomes diachronically younger towards the south from the TMB to GMB
	Syn- to late D_B	1.88-1.87	Gneissic tonalites, locally pyroxene-bearing in the EGC, WUC and SVB	S_C foliated showing a complex pattern of later shear band structures, all the D_{E-H} granitoids and dykes cut the tonalite			Forms large homogeneous intrusions (e.g. Hindby intrusion)
	N-S COLLISION - A NEW CONTINENTAL CRUST FORMED						
E_3	**D_C**	1.88-1.87	Granitic neosomes to a in decreasing extent after D_B	Moderate to tight folding with weak E-trending axial plane foliation or crenulation deforming the $D_{(A)-B}$ structures; the first penetrative deformation in the syn-/late D_B tonalites	N-S contraction	Collisional event in the ductile stage causing crustal shortening	C. similar ages of the D_C and D_B suggest continuous overall D_C collision and local D_B extension, both becoming diachronically younger southwards
	SW-NW TRANSPRESSIONAL COLLISION						
Transition from E_3 to E_4	**D_D**	1.88-1.87	Pyroxene-bearing quartz-monzonites in the CFGC	Open to tight folding causing ellipsoidal D_{C+D} dome-and-basin structures especially in the SVB, no significant foliation identified; developed into intensive D_4 shearing causing block structures in the northern terranes (e.g. CFGC and TMB); deformation was more zonal in the north than in the south	NE-SW transpression; related SE-NW oblique extension (e.g. in the CFGC)	Ductile oblique collisional event causing crustal shortening; intense movements of crustal blocks indicating escape tectonics model of deformation	The quartz-monzonites of 1.87-1.86 Ga[14 and15] establish the closing of D_D in the northern terranes
	COOLING STAGE						
The cooling stage after the D_D varied in duration in differet areas. In the northern terranes cooling began after D_4 and deformation developed to become more zoned in character. In the south (SFGZ) thermal activity was in places nearly continuous, but local cooling stages of c. 30 Ma occurred.							
	FORMATION OF THE SOUTHERN FINLAND GRANITOID ZONE (SFGZ) IN OBLIQUE EXTENSIONAL TECTONIC REGIMES						
E_4	**D_E**	c. 1.87-1.84	Strong tonalitic to granitic magmatism with minor gabbros; pull-apart-basin supracrustal rocks (see details below)	Strong horizontal S_{Eext} foliation with top-to-SE movement in the SFGZ; often totally destroyed the previous D_{A-D} structures; complex D_E shear band structures in previous rocks	C. NW-SE oblique extension during overall NE-SW transpression	Oblique extensional zones developed under NE-SW transpression between the the major N-trending shear zones (BBZ, RKZ and TIB)	
	Early D_E to mid-D_E	1.87-1.84[13]	Garnet-bearing tonalites and contemporaneous pegmatitic granites predominantly in the EGC; microtonalite dykes	Metamorphosed intrusions and dykes, often garnet bearing; cut the syn-/late D_B tonalites; remelt by the later metamorphic events, e.g. during D_H.	NE-SW to E-W dilatation		Early pegmatitic granite borders of the early tonalitic dykes indicate increasing temperature during their emplacement
	D_E	After 1.87-1.86[7]	Jokela sedimentary-volcanic association: quartzites, conglomerates, pelitic metasediments and volcanic rocks	Shows one prograde metamorphism to medium-grade and low pressure, strong S_E and later deformations, very weak foliation preceeding S_E; cut by D_{E-H} granitic magmas	Upper crustal oblique NW-SE extension	Sedimentation and volcanism in a pull-apart-basin in a high-energy environment; later change to deep water sedimentation and volcanism	Corresponding associations occur and are generally preserved in the intersections of the major E-trending shear zones (predominantly D_H) and D_I structures.
	Late D_E	c. 1.86-1.84	Tonalites, granites and gabbros	Show only weak contractional D_E deformation structures and are cut by the late D_E granitic dykes; also composite dykes with pegnmatitic granites; often emplaced along S_{ext} planes			Lower-crustal intrusive magmatism is possibly related to upper-crustal volcanism e.g. in the D_E pull-apat-basins
	D_F	c. 1.86-1.85[17]	Granitic intrusions in eastern Finland (Maarianvaara)	Zones of folding with N-trending axial planes in eastern Finland[16]; shear zones bordering the Central Finland block; Hiidenvesi shear zone in the WUC	E-W contraction	Related to escape tectonics causing eastwards movement of crustal blocks in central Finland	D_F structures are local and not significantly developed in southern Finland; stress probably released along the major E-trending shear zones in the south
	D_G	c. 1.84	Minute granitic veining	Open to moderate large-scale folding locally with granitic veining in the axial plane; shearing especially along the early shear zones between granitoid and supracrustal terranes	N-S contraction	Collisional crustal shortening	Deformation D_F occurred simultaneously with the D_E, suggesting different local stress fields in different parts of the Svecofennian domain; situations of this kind are characteristic of escape tectonics
	D_H	1.83-1.80	Granodiorites, granite and pegmatitic granite dykes	Extensional recumbent folding F_{Hext} with strong horizontal Shext and contractional folding with NE-SW-trending axial planes, medium- to high-grade metamorphism at low pressure and strong partial melting of earlier granitoids and gneisses	NW-SE transpression	Rotation of the stress field into NW-SE caused oblique contraction in the SFGZ and closing of the D_E pull-apart-basins	In high-grade areas (e.g. WUC and EGC) the change from D_E to D_H magmatism was transitional; patchy occurrence of the D_H granites refers to local oblique extensional zones during continued transpression
		1.83-1.78	Diabase dykes	Weakly deformed amphibolite facies N-S- and E-W-trending diabase dykes	Oblique dilatational zones during the overall NW-SE transpression		There are also gabbroic rocks (D_H?) within D_H granites, indicating wider deep-seated magmatism and heat flow during D_H
	POST-TECTONIC MAGMATISM AND FADING OF THE SVECOFENNIAN OROGENY						
E_5	**D_I**	c. 1.8		Late deformation in the N-S-trending major deformation zones (BBZ, RKZ and TIB); large-scale folding with N-trending axial plane forming open D_{G+H+I} dome-and-basin structures	C. ESE-WNW contraction	Crustal shortening and shearing along the major shear/fault zones	The BBZ, RKZ and TIB evolution initiated during the D_D transpression and continued during the D_{E-H}; the D_I structures deform the SZGZ; the deformation style was brittle in the north and ductile in the south until the fade of the Svecofennian orogeny
		1.8-	Homogeneous granitic intusions (stocks)	Post-tectonic to the major Svecofennian deformation phases, but are often sitting close to the intense D_I zones, like in the BBZ or RKZ			Post-tectonic or late tectonic to the D_1 (?)
POST-SVECOFENNIAN EVENTS							
	D_P	**RAPAKIVI STAGE**					
		1.65-1.52	Rapakivi granites, quartz-porphyry and diabase dykes	Drag folding, zonal semi-ductile dextral shear zones, jointing in the direction of diabase dykes; large-scale listric faulting[8]		Crustal extension	Rapakivis were set into the intersections of the late Svecofennian high-strain zones (D_E, D_G, D_H and D_I); the diabase dykes are at least partly controlled by ductile shearing structures like the Hiidenvesi shear zone in the WUC and jointing
		RIFTING STAGE					
		c. 1.25	Sandstone and mafic diabase	Open dragfolds, weak fractual cleavage, brittle faults		Upper crustal extension	
		CALEDONIAN OROGENY					
		c. 450 Ma		Brittle faults, reactivation of pre-existing structures and possibly low-angle brittle thrusting faults; fluid actvity in preexisting faults; U-mobilization(12) and remagnetization(13)		Reflections of Caledonian orogeny	
		POST-GLACIAL EVENTS					
		<10 000 a		Minor faults deforming glaciogenic sediments and recent earthquakes[10]	Present-day c. NW-SE stress field[11]	Post-gacial isostacy and modern plate-tectonics(?)	Reactivation along pre-existing brittle structures, joints and faults

(1) Korsman et al. (1999; and references therein), (2) Väisänen & Mänttäri (2002), (3) Hopgood et al. (1983), (4) Patchett et al. (1981), (5) Suominen (1991), (6) Pajunen et al. (2006), (7) Lahtinen et al. (2002), (8) Korja & Heikkinen (1995), (9) Elminen et al. (2008), (10) Kuivamäki et al. (1988), (11) Stephansson et al. (1986), (12) Vaasjoki (1977b), (13) Mertanen et al. (2008), (14) Mäkitie & Lahti (2001), (15) Lehtonen et al. (2005), (16) Koistinen 1981 and (17) Huhma (1986).